A BI-LEVEL FRAMEWORK FOR AIRCRAFT DESIGN UNCERTAINTY QUANTIFICATION AND MANAGEMENT

A Dissertation
Presented to
The Academic Faculty

By

John Mark Mines

In Partial Fulfillment
of the Requirements for the Degree
Doctor of Philosophy in the
School of Aerospace Engineering

Georgia Institute of Technology

May 2019

A BI-LEVEL FRAMEWORK FOR AIRCRAFT DESIGN UNCERTAINTY QUANTIFICATION AND MANAGEMENT

Approved by:

Professor Dimitri N. Mavris, Advisor
School of Aerospace Engineering
Georgia Institute of Technology

Professor Daniel P. Schrage
School of Aerospace Engineering
Georgia Institute of Technology

Dr. Jimmy C. Tai
School of Aerospace Engineering
Georgia Institute of Technology

Dr. Jason A. Corman
School of Aerospace Engineering
Georgia Institute of Technology

Dr. Joseph Scott Wilson
Mission Systems
Northrop Grumman Corporation

Date Approved: March 28, 2019

Rather than love, than money, than fame, give me truth.

Henry David Thoreau

To my family,

whose shoulders I stood on to see further.

and,

To my wife,

who supported me through graduate school,

which turned out to be a non-trivial exercise.

“Always remember there was nothing worth sharing like the love that let us share our name.”

-The Avett Brothers

ACKNOWLEDGEMENTS

I thank my thesis advisor, Dr. Dimitri Mavris, for building such a unique aerospace graduate laboratory that has given me invaluable experience. I would not have finished in a timely fashion without Dr. Jimmy Tai, who sacrificed his time to meet with me so frequently. I would like to thank Dr. Jason Corman for enabling me to utilize his team's design environment, and Dr. J. Scott Wilson for allowing me to advance his personal work, as well as his encouragement throughout the defending process.

In addition, I indebted to the RADE team, specifically Adam Cox and Coleby Friedland, for answering my frustrated questions. I thank Eric Inclan, for his zeal for science, and John Robinson, for reminding me never to take things too seriously.

I cannot thank my family enough for their unwavering support, unfailing love, and unselfish sacrifice. Much has been invested in me to reach such a point of academic achievement, and it is the result of decades of perseverance by my parents, Michael K. and Janice L. Mines.

I would like to thank my wife, Kendall R. Mines, who ran, walked, and crawled through this journey with me. I am deeply grateful for her many sacrifices, and the challenges she overcame that no one else will ever see. Her strength made all the difference at the inflection points.

And finally I would like express a special thanks to my grandparents: to my grandpa, Keith G. Mines, for his financial support of my academic career; and, my grandfather, Dale E. Gillan, for financing my speech pathology classes all those years ago, which taught me that anything is possible.

Thank you all,

John Mark Mines

Atlanta, 2019

TABLE OF CONTENTS

LIST OF TABLES

LIST OF FIGURES

SUMMARY

Aircraft design and development is a high-risk process. The recent obstacles with the Boeing 787 Dreamliner and Lockheed Martin F-35 Lightning II programs demonstrate the difficulty in achieving profitability from bringing a next-generation aircraft from concept to reality. A review of the design process reveals that the design freedom falls precipitously during the conceptual phase while the uncertainty remains high until the preliminary phase. This contrast means that important decisions are made under high levels of uncertainty, increasing the likelihood of future problems in the program. This phenomenon encapsulates the high level of risk confronting aircraft manufacturers: the expenses required represents serious investment, while the complexity represents high likelihood that issues will arise.

The recency of these two aircraft programs shows that the level of risk has yet to be adequately addressed. A review of work in this area reveals that methods do exist that quantify design uncertainty as well as capture common safeguards against unfavorable uncertainty realizations; however, two main capability gaps currently inhibit the effectiveness of reliability-based methods. The first gap is an inability to explicitly model design alterations (called *mitigation*) within a physics-based modeling environment. This prevents accurate assessments of design modifications applied in response to uncertainty. The second gap is a lack of data-based processes to describe and correlate sources of uncertainty. Uncertainty sources are typically assumed to be independent with prescribed distributions without data-based justification.

This thesis addresses these capability gaps. The first gap is addressed by integrating a wing-level, physics-based design environment (the Rapid Airframe Design Environment,

or RADE) with a vehicle-level, empirically-based design environment. RADE is a toolkit that utilizes a series of finite element modeling tools to modify wing geometries and perform structural sizing. The selected mitigation action, taken from the historical example of the Sutter Twist, is geometrically twisting the outboard wing after the wing has been structurally sized. This design change is applied directly to the geometry, and affects performance (such as span efficiency) and wing-level constraints (such as tip deflection).

The second capability gap is addressed by determining the most relevant sources of uncertainty with respect to vehicle- and wing-level design environments. Because this work relies exclusively on models to perform analysis, the primary focus is on model uncertainty. A sub-category within model uncertainty (discretization error) is selected for quantification. The error is characterized using Richardson's Extrapolation Method which varies the mesh size of the finite element model to extrapolate the ideal solution. This method is applied to a sampling of wing designs to form a error dataset which is then fit to parametric distributions and tested for correlation using Pearson's Correlation Coefficient. To maintain the found correlation, the dataset is used to fit a t copula (an n-dimensional joint probability distribution). The copula maintains the relationships between the variables and can be sampled directly. Accounting for correlation is seen to affect the reliability estimation by as much as 10%.

The physics-based and empirically-based environments are integrated into a single environment to perform bi-level reliability analysis. Because the two environments have different levels of fidelity, shared variables are not guaranteed to agree. The two environments are bridged using take-off gross weight, wing skin weight, wing ribs and spars weight, and span efficiency. The convergence is shown to be robust against various initial guesses and across the design space. After integrating the two environments, the presence of wing-level constraints is shown to greatly affect the reliability assessment. Because the vehicle-level environment has no awareness of the wing-level constraints (they are "unknown," or uncertain), vehicle-level optima tend to fail wing-level constraints. Therefore, the integrated

environment greatly improves reliability estimation and conceptual design selection by reducing downstream uncertainty.

The methods developed herein are used to form a framework for reliability assessment using bi-level design analysis (RABiDA). This framework is demonstrated on a 300 passenger airliner design scenario. An optimization is performed to determine a Pareto Front in the objective space where economic block fuel and reliability are the optimization criteria. The results show two clusters form along the Pareto Front, distinguished by a discontinuity along the Front. These two clusters had mutually exclusive design spaces, meaning that the difference in reliability was not margin values but design values. These two clusters form two design loci that management could select with some flexibility.

For contrast, an optimization is performed to maximize compliance (satisfying constraints without the use of mitigation). The Pareto Front that maximizes success is dominant with respect to both objective criteria; however, the optimization criteria do not take into account the programmatic effects of mitigation.

The contributions of this work are mitigation modeling, data-based uncertainty quantification, and bi-level environment integration. The mitigation action is explicitly modeled neglecting the need of translational k-factors. Applying Richardson's Extrapolation Method allows for parametric distributions to describe the discretization error (rather than be prescribed a priori) and allow the data to be tested directly for correlation. The structural wing weight convergence iteration bridges two environments of varying levels of fidelity allowing downstream constraints to be known at the vehicle level. Finally, each of these additions to the state-of-the-art is included in a completed reliability-based conceptual design optimization.

CHAPTER 1
INTRODUCTION AND MOTIVATION

Humans have always been engineers: prehistoric Homo sapiens utilized raw resources to hunt, kill, and eat. The tools resulting from these engineering abilities resulted in a competitive edge in nature, allowing us to grow to a population of billions. Today, our engineering has become far more advanced, but the principle remains the same: the group with the most advanced engineering sustains a greater probability of survival. In truth, the contest before was between species; today, the contest is between companies and countries. Nonetheless, the goals of survival and success still remain.

Today, the complexity of the engineering process is difficult to describe. Our gadgets fail to resemble the original resources used in their construction. The engineering process now requires ingredients from all over the world transported along global supply chains, local languages, and commercial entities. Today, tools make tools, codes write code, and machines make machines. Even the most mundane objects are highly specialized to maximize performance and minimize cost. The aerospace industry is certainly no exception to these trends.

Undoubtedly the first engineers relied on trial and error to improve their creations. In situations where resources such as time, material, and labor are abundant, this process is sufficient. However, in today's cutting edge, dynamic marketplace, trial and error is no longer a viable approach to engineering design.

Design is a highly competitive process inundated with uncertainty and possibility. These two characteristics form the motivation of this thesis: how can we safely dive into the unknown to turn on the light? Being an aerospace engineer, the field of choice will be aerospace engineering, and the design process of choice will be aircraft design. Though, in truth, these principles hold for all engineering design applications, such as smart phones,

and all aerospace applications, such as rockets or satellites. This first chapter will introduce the aircraft design process, its challenges, the economic impact, and opportunities for improvement, which will become the focus of this work.

Motivational Question
How can the level of risk inherent within the aircraft design process be improved?

1.1 The Aircraft Design Process

The aircraft design process is the series of steps taken that result (hopefully) in a flyable plane. As described by Raymer [1], it typically starts by defining the requirements the aircraft must satisfy. These requirements are defined with a focus on the end customer: range, speed, cost, etc. Various concepts are developed that meet these requirements, then refined with high-fidelity analysis eventually prepared for production. The design process ends when a single design is determined. Here it is prudent to be rigorous about the use of the term "design": for this thesis, design is either an action (verb) or product (noun). When used as a verb it describes the overall process of determining the design. The term determining refers to the iterative process of analysis to conclude on a singular design. The design is fully complete when each variable value has been found, and the values agree with each other (e.g. sum of all weights is equal to gross weight). Design used as a noun, such as in the previous sentence, refers to a unique set of values. A design is not (and never can be) equivalent to a flying aircraft. Instead, a design is a blueprint: a unique set of values that the airplane *should* be, but may ultimately embody. A flying airplane is a single realization of a design, just like a building is a realization of a blue print. However, no matter how many airplanes are built, there is still only one design.

The precise process taken by aircraft designers to create a new or derived concept varies by entity. Unfortunately, these processes and procedures tend to be proprietary and therefore publicly unavailable. However, Raymer has established a formal aircraft design pro-

cess consisting of three major phases as showing in Figure 1: conceptual, preliminary, and detailed design [1]. Raymer also at times adds a prior step to the design process for requirements engineering. The entire process includes seven stages, appending manufacturing, production, and operations and support to the design stages detailed by Raymer [2]. Raymer's classification is the most popular approach to aircraft design, though other segmentations exist [3, 4].

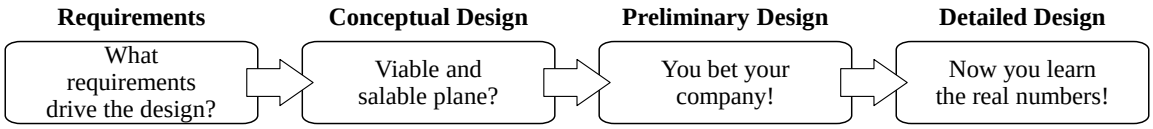

Figure 1: Three Phases of Aircraft Design, adapted from [1]

1.1.1 Requirements

Conceptual design is often called the first phase of the design process because typically requirements definition is not often classified as "design"; nevertheless, the design process depends on it. The requirements are typically first defined in customer-centric language, such as requiring an airliner to fly from the Los Angeles International Airport (LAX) to the Hong Kong International Airport (HKG), or specifying a number of passengers and cargo payload. Requirements are typically written by the customer rather than the engineer. Consequently, these requirements are then translate to quantifiable metrics in a process called requirements engineering. The result is a set of constraints and goals that the design must satisfy. The route from LAX to HKG becomes a design mission (or sizing mission) of 6,300 nautical miles. The mission profile will also be specified, which will contain more detail about the design mission such as taxi, take-off, climb, cruise, descent, and loiter. Additional requirements come from regulatory bodies such as the Federal Aviation Administration (e.g. fuel reserves, cruise speed, field length for take-off and landing).

1.1.2 Conceptual Design Phase

Defining the requirements allows for concept trade studies. A concept is a specific aircraft configuration, such as a narrow-body fuselage with two wingtip mounted turbofan engines and a T-tail. Requirements are merely a list of chores or constraints: concepts are specific configurations that might satisfy the requirements. Here is where the overall size and shape of the vehicle take shape, though at a low level of detail, allowing for a quick analysis of a wide variety of concepts. Because there are many consequential decisions to be made (number and type of engines, type of tail and fuselage, type and number of high-lift devices, etc.), the combinatorial space is prohibitively large. Therefore, an analysis of alternative concepts is performed, where different designs or a family of designs are evaluated against one another [5]. The goal here is to explore the space efficiently and effectively. In order to compare potential configurations or to explore the entire design space of a specified configuration, lower fidelity tools are used to get approximations of performance values for design points. These tools focus on the key disciplines of aerospace engineering, such as aerodynamics, propulsion, and performance, and may rely on empirical data rather than rigorous physics-based analysis. The more precise disciplines, such as stability and control, are postponed until preliminary and detailed design. The more substantial pieces of the aircraft are the center of focus here, such as the wing shape and area, fuselage dimensions, and engine thrust and weight. The vehicle level analysis results are expected to be rough estimates, but the trade-off during this phase is the agility to compare a large number of designs. The rest of the design phase is dependent on the design point selection, and about half the cost of the program is committed once conceptual design is completed.

1.1.3 Preliminary Design Phase

Once the major decisions have been made about the new design (particularly the configuration and size), the preliminary design phase begins. Here, the decisions made during conceptual design are considered “locked in,” or “frozen”: these decisions cannot be changed

throughout the rest of the design process. This shows how the aerospace industry has classified each of its stages: within each phase, the decisions are fluid, constantly changing with new analysis and test; however, once the phase has concluded, the decisions are written in stone. This is largely a result of the expansive combinatorial space: for each singular conceptual design, there are thousands of decisions to be made (values to determine) in the preliminary and detailed phases. Put simply, performing the phases simultaneously is currently too complex [6]. Raymer states that this is a crucial schedule milestone as "it allows other designers to begin serious development of structure and subsystems without ear that their work will be invalidated by later changes." During preliminary design, the low-fidelity tools used during conceptual design are swapped out for higher fidelity or physics-based tools. Whereas conceptual design tools are typically based on empirical regressions, preliminary design tools are typically based on physical modeling. Common techniques include computational fluid dynamics (CFD) and finite-element methods (FEM). The key components during this phase are internal structures, landing gear, and control systems. The major pieces move into fabrication and testing. Here, the analysis and testing effort intensifies, as does the cost of the program; indeed, recall that the previous analysis has been mostly empirical or low-fidelity. From Figure 1, Raymer satirically says that this is where you "bet your company" because not a lot is known about the chosen conceptual design until the money is spent to build and test the major pieces. Entering this phase is a gamble.

1.1.4 Detailed Design Phase

The detailed design phase is when the each of the thousands of aircraft parts are designed and analyzed. This is the most expensive phase of the design process: every element of the aircraft must be analyzed and tested to ensure usability. All previous decisions are still locked in, though subtle changes to the design can be made at this stage with the remaining degrees of freedom. Parts of the design that have hitherto been neglected are

now created: tracks, brackets, structural clips, doors, racks, and others. Here, production design coalesces with product design, as the engineers determine how exactly the aircraft is to be manufactured and assembled. This phase ends with the full fabrication and assembly of the aircraft. As Raymer notes, this phase does bring the "real numbers" because the aircraft itself is finally built and tested. The design is now fully known and frozen (fixed).

1.1.5 Design Phase Distinctions

As previously noted, conducting aircraft design all at once is currently too complex to handle: the design space is too large, the math is too cumbersome, the software programs are too slow, and many other obstacles exist. As a result, the overall process has been discretized into the aforementioned phases. In fact, more than discretized, it has been specialized: over time groups have dedicated themselves to specific pieces of the aircraft puzzle, either internally at the large aircraft manufacturers or externally by starting new companies specializing in software development or prototyping. This specialization allows each entity to master the much smaller problem, increasing efficiency and detailed know-how, but there is a drawback: the final design is destined to be sub-optimal. For example, the conceptual design is selected based on low-fidelity models to truncate the complexity of the analysis. Put another way, it is selected based on a number of assumptions. Worse, this selection is *final* as the design phase progresses. Never mind if the aircraft requires a new manufacturing process when detailed design rolls around. At that point, the detail design engineers must simply "figure it out." The program has become too big to cancel or start over. When preliminary and detailed phases come around, whatever new knowledge is gained about the selected concept does not feedback to conceptual design. If any of the assumptions were found to be errant (which is inevitable), the designers can only use the remaining degrees of freedom. They cannot "go backwards." This almost guarantees program delays and cost overruns. Therefore, until aircraft can be designed with as much forward knowledge of the design as possible, the final result is sub-optimal.

Observation

The complexity of aircraft design and development has resulted in discretization into design phases, with specialists in each phase making significant decisions without feedback from downstream analysis.

1.2 The Economics of Aircraft Design and Development

Because aircraft are so difficult and expensive to create, there are a relatively few number of producers. In the civil space the major players are The Boeing Company and Airbus SE. In the military space Lockheed Martin and Northrop Grumman are the largest. These manufacturers are well known because they employ large numbers of people and operate supply chains all across the globe. Smaller players in the civil space are Bombardier Aerospace and Embraer S.A.

In the past couple decades the aerospace industry has seen a high amount of consolidation. Cessna, Rockwell International, McDonald Douglas, and Sikorsky (helicopters) are a few names that were absorbed by the remaining companies. Perhaps the best narrative to illustrate this trend is Orbital Sciences Corporation, founded in Virginia in 1982. For 32 years it operated as a single entity, until 2014 it merged with Alliant Techsystems to form Orbital ATK, Inc. In 2017, Northrop Grumman announced its plans to acquire Orbital ATK for $9.2 billion (FY2017) [7], which was completed in 2018, into a new division called Northrop Grumman Innovation Systems. In four years, Orbital Sciences underwent a merger and an acquisition, and is now no more. In fact, Northrop Grumman has undergone nine such acquisitions in the last 25 years, including Westinghouse Electronics and Scaled Composites. In 2017, the largest takeover came from United Technologies Corporation acquiring Rockwell Collins for $30 billion (FY2017) [8].

While the aerospace industry is not the focus of this thesis, design risk is. The consolidation of the industry is emblematic of the underlying nature of the risk in aerospace design

and development. Put simply, larger companies are more stable, diversified, and efficient (theoretically). They can absorb the enormous risk to innovate. A smaller company with few offerings cannot ebb and flow with the market as well as a larger company with several offerings. This approach has been championed by Boeing, who strives to have a foot in both the military and civil markets to balance its portfolio.

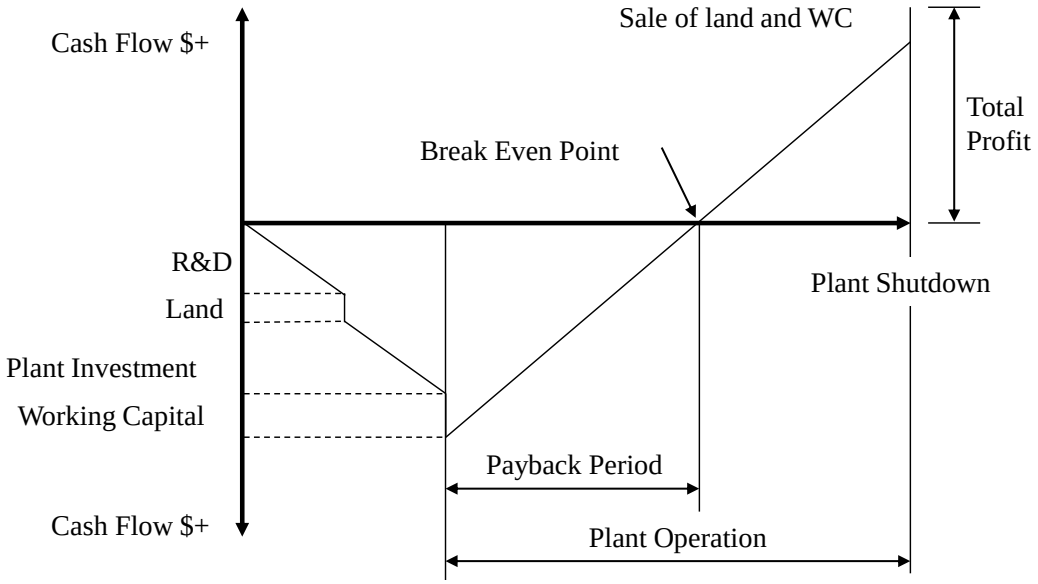

Figure 2: Notional Cash Flow Diagram of an Aircraft Development Program [9]

Figure 2 represents the notional cumulative cash flow of an aircraft design and manufacturing company. The process starts with research and development. This stage represents the first sunk cost to the company. Once this stage has completed, property, plant, and equipment (PP&E) must be purchased to begin the manufacturing process. Assuming that the design is producible and the manufacturing process progresses, deliveries begin which bring revenue. At this point the cumulative cash flow becomes less negative, though capital is still required to produce the aircraft. Hopefully, the aircraft sells enough units for the company to break even. At this point, the company has made no profit: it has simply recouped the initial investment and the cost to produce the sold vehicles. Because this process can take on the order of tens of years, the time value of money must also be incorporated for the break even analysis for aircraft. If the aircraft continues to be produced and sold, the

company now produces a profit. When the aircraft is retired, the land and plant can either be sold or re-purposed, adding to the profitability of the aircraft or decreasing the cost of the next production line.

There are two main takeaways from this diagram: one, that companies are required to invest a large amount of capital up front; and two, when this investment is committed, there is no guarantee of profit. As demonstrated by the diagram, aircraft companies spend most of the life of the aircraft in the negative cash flow regime [10]. The payback period is typically ten years for commercial aviation [11]. Figure 2 suggests a financial barrier to innovation: the additional cost to research and develop technology in tandem with the cost of retooling and re-machining the production process must be balanced by an increase in revenue from aircraft sales. Larger upfront investments result in larger risks, with potential larger rewards. This is where the phrase that states technology must "buy its way" onto the aircraft comes from: if the technology does not increase profitability enough to compensate the increased risk, it will not be included in the design.

Some aircraft designs have an extremely long tenure. The Boeing 747 made its first flight in 1969, which was also the year man first went to the moon. Versions of the aircraft are still in production today (as of 2019)! The most recent version, the Boeing 747-8, was first delivered in 2011, 42 years after the first version. For a product with such a long life cycle, the years spent during the investment period may seem minimal, though not every aircraft is as successful as the 747. Hopefully each design that reaches production will still be viable over 40 years later.

Observation

The immensity of the upfront capital, payback period, and potential revenue longevity characterize aircraft development programs as high-risk high-reward endeavors.

Figure 2 illustrates the cumulative cash flow for a new commercial aircraft development program. Figure 3 illustrates the comparison between different types of develop-

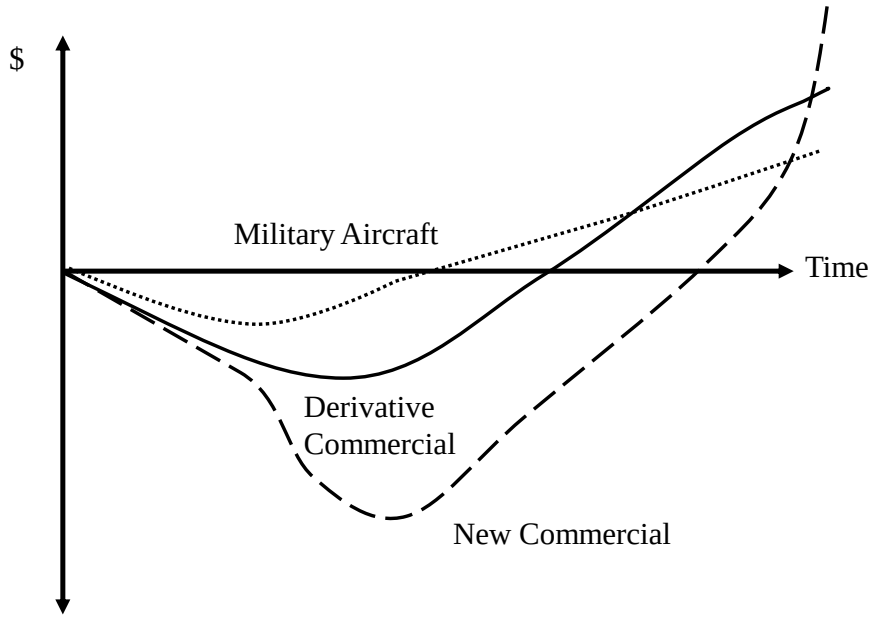

Figure 3: Normalized Cash Flow for Military, Commercial Derivative, and New Commercial Development Programs [9]

ment programs: military, derivative commercial, and new commercial. The most important takeaway is that the new commercial program is the most risky, with the highest upfront investment, and the most rewarding, with the highest profits.

There are other options, however. Military aircraft typically do not carry as much upfront cost due to the presence of a sponsoring entity, such as a government agency. A derivative commercial program relies heavily on the previous design iteration, utilizing R&D, property, plant, and equipment used beforehand. There are also less costs in training and tooling. To decrease risk even further, an aircraft manufacturer could keep the same design but "re-engine" the aircraft; that is, implement newer, more efficient engine designs to improve aircraft performance. In this way, civil aircraft developers have many options: they could create a new design, modify an existing, replace the engines, or neglect the pursuit altogether.

Observation
New commercial programs have the highest risk and highest potential reward.

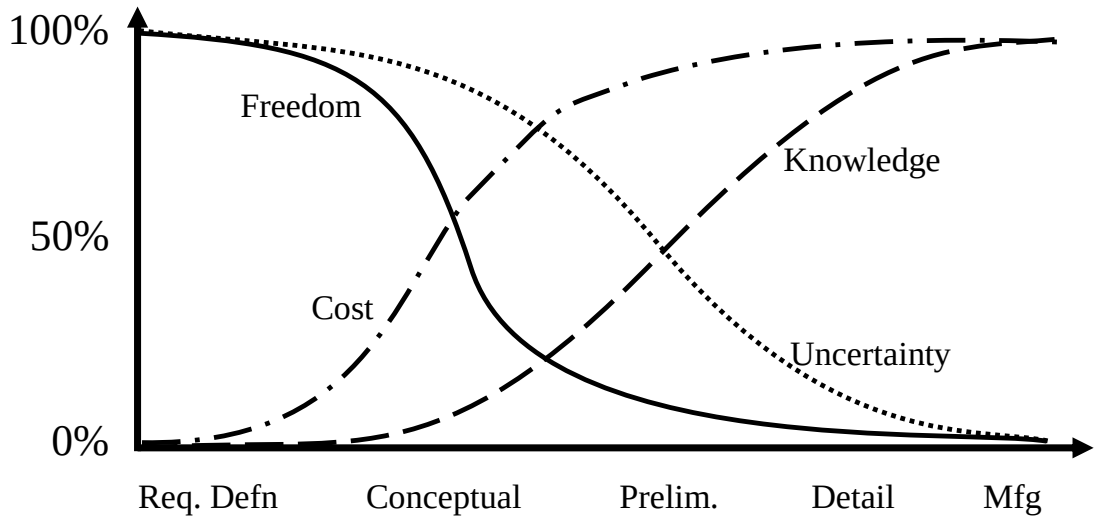

Figure 4: Design Process Paradigm Shift [13]

1.3 Design Freedom and Uncertainty in the Conceptual Design Phase

We will now investigate further how cost and uncertainty vary during the development program life cycle. Though the costs of an aircraft are expensed over the entire cycle, the costs are *committed* (or determined) in advance. This trend is illustrated in Figure 4 [12, 13].

Figure 4 illustrates four different curves: cost committed (-.-), design knowledge (- -), design uncertainty (.), and design freedom (-). The x-axis the design process, beginning with requirements definition and ending with production. The y-axis is a percent level, similar to a cumulative distribution function, for each of the curves.

There are two pairs of curves shown in Figure 4 that act as opposing forces. The first pair is the freedom and cost curves and the second pair is the knowledge and uncertainty curves. As one curve in each of the pairs increases, the corresponding curve decreases.

Design freedom represents the flexibility remaining in the design itself. It reflects the number of characteristics yet to be determined or that can be changed. It drops steeply during the conceptual design phase. This is because major limiting decisions about the design are made while it is still a concept. Similarly, the cost committed steeply increases during

the conceptual design phase: nearly 50% of the cost of the entire program is committed and 50% of the design freedom is lost the during conceptual design phase [5]. Clearly, as decisions about the design are formed, their associated costs are committed.

The design knowledge represents the level of measurement of the design. As demonstrated by the curve, not a lot is known until it can be built and tested during the preliminary and detailed design stages. According to Raymer, this is where the "real numbers" are learned. Lastly is the uncertainty curve, which runs contrary to the design knowledge curve. The uncertainty is high until the design knowledge increases.

This chart is known as the "Design Process Paradigm Shift": it illustrates the need to shift the freedom and cost curves to the right and shift the knowledge and uncertainty curves to the left. As it stands, the most significant decisions are made during the conceptual design phase; importantly, this is also the design phase where the uncertainty is the highest. These trends were first discussed at the 1996 Strategic Planning Workshop hosted by the National Science Foundation [13]. Since then, the design process has been the subject of intense effort to increase the knowledge of the proposed design before the costs are committed and freedom is lost. This thesis is in tandem with that effort.

Observation

The most consequential design decisions occur during the conceptual design phase; further, these decision are made when design knowledge is low. Therefore, the most significant improvement to the aircraft development program decision-making process could be made by conducting a better informed conceptual design phase.

The conceptual design phase can either be improved by shifting design freedom toward later design stages or shifting design uncertainty curve toward earlier design stages, better decisions can be made. Hence, if an effort made to address the level of risk in an aircraft design process, the conceptual design phase would be center focus. But, before we formalize our research objective, we should answer two questions: first, what is the source of the

uncertainty in the conceptual design phase; and second, how does the conceptual design phase affect the degrees of freedom of the design itself.

1.3.1 Design Uncertainty

As aforementioned in Section 1.1.2, the conceptual design phase is completed using low-fidelity models. This is largely because the combinatorial design space is prohibitively immense. Therefore, we want to explore the space quickly but accurately. Remember: any dimensions that are collapsed ("doors that are closed") during the conceptual design phase cannot be re-opened. Well, if we want to reserve the design freedom as much as possible, why not just use high-fidelity analysis?

There are two problems with this approach. First, modern high-fidelity tools are simply not high enough. Raymer states: "Even with [an] extreme level of design sophistication, the actual airplane when flown will never exactly match predictions" [1]. Further, Raymer also states that in the time taken to perform the highest level analysis on a single design, ten good aircraft could have been designed and flown (learning the *real* numbers). So, high-fidelity models would take too long for not good enough results. Second, the market is too dynamic. Requirements, customer preferences, and competition change quickly. Recall Figure 2: the more resources spent on R&D, the greater the pressure to recoup the investment. Better analysis means more time and cost which prolongs the payback period, and gives the competition more time to release their new design.

This brings to light an interesting characteristic of the conceptual design uncertainty: it is self-inflicted. The uncertainty is not a result of natural randomness, or a lack of physical understanding (though, in truth, we do not fully understand all of the physics, but for civil applications this does not constitute the majority of the uncertainty). The majority of the uncertainty comes from our own decision to choose low-fidelity models over physical testing. The uncertainty is an artifact of the nature of the industry rather than physical nature. As a result, it *could* be reduced, but rather, we choose not to reduce it because reducing it

would be too costly.

Observation

Part of the conceptual design uncertainty can be characterized as man-made. It is a result of the complexity of the problem in addition to the expedience required, rather than solely a result of physical complexity.

A second observation can be made here as a corollary: if part of the uncertainty is indeed self-inflicted, then it can be reduced. Later we will discuss the different types, sources, taxonomies, and modeling approaches of uncertainty; but, here, without any rigorous literature review, it simply becomes apparent that if the uncertainty is indeed created by the chosen approach, then it is probable that the uncertainty can be affected by a different approach. This corollary is termed an "observational hypothesis" to distinguish it from the future hypothesis which will be formulated more rigorously.

Observational Hypothesis

If a portion of the uncertainty is man-made, then it can be reduced.

This observation helps motivate an effort to address design uncertainty because it gives hope it can be changed. Thus far we have focused only on the problems and challenges confronting aircraft design, but here we see a glimmer of light. Reducible uncertainty motivates us with the possibility it can be removed. If, on the other hand, the uncertainty did not appear to be removable (e.g. it was a result of complex physics that have yet to be fathomed), then our research efforts should be placed elsewhere, such as fundamental sciences.

1.3.2 Design Freedom

Design freedom can broadly be defined as the number of characteristics that are flexible, meaning they are yet to be determined or can be changed. They are not "frozen." Recall

that freezing crucial aspects of the design is necessary for "serious development" (Raymer) of subsystems because designers know that their work will not be invalidated. "Freezing" is necessary to breakdown the problem into smaller, approachable pieces. Not all pieces can be addressed simultaneously. That is why freezing occurs before serious *subsystem* development: the systems themselves must be solidified.

When design freedom is preserved, the design itself contains the possibilities of what it could become. Rather than a single house, it is more akin to a neighborhood: plenty of closely related possible realizations. Sometimes it can be called a family of alternatives. The "design" actually represents several potential designs: the final one has yet to be determined. Theoretically, this is a beneficial approach; practically, it is a headache. Continually keeping as many options as possible makes visualizing the end result difficult. Hence the tendency to freeze, to concrete a decision so that the path can be set.

In systems analysis, this is called a "one-to-many" relationship. In the housing analogy, for one neighborhood there are many houses. Similarly, one book has many pages, but all the pages belong to one book. This concept is important because each design phase distinction is a one-to-many relationship. For each design point in conceptual design, there are thousands of possibilities in preliminary design. For every design point in preliminary design, there are thousands of design points in detailed design. Again, this is how the design problem is too complex to confront at once: to simultaneously consider all the billions of possibilities is currently impossible (or at the very least impractical).

An example here will help illustrate. An aircraft wing is composed of thousands of parts, including everything from the wing skin material to the nuts and bolts to the fuel tanks. Due to the use of low-fidelity tools in the conceptual design phase, these thousands of components are aggregated into a few, high-level metrics like aspect ratio, span and wing area. Conceptual design simply cannot comprehend the connection between a rib and a spar using only aspect ratio and wing area. It assumes these details will be settled later. As the development program progresses, the higher fidelity analysis introduces more

variables, or more degrees of freedom; however, importantly, these new degrees of freedom always affect the overall performance much less than the prior phase variables. There are thousands of nuts and bolts on an aircraft, but not one of them is considered in conceptual design. One conceptual design variable, such as aspect ratio, will determine performance far more than a single bolt. (It only takes one bolt, however, to violate a constraint and fail a design, which will be discussed later.)

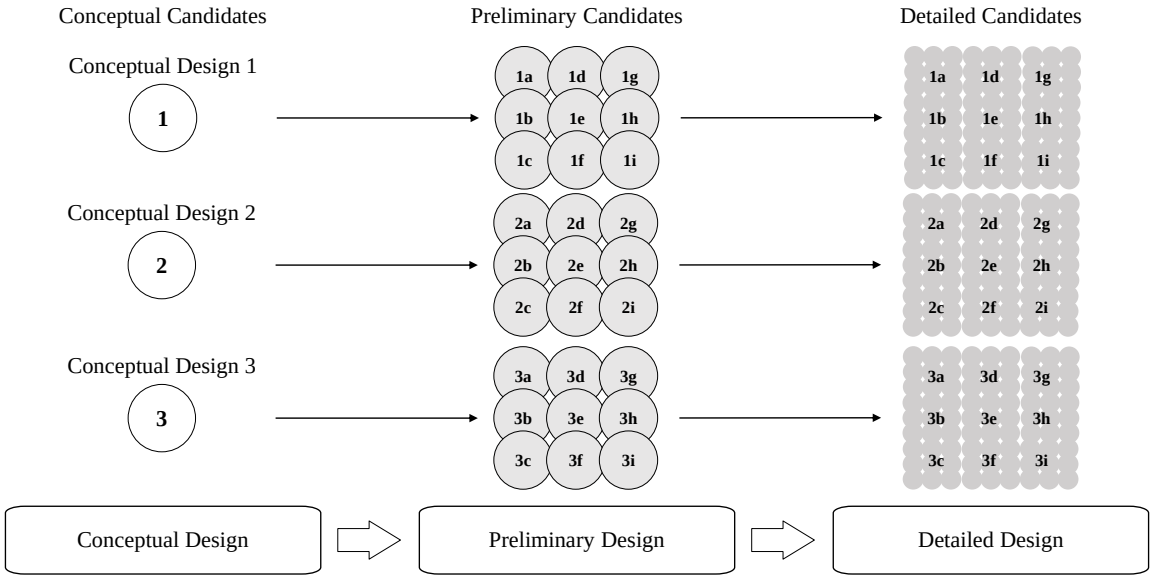

Figure 5: One-to-Many Illustration: One-to-Nine for Conceptual-to-Preliminary and Preliminary-to-Detailed Design Phases

Figure 5 illustrates the increasing dimensionality with each passing design phase. Imagine these three designs have three different aspect ratios (e.g. 9, 10, and 11). The preliminary candidates could be uniquely defined using preliminary variables, such as spar length, rib spacing, rib angles, wing twist, etc. They are introduced because they are required to describe the design on a preliminary level. It is also important to note that the ratio of possible preliminary designs to conceptual designs is dependent on the concept chosen: a concept with a high aspect ratio will form a larger planform area, increasing the required number of ribs in the wing. Each rib will have several variables to describe it (location, thickness, angle, etc.), such that the number of variables in subsequent phases increases. Therefore, in practice, the mapping ratio is not fixed.

Here, only three conceptual designs are depicted, with a constant one-to-nine mapping at the preliminary and detailed design phases. Even with this enormously small example of three conceptual designs, there are 243 detailed candidates. This illustration demonstrates how the design freedom is so significantly decreased during conceptual design: with each degree of freedom that is closed, thousands of potential designs are categorically eliminated.

Observation

Design freedom is dramatically decreased during the conceptual design phase because the phases have a one-to-many relationship; therefore, any decisions made during conceptual design have significant cascading effects on downstream phases.

1.3.3 Techniques to Safeguard Against Uncertainty

In the conceptual design phase, design freedom falls precipitously without much change to the uncertainty. Therefore, when uncertainty is "realized" in the preliminary and detailed phases, not many options remain to respond. Few knobs are left to turn. So, designers have learned to address this issue proactively through margin. *Design margin* is an important concept in this thesis, as is its reactive counterpart *mitigation*. They are two sides to the same coin: both are used to account for design uncertainty while the former occurs proactively (before uncertainty is realized) while the other occurs reactively (after uncertainty has been realized).

The term "realized" is also important. Its use here will be identical to the common usage: to become aware. As demonstrated by Figure 4, design uncertainty exists until the end of the design process. It decreases because we are becoming more aware of the design. Some of its characteristics will be identical to predictions, some will not. That is why, at the end of the design process, the uncertainty goes to zero. Once it is finished, the design is fully known. All the uncertainty has been realized, and therefore it has been expunged.

Table 1: Various Types of Margin

Margin Type	Description	Uncertainty Sources	Examples
Requirements	Excess constraints	Constraint values	Range
Design	Excess dimensions	Design characteristics	Empty weight
Operational	Excess resources	Flight conditions	Fuel

Design Margin

Margin has an old history in engineering [14]. Generally, margin is a small gap or difference. Examples include a piece of paper with one-inch margins or winning by a narrow margin of victory. More specifically it means excess: the exceeded amount required to achieve an objective. The margin on the side of a paper is not used; therefore, it is termed "margin." It is extra. It provides a cushion should more space be needed. There is an additional definition in the Oxford English Dictionary stating "Deposit an amount of money with a broker as *security* for an account or transaction" [15] (emphasis added). Margin can be considered as security: a little extra something (space on a paper, money in an account, range for an aircraft) to be rather safe than sorry.

In engineering, margin is added to create excess. The excess can be placed in three general categories: requirements, design, and operational.

Table 1 describes the different types of margin. For example, the requirements for an aircraft might dictate a range of 2,000 nautical miles. To account for unforeseen uncertainty, the designers might instead design the aircraft for 2,200 nautical miles resulting in a 200 nautical miles margin, or a 10% margin. Then, if the aircraft has more drag than expected and only flies a range of 2,050 nautical miles, then it still satisfies the original range constraint. Similarly, for design margin, the expected take-off gross weight might be predicted to be 600,000 pounds; but, due to experience, designers may know that wings and engines tend to "end up" overweight. Therefore, they scale everything up by 5% to a expected take-off gross weight of 630,000 pounds, or 30,000 pounds of margin. This is an

example of design margin: the dimensions were sized to handle a heavier aircraft. Military requirements provide the epitome of operational margin. MIL-PRF-7700F, for example, requires that 5% fuel extra is carried during missions [16]. Should the fighter need to land at a different base, excess fuel is available to acquiesce.

You may wonder: why 5%? It seems this value should change for the vast amount of missions that the military performs. Typically, margin values are "rules of thumb" from expert judgment or historical data [17, 18, 19, 20]. Further, the industry standard for a metallic aircraft structure safety factor is 1.5 [21]. The roundness of these numbers exemplify the lack of mathematical rigor in their derivation.

There are two key aspects of margin that are significant for our purposes. First, margin is considered proactive because it takes place during aircraft sizing. The design will be scaled to match the range margin or weight margin or fuel margin. Further, because margin is considered during sizing, the entire aircraft is affected. A longer range will scale the wings, the engines, the fuel tanks, and everything else. As a result, the three different types of margin are only different vantage points on the same focal point. Range margin will have an extremely similar effect as fuel weight available margin. Consequently, the different types are only discussed as a matter of discipline or organization; practically, they affect the final design similarly. The types will not be distinguished throughout this work, but have been included as a helpful tool to introduce the concept of margin.

The second key aspect to margin is that it is absolutely ignorant of uncertainty. Because the entire design is scaled, a whole variety of uncertainty is protected against. A cushion in maximum range guards against greater fuel consumption, smaller fuel tanks, and greater drag all at once. The margin simply does not care. This is margin's greatest strength and weakness. The benefit is that no traceability analysis of uncertainty needs to occur: all is protected to an extent. There is no localized protection, only global scaling. It also cannot be undone - once the size is determined, it cannot be made smaller or lighter. Finally, margin decreases performance: a heavier aircraft requires bigger engines that produce larger

thrust. Higher thrust results in higher fuel consumption which increases operating cost for the customer. Essentially this makes margin a gamble.

To summarize, margin affects the entire design by irreversibly increasing size, which increases cost and decreases performance. But, the benefit is an increase in probability that the design will meet all performance requirements and a decrease in probably that the design will need to be re-designed downstream. This re-design has different levels from small design changes to re-sizing the design altogether. This leads us to the reactive response to uncertainty, termed design mitigation in this thesis.

Design Mitigation

Calling on the Oxford English Dictionary again, mitigation is defined as: "the action of reducing the severity, seriousness, or painfulness of something." Here, mitigation will be reducing the painfulness of constraint violations. Specifically, mitigation is a type of action or design change taken to satisfy a previously violated constraint caused by a negative uncertainty realization.

Uncertainty is realized via a newly available test or analysis. It is new, not because of technology, but because the design has matured to a testable stage. The wing, for example, can only undergo wind tunnel testing when an outer-mold line has been designed and built. The wind tunnel test will remove uncertainty with knowledge gleaned from the results. The test may reveal that the drag is much higher than previously predicted. This would be a negative uncertainty realization. With the new drag numbers, the design team assesses a new range calculation which now, with the new data, falls short of the range requirement. This would be a constraint violation. However, if the aircraft has already been sized and the excess range or fuel capacity is insufficient to satisfy the constraint, then the design has failed a requirement. At this point, the design is called *non-compliant* (whereas if the realized uncertainty did not cause a violation in any constraints it would called *compliant*). Compliant means a design satisfies all constraints. As-is, the design does not comply with

all the performance constraints, and therefore does not satisfy the customer requirements.

Something must be done. The design team now scrambles to adjust the design to somehow satisfy the range constraint. Is there a new technology that can be applied? Is there a new material that is lighter or more aerodynamic?

Previous authors in this space have referred to these changes as recourse [22] and mitigation actions [23]. These terms seek to capture the remedial aspect of the design process, where a set of corrective actions are taken in response to an unpredicted event. The NASA Systems Engineering Handbook requires metrics that track feasibility, termed Technical Performance Measures, are monitored and bounded for effectiveness [24]. The key point here is that a change is made (recourse, action, etc.) in response to an adjusted performance metric caused by new information.

This leads us to the two key aspects of mitigation: first, that it is reactive because it occurs after uncertainty has been realized; and second, that it is a localized change tailored to the specific constraint violation. Unfortunately there is no guarantee a negative uncertainty realization can be mitigated.

If the team cannot manipulate the design to satisfy the range constraint, the wing may be need to be re-designed or the program may be canceled. Redesign means going backwards. The frozen characteristics of the design are changed to satisfy the constraint; however, the other disciplines must be notified of the change. This change may invalidate their progress requiring everyone to reset. If this is too costly, it may be best to just cut the losses and cancel the program.

If a solution is found, the design is now called *recovered*: negative uncertainty was realized, resulted in a constraint violation, but was mitigated by a design change (mitigation action). The design process may not progress as if the design was compliant. One last term that is important to introduce is *reliability*. Reliability is the probability that the design will either be compliant or recovered. It is the probability that the design will continue forward towards production.

Unfortunately mitigation can be expensive as well [9]. The cost of changing the design increases exponentially in the preliminary and detailed phases. Recall that each of these phases as its own set of variables; therefore, a "change" constitutes a deviation from a previously frozen value. It can also mean production of the same components with small changes. This is also called re-design or re-work.

Though not extensively detailed, mitigation is a ubiquitous part of any aircraft design process. The Boeing Dreamliner, for example, required mitigation actions. The Seattle Times reported: "The first 40 out of the Everett factory required massive and repeated rework, and the next 10 to 20 also need modifications because of design changes after flight testing" [25]. Here, the flight testing produced information about the Dreamliner that was previously unknown (or was uncertain). Mitigation was applied after the uncertainty was realized.

Unfortunately margin and mitigation are not categorically more or less expensive than each other. Costing data is not readily available for a given mitigation action, nor detailed data regarding the frequency sum of actions taken. As a result, cost is not often regarded in uncertainty quantification.

Mr. Sutter Does the Twist

The most well-documented mitigation action is regarding the Boeing 747 Jumbo Jet. Joe Sutter was the lead designer of the 747, and he details his adventures in his autobiography [26]. Unfortunately, there was a time when the 747 was non-compliant: at the termination of aerodynamics testing, the structures testing began to show the outboard wing was carrying a larger load than predicted. Sutter recalls: "Because of the accelerated pace of development, this realization came quite late in the design process... A new wing simply wasn't an option; we would have to fix what was wrong with the current wing...". Sutter and his team proposed and implemented the idea of only twisting the outboard wing while leaving the inboard wing intact, which completely solved the loads problem but was "one

tenth as difficult and costly as twisting the entire wing." The press designated this savior as the "Sutter Twist."

This is a textbook example of mitigation. The prediction from conceptual design of the loads on the outboard wing carried uncertainty. Negative uncertainty was realized only after the wing was sized and tested aerodynamically. When the internal structures testing began, new information showed a violation in a loading constraint (negative uncertainty realization results in a violated constraint). To his manager, re-sizing the wing seemed to be the only option. Therefore, the task was for Sutter and his team to fix the current design in any way they could without moving backward in the design process. After some delay, they were able to salvage, or recover, the wing design at one-tenth the difficult and cost.

Reliability Assessment Overview

While in the midst of introducing our problem, we have sufficient knowledge to map a general flowchart of a design process under uncertainty. The sequential nature of the design process is the foundational element: it allows the entire program to be broken down into solvable pieces but requires a forward progression. Uncertainty is realized as the design progresses through the design process. Mitigation is only applied to non-compliant designs. If a solution is found, the non-compliant become recovered, but if a solution cannot be found, the design is considered a failure.

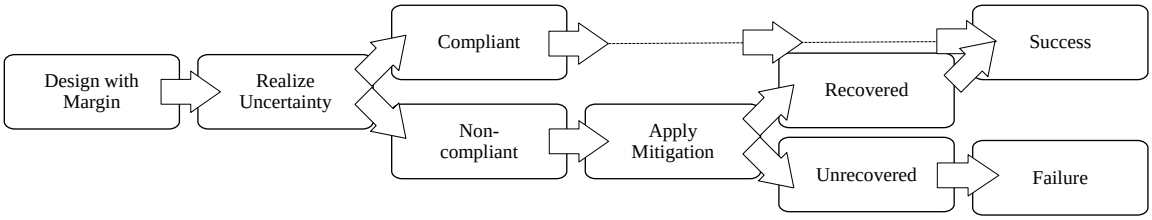

Figure 6: Introductory Diagram for Reliability Assessment using Margin and Mitigation under Uncertainty

Because a design is uncertain, it may eventually take different shapes; or, in another way, it has multiple possible future states. Given bounds, all future states could be tested

to paint a picture of expected overall reliability. If all of these future states or scenarios are equally likely, then a single design could be described as having a level of reliability equal to the proportion of the success states to the failure states. Now we are able to define *design reliability*.

$$Reliability = \frac{Number\ of\ compliant\ scenarios + Number\ of\ recovered\ scenarios}{Total\ number\ of\ scenarios} \tag{1}$$

Reliability is expected to be inversely related to performance. If both margin and mitigation are effective, we expect reliability to increase and performance to suffer. Because the specific future state that will come to reality (be realized) is unknown, reliability is ultimately a probability.

Unfavorable and Undefined Uncertainty Realizations

The uncertainty realizations are important for consideration insofar as they result in constraint violations. Because there are multiple levels of fidelity throughout the design process, not all constraints are considered at once. Hence, some constraint values will not even be estimated during conceptual design. Because these variables are not even defined, they are difficult to protect against.

We would like to distinguish between these two types of uncertainty realizations. The former is characterized by an estimate value with an eventual *error*. The latter is characterized by a complete ignorance of the value with an eventual *reveal*.

In the range constraint example, the range was violated due to an increase in drag. This would be an unfavorable uncertainty realization because the drag was underestimated. The error is the difference between the old estimate and the new estimate.

In the Sutter Twist example, it seems the design violated a wing-level constraint: he states that the outboard wing was carrying too much load. This implies a violation of a

tip deflection constraint or perhaps a root bending moment constraint. In other words, the wing is deformed too much by aerodynamic loads. Conceptual design tools (like the ones used in this thesis) have no awareness of wing tip deflection or root bending moment. They are not defined variables. Therefore, when the value is revealed through higher-fidelity analysis, the value is introduced rather than updated. There is not an error because there was no initial prediction.

In terms of reliability and mitigation, we are only concerned with constraint violations. There are two key difference between unfavorable and undefined uncertainty realizations. The first is that margin cannot directly safeguard against undefined uncertainty realizations. Margin can must be quantified during conceptual design in order to affect sizing, but this design phase does not define downstream constraints. The second key difference, which is a corollary to the first, is that because the constraint is undefined, it is *not* a result of incorrect assumptions. Many of the downstream complexity is encapsulated in the form of efficiency factors. The range constraint could have been violated due to a lower Oswald efficiency factor or span efficiency. Margin protects against these error if the physics turns out to be different than expected, but there is no assumption or efficiency factor for tip deflection.

In summary, margin cannot guard against undefined uncertainty realizations because they are not caused by erroneous assumptions in the conceptual design phase. Or, to be put another way, excess size does not cushion against all constraints.

Observation

Because downstream constraints exist that are undefined at the conceptual design level, some constraints cannot be safeguarded against via margin.

1.4 Recent Examples

Thus far we have gained a foundation for the aircraft design process and its challenges. We will end with a brief description of some recent examples that could have benefited from increased reliability. These examples will demonstrate that design uncertainty is still an obstacle today, even though the paradigm shift effort to shift uncertainty from Figure 4 was released more than 20 years ago.

1.4.1 The Boeing 787 Dreamliner

Following the deregulation of the air travel industry in 1977, airlines and passengers alike flooded the market. The increase in passengers from about 240 million to 640 million from the late 1970's to the late 1990's attracted aircraft manufacturers as well. At the end of this period Boeing was in the midst of losing market share to Airbus. To respond to Airbus' new dominance, in 2003, Boeing began developing a new aircraft: the 787 Dreamliner. This aircraft was design with efficiency in mind. The primary structure of the Dreamliner was designed to be 50% composite materials rather than the usual aluminum industry standard. This would allow the aircraft to be lighter and therefore more fuel efficient as well as increase range [27]. The composite materials should also decrease maintenance cost [28]. The idea was that this increased range and fuel efficiency would allow airlines to fly direct between any two cities, increasing the operational flexibility of the aircraft [29]. A comparison between the Dreamliner and the Airbus A380-800 is included in the Table 2. At the same speed and longer range, the Dreamliner weighs less than half of the A380. Though the passenger capacity was much lower than other aircraft of similar range, the cost-per-seat mile was expected to be 10% lower than any other aircraft [29].

By the end of 2008, Boeing had received a total of 895 orders from 50 different airlines for the Dreamliner, making it the fastest selling plane in aviation history. However, by this time, Boeing had begun announcing a series of delays, which would end up delay-

Table 2: Comparison Between Boeing 787 Dreamliner and Airbus A380-800 [29]

Airline Family	Max Range (nmi)	Max Capacity (passengers)	Empty Weight (lbs)	Cruise Mach
Boeing 787-9	8,500	330	254,000	0.85
Airbus 380-800	8,200	555	610,000	0.85

ing the release of the Dreamliner by more than two years. The innovative design of the Dreamliner increased the expected performance of the aircraft but this improvement came with a production challenge. For the Dreamliner, the supply chain specifically proved to be an immense challenge largely caused by the composite material component manufacturing process. These delays frustrated customers and postponed revenue for Boeing; however, the production cost itself of the aircraft was much higher than anticipated as well. The production cost of the aircraft was finally lower than the sale price of the aircraft in 2016 [30]. Boeing estimated that the Dreamliner will break even on *manufacturing costs only* 10 years into production, or in 2021 [25]. Due to the sunk costs of almost $33 billion (FY2015), some analysts believe that Boeing will never make a profit on the Dreamliner program [31].

The Boeing 787 Dreamliner case illustrates the risk in dramatically advancing the state-of-the-art. Though the design may be technically superior to the other aircraft on the market, Boeing may never make a cent of profit on the aircraft program. This recent case inhibits the ability and desire of engineering design companies to deviate from the norm. The result is plenty of derivative aircraft programs and few new aircraft programs.

1.4.2 The Lockheed Martin F-35 Lightning II

Then there is the most expensive military weapons system program in history to consider. The roots of the program started all the way back to 1992 with the Joint Strike Fighter program. Two contracts were awarded to build prototypes in 1996: one to Boeing, one to Lockheed Martin. In 2001 Lockheed Martin won the contract for the X-35 concept

with the proposition of commonality. There were to be three variants of the concept: one each for the Air Force, Marine Corps, and Navy (designated F-35A, F-35B, and F-335C, respectively). The initial commonality estimates were between 70%-90% among all three versions, but eventually fell to 20% [32]. In 2009, the Pentagon estimated that the program was two years behind schedule. In 2010, over half a billion dollars was withheld from Lockheed Martin due to the schedule delay, with Major General David R. Heinz being removed from command of the program as some estimates of the price tag had increased over 50%. By 2014, the program was "$163 billion over budget and seven years behind schedule" [33].

At the time of this writing, the F-35 is still announcing delays in some of its variants. Senator John McCain, chairman of the Armed Services Committee, recently tweeted: "after years of delays & massive cost overruns, another reminder that the true cost of the F-35 program is still TBD" [34].

Though the Boeing 787 Dreamliner and the Lockheed Martin F-35 Lightning II share a similar story line of cost overruns and schedule delays, the worries are different for the two companies. For the F-35, the sunk cost was absorbed largely by the United States government and its allies. For the Dreamliner, Boeing shouldered the brunt of the risk. In some respects, then, the risk to Lockheed Martin was significantly diminished compared to the risk that faced Boeing. As previously stated, Boeing will likely not make much profit if any off of the Dreamliner, but Lockheed Martin is guaranteed by contract to sell the F-35 to the US government. However, the debacle of the design and development of the F-35 will leave a burden of caution for future defense procurement contracts. In the wake of the vast increase in price for the F-35, future designs for the US government will most likely increase restrictions on cost creep and schedule delays. Therefore, future design programs, both commercial and military, are motivated to partake in the "paradigm shift."

The Boeing 787 and the Lockheed Martin F-35 highlight the need for an improved aircraft design process. These companies are two of the largest and most prolific aircraft

designers in the world, yet at the time of this writing, are still suffering challenges with these two designs. From the recency (and concurrency) of these issues, we can conclude that aircraft design is *still* a major risk for aircraft companies. This leads to the motivational problem for this thesis:

Motivational Problem

The recency of these examples demonstrate that the level of risk associated with aircraft design remains a significant challenge.

Therefore, the eventual goal of this thesis should be a contribution addressing this problem. Ideally, advances can be made to the conceptual design process to decrease the associated risk to allow for better performing and more reliable aircraft.

1.5 Summary and Thesis Framework

1.5.1 Definitions Summary

This chapter introduced aircraft design and its challenges. A number of frequent terms were defined and are summarized here:

Summary of Defined Terms

- Uncertainty Realization: a possible future state of a design
- Unfavorable Uncertainty Realization: an error between the predicted value and found value realized by new analysis or testing that could result in a constraint violation
- Undefined Uncertainty Realization: a constraint value (hitherto unknown) revealed by new analysis or testing
- Margin: excess performance considered in aircraft sizing included as a safeguard against undefined uncertainty

- Mitigation: local design change performed in response to a specified constraint violation
- Compliant: satisfaction of all constraints; no mitigation required
- Non-compliant: negative uncertainty realization resulting in a violation of one or more constraints
- Recovered: a previously non-compliant design that satisfies all constraints due to a design change (mitigation action)
- Reliability: the probability that a design will satisfy all requirements

This chapter has introduced content pertinent to this thesis as well as a motivational problem supported by high-profile recent examples. Companies that design and manufacture aircraft face an overwhelming obstacle when it comes to producing both innovative and reliable designs. The sunk costs are steep early into the design process, with break even points temporally distant from the initial investment for research and development. The decisions made at this point are the most significant of any decisions during the entire aircraft program; yet, this phase is plagued with uncertainty. Due to the complexity design, aspects of the aircraft are fixed early in the design process, which can only be changed later at great cost. This introduction leads to the Research Objective:

Research Objective

The objective of this to discover, investigate, and implement techniques that decrease the risk associated with the aircraft design process.

1.5.2 Thesis Framework

The first two chapters of this thesis work to introduce, motivate, and provide the background required to make a substantial contribution to the state-of-the-art. Chapter 3 will review current aircraft design reliability based methods to determine what capability gaps

(if any) exist. This will lead to three opportunities for improvement, which are described in Chapter 4. A more detailed literature review is also provided in this chapter. Filling the gaps will require the development and testing of new methods which will completed in Chapters 5, 6, and 7. A entirely new framework is developed integrating the new steps with the most-applicable benchmark method. A layout and full implementation of this new framework, later termed RABiDA, is given in Chapter 8. A summary of the research questions, experiments, results, and conclusions is given in Chapter 9.

CHAPTER 2
BACKGROUND

Before the motivational question can be addressed, there are several terms and definitions that need to be settled. The first area to cover is the early stages of the design process. This is highlighted due to the collapse of design freedom under high uncertainty. The next area is to distinguish the difference between probabilistic design and deterministic design, as well as various probabilistic methods. Next is to cover ways to safeguard against uncertainty supported by historical examples. This background will form the guidelines for the literature review in Chapter 3.

2.1 Early Stages of Design

The initial three stages of the seven-stage process described in Chapter 1 were requirements definition, conceptual design, and preliminary design. The requirements definition is not strictly a part of the design process, so its background will be relatively brief. Then, the background of conceptual and preliminary design will be given to get acquainted with their terms and methods.

2.1.1 Requirements Definition

The requirements are usually defined outside of the design process due to their non-technical origins. They are enumerated using market research or government declarations. Still, they are essential to the process because they form the guidelines for the technical decision-making process. The two noteworthy types of variables introduced by requirements are constraints and objectives. Constraints are behaviors the solution *must* perform whereas objectives define preference. Range is an example of a metric that can be either a constraint or an objective. In one case, a customer may specify that the aircraft must fly at least

2,000 nautical miles. Here, range is a constraint. In another case, a target range may not be specified, but larger ranges are preferred. Here, range is an objective. It distinguishes the "better" designs by encapsulating customer preference.

Requirements can have a larger effect on the success of a program than the engineering process. Consider the Airbus A380. It was designed to carry a lot of people a very long distance. The requirements specified that in the passenger (about 500 people) constraint. However, these requirements turned out to be suboptimal. The A380 gambled on high-capacity, long-range flights utilizing the "hub-and-spoke" network of airports. From 2007 to December 2018 (entire production life at the time of this writing), 234 A380s were produced [37]. Boeing, however decided on a new development program aimed at smaller, fuel-efficient aircraft, betting on an increase in direct flights between smaller airports. The passenger constraint much smaller: about 250 people. From 2011 to 2018, 781 787s have been produced [38]. That is more than three times the sales volume of the A380, and, unfortunately for Airbus, the A380 does not have triple the price of the 787.

In February 2019 Airbus announced that it is stopping A380 production with its final delivery in 2021 [39]. Orders are still coming in for the Dreamliner. This case study shows the impact of requirements. As we saw in Section 1.4, the 787 certainly had plenty of development issues, but the cost is only half of the equation.

2.1.2 Conceptual Design Process and Formulation

There are four sub-stages in the conceptual design phase: analysis of alternatives, constraint analysis, sizing & synthesis, and performance analysis.

Analysis of Alternatives

The output of the requirements definition is a list of behaviors with quantified values. The inputs to conceptual design are mission profile, range, passenger class, among others. The assumption is that regardless of the shape or "look", *any* concept that can satisfy the re-

quirements should be considered. The first step of conceptual design is performing a trade study between these configurations which is called an analysis of alternatives. The alternatives refer to variations in configuration that could possibly perform the given mission.

This step is the focus when evaluating advanced concepts. An advanced concept is anything apart from the standard tube-and-wing aircraft design. Current aircraft do not "look" much different than the de Havilland DH 106 Comet, which was the first jet airliner. Advanced concepts could be pushing the norm with respect to propulsion, aerodynamics, materials, or production processes. Examples include electric engines and using a wing support truss system. Traditional concepts are usually chosen due to the wealth of experimental data and experience on their performance.

Design Point Selection: Energy-based Constraint Analysis

Each concept can be further described using dimensionless parameters. These ratios define the relative characteristics of the design. The thrust-to-weight ratio (TWR) and wing loading ratio (WSR) are the two most common vehicle-level design point parameters. Prescribing a value to TWR constrains the relationship between thrust and weight, but not the individual magnitudes.

$$TWR = \frac{Takeoff \;\; Thrust}{Takeoff \;\; Gross \;\; Weight} \tag{2}$$

Describing the concept like this is useful for energy constraint analysis, as shown in Figure 7. The various segments of the mission profile are decomposed, such as takeoff, landing, and cruise (other examples can include climb, maneuver, and loiter). For energy constraint analysis, the aircraft is assumed a point (no geometric definition) and the forces in precisely parallel or perpendicular directions (thrust and drag are exactly parallel). Clearly these assumptions are simplified, but they give a starting location. Thus, the aircraft starts as a point called a *design point*.

Figure 7 shows the feasible region for a design point. It must have sufficient TWR for

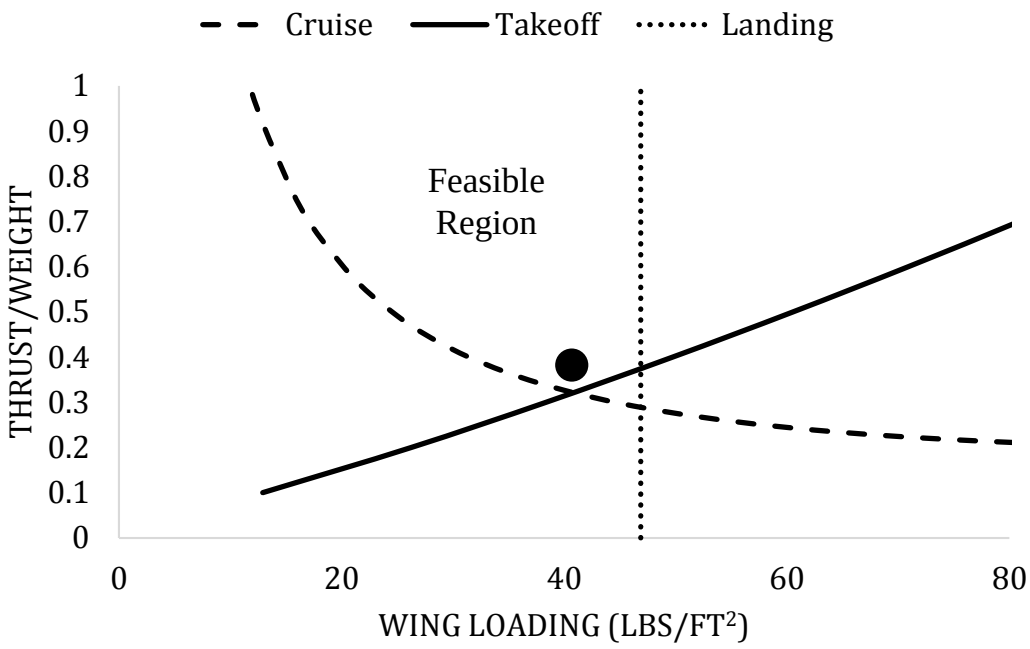

Figure 7: Design Point Selection using Constraint Analysis

cruise and takeoff, and it must have minimal WSR for landing. Again, the design has no size at this stage, so no gross weight or thrust is known, but the ratio between the two can be determined and fixed.

Sizing Analysis

The next step is to give the design a size. Raymer states clearly: "Sizing is the most important calculation in aircraft design - more so than drag, or stress, or even cost (well, maybe not cost)" [1].

The process of sizing is to determine how large (magnitudes) the design point needs to be in order to complete the required mission. Sizing is often accomplished iteratively until the fuel balance (fuel available is equal to fuel required) is complete [40].

First, a takeoff weight is guessed (for this thesis, the terms takeoff weight, takeoff gross weight, and gross weight are all equivalent). The weight components are estimated as fractions of the gross weight. Performing mission analysis will result in a fuel required estimate. If the fuel available is greater than the fuel required, the size is feasible. If not,

the process is repeated for a larger gross weight. If the available fuel is much greater than the fuel required, then the process is repeated for a smaller gross weight.

In order to perform sizing analysis, much more data about the aircraft must be known other than its dimensionless parameters. For example, ample mission data must be available for flight conditions and constraint analysis. Further, some disciplinary data must be known such as the drag polar and propulsion characteristics. These parameters, which are often estimations, have a significant effect on the final size of the vehicle. Typically, this step relies heavily on empirical (historical) data rather than physics-based approaches.

Performance Analysis

Once a size is deemed a candidate for the design point, it is evaluated at every step of the mission profile to evaluate overall performance. Hence, this step is aptly named performance analysis. The analysis is at a slightly greater granularity than sizing. For example, during sizing, the range may be estimated using the Breguet Range equation given in Equation 3:

$$Range = \frac{V}{TSFC} * \frac{C_L}{C_D} * \ln\left(\frac{W_i}{W_f}\right) \tag{3}$$

where V is velocity, TSFC is fuel-specific thrust consumption, C_L is lift coefficient, C_D, W_i is the initial (gross) weight, and W_f is the final (landing) weight. This is a quick way to estimate range using aerodynamic, propulsion, and weight relationships. During performance analysis, however, an engine deck is created. An engine deck is a series of propulsive performance values (thrust, fuel consumption, etc.) at various points in the sky (pressure, density, temperature). This deck is used to calculate the entire fuel consumption of the mission rather than using the Breguet Range equation.

This is an example of a shift in model fidelity. An engine deck is created by a conceptual design engine tool. It is far more rigorous compared to the Breguet Range equation (and far more simple than preliminary design analysis). Because weight is found iteratively, the

range equation is simplified. But now that a weight is specified, deeper analysis can be performed. This small example will be repeated on a larger scale when conceptual design transitions to preliminary design.

Multiple mission profiles can be used for analysis or constraint cases. Examples include flying on a hot day or landing at a high altitude airport. For conventional designs, current conceptual design methodologies integrate sizing & synthesis and performance analysis [41, 42].

2.1.3 Preliminary Design

Conceptual design is concluded when a concept is chosen (analysis of alternatives), the energy constraint analysis is performed (design point selection), the design has converged on a fuel balance (sizing), and it satisfies all mission constraints (performance analysis). These steps can be integrated into an optimized process in order to find the *best* conceptual design. Once the design is frozen, the design point and size are unchangeable. The characteristics prescribed in this phase propagate throughout the rest of the development process. Subsequent to the conceptual phase, the design is given to a series of experts in various fields (propulsion, aerodynamics, and structures).

During the preliminary phase the disciplines cannot be in constant communication with each other; therefore, the characteristics determined in conceptual phase (takeoff weight, takeoff thrust, fuel capacity, lift/drag, etc.) now become agreements, or constraints. For example, the engine is designed to a take-off thrust. If the wing and fuselage weight estimations change drastically, the engine may need to be redesigned because the priori thrust level was insufficient. This is why the accuracy of the assumptions and expectations made during the conceptual design phase is important.

The end of conceptual design is marked by this change: the design moves from a single team to multiple teams. If the propulsion team finds out that the engine will require more fuel than necessary, then the wing may have to be re-designed for great fuel tank capac-

ity. This may render the aerodynamic or structural analysis irrelevant, which requires new analysis and ultimately program delays. This example prompts the need for margin: hopefully, the margin is sufficient to cover any shortcomings the teams may find. This keeps the development process running smoothly [43].

2.2 Modeling, Simulation, and Optimization

The engineering design of complex systems such as aircraft or spacecraft are exceedingly difficult because a single person or small group is insufficient to fully understand all the disciplinary knowledge required for design [44]. Subject matter experts, who spent careers gaining experience, held the decision-making authority, but this is shifting. Decisions made by lauded subject matter experts can now be described using empirical relationships or physics-based analysis. Computers can be the integrators we never were; they can hold terabytes of data and perform billions of calculations without being paid overtime. As the advance in computing power and physics-based modeling continues, larger chunks of the design process are integrated into single formulation rather than a series of independent processes. To borrow a metaphor from chemistry, the design process is becoming much more of a compound rather than a mixture; or, to borrow a phrase from antiquity, the whole is greater than the sum of its parts.

The three ingredients required to produce these new computationally-driven insights are models, simulations, and optimization. A model is a mathematical representation of reality. An equation is the simplest form of model. The implied assumption is that the model represents the system under review, which is often not entirely true. Still, models can provide useful insights. A simulation is a specific set of inputs to a model. Where a model is general, a simulation is specific. Optimization is the process of determining which set of inputs to the model result in the most preferred output. In this case, a design would be a simulation, or a set of simulated performance values, and the optimization process would result in the most preferable simulation.

2.2.1 Modeling and Simulation

The simplest example of a model and simulation would be determining the volume of a rectangular cardboard box. From mathematics, we can estimate the volume as the length multiplied by the width multiplied by the height as given in Equation 4 where l, w, and h are length, width, and height, respectively. This is a model because it represents a generic box: no values of l, w, and h have been specified. A number of assumptions have already been made for this model to be developed, namely: the box is a perfect rectangle, the thickness of the cardboard is uniform, and no deformities exist, to name a few.

$$Volume = Length * Width * Height = l * w * h \tag{4}$$

Table 3 shows the results of three simulations. The inputs to the model were varied and the model was executed to produce the output. Between these three scenarios, if maximum volume is preferred, box 3 is the best.

Table 3: Sample Simulations of the Box Volume Model

Simulation	Length (in)	Width (in)	Height (in)	Volume (in^3)
Box 1	10	4	3	120
Box 2	7	7	2	98
Box 3	5	5	5	125

2.2.2 Optimization Formulation

But the model and the simulation do not directly impact decision making. Instead, what if we asked the question: *which values of l, w, and h would yield the largest volume?* We have now entered the field of optimization. Optimization seeks the unique set of inputs that, using the model, yields the most desirable set of outputs. If we wanted to *minimize* material costs (sum of l, w, and h) and *maximize* volume (product of l, w, and h), we would use optimization.

Optimization requires us to define preference. The results are the inputs that are "best." For the box, that could be using the least material, fitting the most onto a truck or cargo aircraft, or carried most easily by hand. We may even add constraints, such as the box may not be greater than six inches high, or must not be twice as long as it is wide. These boundaries restrict which set of l, w, and h are the "best."

We can now formalize a generic optimization formulation as follows:

$$\text{Minimize} : f(x)$$

$$\text{with respect to} : x$$

$$\text{such that} : g_i \leq 0 \; \forall \; g$$

f(x) represents the objective function (volume, in the previous example). The result of this function is the objective, or metric that determines preference. For an airliner, this could be takeoff gross weight, block fuel, or acquisition cost plus operating cost. In standard form, optimization problems are always described as minimization problems; maximization can be performed by minimizing the negative of the objective function. x represents the design variables, or the variables we directly affect. In the box example, the design variables were l, w, and h. Last are the constraints (g), which restrict the combinations of design variables (the box must not be more than twice as long as it is wide). They may reflect physics (deformation) or outside influence (USPS requirements). They are formally described as less than inequalities.

Optimization has proven especially useful in engineering design. For complex vehicles, trail and error in unacceptable. Therefore, computers are used instead. As aforementioned, subject matter experts have been replaced by disciplinary-level computer algorithms which can be integrated into a single environment known as multidisciplinary design analysis (MDA) and multidisciplinary design optimization (MDO) [45, 46, 47]. MDA and MDO gained popularity in the late 1990's [48] along with the increase in popularity and power of

computers.

The standard form for optimization can be applied to our motivational problem; but, it needs to be transformed to apply. First, there is no mention of uncertainty. The box example assumed the result was deterministic (that l, w, and h *always* equal volume). Second, there is no inclusion of margin or mitigation. Last, there is no temporal aspect included in the formulation (no "freezing" of the design space). Therefore, we will need to develop an optimization formulation specific to our motivational problem.

Observation

Standard form optimization is insufficient to cover the complexity of the motivational problem. Uncertainty, margin, and mitigation need to be included as well as the discretization of design variable spaces between design phases.

Note here a new use of the word "design." In optimization, the design variable designation distinguishes the independent (control) variables from the dependent (response). The result of the optimization is a set of values for the design variables that lead to the most preferred outcome. Design is an adjective describing the type of variable rather than a noun. Whenever the phrase "design variable" appears, it is referring to the optimization nomenclature which is completely agnostic to the aircraft nomenclature.

2.2.3 Constraints

Constraints define whether or not a design is feasible. While the same metrics can be used as constraints or objectives (range, fuel, cost, etc.), constraints are distinguished by their binary response. Constraints are either satisfied or violated. A feasible design passes *all* constraints, whereas an infeasible design fails one or more constraints. This is referred to as a constraint satisfaction problem (CSP). They could also be referred to as "hard" constraints. In reality, constraints may have a little bit of leeway. To capture this, a number of "soft" constraint formulations have been developed (e.g. partial constraint satisfaction,

hierarchical constraint satisfaction, and soft constraint relaxation) [49, 50, 51].

The most straightforward approach to capturing all relevant constraints is by level: vehicle (constraints that are enforced on the design as a whole), system (constraints enforced on the main components), and sub-system (or component; constraints enforced within the system). There is some nomenclature redundancy here: some refer to the engine as a "system" while some refer to it as a "sub-system" relative to the aircraft as an entire system. This thesis will try to avoid the confusion by referring to the whole aircraft as the vehicle, systems by specific name (e.g. wing), and the decomposition of system as components. This designation implies the aircraft is a "system-of-systems."

Vehicle Constraints

The vehicle constraints are the most intuitive because they are most similar to the requirements definition. The aircraft must go this far (range) carrying this many people (payload) at this speed (Mach number) at this cost per flight (block fuel). These are typically the contractual constraints on the vehicle; it must perform this way to satisfy the customer or be sell-worthy. There are also a number of performance requirements to operate at airports such as runway length. Other performance requirements can include stall speed, maximum speed, and endurance. As a whole the aircraft must be stable, so constraints are on lateral-direction static stability, dynamic stability, and controllability during stall [52]. Lastly, there can be manufacturing considerations for producibility, cost, and safety.

System Constraints

The system constraints are on the main pieces of the aircraft: engine, wing, fuselage, landing gear, etc. They are typically enforced at the onset of preliminary design when the concept has been frozen such that the disciplinarians can dive into the detailed analysis required for system design. An engine, for example, would have thrust, temperature, and weight constraints. A wing would likewise have a weight constraint, as well as a root

bending moment constraint, induced twist, flutter, buckling, tip deflection, minimum gage, limit-cycle oscillations, and aileron reversal constraints [53, 54, 55]. Clearly the number of constraints grows with each design phase.

These constraints are almost independent of the vehicle constraints because the analysis is almost independent: FLOPS cannot compute buckling or flutter. It has no comprehension of these phenomena. Therefore the likelihood may be high that these constraints will be violated for the generic design of the system: the vehicle was not selected with these constraints in mind. In the face of a constraint violation, a designer must satisfy the constraint *without* violating one of the vehicle level constraints.

Component Constraints

The components make up the system, and each have their own constraints. Considering structures only, there are six basic types of structural loading: tension, compression, shear, bending, torsion, and thermal [1]. Each of these loads has an associated constraint. As an aircraft must perform well over time, additional considerations can include creep, corrosion, and fatigue [53]. Each component in the entire vehicle will have an associated stress. Instead of reporting each one, it is common to only check material failure modes such as maximum shearing stress, maximum distortion energy (von Mises stress), and maximum normal stress [56].

Constraint Aggregation

The number of constraints greatly increases as we move from the vehicle to the component level. Relatively speaking, the vehicle only has a few (10-20) constraints. The components, however, each have a set of constraints, and there could be thousands of components, with each component having an infinite amount of constraints (stress at every point along the continuum) [57]. Evaluating this many constraints is a problem for two reasons. First, keeping track and evaluating all these equations for a single design is unrealistic because

the set of constraint is evaluated for every potential design. Second, this many constraints makes finding the feasible space very difficult. As a result, an approach called constraint aggregation is often employed. As the name implies, multiple constraints are aggregated into a single value. For example, instead of checking every tensile stress value for each component in the wing, we need only check the maximum value. If the maximum value exceeds the constraint, then the entire wing fails, and if it satisfies the constraint, then we know that all of the stresses satisfy the constraint as well.

One difficulty with using constraint aggregates is they do no carry gradients. Therefore, gradient-based optimization approaches cannot be employed to determine the feasible space given an infeasible point. This will be an important note to remember when determining an optimization approach. Still, to get around this, a number of alternative constraint aggregates have been developed such as the KS metric [58, 59, 60] and P-norm metric [61, 62]. These approaches attempt to aggregate the local constraints into a global constraint while still being applicable to gradient-based methods.

Using the local stress constraints has been to provide better results than single global constraint [63, 64] but at much greater computational expense. Furthermore, each design is not guaranteed to have the same number (or size) of components, and therefore the number of constraints can very from case to case [65]. Therefore, constraint aggregates allow designs to be compared to each other in an efficient but imperfect way.

Load Cases

During energy-based constraint analysis, each mission segment (take-off, cruise, landing) formed a constraint on the design point. Similarly, load cases that may be encountered throughout the life of the aircraft are considered as well. Many types of load cases exist such as:

- Airloads: maneuver, gust, control deflection, buffet
- Inertia: acceleration, rotation, vibration, flutter

- Landing: vertical load factor, braking
- Powerplant: thrust, torque, gyroscopic
- Other: bird strike, crash, fuel pressure

The largest load the aircraft is expected to encounter is called the limit (or applied) load, but the aircraft is designed toward a larger load. This difference is referred to as a safety factor, which is usually 1.5. The safety factor value is an industry standard (traditional value). The typical limit load factors for a given type of aircraft is described in Table 4.

Table 4: Typical Limit Load Factors (adapted from [1])

Type of Aircraft	Maximum Load Factor	Minimum Load Factor
General Aviation	2.8	-1.5
Transport	4	-2
Strategic Bomber	3	-1
Fighter	9	-6

Constraints are assessed for each load case; consequently, the number of constraints increases again. For every load case there is a maximum tensile stress, bending moment, tip deflection, etc. Consequently, the number of load cases greatly impacts the number of constraints on the design.

2.2.4 Surrogate Modeling

Models are not always simple. Determining the volume of a rectangular box is simple; determining the maximum stress in a flexible wing is not. In engineering design, optimization usually cannot be performed analytically (such as taking a derivative). Further, high fidelity models can take several hours or even days to execute a single simulation. In this case, how can optimization be performed? One popular solution is to develop a surrogate model which is a simplified set of equations representing the behavior of a more complex model. Generally, a surrogate is a substitute or replacement [15], most commonly heard

when discussing the use of a surrogate mother (a woman carrying a baby that is not biologically hers). The utility is the same with a surrogate model: the physics-based model cannot be used to perform the optimization; therefore, a replacement model must be used.

Developing a surrogate model starts with a design of experiments (DoE). The design refers not to the experiment itself but to the set of experiments (or simulations) that are conducted. A DoE is an thoughtful consideration of which simulations to execute, desiring to gather the maximum amount of information with the least number of model executions. Next, the results from these simulations are used to form a response surface [66]. When first developed in 1951, the authors suggested a second order polynomial as the surrogate model. Even with the approximation of using a simplified model, the ease of estimation and broad application resulted in its proliferation today. There are many assumptions and checks that need to be performed when developing surrogate models, which will be explained in more detail when they are developed as a part of this thesis. The main takeaway here is that approximate models exist which enable optimization to be performed even when the multidisciplinary tools require several hours to finish.

2.2.5 Uncertainty in Aircraft Conceptual Design Optimization

Multidisciplinary design optimization (MDO) is no stranger to reliability methods. In fact, multiple surveys have been completed just on reliability-based methods in MDO [67] and engineering design [68]. Structural engineering is the field that has the most extensive history in reliability-based design. The methods in this thesis have focused on reliability-based design techniques that rely on the realization perspective; that is, scenario analysis is used as a way to forecast potential uncertainty impacts. Other forms of uncertainty quantification exist as well, such as using worst-case or lowest percentile to describe reliability. The realization method has been compared to the worse cast method (or 95th percentiles) and shown that results are better for realization method [69].

Reliability takes on many forms and definitions throughout the literature. A design may

have a single reliability aggregate, or may be a set of component reliability values. This calculation is very computationally expensive. Uncertainty at the subsystem level often requires iterative analysis due to coupling [70]. For multidisciplinary systems each system has an associated uncertainty with an interaction effect on coupled systems. This results in an iterative loop which is quite cumbersome. There are some techniques to increase the computational efficiency of this process, but it remains an issue to MDO [71, 72].

Uncertainty Multidisciplinary Design Optimization

While the baseline methodology provides a basis for uncertainty multidisciplinary design optimization (UMDO), there are a number of approaches in the literature to accomplish this feat. The 90's and early 2000's saw a rise in the use of MDO as computational speed increased and problems became more complex [73, 46]. The computational optimization field flourished, allowing for complicated but integrated environments to find optimal results from a vast design space. Now, with MDO as a solid foundation, the current literature turns to including uncertainty, or probability, into these MDO environments. These formulations vary in number of optimization loops, computational complexity, and types of uncertainty. For references on exhaustive review of these methods, see [67].

2.3 Uncertainty Realization Timeline

We need to ensure we understand the specific nature of the design uncertainty. We will be using the Sutter Twist as the epitome of the uncertainty realization process, and conclude with another example in the F-135 program.

There are three distinctive characteristics of design uncertainty that emerge from the Sutter Twist example:

1. Uncertainty becomes realized over time: the outboard load violation was only realized after loads testing.

2. The design process consists of a single design: Sutter tested one wing design rather than several design realizations.

3. Size cannot be used to respond to uncertainty without redesign: Sutter preferred the twist to redesign because it was easier and cheaper.

2.3.1 1) Uncertainty Becomes Realized Over time

The first aspect of the uncertainty was that it became realized through loads testing. This may seem obvious, but the distinction is critical to modeling uncertainty accurately. The value could have been assumed, estimated, or left vacant, but it was not known. It was only known when it was measured. This is now referred to as *realizing* (or reducing) the uncertainty. Before the test the loads were unknown (or assumed or guessed), but after the testing, all other possibilities of loads are eliminated. Only one possibility is left which is the actual result.

The behavior now shifts from the uncertain to the known. Yesterday we were not 100% sure what the weather will be today, but tomorrow we will have 100% knowledge of what the weather was today. What was uncertain is now known.

This calls for the need to include the temporal aspect of aircraft design. In optimization (and mathematics in general), all variables are considered equal. But in reality, some variables were defined yesterday that cannot be changed today, while others are uncertain that will not be known until tomorrow. This decomposes the optimization formulation into a series of optimizations (even a series of *probabilistic* optimizations). Design is not done in a moment; it is done over time.

This likens uncertainty analysis to the field of scenario analysis, or analyzing possible future states relative to a constant present state. Though many future states may be considered, only one future state will be realized. The possibilities are erased as time progresses until only one state remains. Before the loads testing was performed, the team knew there was some uncertainty in their estimations. To them, the center of pressure could have been

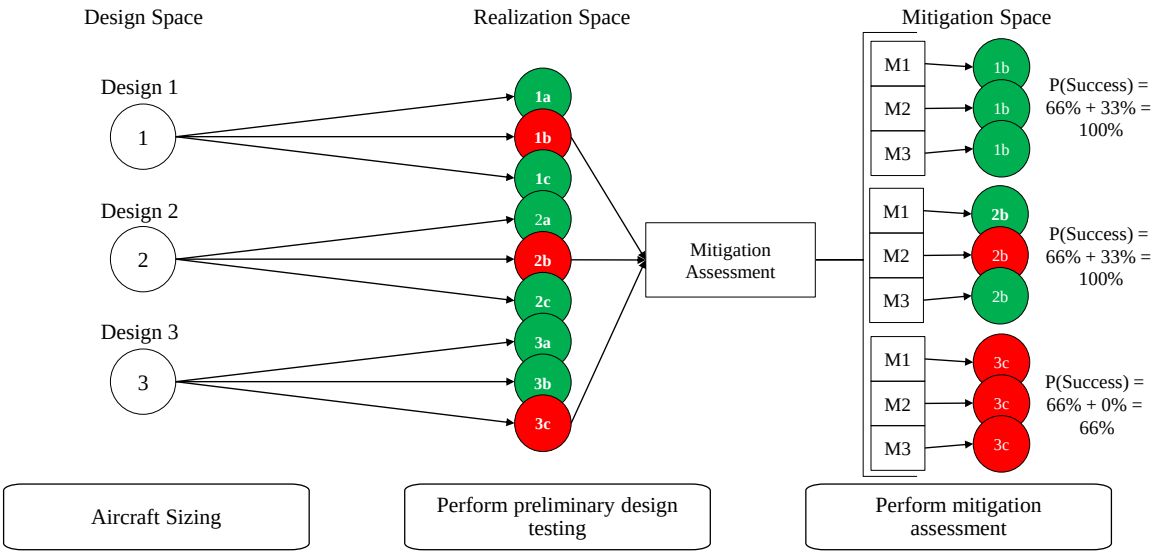

Figure 8: Process for Mitigation Assessment for Conceptual Design Realizations. Green illustrates compliant or recovered realizations.

within some predefined bounds with some predefined probabilities. But, at the conclusion of the testing, only one possibility was realized.

So, this is the way the design process should be modeled as well. Figure 8 represents the way this could be implemented in a computational model. A given design (designated Design 1, 2, or 3) has many potential *realizations*, or possible future states. The future state is determined by the true value of performance, which at this stage in the design process is clouded in uncertainty. Some instances will satisfy all the constraints, while some instances will not. In Sutter's case, the lift distribution shifted outward such that the structure could not maintain the load. The lift distribution could have easily been missed inward instead of outward. This may not have caused a structural concern. In the same way, some realizations may not violate any constraints. These realizations will not require any actions or design changes. The realizations that cause a violation in constraints, however, will needed to be assessed.

In Figure 8, the green realizations are compliant. These points do not undergo mitigation assessment because there are no violated constraints to re-assess. Similarly, the red realizations are the potential future states that will require mitigation. If the realization is

able to be changed to satisfy all constraints, the realization is now called recovered. If no mitigation can bring feasibility to the realization, then it is called failed.

It is important to note that the number of mitigation actions that can recover the realization is irrelevant. The reliability assessment only weighs whether realizations can or cannot satisfy all constraints. This is shown in Figure 8 with realizations 1b and 2b. Even though all three mitigation action strategies (unique actions or unique amount of an action) recover 1b, it has the same recovery as 2b. Sutter may have had three options when performing the wing twist, say decreasing twist (increasing washout) by -0.10°, -0.20°, or -0.30°. How many of these twists satisfy the constraint is irrelevant. The only question to consider is whether *any* mitigation is available to recover the realization. Sutter may have had ten other options he attempted before twisting the wing, but he only needed one option to work.

Capturing the effects of the future states allows the design knowledge to propagate upstream. In other words, it increases information earlier in the process. Capturing the uncertainty and associated responses to recover the realizations (if any) results in an improved reliability assessment.

2.3.2 2) Design Process Consists of a Single Design

The most intuitive example of uncertainty realization is chance (a throw of a die or a game of roulette). For design, this first appeared necessary for mass production and replaceable parts. Then, the goal of uncertainty quantification is to decrease the difference between like parts. This is called *robustness*. The goal of robust design is to minimize the sensitivity to noise or variance [74]. The "goodness" of the design is actually of second importance: the key is to be the *same*. The goal is reproducibility. Robustness became very popular with the rise of industrial manufacturing where millions parts were produced from assembly lines [75]. In this case, however, the design itself is not the main concern as much as successfully producing the part as similarly to the blueprint as possible. If it the part does not fit as designed, it is worthless; therefore, the optimization here is to minimize the number of

these defects as possible.

This is not the case with early design. Sutter only ever tested one wing. He was not concerned about the similarity between wing designs; indeed, there was only one design to test. He references a singular wing rather than a plural set. Therefore, to replicate his reality, we do not necessarily care how *sensitive* the design is to noise as in robustness, only that it satisfies all constraints (such as structural loading). This is called *reliability*. Reliability is not concerned directly with variance. The goal of reliability is to minimize the probability of a system or component violating a performance constraint, or failing, during some specified time period [76, 68]. The resultant distribution of outcomes is only relevant to reliability in the determination of the probability of failure, or conversely the probability of success. The standard deviation or variance of the distribution is not directly weighed. The differences between robust design and reliability-based design are highlighted in Figure 9.

Figure 9: Comparison between Robust Design Optimization (left) and Reliability-based Design Optimization (right)

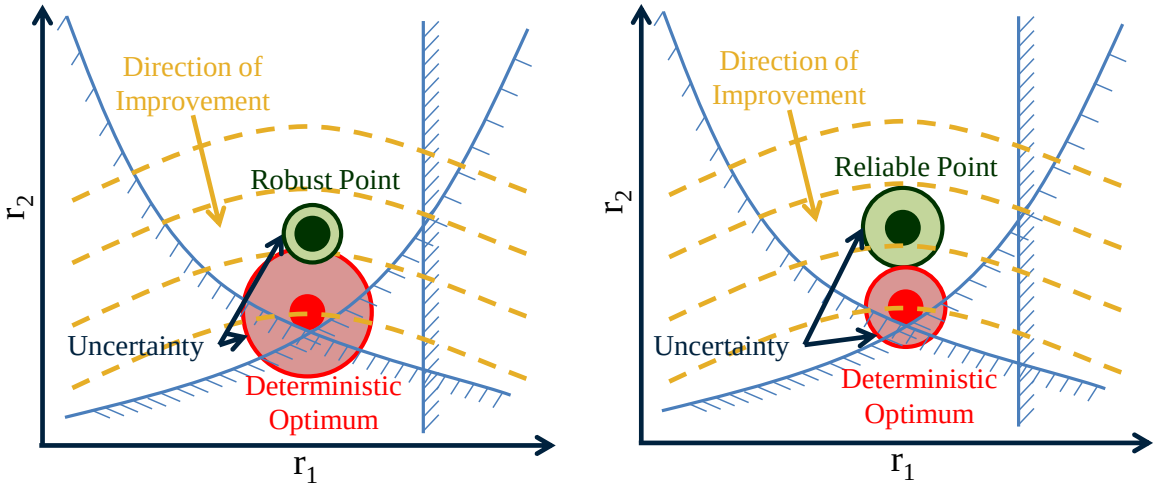

(a) RDO: Minimize sensitivity to noise (area of outer circle)

(b) RBDO: Minimize infeasible possibilities (portion of outer circle in infeasible region)

Pictured on the left in Figure 9 is Robust Design Optimization (RDO) and Reliability-based Design Optimization (RBDO) on the right. Two points are highlighted for illustration: the red point is the deterministic optimum, and the green point a less preferable point from a response perspective (r_1 and r_2 are two sample response parameters). In both cases,

the red point is preferable to the green point with respect to the response variables; however, the red point is not preferable from an uncertainty perspective. For RDO, the variance of the design is very important. The cloud of uncertainty around the red point illustrates the distribution of possible future states of the design. The green point has a much smaller distribution than the red point, or less variance. Thus, the green point is a more robust point. This is assuming that both the red and green points were affected by the identical uncertainty conditions. While the green point may not perform as well the red point deterministically, the green point could be chosen as the preferred design due to favoring the robustness (and predictability) rather than solely performance.

The figure on the right in Figure 9 tells a similar tale. Here, both the red and the green points have high variance relative to the green point in the RDO figure (large area of potential future states, or "cloud"). Again, the red point performs better than the green point, and again, the green point accounts for the uncertainty more favorably than the red but this time not due to cloud size. The figure illustrates that part of the red point's distribution is actually violating at least one constraint. This would result is a less than 100% reliability for the red point. This point could have about a 60% probability of success (satisfying all constraints), or a 40% probability of failure (violating one or more constraints). The green point, on the other hand, has a 100% reliability, as all the possible points within its distribution satisfy all the constraints.

Both RDO and RBDO have their place in engineering design. The question at hand is which approach is better suited for capturing design uncertainty. Thankfully, this question has already been asked by Huyse at NASA Langley Research Center [77]. His classification matrix is demonstrated in Figure 10.

Huyse classifies uncertainty approaches by the impact and frequency of uncertain events. For RDO, the frequency of the event is high but the impact of the event on performance is low. On the opposite end of the matrix is RBDO, where the frequency is low but the impact is high (or catastrophic). This matches the story from Mr. Sutter and his twist: if he and

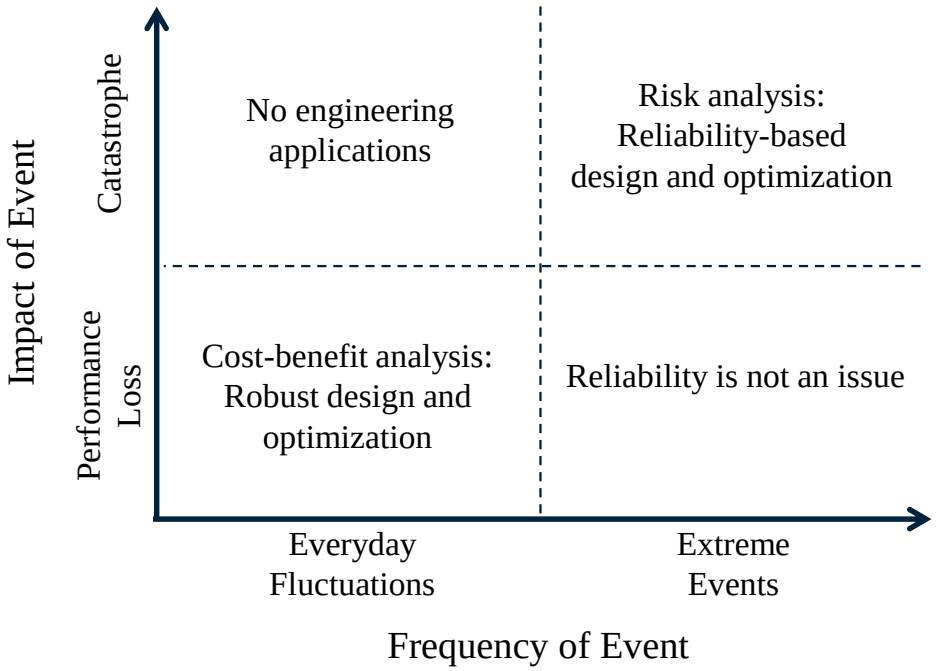

Figure 10: Comparison between Applications for Robust versus Reliability-based Design Optimization [77]

his team did not find a way to support the outboard loading, the wing would need to be re-designed. This describes a catastrophic event. Similarly, the field of structural engineering commonly uses RBDO as failures result in catastrophe [78, 79, 80, 81]. Therefore, RBDO is a better fit for modeling design uncertainty.

Observation
Reliability-based Design Optimization provides the best foundation for a framework aimed to selecting the conceptual design that both performs well and accounts for design uncertainty.

2.3.3 3) Uncertainty in Performance, Not Size

This characteristic derives its importance again from the temporal nature of design. The wing had already been designed, which in this case meant sized in conceptual design. Now that the conceptual design decisions were frozen, preliminary design allowed the wing to be constructed and physically tested, which is where the uncertainty was realized (went from

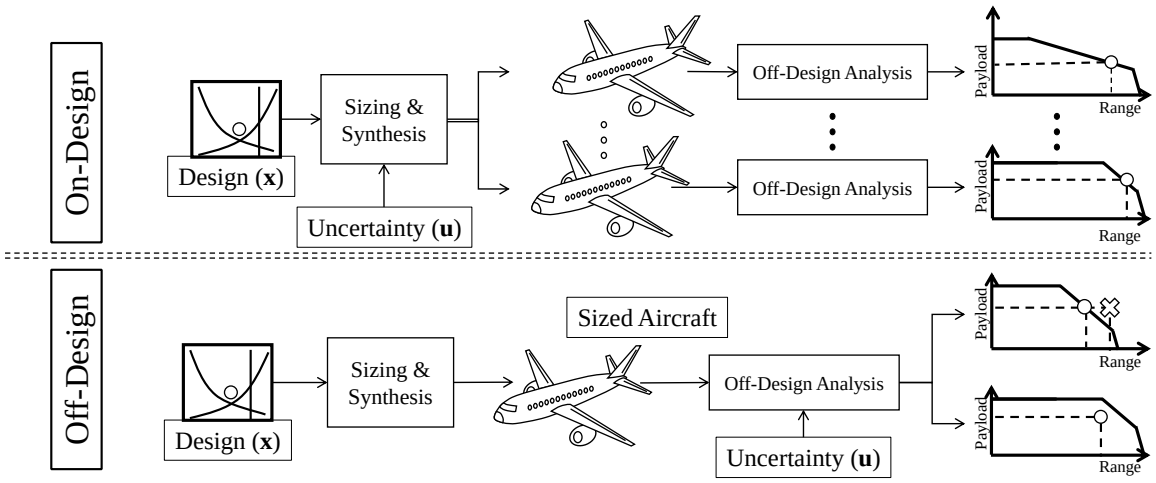

Figure 11: Comparison between On-Design Uncertainty and Off-Design Uncertainty [23]

a series of possible values to a known, singular value). Now there was a decision to make: go backwards to re-design (and give the other disciplines new values for the re-designed wing), or fix the current wing.

Sutter did the latter, which he said was one-tenth as difficult and costly. But there is another subtle hint to the characterization of uncertainty here, and that is how it affects performance which is highlighted in Figure 11.

The top timeline in Figure 11 represents uncertainty that is captured during the sizing process, while the bottom time-line represents uncertainty that is implemented during the performance analysis process. These two stages are also referred to as "on-design," while the size of the aircraft is being determined, and "off-design," where the design is being evaluated at multiple points in the sky with a fixed size.

Uncertainty that is incorporated during sizing would result in aircraft of very different sizes. This type of model best describes uncertainty in the requirements of the aircraft. For example, there may be uncertainty about the expected range of the new aircraft design. For this type of uncertainty modeling, Mr. Sutter would have received a memo from his boss that the aircraft is now supposed to fly a different mission than before. This is a "top-down" uncertainty, where the uncertainty is from the requirements, customer preferences, or market research. Instead, the motivational problem illustrated a "bottom-up" uncertainty,

where the physics of the design itself illuminated the error.

This discussion is reminiscent of the distinction between the different types of margin. Before, requirements, design, and operational margin affect the design similarly. Here is the case: the uncertainty is specifically design uncertainty. It is realized via physics during performance analysis. Therefore, it needs to be captured during the preliminary design step rather than the requirements definition.

However, because there is not a sizing and synthesis loop post-conceptual design, the rest of the disciplines cannot be altered in response to the uncertainty. Recall that for margin an increase in empty weight is captured through sizing, such that the wings can be sized to fit more fuel and the engines can be enlarged to produce more thrust. This is not the case for mitigation. A realization of uncertainty will change the performance of the aircraft; indeed, the Sutter Twist changed both the structural and aerodynamic properties of the wing. The rest of the aircraft, though, cannot be resized to compensate for the loading calculation error.

Observation

Design uncertainty is realized post-sizing; therefore, it cannot be redressed via sizing (without re-design) and it disrupts the synthesis of the conceptual design point.

A simple corollary follows that if the design uncertainty is indeed realized during preliminary design, then a design process that desires to capture this uncertainty must include the preliminary design phase (same with mitigation). This makes sense, as mitigation actions (such as wing twist) often are lower fidelity than the conceptual design phase will allow.

2.3.4 F-135: Historical Example of Margin, Uncertainty, and Mitigation

An additional example to the Sutter Twist is included with the F-35 engine: the F-135. Pratt & Whitney also had some issues arise with the design and manufacture of their piece

of the aircraft, specifically the short take-off and vertical landing (STOVL) version. The following is an excerpt from an article interview with the director of the F-135 program, William Gostic.

> Currently, the STOVL F-135 is 72 lb. below the specification weight and 230 lb. above target weight. By definition, target weight is that which is 6% below the engines not-to-exceed-weight; specification weight is that which is 3% below the not-to-exceed weight, Gostic said. All performance calculations are made using the not-to-exceed weight. Right now we have a plan to get the STOVL engine to the target weight, and have identified a number of things to actually get the engine below the target, Gostic said. [82].

The quote from Gostic clearly demonstrates the importance of satisfying vehicle-level metrics. The design process had moved from conceptual design (determining the vehicle as a whole) to preliminary design (determining the major systems). It is interesting to note that Gostic discusses the importance of engine weight rather than thrust. It seems as though the thrust requirement had already been met, but there was serious ongoing work to decrease weight. This shows that weight is an important metric for any system, not just structures, most likely because it affects the entire take-off gross weight.

Gostic was given a "not-to-exceed" weight. This was the value used in the calculations for the other components, as described in the quote. The F-135 engine was below this weight (and the specification weight) but above the target weight. This shows both the use of margin and the use of mitigation. The not-to-exceed weight was used in the performance calculations even though the engine was not that heavy: there was an engine weight margin equal to the not-to-exceed weight and the target weight. Second, the team had identified a number of corrective actions to decrease the weight after it had been designed (mitigation actions). This is interesting because it shows mitigation being used as a matter of preference (weight reduction) response to a constraint violation (exceeding not-to-exceed weight).

Mitigation could affect the financial aspect either through development delay, technol-

ogy acquisition, or production costs. For example, the Sutter Twist did not seem to have major performance degradations associated with the design change, but the excerpt is clear that the design process was slowed, or stopped, due to the realization of uncertainty. It is possible the fixes themselves are not as costly as the time taken to fix them. Due to technical delays, the A400M military jet and A350 wide-body programs cost Airbus a combined $1.55 billion (FY2016) solely from production delays [83]. The A350 price tag is between $275 and $360 million (FY2017), which means that the production delay cost would be equivalent to giving away five aircraft for free when it produces about 10 per month [84]. This information, combined with the accounts of Sutter and Gostic, leads to the observation that mitigation is not viewed through the same lens as margin. While the goal of margin is to balance performance with reliability, the goal of mitigation is to balance viability with feasibility. In other words, mitigation must be done quickly.

2.4 Uncertainty Classifications and Descriptions

Probabilistic design explicitly places the limits of knowledge within the decision making process. It aims to include the source of uncertainty and propagate its effects to the constraints and performance. As aforementioned, aircraft development is an immense investment. The decision-making process is crucial to the success of the company and the program; as a result, if uncertainty is to affect this decision-making process, the approach must be rigorous to affect change.

2.4.1 Epistemic and Aleatory Uncertainty

While probabilistic design is relatively new, the study of uncertainty is not, going all the way back to the Greeks who first studied uncertainty in the 4th century BC [85, 86]. Epistemology, the branch of philosophy concerned with the study of knowledge and its limits, comes from the Greek *episteme*, meaning knowledge, and *logos*, meaning theory. Similarly, epistemic uncertainty (also called reducible or subjective) describes the unknown

caused by a limit in understanding [87]. Aleatory uncertainty (also called variability, irreducible, inherent, or stochastic), on the other hand, is inherent. The root *alea* from the word aleatory is the Latin word for dice: the quantity can change from draw to draw [88]. This distinction has become commonplace in uncertainty quantification and management because the epistemic uncertainty can be reduced, and therefore it should be the focal point of uncertainty management methods [89]. Aleatory will simply always be there: it should be accounted for but cannot be reduced.

Here is an example to demonstrate the importance of classifying uncertainty. Figure 12 shows the discrete probability distributions for two different dice: the left-hand die is perfectly balanced whereas the right-hand die is loaded (unbalanced). We assume that we cannot know which number will result with the left-hand die: the uncertainty is irreducible. Then, we can only assign a probability to each potential outcome (1/6 in the case of a six-faced die). The exact distribution of weight in the right-hand die is unknown; still, it will affect the probability of any given result. Describing the right-hand die as uniform distribution (1/6 for each face) would be inaccurate. If, for example, the die was weight such that the number 6 would result in half the throws, the PDF could be accurately formed giving the face 6 with a 50% change of occurring with each other face a 10% chance of occurring.

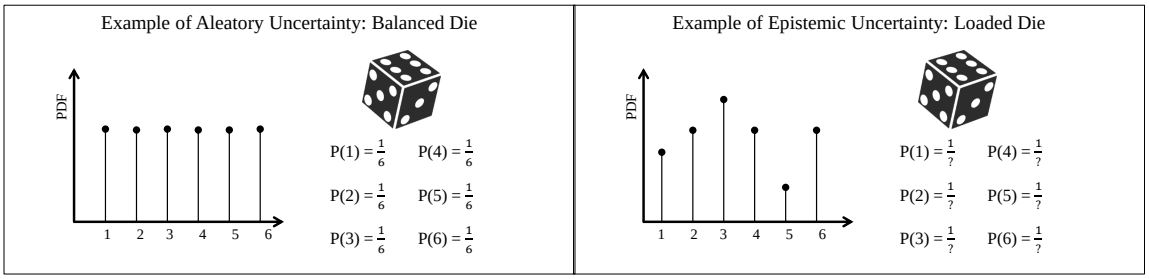

Figure 12: A Tale of Two Die: An Example of Aleatory and Epistemic Uncertainty

This highlights the distinction between aleatory and epistemic uncertainty. Applying a uniform distribution to the right-hand die would result in more error than the left-hand die, but this additional error would be due to epistemic uncertainty, not aleatory.

A more common example illustrating in the sciences is measurement. The measurements of a 10 feet long table would be uncertainty if the measuring tool was a 12 inch ruler. If the table was measured 100 times, the aleatory uncertainty may balance out and the average could be close to the actual length. This is why experiments often tout the importance of repetitions. However, an assumption was made that the ruler was indeed 12 inches. Consider if it is not; maybe it is actually 11.95 inches. Now, no matter the total number of measurements, each would be impacted by the imprecise ruler. It will give an overall estimation of the table length (probably reliably within 10% difference) but will *never* result in the actual value, unless the epistemic and aleatory uncertainty perfectly offset. This is an example of *systematic* uncertainty: numerous draws do not cancel each other out [89].

Aleatory uncertainty is often characterized by a random variable which takes on various values within a range of defined bounds. A roll of the dice is a prime example of aleatory uncertainty. Though the actual result from a single roll is uncertain, the value may only exist within a set range defined by the numbers on the face of the die. Appropriately, aleatory uncertainty is often modeled via PDFs. Epistemic uncertainty, on the other hand, is much more difficult to model. English economist, journalist, and financier John Maynard Keynes expresses epistemic uncertainty as thus:

> "By 'uncertain' knowledge, let me explain, I do not mean merely to distinguish what is known for certain from what is only probable. The game of roulette is not subject, in this sense, to uncertainty... The sense in which I am using the term is that in which the prospect of a European war is uncertain, or the price of copper and the rate of interest twenty years hence... About these matters there is no scientific basis on which to form any calculable probability whatever. We simply do not know." [90]

Keynes was distinguishing epistemic from aleatory uncertainty: aleatory uncertainty is best described by probabilities, such as the game of roulette. However, the process to de-

fine some values of the future, such as the interest rate in 20 years, is unknown. We do not know how to do it. The design process of a complex aerospace configuration relates more to the uncertainty of war than a throw of the dice. Indeed, the uncertainty that dominates the aircraft design process is epistemic uncertainty rather than aleatory uncertainty [23]. In fact, in the conceptual design phase specifically, only epistemic uncertainty exists. This is because there is no natural process at work: only computer models and empirical relationships, which are deterministic (repetitions would yield the same results). The relationships themselves carry epistemic uncertainty introduced by a lack of understanding and simplifying assumptions. Therefore, the key type of uncertainty we are interested in is epistemic uncertainty.

Observation

The type of uncertainty inherent in the conceptual design process is epistemic uncertainty because no natural or irreducible processes are used. Therefore, by definition, the conceptual design phase uncertainty is reducible.

The good news is that work can be done to reduce epistemic uncertainty [91]. As the design becomes more physically testable, the results become more susceptible to aleatory uncertainty. However, during testing, aleatory uncertainty can be accounted for by using repetitions: the "true" value will become apparent after several measurements.

This uncertainty classification is popular because it is practical. It does not, however, perform well under extreme conditions. Some argue that all uncertainty is epistemic because if *everything* was known the outcome could be predicted. Aleatory uncertainty, then, can be reduced. Conversely, though epistemic is described as reducible because it is related to ignorance, some ignorance cannot be reduce, even in principle [92]. The classic example of this paradox is Heisenberg's uncertainty principle. The principle states: "the more precisely the position of some particle is determined, the less precisely its momentum can be known, and vice versa" [93]. The study of quantum mechanics has shown that we

can never know where a particle is: this knowledge would require infinite kinetic energy (or momentum) for us to exactly locate it [94]. Therefore, we do not consider particles to have exact locations; instead, we describe its location using a probability distribution. To reiterate: the exact location (truth) cannot be known. Instead, the location is described using a list of possible locations with assigned probabilities.

For aircraft design, we are dealing with unknowns that will be revealed in time. Therefore, we need not fret about whether the knowledge is knowable or not.

2.4.2 Probabilistic Modeling

Quantum mechanics is fun, but it is also serves as an analogy to design uncertainty. We assume that the "truth" value (location of the electron, or future state of the aircraft) *cannot* be known. The set of probabilities is known as a PDF: probability density function [95]. The value of a PDF at a given point is the probability, or *relative likelihood*, that the value of the random variable would equal that point. The "random" variable is the variable whose ultimate value is uncertain. Recall the die example from Section 2.4.1: the value of each face was described by a discrete PDF. The function is discrete because only some values are possible (1, 2, 3, 4, 5, and 6 in this case). The random variable f (representing which face will result on top) is described by a discrete, uniform distribution between 1 and 6. A PDF is continuous when *any* value between bounds is theoretically possible, such as the weight of an aircraft or the length of a table.

Probability density functions are not new and are the most common approach in transforming deterministic design into probabilistic design. The paradigm shift is from a single point to a collection of points, from algebra to statistics. DeLaurentis and Mavris define uncertainty as "the incompleteness in knowledge (either in information or context), that causes *model-based predictions* to differ from reality *in a manner described by some distribution function*" (emphasis added) [96]. PDFs are so prolific that these authors have used them in their definition of uncertainty.

During conceptual design, the wing weight could deterministically be calculated as 60,000 pounds. But this cannot be known. In fact, the probability that it is *exactly* 60,000 pounds is exactly zero. Instead, the final wing weight could be a range of weights from 40,000 to 75,000 pounds with the most likely (highest probability) weight being 60,000 pounds. The ease of PDFs is their parameterization: a distribution of infinite points can be described using only a couple of parameters. For this example, a triangular distribution could be used bounded by 40,000 and 75,000 pounds with a maximum at 60,000 pounds. A normal distribution, for example, only requires two: mean and standard deviation.

There are many challenges with describing uncertainty using PDFs, namely: which distribution should be used? How should it be bounded? What parametric values should be used? And so on. The key difficulty is that each of these choices carry uncertainty, which, in turn, is a source of uncertainty.

This is where quantum mechanics differs from engineering design: in design, the possibilities are boundless. This is not as optimistic as it may appear: we want the analysis to be bounded but there is always a non-zero probability of a catastrophic event occurring with devastating consequences [53]. PDFs capture this effect, (a normal distribution, for example, approaches both negative and positive infinity) but these extremes increase the difficulty of the reliability calculation. A distribution sample would require millions of points to ensure the tails are represented because they are, by definition, extremely unlikely to occur. If these extremes are not of interest, a normal distribution could be truncated into a triangular distribution.

2.4.3 Challenges in Capturing Uncertainty

The PDF matches each potential outcome to a probability. This tends to work well with aleatory but not epistemic uncertainty because it is difficult to characterize what we do not know. Usually aleatory uncertainty can be isolated and even eliminated using repetitions, whereas epistemic uncertainty is not revealed via frequency (recall the incorrect ruler ex-

ample from Section 2.4.1). This is why epistemic uncertainty is often related to systematic error, or error that is caused by the measurement procedure, rather than random error, or error that is caused by variable environmental factors. Recalling the Sutter Twist example from Section 1.3.3, the number of aerodynamics tests could not have predicted the outboard wing loading problem before loads testing. It was simply not asking the right questions.

Therefore, nothing could have been done to predict the loads problem: it could only be revealed by loads testing. Increasing the number of empirical calculations or aerodynamics testing would not have helped. They were systematically incapable of reducing the loads uncertainty.

If a PDF is chosen, the selection itself introduces uncertainty termed *ambiguity*, defined as "uncertainty about probability, created by missing information that is relevant and could be known" [73] which unfortunately has a great impact on the results of the simulation [97, 98]. Note that ambiguity is another form of epistemic uncertainty because it could be known (reduced), but it is not. Note also that this is different than Thunnissen's definition of ambiguity. It is the probability of a probability. Often, because no knowledge can be known of epistemic uncertainty, the input distributions to model epistemic uncertainty variables is uniform, as stated by Laplace's Principle of Insufficient Reason [99] which essentially states that any other distribution introduces more uncertainty. Any other distribution would denote a measure of knowledge.

Due to these concerns, some authors have argued that PDFs are not the preferred method for propagating uncertainty, though this is an old debate [100, 101, 102, 103]. While the debate rages on, using probability for risk and uncertainty assessment is the most common approach. While this is certainty an imperfect method to modeling uncertainty, it allows uncertainty propagation to be assessed throughout the design process.

Observation

Characterizing uncertainty using a PDF requires a number of parameters to be defined, thereby potentially adding unnecessary ambiguity. Therefore, describing epis-

temic uncertainty using PDFs is an imperfect method to integrate uncertainty into the design process.

Note that the ambiguity referenced here is the statistical ambiguity recently defined rather than the communicative ambiguity defined by Thunnissen.

2.4.4 Classifications in Engineering Design

While aleatory and epistemic uncertainty are the most commonly used types of uncertainty, there are many ways [104, 96, 77, 105, 106] with each field typically having its own taxonomy [107, 108]. While we will dive deeply into uncertainty categorizations in Chapter 4, we can introduce an applicable taxonomy here as background.

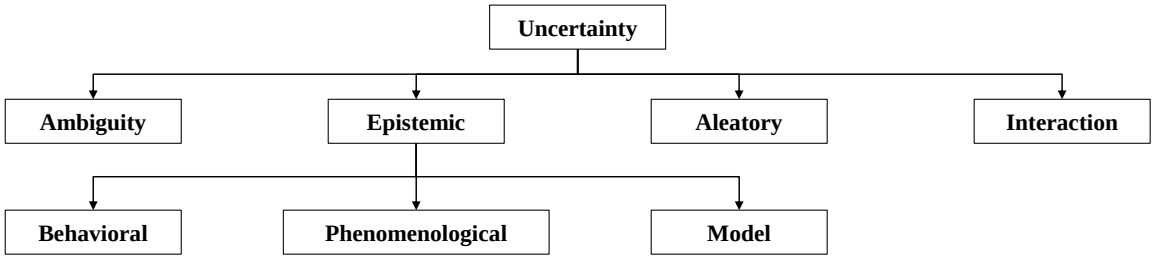

Figure 13: Thunnissen's Taxonomy for the Design and Development of Complex Systems [104]

Thunnissen has provided a framework for classifying uncertainty across multiple fields of study [109] but the one most important for our purposes is the taxonomy for the design and development of complex systems. His taxonomy is illustrated in Figure 13. In design, there are two extra categories: ambiguity and interaction. Ambiguity is caused by human communication and negligence (e.g. contract language). An example would be confusing the difference between block fuel (fuel required to get from gate to gate) and mission fuel (fuel required from takeoff to landing). Another example would be stating in the contract that the design perform "satisfactorily" without explicitly defining that expectation. Interaction is a sort of "catch-all" category that describes emergent uncertainty between the other categories.

Our focus is on epistemic uncertainty, which Thunnissen decomposes into three deeper sections: behavioral, phenomenological, and model. Behavioral describes how organizations act, and has four main sources: design, requirement, volitional, and human. These definition differ from the terms used in this work thus far because they refer to human impact. Phenomenological is categorized as epistemic because it is caused by natural processes we do not fully understand; again, this is true, but not immediately applicable to our purposes because conceptual designs uses low-fidelity models.

Finally, this leads to model uncertainty, which is most aligned with our problem. Therefore, they key source of epistemic uncertainty for our purposes is model uncertainty.

Observation

Model uncertainty is the subcategory of epistemic uncertainty that is most applicable to the motivational problem.

A Note on Uncertainty vs. Error

Thunnissen further decomposes model uncertainty into approximation error and programming error. Notice the subtle change in terminology between model *uncertainty* and *error*. Error implies a difference between a given value and a *true* value. Take approximation error, for example. Approximating π as 3.14 introduces error because the true value of π is known (or, at least, can be approximated with much greater accuracy than the third significant digit). Uncertainty, on the other hand, states that the value is not or cannot be known.

The goal of uncertainty quantification is not to get the "right" answer. In many ways the actual realization is not as important as the decision-making process. As designers, we are not playing the lottery and hoping to get lucky. We are after repeatable processes that will reliably produce superior results.

2.4.5 Classifications in Aerospace Engineering

We started with broad uncertainty classification (epistemic and aleatory) and determined that epistemic was more suitable to the problem at hand. Then, moving toward engineering design resulted in a focus on model uncertainty within epistemic uncertainty. Now, moving specifically toward the aerospace engineering discipline we would expect a well-defined, standardized taxonomy for model uncertainty. Unfortunately, this is not the case.

Instead, authors tend to place uncertainty on the most likely suspects, such as customer requirements, low fidelity in analysis tools, manufacturing tolerances, and immature technologies [110]. DeLaurentis and Mavris [96] summarize a classification in aerospace engineering from a set of previous authors including controls, systems design, structural design, computational modeling and simulation, and complex systems design [111, 106, 112, 113].

Observation
No single taxonomy has emerged as the industry standard in aircraft design for classifying epistemic or model uncertainty.

A short background on the types of uncertainty revealed two major findings: first, the uncertainty is epistemic and therefore effort can be made to reduce it; second, the field has not come to a consensus on uncertainty classification. The first observation is significant because it motivates uncertainty reduction efforts. The second observation creates an opportunity for improvement.

2.5 Background Synthesis and Thesis Scope

Chapters 1 and 2 have included a number of observations that will form the foundation for this thesis' research questions and method development. In order to contribute to the state-of-the-art, the next chapter will delve into the most influential techniques for aircraft design and uncertainty quantification. But we cannot survey the entire fields of aircraft design and

uncertainty quantification. Clearly, aircraft design is complex and immense: it would be a fool's errand to tackle the entire process in one thesis. Therefore, we would like to scope the problem down to its core. The following is list of key notes from the first two chapters:

- The research objective highlighted the need to address uncertainty is the design process.
- The paradigm shift highlighted the drop in design freedom during the conceptual design phase but the increase in design knowledge during the preliminary and detailed design phases.
- Optimization standard form needs to be drastically re-formulated to include uncertainty, margin, mitigation, and "freezing" of the design space.
- Both Sutter and Gostic demonstrate real examples where uncertainty, margin, and mitigation significantly affect the success of an aircraft development program.

We would like to focus on the conceptual design phase because that is when the design freedom is lost; however, we would also like to focus on the preliminary design phase because that is when uncertainty is realized and mitigation is applied. Therefore, the scope of this thesis is illustrated in Figure 14.

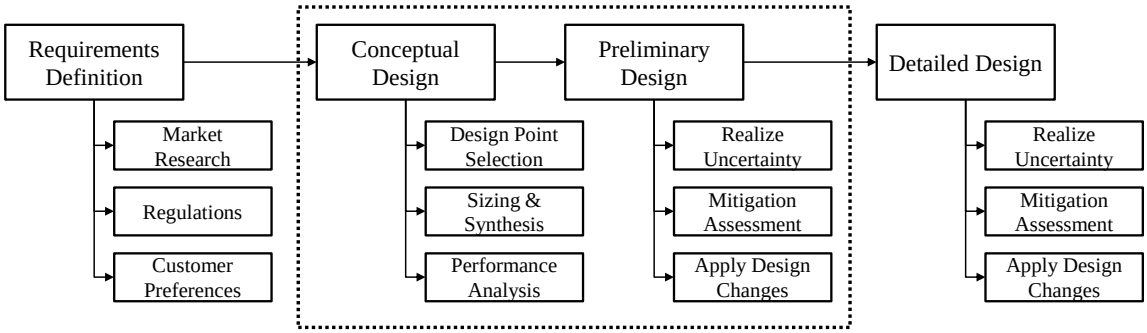

Figure 14: Scope of Thesis within the Aircraft Design Process

The dotted line indicates the focus of this work. This will allow all the ingredients hitherto described to be included in the problem formulation: uncertainty, margin, mitigation,

changing design spaces, constraints, performance, and reliability. Therefore, we will need to look into three main areas in the literature review: conceptual design, preliminary design, and uncertainty quantification methods. The next chapter (Chapter 3) will skip to the chase: what are the current methods that capture this entire process?

CHAPTER 3
REVIEW OF RELIABILITY-BASED DESIGN METHODS

The fields of aircraft design and uncertainty quantification are wide and deep. There is simply far too much published material to effectively or efficiently sort through all the past and ongoing work. The introduction and background were a bit more thorough than a typical thesis to enable a limited scope at this juncture: we wish to stick as closely as possible to the 747 Sutter Twist and F-135 weight reduction. Therefore, the scope of this literature review is limited to reliability-based methods that capture all the ingredients: reliability-based optimization, aircraft conceptual design, aircraft preliminary design, uncertainty quantification, and uncertainty safeguards (margin and mitigation). This review will lead to a benchmark method that represents the state-of-the-art in aircraft design RBDO. Unfortunately, this method falls short of capturing all the necessary ingredients. This presents opportunities for improvement which are the center of attention in Chapter 4.

3.1 Aircraft Design Reliability Optimization Methods

3.1.1 Earliest Methods

One method will be mentioned to give a short history. Uncertainty quantification goes back to at least 1998 with respect to design in the aerospace field [114]. Mavris records competitive pressures, greater safety, environmental consciousness, and maturation of technology as motivators to incorporate margin assessment. Mavris' work and Figure 15 shows that the earliest margin models emphasized the uncertainty and its effect over the ability to diminish the uncertainty. When probabilistic methods first emerged, the focus was on how changes in the design point affect the variability of performance. Indeed, Mavris concludes: "The primary conclusion of this study is that component uncertainty has a significant impact on

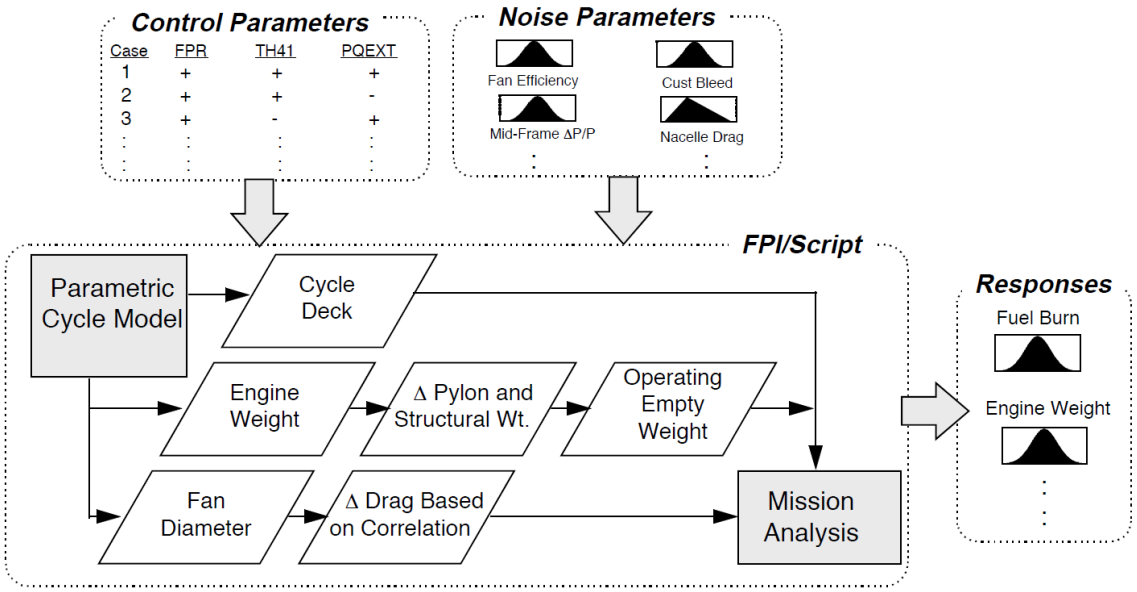

Figure 15: Analysis Flow Chart from [114]; Example of Uncertainty Analysis in Aerospace Design in 1998

vehicle performance." Then, the margin space emerged as an extension of design space; in fact, they tend to share the exact same variables.

3.1.2 Current State of Margin Quantification in Aircraft Design

Though margin has been used extensively throughout the history of engineering design, the quantification of margin is a somewhat new and recent [115, 19, 116]. However, as observed in Section 1.3.3, margin application has a direct effect on performance and reliability. Recall that margin is proactive: it is determined before uncertainty is realized but also unable to be increased or decreased after uncertainty is realized. If margin is the only technique to account for uncertainty, no responses to uncertainty are possible. Should the vehicle show sub-par performance during preliminary or detailed design testing, changing the margin is extremely difficult, if even possible [6]. In one extreme, applying too much margin results in an over-sized vehicle, while applying too little margin runs the risk of redesign or cancellation. Therefore, an important step in the engineering design process is margin quantification and determination [117]. Excessively conservative decision making

will result in an uncompetitive aircraft final design, whereas risky decision making may result in cancellation.

Because margin cannot be changed after sizing, it must be set *before* design knowledge is increased. Now, with modeling tools that capture the effects of margin on reliability and performance, the specific margin values can be determined with a level of confidence of possible future scenarios rather than based on subject expert knowledge. This prompted development in the areas of uncertainty propagation and forecasting. Further, the positive impact of margin cannot be quantified without an uncertainty quantification process. Otherwise, historical margins or values based on expert judgment would be used, though no one would ever really know if the applied margin was too much [16].

Closely related to aircraft design is spacecraft design. Margin is extensively studied in the spacecraft design realm though it is extensively described only in terms of mass [118]. During conceptual design the total weight of the spacecraft is frozen (similar to aircraft), but the restriction is much more severe because spacecraft propulsion is much more complex than air-breathing propulsion. Therefore, extensive work has been done for design toward margin as well as sequentially releasing margin throughout the design process. Margin quantification remains a rich field of ongoing work despite the significant progress compared to aircraft design. In order to determine margin for a novel concept, Robertson draws on the shipbuilding, financial, and scheduling to derive four main components to margin quantification: predetermined percentage, historical regression, expert opinion, and simulation analysis [119, 120].

3.1.3 Capturing Temporal Aspect of Design

Scheduling comes the closest to including the time element in the margin quantification process. This temporal aspect has been attempted to be included in the aircraft design field. A novel approach to capturing the design "freezing" phenomenon was proposed by Nam in 2008 [121, 122]. The work was motivated by the significant impact of conceptual design

decisions made when design knowledge is extremely low. The basic idea was to discretize conceptual design space in a series of steps such that certain design variables could be left undetermined. Each step required its own formulation and analysis tool. This would allow margin to be applied to components which were sized during conceptual design, but could be sized subsequently to prior conceptual design steps. This idea was called Multi-Stage Reliability-based Design Optimization (BDOMSRBDO) [121, 123].

MSRBDO is based on three assumptions: reducible uncertainty, retained design space, and decisions toward feasibility. The first and last assumptions are identical to implicit assumptions of this thesis: the first being that the uncertainty is repeatable (not aleatory) and reducible (epistemic), and the second being that designers make decisions in order to achieve technical feasibility. The key differentiation is the assumption of a retained design space from stage to stage. As defined by Nam: "Designers hold a certain degree of design freedom that can be exploited to correct the decisions made at previous stages with increased knowledge." This assumption allows the inclusion of mitigation, or some exercise of changing the design in response to increased design knowledge. Because the design space is retained, no consequence is caused by the delay of decision making: the change in formulation to allow for discretization structures the process to allow for late stage decisions without penalty.

An implicit fourth assumption is that this discretization is possible. Nam describes that a crucial step in the process is *stage definition*, which would replicate the design reviews of an actual process. This is an ideal scenario; however, analysis tools suitable for each stage are required. This would require new tools for each stage as currently there are only a few conceptual design tools (that revolve around sizing). Therefore, this approach is novel for aircraft design risk-reduction, but is currently disabled by the lack of design tools to represent the multiple stages. In theory these tools could be developed, but Nam has not gone far enough to explicitly map reported design stages to hypothetical analysis tools. As a result, this approach is considered novel but too rudimentary to be implemented.

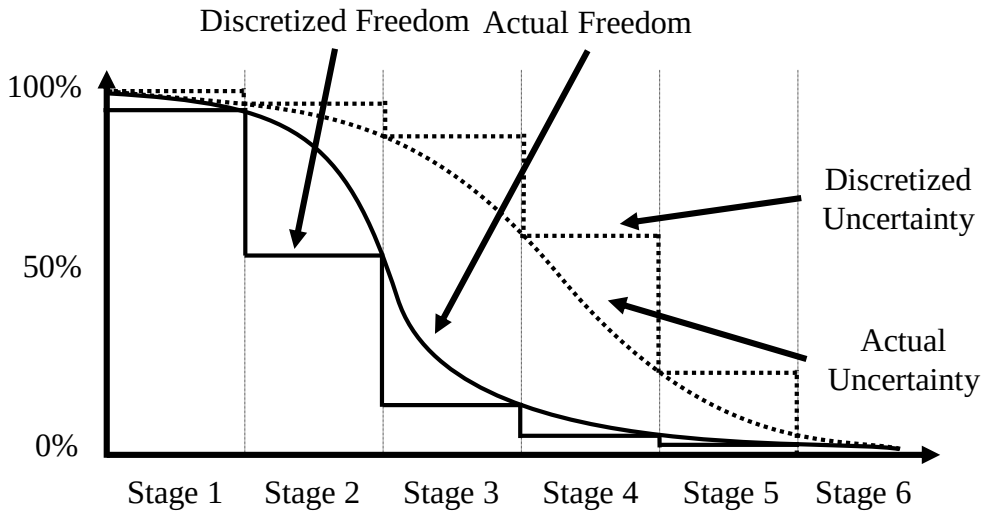

Figure 16: Discretized Design Stages fro Multi-Stage Reliability-based Design Optimization [121]

3.1.4 Introducing Design Changes via Stochastic Programming

There is a precipitous decrease in amount of work published on responses to uncertainty compared to proactive measures against uncertainty. The difficulty is the change in optimization formulation: margin variables share many similarities with design variables whereas mitigation does not. In this case it takes a tailored approach to aircraft design for the work to be useful here.

Similar to reliability-based design is a field called stochastic programming. This field was developed in the 1950's when applying uncertainty to linear programming [124]. Dantzig and Beale created a method under stochastic programming that include the concept of recourse, or the capability to respond to constraints under uncertainty. This is probably the first time a statistical method introduced the idea of reactive design. Choi applied stochastic programming with recourse to aerospace problems (fuel cells, specifically) [22]. The idea is that designers could respond to uncertainty reactively with recourse.

Choi describes the motivation for his work in 2008: "the logical next step in uncertainty modeling is capturing the remedial aspect of design. If a design has failed one or more

constraints, often designers do not simply return to the drawing board. Instead, recourse measures are taken in an attempt to salvage feasibility. This work is intended to capture this practice in the modeling process" [22]. This would lead to what is now, or has been in this thesis, called mitigation. Using the advances in stochastic programming, Choi developed a method to apply recourse in aerospace design, acting as the bridge between the two disciplines.

While this marriage was novel at the time, obstacles still faced the stochastic programming approach. Stochastic programming assumes that recourse is always available; or in other words, all the uncertainty realizations are recoverable. Therefore it cannot be used to calculate reliability. Further, stochastic programming only allows for a single design space; as a result, the recourse variables are identical to the original design variables. For aircraft design, this would be equivalent to applying recourse through aspect ratio or fan diameter: once the sizing is complete, these variables are difficult to change. Instead, aircraft design dictates a new set of variables for each design phase to replicate the actual process. Consequently, the stochastic programming method with recourse is not directly suitable for this problem without modifications.

3.1.5 Designating A Unique Mitigation Space

Both Nam and Choi worked to incorporate mitigation actions without the trouble of isolating from the design space. Nam tackled this by sequentially fixing design variables in a multi-stage approach. Choi incorporated recourse which shares a variable space with the design variables. Finally, in 2015, Wilson published a new approach to retroactively account for uncertainty using a unique variable space [23]. He termed his version of recourse "mitigation," and differed from recourse in that it had a unique variable space independent of design variables. The dictionary definition of mitigation is "the action of reducing severity, seriousness, or penalty of something" [15]. This is an aptly named term, though it is a direct descendant of the recourse and MSRBDO approach of Choi and Nam, respectively,

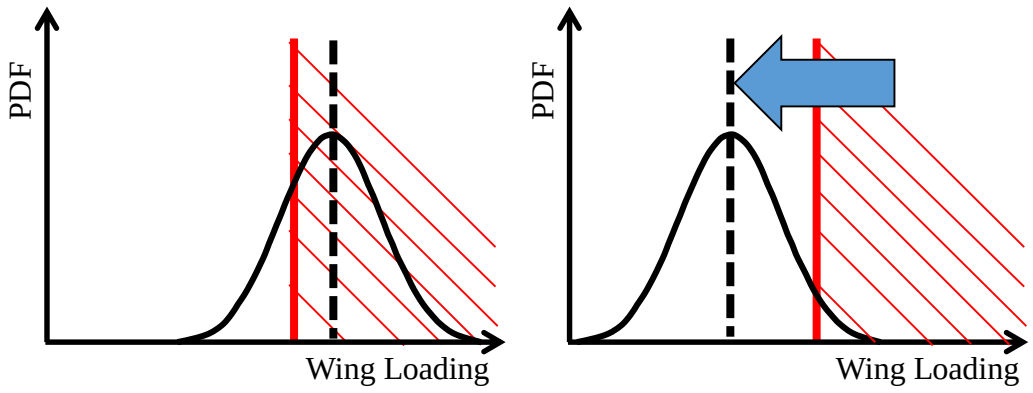

Figure 17: Effect of Mitigation (Recourse) on Probabilistic Performance

in the act of applying design changes as a form of uncertainty reduction.

The key differentiator of Wilson's work is that there is no assumption that the design changes occur in the design space. Both Choi and Nam (and followers) required that mitigation remain in the design space. Wilson notes that no major paradigm shift in aircraft design need occur; indeed, chief engineers have been making design changes since the beginning. These changes are often proprietary and unpublicized, or published years after the success of a program as is the case with the Sutter Twist.

The removal of the retained design space assumption from Nam's work opens up a new space of possibilities; however, some key language remains common ground between the two works. The key commonality is "degree of freedom." All three authors agree that an assumption must be made that the change is *possible*. Because Wilson does not assume that some design space is retained, he makes the assumption that the design changes are relatively small. This assumption is justified by Raymer, who states that gross changes to the design indicate a failure in the conceptual design process itself. Therefore, Wilson's mitigation can be generally described as within the preliminary design space as opposed to the conceptual design space. This way, the temporal aspect of the design process remains without the need for multiple conceptual design tools.

3.2 Defining the Benchmark Method

From the literature search, the closest methodology that captures mitigation quantification is Wilson's method. Consequently, his method will be described in more detail in this section, specifically with respect to mitigation implementation.

Wilson uses conceptual design tools to capture the overall effect of small design changes. The optimization formulation used by Wilson is based on performance and reliability, with the performance objective metric of block fuel. Mitigation is often characterized by a performance penalty such as additional weight, such as for additional fuel capacity or additional high lift devices. Takeoff weight is assumed to be fixed, so additional component weight subtracts from available fuel weight for the range constraint calculation; or, in the case of the economic mission used for the objective calculation, the additional component weight increases the amount of fuel needed for the economic mission, thus penalizing the designs that need mitigation.

The heritage of Choi, Nam, and Wilson will act as the foundational work for the current strategy for risk-based aircraft conceptual design, particularly with respect to reducing the severity (mitigation). The method is called ARMOUR: Aircraft Recovery through Mitigation and Optimization under Uncertainty for Reliability.

Observation

The ARMOUR method represents the current aircraft conceptual design state-of-the-art in terms of capturing uncertainty safeguards (margin), uncertainty realization (bi-step analysis), and uncertainty responses (mitigation). Therefore it will be used as the benchmark method.

In the words of Nam: "...a weight penalty alone may not be a correct measurement of all the consequences of infeasibility from the program management perspective, particularly if infeasibility could jeopardize continuous funding for the development program." Clearly, there are non-performance effects of non-compliant. For conceptual designs to be

considered vis-a-vis, the relative impacts of the mitigation levels should to be captured. There is a sizable obstacle to determining this preference, however. Ideally, cost would be the determinant between margin and mitigation, but gathering cost details is improbable for academic work. So there is a capability gap here for future generations, but neglected for the current work.

There is another capability gap, however, that is lower hanging. Recall from Figure 4 that the design uncertainty drops during preliminary design rather than conceptual design. Further, mitigation actions, such as Mr. Sutter's Twist, tend to be *physical* changes made directly to the design. Conceptual models do not support this functionality because no physical model is created. Therefore, there is a substantial opportunity to contribute to the state-of-the-art by integrating the preliminary design phase into the reliability-based design optimization.

Capability Gap

The current state-of-the-art aircraft conceptual design RBDO methodology (ARMOUR) does not extend into the preliminary design space.

Wilson cleverly changes the optimization settings within the conceptual design environment to shift from sizing & synthesis to performance analysis. Essentially the "step" in the process that brings new knowledge is within the conceptual design phase. This represents the general format but rather simulates new knowledge than actually gathers it. Therefore, the quest is to go beyond the conceptual design phase (or at least empirically-based tools) to the preliminary design phase.

Perhaps the most important ingredient to the RBDO methodology is the uncertainty. The sources of uncertainty need to be categorized, selected, modeled, and mitigated. The presence of the mitigation actions are only necessitated by the unfavorable uncertainty realizations. However, the aforementioned methods do not provide rigorous processes for defining and characterizing the uncertainty used within the method. Wilson's method uses

probability density functions to represent a weight, drag, and fuel flow uncertainty sources, but there is not a method to define the distributions or its bounds. As a result, uniform distributions are sampled independently. The uncertainty directly affects the reliability and performance: it needs to be rigorously derived. If a trustworthy process cannot be developed to describe the uncertainty, the results of the method will be ineffectual.

Uncertainty quantification and management is a rich field in the literature, and will be reviewed extensively in the next chapter. For now, it suffices to say that there is an opportunity to enhance the conceptual design selection process by providing a method to generate, select, and characterize sources of uncertainty.

Capability Gap
The benchmark method does not include a process to generate, select, and characterize the sources of uncertainty that result in non-compliance.

There is, however, a detailed discussion as to which reliability methods should be used (sampling methods versus constraint approximation). The process used, then, is not the subject of improvement but rather the uncertainty sources and associated characteristics (distribution type, parameters, independence, etc.) that is open to improvement.

3.2.1 ARMOUR Process

As illustrated in Figure 18, the realizations that receive mitigation are only recoverable points. This is a subset of the total realization space. In a realistic model, a given conceptual design may have around 80% compliant points, 15% recoverable points, and 5% failed points. This would result in a reliability of 95%. For this design, mitigation would only be applied to the 20% of realizations. The outcome of the overall environment is to make a conceptual design selection. In order to make this selection, the *designs* must be compared, rather than the realizations. Thus, the information about the realizations must be aggregated into comparable metrics across designs. The benchmark method used block fuel, averaged

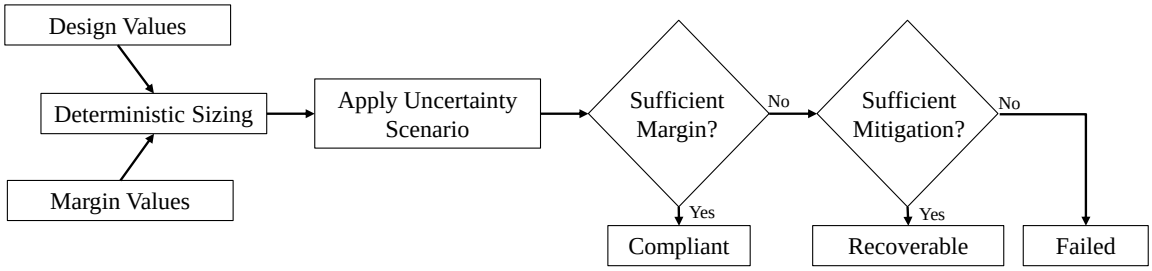

Figure 18: Flow Chart for Uncertainty Realization Analysis, visualized from [23]

across all non-failed points. The aggregation usually comes in the form of an arithmetic mean. If the realization population size was 10,000 points, then 9,500 block fuel values would be averaged together to form a single block fuel value. This value would represent the performance of the conceptual design.

3.2.2 Defining P(Compliance), P(Recovery), and P(Success)

The percentage of realizations that are compliant is also called the *probability of compliance*, also denoted as P(Compliance). The percentage of realizations that are recoverable is also called the *probability of recovery*, also denoted as P(Recovery). Because "reliability" is a general term, a more refined term is the *probability of success*, also denoted as P(Success). Here, success refers to the ability to complete the design process, so this could be called the probability of design completion. P(Compliance) could be viewed as the reliability with respect to margin. Similarly, P(Recovery) could be reliability due to mitigation. The mathematical definitions of these terms are defined as follows:

$$P(Compliance) = \frac{Number\ of\ feasibility\ realizations}{Total\ number\ of\ realizations} \tag{5}$$

$$P(Recovery) = \frac{Number\ of\ recoverable\ realizations\ due\ to\ mitigation}{Total\ number\ of\ realizations} \tag{6}$$

$$P(Success) = P(Compliance) + P(Recovery) \tag{7}$$

Note that P(Recovery) is relative to the entire realization population rather than the non-compliant points. Consequently, if all the non-compliant points are recoverable, the P(Recovery) is not 100%, but 100% - P(Compliance). This is for the simplicity of Equation 7.

3.2.3 Tools Needed for Methodology

In order to produce a new method to fill the capability gaps, the ingredients must be enumerated. The benchmark method provides some suggestions as to how the overall RBDO approach can be done. Filling the capability gaps will require more attention, and is the focus of Chapter 4.

Aircraft Conceptual Design Tools

A set of conceptual design tools are needed to perform an aircraft design optimization methodology. Thankfully, the field of Multidisciplinary Design Optimization (MDO) has been advancing for the recent decades to enable conceptual design models to include multiple disciplines [125]. The key enablers for aircraft MDO specifically are NASA's Flight Optimization Software (abbreviated FLOPS) [126] and Numerical Propulsion System Simulator (NPSS, also developed by NASA) [127]. FLOPS is based on historical regressions of aircraft data, specifically weight data. It runs using a code structure similar to C++ with an input file executed from a command line. NPSS is similar but relies more on fundamental thermodynamic relations to perform engine sizing. More importantly it can be used to build the engine deck (described in Section 2.1.2). These two codes can be integrated, and indeed have been at the Aerospace Systems Design Laboratory (ASDL) at Georgia Tech into a single environment called the Environmental Design Space (EDS) [128].

3.2.4 Aircraft Preliminary Design Tools

The capability gap highlighted the need to extend into the preliminary design space. Though, to be clear, the new tools may not technically be considered "preliminary." They main obligation the new tools must fulfill is that they are physics-based, or that they generate and analyze a physical model (for the purposes of both mitigation modeling *and* uncertainty quantification). This will most likely result in the addition of a computational fluid dynamics (CFD) tool or a finite element model (FEM) tool depending on whether the aerodynamics or structures are emphasized. The new level of fidelity will also yield an opportunity for uncertainty realizations to occur as is reflected in an actual design process.

Surrogate Modeling

While this environment is extremely useful, it is nonetheless time consuming. Therefore, previous approaches have utilized surrogate modeling to increase the efficiency of design optimization. A surrogate model is a representative equation that captures the trends within a specified design space [66]. A design of experiments (DoE) is conducted within the specified design space, and statistical methods are used to fit regression equations within the space. Then, goodness of fit tests are conducted on the regressions to evaluate accuracy and predictability power. When the equations are validated, they only require a second to run, greatly increasing the speed at which optimization can be performed. This technique has already been discussed in Section 2.2.4.

Uncertainty Propagation

Similar to EDS, a Generic Tool for Uncertainty Propagation (GTUP) has been developed at Georgia Tech [129]. This tool was developed in MATLAB for the optimization. Wilson's approach used a genetic algorithm as the optimization algorithm and surrogate equations to predict the performance metrics for both the objective function and the constraints of a given conceptual design under a specific set of uncertainty values. Then, mitigation values

could be added to non-compliant realizations to determine recoverability. The surrogate equations again can predict the performance to determine final performance for recoverable points. The performance metrics are averaged across all non-failed realizations to describe the conceptual design. These values are recorded within the optimization process until the exit criteria are met.

3.2.5 Conceptual Design Selection

Wilson's method is visualized in Figure 19. The process begins with defining the design (x) space, margin (h) space, uncertainty (u) space, and mitigation (m) space. The aircraft models are evaluated in the design of experiments resulting in surrogate equations for each performance and constraint metric. The variable spaces and surrogate equations are passed to GTUP for optimization. The output of the optimization is a Pareto Front of conceptual designs. The Pareto Front is across two axes defined by performance and reliability. In the benchmark method, this would be expected economic block fuel and P(Success).

3.3 Summary

3.3.1 Capability Gaps and Research Objective

Here we can begin to formulate research questions based on the capability gaps found in this review of RBDO aircraft design methods. In Chapters 1 and 2 we determined an overall motivational problem of the high design uncertainty during the conceptual design. Now we have done a literature review where we found that some methods exist that address these concerns, but some gaps remain, namely:

Capability Gap 1
The current reliability-based design optimization methods do not extend into the preliminary design space.

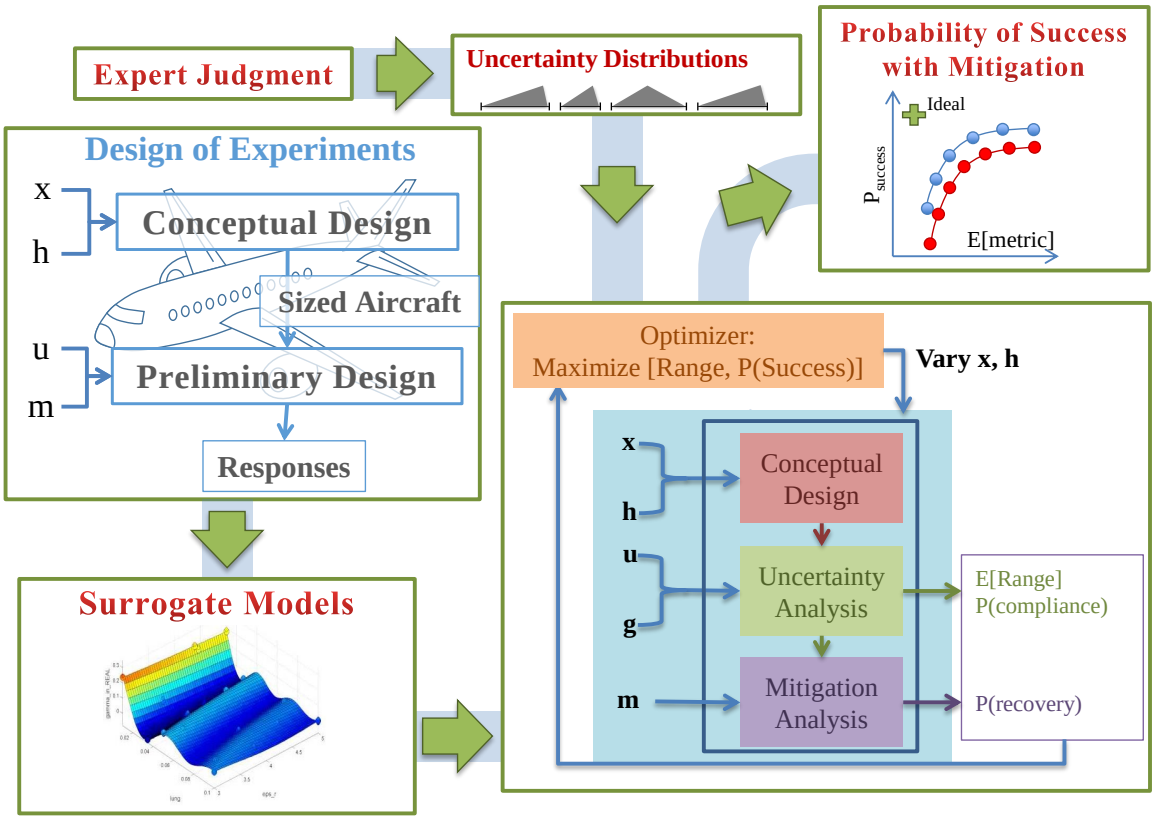

Figure 19: Visualization of Aircraft Conceptual Design under Uncertainty [23]

This gap is a concern because the uncertainty is realized during the preliminary design phase, and mitigation actions tend to be physical design changes (therefore should be captured via a physical model).

Capability Gap 2

The benchmark methods do not include a process to generate, select, and characterize the sources of uncertainty that result in non-compliance.

While many uncertainty quantification approaches exist in the literature, none seem to be implemented in the benchmark methods.

These two capability gaps form the basis for this thesis. Now that these gaps have been defined, the following steps will be taken to fill them:

1. Perform focused literature review into each gap.

2. Enumerate candidate methods.

3. Select the best method from each list of candidates for experimentation and testing.

4. Design an experiment to test the new method.

5. Analyze the results to conclude whether the method has filled the capability gap.

These steps will be repeated for both capability gaps. Assuming that methods will be found that sufficiently fill the stated capability gaps and that the testing of the methods will show successful implementation, they should be integrated into a new benchmark reliability-based design optimization methodology. This process of linking all the necessary parts together is summarized in the last "capability gap:"

Capability Gap 3
No process exists in aircraft conceptual design that performs design selection based on a bi-level design phase approach with uncertainty quantification and correlation.

Clearly Capability Gap 3 is a fallout from Gaps 1 and 2. However, the goal from the original Research Objective is to advance the state-of-the-art with respect to reliability-based methods. Therefore the approaches demonstrated to fill Gaps 1 and 2 should be fully integrated into a single method. Because the new method will perform a reliability assessment and is distinguished by its bi-level (vehicle- and wing-level environments) design environment, the developed method is called Reliability Assessment using Bi-level Design Analysis, or RABiDA. The general research objective is now refined.

Research Objective
Develop an integrated vehicle- and wing-level design environment with uncertainty characterization and correlation to perform reliability-based design optimization.

Statistical versus Physical Models

Research Question 1 calls for a physical model; but, this is not because physical models are "better" than statistical models. Conceptual design tools (like the ones that will be used in this work) are typically statistical models, meaning that they regress outputs against inputs using empirical data. Just because they are low-fidelity (not complicated) models, they are not inferior to physical models. Indeed, they are more accurate and reliable because they are based on real, observed data whereas the physical models are theoretical results inhibited by simplifying assumptions. The general rule is that when data is available, use statistical models.

So, why go through all the pain and suffering of developing a physical model? There are three reasons, two of which are unique to this work.

The first reason is that the empirical data does not characterize advanced concepts. Because it is statistically-based, it cannot predict anything that is not in the database. Thus, whenever a new concept is suggested, statistics cannot be used. This first reason is the general motivation for physics-based models rather than sole reliance on statistical models. However, it does not apply to this work because we have already down-scoped the problem to conventional designs (Section 2.1.2).

The second and third reasons motivate the use of physics-based models. They are uncertainty and mitigation. As hitherto described in spades, uncertainty is realized during the preliminary design phase. To capture this trend is to require a step along the design process such as moving from statistical models to physical models. Eventually a physical model is required.

Mitigation modeling is the final reason. To be considered, mitigation is either explicitly modeled as an input to the model or as a transform function used to encapsulate its effects. Because mitigation has not been extensively studied to the point of publicly available transform functions, it must be modeled explicitly because we simply do not know the effects a prior. Therefore it needs to be a collection of inputs to the model, where model execution

will give us the knowledge of its effects.

3.3.2 Research Questions

In association with the three capability gaps, the research objective can be decomposed into three research areas: developing a physics-based design environment, quantifying and correlating uncertainty sources, and bridging the two environments into a single, integrated modeling environment.

Research Question 1

The first research area is finding or developing a preliminary design environment. This allows for uncertainty to be realized as well as the mitigation actions to be modeled explicitly. While an entire preliminary design environment would certainty move toward an integrated design process, it is unlikely that such a high-fidelity environment would be efficient enough to perform optimization. Therefore we can scope the search down to a *physics-based* model. This distinction is made to decrease the computational load of the environment while keeping an increase in model fidelity between the two environments. The second limiting assumption is a focus on a particular aircraft system. Candidates for selection include the engine, wing, and fuselage. Each of these systems has a significant effect on the vehicle-level metrics and conceptual design selection. Selecting a single system will further limit the scope to improve computational efficiency. To stick with the historical motivational problem of the Sutter Twist, the wing is selected. Therefore, we desire a physics-based, wing-level design and analysis environment. This scope is reflected in Research Question 1.1:

Research Question 1.1
What tools are needed to perform physics-based, wing-level design and analysis?

If more than one are required, how can these tools be integrated to form a single wing-level design environment?

At this time the subsequent sub-questions to Research Question 1 cannot be formulated, but we fully expect questions to arise during the next literature review in Chapter 4. We can surmise that there will be an environment that will be found and need to be tested for accuracy. Further, we can expect to need to develop a mitigation application approach. These expectations are reflected in Figure 20.

Research Question 2

The second research area focuses solely on uncertainty modeling. The benchmark methods had little to no discussion as to the process of characterizing the sources of uncertainty and testing for accurate implementation. As the uncertainty directly affects the reliability assessment, this gap needs to be addressed.

The first step in characterizing the uncertainty is enumerating a list of possible sources and determining which are most relevant to the problem at hand. This task is given in Research Question 2.1:

Research Question 2.1

What are typical categorizations of uncertainty, and which are most prevalent to design uncertainty?

In the benchmark methods the uncertainty was implementing using independently sampled PDFs. While not yet formalized, we can guess that two areas of research for this work will be describing these PDFs more rigorously and testing for correlations or dependencies between the uncertainty sources. This expectation is reflected in Figure 20.

Research Question 3

The third research question cannot be asked at this point because the results from Research Question 1 and 2 are unknown. If no physics-based modeling environments exist and cannot be developed, then it cannot be integrated; or, similarly, if no approach can be found to characterize the uncertainty sources, it cannot be integrated into a new environment. If, on the other hand, a physics-based modeling environment or uncertainty quantification candidate is found (or created), Research Question 3 can be formulated around integrating the two environments into a single, consistent environment. Assuming that a suitable environment will be found, Research Question 3.1 can be formalized:

Research Question 3.1
How can two design environments of varying fidelity be integrated to agree on performance estimation?

We assume here that the new uncertainty process will be amenable to the reliability-based design optimization such that it does not warrant a formal research question. This, along with all the research questions, will be investigated in the next chapter. There is one last research question to ask which relates to the integrated environment. That question is: what light has been shown on conceptual design selection? What darkness has been removed by a new level of understanding? If nothing new is shown by the developed approaches, then the capability gaps were not significant. Therefore, we wish to demonstrate the power of the new approach by answering this final research question.

Research Question 3.2
What impact integrated environment have on conceptual design selection relative to the benchmark method?

Each of these research questions and their expected decompositions are given in Figure 20.

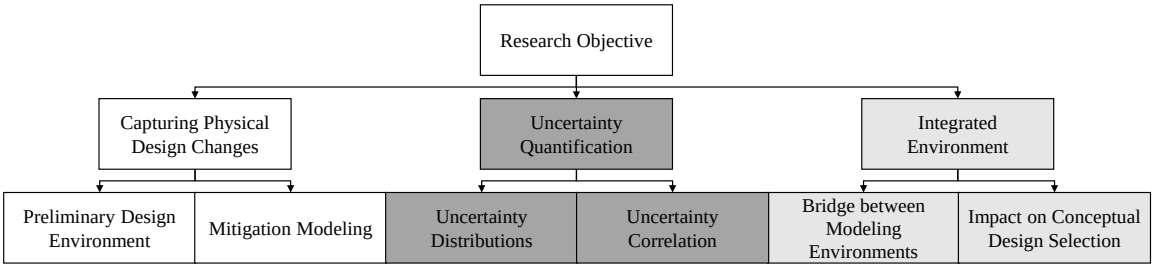

Figure 20: Research Objective Decomposition with Sub-Research Questions

CHAPTER 4
RESEARCH QUESTION DEVELOPMENT

After a literature review of RBDO aircraft conceptual uncertainty quantification methods we found two main capability gaps: one with respect to physics-based modeling and one with respect to uncertainty quantification and correlation. The third capability gap exists by default of the first capability gap: if no reliability-based method includes a physics-based design environment, then a bi-level environment has yet to be developed. The research questions poised at the end of Chapter 3 will be addressed first, but we expected to require further review of literature as well as more questions to be prompted. Each section of this chapter is dedicated to the formalization of the research questions and hypotheses to address the three capability gaps in current RBDO aircraft design methodologies.

4.1 Research Question 1: Physics-based Design Environments and Mitigation Modeling

The glaring gap in the baseline method is the exclusion of a physics-based design tool to show a sequential step in the design process. The method includes mitigation actions, though they are general and applied at the conceptual level such that the actions are not physically defined within the model. To allow the actions to be characterized at a physical level, a preliminary design tool needs to be included.

4.1.1 Research Question 1.1: Physics-based Design Environment

The first part of the first Research Question was formalized at the conclusion of Chapter 3.

Research Question 1.1
What tools are needed to perform physics-based, wing-level design and analysis?

If more than one are required, how can these tools be integrated to form a single wing-level design environment?

There are many tools associated with the major components of the aircraft, though the wing and the engine are the most obvious choices. The engine would be an interesting choice and could be built off of Gostic's example from Section 2.3.4. However, Sutter provides more information in his description relative to Gostic. So, as this particular example has never been implemented, we will seek to develop a method that allows wing-level constraints to be recovered via wing twist modification.

Even with the choice of the wing there still exists a selection of aerodynamics or structures. As described by Sutter, the aerodynamics was completed before and independently of the loads testing. So, we could focus either on the aerodynamic analysis of the wing (CFD) or the structural analysis of the wing (FEM). Again, as the Sutter Twist was based on the loads testing, we will select the structural design of the wing. Therefore, we have refined Research Question 1.1 to the wing-level and to structural sizing.

Revised Research Question 1.1

What tools are needed to perform physics-based, structural wing-level design and analysis? If more than one are required, how can these tools be integrated to form a single wing-level design environment?

The most common approach to structural analysis is finite-element analysis (FEM). FEM discretizes components into a finite number of elements (hence the name). Realistically continuum mechanics govern the behavior of materials and bodies. However, the complexity of high fidelity continuum mechanics is computationally prohibitive, which is why FEM has gained a major foothold in the structures community.

Obstacles to Efficient, Physics-based Structural Sizing

While the popularity has grown considerably, there are still many obstacles to using FEM for aircraft design selection.

Structural Design Freedom As mentioned in Section 1.3.2 and Figure 5, a major obstacle between the conceptual and preliminary design phases is the drastic change in degrees of freedom. For conceptual design, only a handful (10-20) variables are required to define a model. In preliminary (or physics-based) models, the number grows significantly due to the presence of geometric definitions. Little is known about the structural geometry or configuration in conceptual design because empirical data does not describe it; however, this definition is a prerequisite for preliminary analysis. While detailed geometric definition creates a few challenges, the challenge highlighted here is the difficulty in mapping the conceptual design to the preliminary design as well as handling a significantly larger multivariate design space.

Essentially this calls for a process to automatically map a conceptual design to a preliminary design. This approach would most likely be heuristic (e.g. a wing of a certain span has a certain number of ribs). If a one-to-one mapping cannot be determined, then the preliminary design may become probabilistic: one conceptual design may have 1,000 potential preliminary design. We're not sure which values in the preliminary design space will be because it has not been decided yet. This is a type of human factors category of uncertainty discussed in Section 4.2.1.

Model Generation Effort To investigate the design space, the generation of structural models needs to be automated and sufficiently generic to handle a design space. Even though the scope of this thesis is limited to conventional designs (Section 2.1.2), a structural model is difficult to generate. In a structural model, the geometry may be approximate: no two components may be "almost" touching: they must connect exactly. Furthermore, a

mesh would need to be generated as well, and reliably. If the structural model and mesh cannot be automatically generated reliably, either design space exploration cannot be performed or the results will not be usable. If the meshes can be efficiently generated, they should also be evaluated using goodness of fit metrics.

Computational Consumption The execution time required for a structural FEM is vastly larger than executing an empirical regression. Therefore, the mesh will need to be fine enough to be usable but coarse enough to be efficient. While the assumption could be made that aircraft manufacturers may have access to high performance computing, this thesis will need to be performable for a doctoral student without access to high performance computing. There also needs to be some sense of what "fine," "coarse," and "efficient" are in this case. For a wing sizing a design with a span of 200 feet, how long is an acceptable run time? This problem is exacerbated by the RBDO methodology. We wish to optimize the design rather than solely analyze a candidate design. So, at least 100 cases will need to execute on the order of a few weeks.

Coupled Disciplines One of the major obstacles is the synthesis between disciplines. We need the design environment to be interdisciplinary. Typically, an advanced CFD code is used to perform a high fidelity analysis of the aerodynamic forces on the wing. These forces translate into loads which result in stresses and deformations in the wing. However, because the wing deforms under these loads, the loads themselves have changed, prompting a new aerodynamic analysis of the new shape. This iteration can be excruciatingly painful when the CFD and FEM models take days to execute. To avoid this issue, some methods make independence assumptions.

While Sutter's tale is a touch outdated, his team seems to have taken a de-coupled approach. The aerodynamics team worked independently of the structures team. While the process could have been iterative, the rush to redesign implies a straightforward progress rather than cyclical improvements. Still, the ideal method would leverage the highest levels

of fidelity in both structures and aerodynamics.

Ingredients for Physics-based Environment

We need an environment that will overcome these challenges. Three are five main functions that the wing-level environment must perform:

- Describe the wing geometry.
- Generate a physics-based model (e.g. mesh).
- Determine aerodynamic loads based on load cases and structural deformation.
- Size the wing structure based on aerodynamic loads.
- Analyze the wing on a number of key metrics (objective and constraints).

Describe the Wing Geometry At the vehicle level, the wing is little more than a collection of rectangles and triangles. Only a few wing-level parameters exist like aspect ratio, sweep, and taper ratio. For a physical environment, a physical model must be generated. This step is essential for OML generation; for example, the values used at the vehicle-level are often aggregates. The vehicle-level taper ratio may be 0.19 (tip chord divided by root chord), but the wing will typically not have a constant taper ratio throughout the entire wing: it varies. This is an example of one metric on the vehicle-level becoming tens of metrics on the wing-level. Therefore, a tool is need to create or accept a wing geometry.

A common tool in the literature is NASA's vehicle sketchpad (VSP). It is a geometry tool developed to evaluate aircraft concepts. In fact, it was developed to visualize the geometry more easily in order to use more complex analysis earlier in the design process [130].

Generate a Physics-based Model Similar to geometry generation, a physical model must be created. This means translating the design from the high level metrics to physical component definition. There also needs to be a process to prepare the physical model for analysis. For an FEM approach, this would be generating a mesh which is "defined as any of the open spaces or interstices between the strands of a net that is formed by connecting nodes in a predefined manner" [131]. Meshes will be discussed further in Section 4.2.2.

Generating a mesh is labor intensive. For an RBDO method, this step needs to be automated. Generating meshes is an old field [132], but we need a tool to perform this with minimal user effort.

Determine Aerodynamic Loads The structural deformation is a direct result of aerodynamic loads. These loads are applied throughout the life of the aircraft. We are especially interested in defining these load cases parametrically such that various cases may be examined (rather than solely focusing on cruise). Therefore, an aerodynamic analysis tool is required. A number of CFD tools are available such as STAR-CCM+ [133] and FUN3D [134]. However, these tools are too intensive for a structural sizing environment. Therefore, a simplified (approximated) aerodynamics tool is needed.

Size the Structure Once the model has been defined and the aerodynamics approximated, the structure must be analyzed and sized. The analysis of the structure results in the deformations and stresses/strains. The sizing portion varies the size (component thicknesses) until the stress and strain constraints are satisfied. There are a number of tools available for this step (LS-DYNA [135], ANSYS [136], MSC Nastran [137]).

Analyze Wing-Level Metrics The analysis is complete when the sizing has been completed. However, because the end result is to perform optimization, this process must be executed using a wrapper that reads and writes data. This allows the process to be per-

formed for a number of different wings while recording the performance values for each. This step transforms a series of tools into an environment.

The Rapid Airframe Design Environment

The list of environments that are currently available to perform all of these steps is extremely short. The conclusive result from the literature search is that the best environment available is the Rapid Airframe Design Environment (RADE) [138, 139]. RADE is a python-based toolkit that performs structural wing sizing with a number of tools that can be used to accomplish our purposes.

Wing Geometry: VSP One of the obstacles to higher-fidelity (physics-based) analysis is the increase in design freedom and the pre-processing effort required. RADE overcomes these obstacles by parametrically generating the structural geometry using VSP. With a VSP file and set of design variables, the end-user can easily generate an outer mold line (OML) using the interface.

Physics-based Model: AFEM RADE utilizes another tool called the Aircraft Finite Element Modeler (AFEM) developed by Laughlin Research [140]. The AFEM software generates meshes for wing components without a human-in-the-loop. The mesh size is variable, allowing the user to define the level of computation time.

Approximating Aerodynamics: AVL The vortex lattice method is used to approximate aerodynamic characteristics of the wing by assuming an infinitely thin lifting surface to compute lift and induced drag. There are four theorems that form the backbone of the vortex lattice method (Boot-Savart, Outtake-Joukowsky, Herman Von Helmholtz, and Portland lifting-line). The Athena Vortex Lattice (VAL) method is software that utilizes the vortex lattice method on aircraft configurations [141]. AVL can be used to compute Oswald's efficiency factor, span efficiency, angle of attack, lift, and induced drag. This tool can be used

as a proxy for CF

Structural Sizing: Nastran Nastran (formalized NASTRAN for NASA STRucture ANalysis) is a finite element analysis software developed by NASA. It is now publicly available and maintained by the MacNeal-Schwendler Corporation (Nastran is often referred to as MSC Nastran) [137]. The source code is used to perform a number of analyses including modal, buckling, flutter, static aeroelastic, dynamic aeroelastic, and design optimization. Nastran requires a bulk data file in order to run. RADE handles this through its model synthesis module which automatically generates the bulk data file from the structural geometry. Nastran can size the wing based on the analysis settings. The most basic function is to size the wing using stress constraints.

RADE Process

A generic process performed by RADE is depicted in Figure 21. The process begins with a VSP file detailing the wing configuration. The geometry is scaled using the design variables (aspect ratio, wing area, etc.) to create the OML geometry. It is then translated into the structural geometry by generated the wing components (spars, ribs, and skin). The material of each part is applied with the user defined properties (e.g. modulus of elasticity). AVL is then used to evaluate the loads using the wing geometry and structural properties. AVL is evaluated after the wing shape (geometry) is created and also the stiffness (derived from the shape and material properties). The loads and structural properties are combined into a bulk data file via the model synthesis module. Nastran is then used to perform structural analysis and sizing.

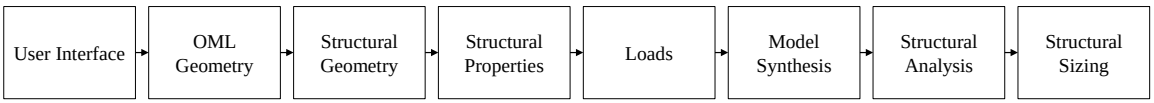

Figure 21: RADE Process for Structural Sizing

Aspect Ratio and Sweep Demonstration We can easily demonstrate the utility of the user interface with RADE. Figures 22 and 23 compare the OMLs of varying aspect ratio and sweep values, respectively. Figure 22 compares a wing with aspect ratio 9 to a wing with aspect ratio 11. Figure 23 compares a wing with sweep 35°to a wing with sweep 39°. Both figures include an overlay to highlight the change in the OML.

Figure 22: Change in Wing Shape: Aspect Ratio 9 and 11

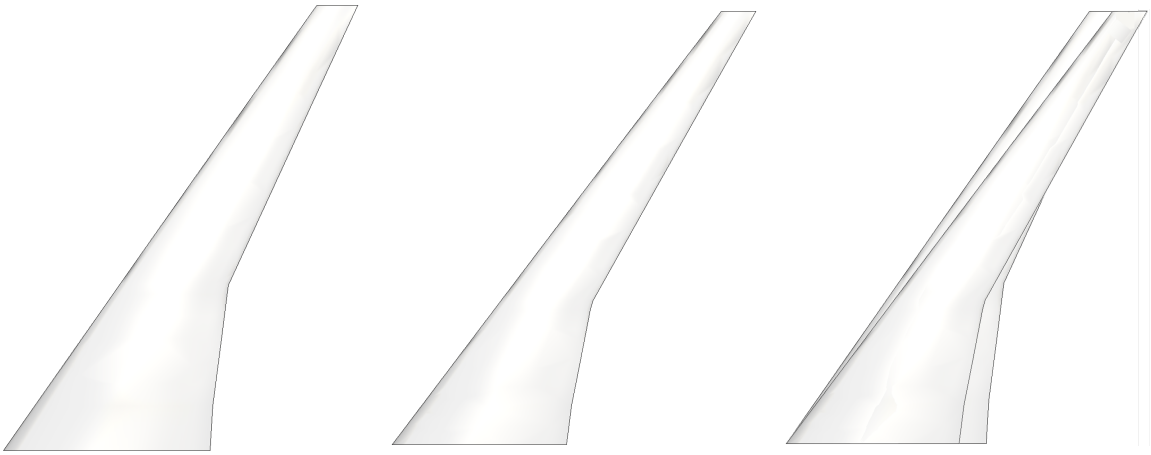

(a) Aspect Ratio = 9 (b) Aspect Ratio = 11 (c) Aspect Ratio 9, 11 Overlay

Note that these images were taken individually and superimposed. Each image normalizes the span such that the two aspect ratios appear to have the same span when they do not. Therefore the only visual change is the higher aspect ratio wing shows smaller chord lengths.

These images were created using the user interface. Only aspect ratio and sweep were changed to take the images. RADE is wrapped such that a single file with a variable matrix can be used to evaluate the number of rows in the matrix. Therefore, we can conclude that RADE appears to be a viable option for a physics-based, wing-level structural analysis and design environment.

Research Result 1.1

Figure 23: Change in Wing Shape: Sweep 35°and 39°

(a) Sweep = 35° (b) Sweep = 39° (c) Sweep 35°, 39°Overlay

The Rapid Airframe Design Environment (RADE) can be used to perform physics-based, structural wing-level design.

While RADE is the environment selected to answer this research question, the components of RADE (VSP, AFEM, AVL, Nastran) are performing the actual analysis. RADE itself is a toolkit rather than a new tool altogether to perform wing design.

This is not a formal hypothesis because it cannot be tested as it is stated. It is more a result of the literature review. Other implementations of physics-based wing design and analysis will not be used to test against RADE's capability. Although, RADE will eventually be integrated with a conceptual design environment. We would expect that the wing weight estimation given by RADE would be roughly equivalent to the conceptual design tool (assuming it is an industry standard tool).

4.1.2 Research Question 1.2: Jig Shape Estimation

The desire for a physics-based environment is twofold. The first motivation is that uncertainty is realized during the preliminary design phase rather than the conceptual design phase. This calls for a change in fidelity between design stages as described by Nam. This step represents the gain of some new knowledge about the design. As depicted in Figure 4, the preliminary design phase represents this change. The second motivation is that the mit-

igation actions require a physical model to be explicitly captured because they are physical changes. We wish to apply these changes directly to the model rather than estimate their effect on the performance by some transformation function. If direct modeling is infeasible, then a transform will be developed instead.

RADE relies on a input VSP file of a wing configuration. The assumption here is that aerodynamic shape optimization has already occurred and now the design has progressed to structural sizing. This process mimics the description of Sutter ("We had pretty much finished our 747 aerodynamics testing... but our structures people began getting lots of troubling data from wind-tunnel testing" [26]). The design was transitioning from aerodynamics testing to structures testing. Therefore, a key assumption for the RADE methodology is that the input VSP file is an aerodynamic shape. The benefit of this approach is that the aerodynamics and structures are decoupled: the flight shape is fixed such that the wing structure can be sized independently [142, 143].

Generally a wing has four different shapes: cruise, jig, production, and elastic [144]. The cruise shape (also called flight shape) is the shape of the wing deflected under a 1g load. Here the "g" refers to the gravitational pull on the entire aircraft. It is equal to the weight of the aircraft rather than the weight of the wing. It is the desired aerodynamic shape to maximize lift over drag. The jig shape is the "0g" shape, or the shape the wing would take without gravity. This shape is also called the manufactured shape. The production shape is also a 1g shape, but here the "g" refers to the wing weight. The elastic shape is the result of elastic effects of flight such as during maneuvers.

So, on which of these wing shape should mitigation be applied?

Initially the flight shape may be desired shape to modify using mitigation actions because it affects fuel consumption and range. Indeed, conceptual design tools care almost exclusively about cruise characteristics. The production shape is the wing under static, 1g conditions. The elastic shape cannot be directly affected: it is result of the wing's flexibility and aeroelastic properties. In fact, all the wing shapes are results rather than controls

except the jig shape. The jig shape is the manufactured shape so it is the shape that can be affected directly. Of course, affecting the jig shape will also affect the cruise, production, and elastic shapes as well. But this is the shape we need to modify because it is the shape we control. Therefore, if mitigation is to be applied to the wing design, then the mitigation action should be applied to the jig shape.

Thought Experiment This hypothesis will not be formally tested. It is more a matter of preference: we could affect the flight shape indirectly via the jig shape. This approach would require a transformation from the jig space to the flight space. Consider the historical example of twist. The jig shape will have a set twist at 0g (no gravity). This exact shape, when in steady 1g flight, will deform to the desired aerodynamic cruise shape. The deformation between shapes is due to gravity as well as aerodynamic forces. We expect that the shape undergoes an induced twist; that is, the wing will be rotated due to aerodynamic forces. Thus, this design will have a jig twist (twist of wing at 0g) and a cruise twist (twist of wing at 1g). The difference between these wing twists is the induced twist.

Now consider we want to twist the wing like Sutter. If we want to twist the cruise shape, we would have to transform what level of twist to the jig shape would result in the final desired twist. The induced twist is a function of the jig twist, so the change in twist is not guaranteed to be constant. Therefore, applying mitigation to the flight shape requires a transformation: we would need to test multiple jig shape twists to determine which would result in the desired flight twist.

$$Twist_{Jig} + Twist_{Induced} = Twist_{Cruise} \tag{8}$$

$$Twist_{Jig} + Twist_{Mitigation} + Twist_{NewInduced} = Twist_{NewCruise} \tag{9}$$

If we were determining the desired flight twist, we could set the mitigation in the flight shape space and assume that some level of twist change to the jig shape would result in the

desired flight twist. However, we do not know a priori what flight twist is needed to satisfy the violated constraint. Therefore, there is no need to place mitigation in the flight shape space when we cannot directly affect it. Placing mitigation in the jig shape space prevents the need to create a transformation between shapes.

Jig Shape Determination

Because the aerodynamic shape is assumed to be an input, RADE will need to determine the corresponding jig shape. This can be done using a fixed-point iteration with the initial guess as the aerodynamic flight shape. The process is outlined in Figure 24.

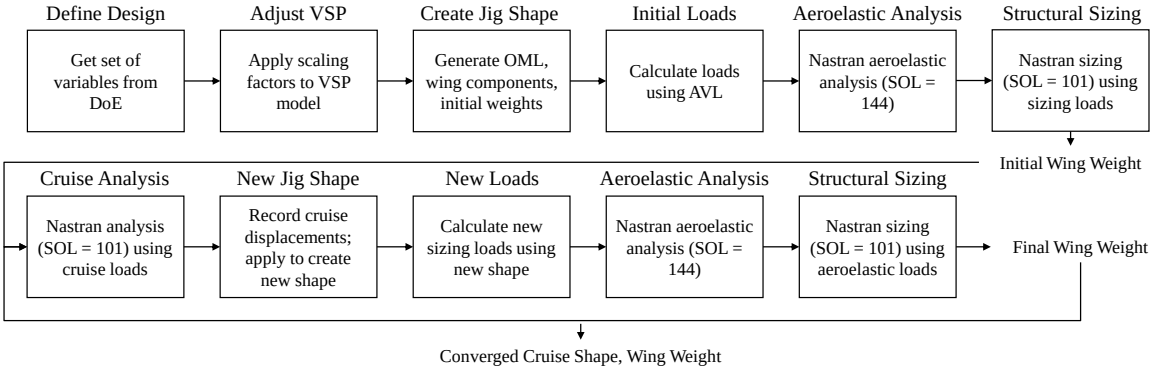

Figure 24: Structural Sizing and Jig Shape Convergence Loop

The first half of the flowchart is identical to the process shown in Figure 21. However, because the jig shape needs to be determined from the flight shape, the design enters a new loop after initial sizing. The first analysis is cruise analysis to determine the displacements at cruise for the given shape. The cruise displacements are then *subtracted* from the initial shape (which is the optimized aerodynamic shape). The term *subtracted* here means that the tip deflection caused by the cruise loads (which will cause an upward deflection) are decreased from the input shape. The jig shape tip deflection is always going to be less than the cruise tip deflection. The new shape undergoes the same sizing process as before. Once sized, the new shape goes through cruise analysis once again to subtract the displacements. This process is repeated until the wing weight does not change.

However, we are not sure a priori how this process compares to other algorithm designs. The default loop is the single loop: both shape and weight are changing simultaneously. This type of loop can be compared to a double loop where the shape is held constant while the weight has a few iterations to converge. This contrast is shown in Figure 25.

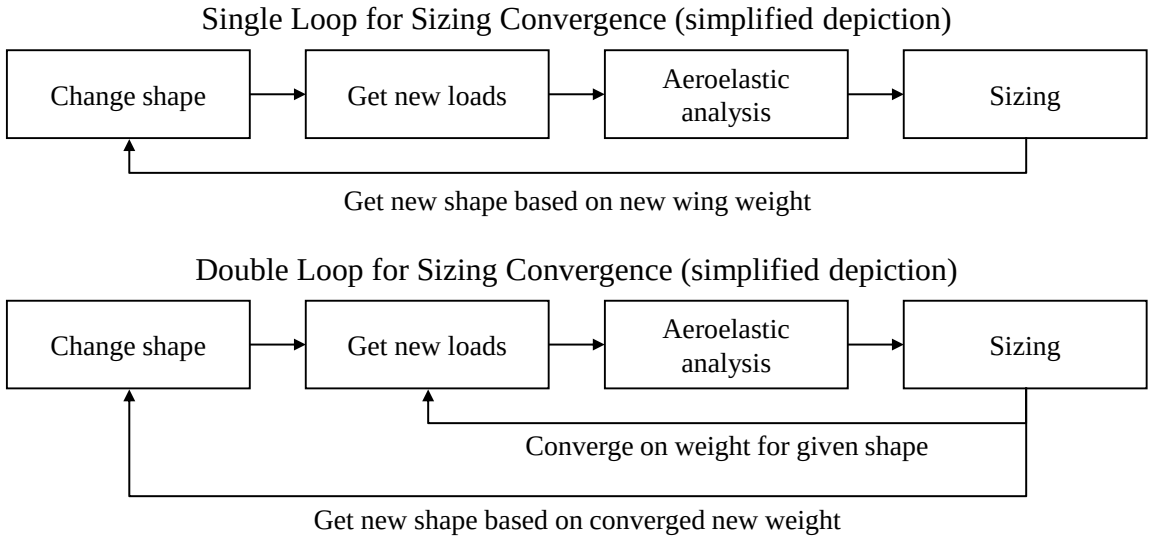

Figure 25: Contrast between Single and Double Loop Jig Shape Convergence

We would like to test to see if this convergence is reliable and how it compares to other convergence algorithms. This results in Research Question 1.2:

Research Question 1.2

How does the sizing algorithm affect final jig shape and size?

This process was published by Corman [139], but he states that the process is untested. We can easily provide a null hypothesis that the default process will perform as well as any other process. However, changing both shape and weight may result in divergence, especially if the initial sizing is extremely high or low. Therefore, we can qualify our hypothesis, restricting it to monotonic convergence:

Hypothesis 1.2

If a single loop convergence that simultaneously alters both weight and shape monotonically converges on a solution, then adding additional loops will converge on a similar (~1%) solution.

In order to make this hypothesis testable we specify the level of similarity between the results. This number is largely arbitrary but necessary to form a proper hypothesis; however, the baseline RBDO method did use surrogate models in the final optimization. As we expect these surrogates to be accurate on the order of about 1-2%, we can accept some approximation error at this point.

We will test this hypothesis against various algorithm designs in Chapter 5.

4.1.3 Research Question 1.3: Mitigation Modeling

Now that we have a physics-based environment and determined the wing shape that will be modified (jig shape), the mitigation actions need to be directly captured in the model:

Research Question 1.3

How can post-sizing physical design changes to the wing be captured in the model?

While this should be simple in concept, we still need a process to implement the changes and demonstrate the change in the responses. As described in Figure 5 there are many variables at this stage in the design process. In fact there are a number of obstacles that the mitigation modeling process must overcome:

- Maintain size and shape from sizing convergence
- Affect geometry parametrically
- Allow for re-analysis

Maintain Size and Shape

Maintaining the size and shape from the sizing loop is vital because mitigation does not size the wing. This is particularly difficult because most formulations assume that the tool is used for wing sizing. Because this is post-sizing, we need a formulation that will not change the size or shape unless the mitigation action is specifically designed to do so. An example of changing the wing size (weight) would be adding an additional fuel tank. An example of changing the wing shape (geometry) would be the manipulating the twist. Ultimately the size and shape of the wing can be changed, but we do not want a process that will automatically scale the rest of the wing due to mitigation actions.

Affect Geometry Parametrically

As illustrated in Figure 5, the number of variables at the preliminary design phase is much larger than the conceptual design phase. Consequently, mitigation could have several hundred variables. The goal is optimization, meaning that the fewer the variables the better. Therefore, the mitigation should be collapsed down to as few variables as possible. For example, rather than defining a mitigation variable for each chord length along the span, using a linearized taper ratio would collapse all those variables into three: root chord, tip chord, and taper ratio. This is highly desirable.

Allow for Re-Analysis

Because we are addressing a capability gap, the effect of the mitigation needs to be demonstrated as clearly as possible. To this end we the implementation will perform the sizing, record output values, apply mitigation, record new output values, and then compare. The change will need to be explicit. Essentially this calls for an option to toggle mitigation on or off.

Utilizing VSP

When considering physics-based design environments, there were a number of obstacles listed in Section 4.1.1. Some of them are listed here as well (number of variables, parametric definition, ease of implementation). In fact, RADE already has the capability to geometrically scale and size wings based on a given VSP file. This was designed specifically to reduced effort on the user. Therefore, we can expect that the same functionality can be used to modify an existing (sized) wing while maintaining the integrity of the wing.

Research Result 1.3

If a parametric tool was used to generate a wing shape from a set of variables and VSP file, then the same tool can be used to parametrically affect the wing geometry without re-sizing.

This will be explored with a sensitivity study in Chapter 5.

4.2 Research Question 2: Uncertainty Quantification and Correlation

Capability Gap 2 describes the gap current RBDO aircraft conceptual design methods in uncertainty modeling. Because most characteristics of the uncertainty are unknown, authors have typically used assumptions to progress the analysis. Before we jump to the implementation of uncertainty in the design process, we will first investigate the types of uncertainties that are most relevant (called uncertainty taxonomies). Then we will move toward common modeling approaches and also correlation techniques. Hopefully methods already exist that can be used to describe and correlate uncertainty within this work's methodology.

The overall process to fill Capability Gap 2 is as follows:

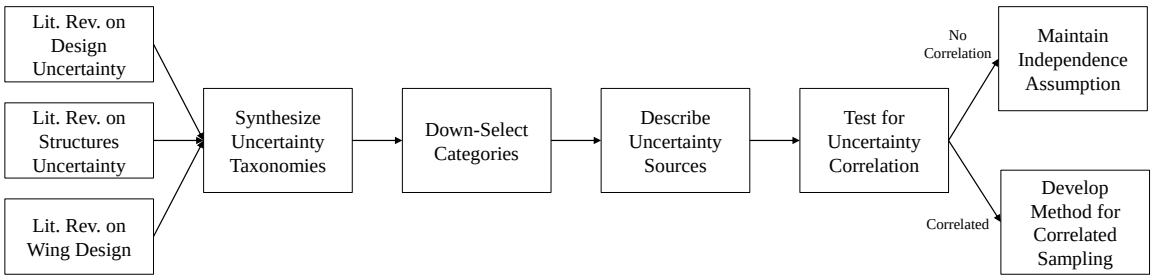

Figure 26: Approach to Fill Capability Gap 2

4.2.1 Research Question 2.1: Development of Uncertainty Taxonomy

Modeling uncertainty requires an acute understanding of the sources, distinctions, and impacts. The goal of developing a taxonomy is collectively exhaust all the sources of uncertainty as well as group individual uncertainties. For example, epistemic and aleatory uncertainty were discussed at length to appreciate the difference between random and systematic uncertainty in Section 2.4.1. Random uncertainty can be isolated and removed through repetitions whereas epistemic uncertainty cannot. Now, uncertainty taxonomies from various fields will be presented and synthesized to develop a new taxonomy for our purposes.

Taxonomy for the Design and Development of Complex Systems

Let's start with the taxonomy introduced in Section 2.4.4 depicted in Figure 13. The main categories of uncertainty were ambiguity, epistemic, aleatory, and interaction. While Thunnissen decomposed each category further, the epistemic uncertainty category was most akin to the current problem (the other categories were ambiguity, aleatory, and interaction), which decomposes into sub-categories of behavioral, model, and phenomenological. Ultimately, we chose to look at model uncertainty. Thunnissen breaks down model uncertainty into three other types: approximation, programming, and numerical. These sub-sub-categories, however, are unsuitable for our purposes because they imply error. Each of these assume there is a "truth" value and that value would be known if we had exact

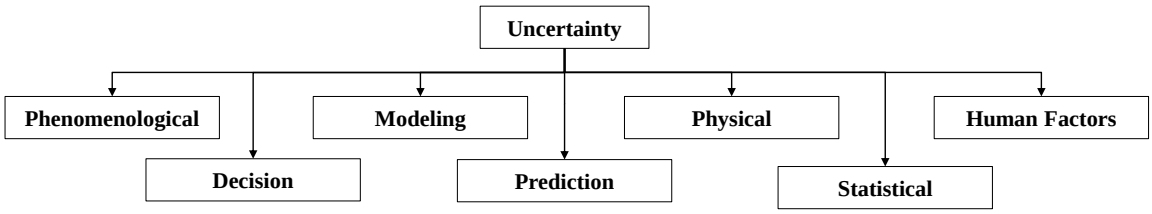

Figure 27: Depiction of Uncertainty Taxonomy for Structural Engineering [53]

precision or coded properly. Numerical uncertainty is closes because it is caused by the discretization of continuum mechanics (a simplifying assumption). Classifying our uncertainty as "numerical", however, would be misleading.

Structural Engineering If we scope the engineering problem down to structural design, we can draw on the field of uncertainty quantification in structural engineering. Melchers [53] developed such a taxonomy for structural reliability depicted in Figure 27 and described in Table 5.

Clearly there are many more categories in this taxonomy compared to Thunnissen's. On the other hand, this is a single level taxonomy whereas Thunnissen's was multi-level. Some categories are similar, such as modeling and phenomenological, and some are new, such as statistical. Some groups have changed names but are very closely related (physical and aleatory, human factors and ambiguity).

Wing Design Uncertainty The first taxonomy presented was of general design of complex systems. The second was specific to structural engineering. The last will be a collection of work around the uncertainty in wing design. Unlike the previous two taxonomies, this list is integrated from many sources rather than taken from a single source. Some authors focused only one some sources while others formed sub-taxonomies. It is summarized in Table 6.

Table 5: Description of Uncertainty Taxonomy for Structural Engineering [53]

Uncertainty Type	Description	Examples
Phenomenological	Unimaginable behavior, particularly characteristic for novel projects or advancing the state of the art	Aeroelastic flutter (Tacoma Narrows Bridge)
Decision	Arises when determining whether or not a limit state has been violated	Crack length (Southwest Airlines [145])
Modeling	Arises from using simplified relationships; difference between observed and predicted responses	FEM, CFD
Prediction	Estimation of some future state of affairs; lack of knowledge about proposed idea	Material behavior
Physical	Inherent randomness of a basic variable	Physical dimensions (manufacturing tolerance)
Statistical	Arises when a simplified PDF is implemented	Distribution (normal vs. uniform), parameter values (mean, standard deviation)
Human Factors	Variation in task performance and gross errors	Ignorance, carelessness, negligence [146, 147]

Taxonomy Synthesis

Table 6 shows a taxonomy solely from previous work in the aircraft wing uncertainty realm, but we can clearly see some similarities between these three taxonomies. There are three categories that appear in each of the taxonomies: aleatory, model, and human. Aleatory uncertainty is present in the first and third taxonomies and present in the second in the form of "physical" uncertainty. Modeling uncertainty (model, modeling, and model form) also appears in all three. Each of the taxonomies represent the human uncertainty but in different ways (behavioral, decision/human factors, and safety factors). Statistical appears

Table 6: Taxonomy of Uncertainty in Aircraft Wing Design

Uncertainty Type	Description	Examples
Material [148, 149, 150, 151]	Estimating material properties (especially composites)	Variation between stiffness Component thickness
Model Form [152]	Modeling approach chosen	Mesh (size and shapes) Sub-component approx (stiffeners)
Parametric [96]	Model inputs with low degree of confidence	Material Properties Loading Conditions
Safety Factors [54, 149]	Decisions made by management as to what is acceptable	Allowable stress Flutter speed
Aleatory [153]	Variation in design or performance due to natural variation in conditions	Component orientation Angle of attack
Statistical [153]	Representing uncertainty using a specific distribution; uncertainty in PDF parameters	Distribution Distribution moments

in the structural and wing design taxonomies while phenomenological uncertainty appears in design of complex systems and structural engineering. This most likely because the wing design taxonomy was developed from published work that focused on implementing the uncertainty, and phenomenological uncertainty is very difficult to capture in design. The most unique category is an added category designated “Inputs” which includes two categories from the wing design literature review: parametric and material. Both of these uncertainties center around the values required for the model to run, such as defining flight conditions or material properties. The synthesis of these three taxonomies is presented in Table 7.

Table 7: Synthesis of Uncertainty Taxonomies

Category	Design and Development of Complex Systems (Thunnissen)	Structural Engineering (Melchers)	Wing Design (Various)
Aleatory	Aleatory	Physical	Aleatory
Model	Model	Modeling, Prediction	Model Form
Phenomenological	Phenomenological	Phenomenological	-
Statistical	-	Statistical	Statistical
Human Factors	Behavioral, Ambiguity	Decision, Human Factors	Safety Factor
Inputs	-	-	Parametric, Material

Developed Taxonomy

The synthesized taxonomy can be translated into the developed taxonomy. Section 4.2.1 will determine which of these categories will be used for this thesis.

Final Taxonomy

The rest of the approach is to be filled in Chapter 6. That Chapter will dive into the technical details of implementing a process to quantify and correlate the uncertainty sources. It would be prudent, however, to down select the categories before launching into the technical details. Table 9 is a table similar to Table 7 given in Section 4.2.1, but the categories have been down-selected.

Aleatory uncertainty is removed because our approach will remain within the modeling process. This thesis does not intend to manufacture or test a wing in a wind tunnel, nor does it intend to simulate that process. As a result, aleatory uncertainty is removed. More precisely, aleatory uncertainty at this stage is exactly zero. This is because the models are deterministic, and therefore repeating experiments would yield the exact same results. Consequently, aleatory is neglected as a category for consideration.

Table 8: Uncertainty Taxonomy for Conceptual and Preliminary Structural Wing Design

Category	Definition	Examples
Aleatory/Physical	Inherent randomness of nature	Component dimensions and orientation, manufactured thicknesses, final angle of attack
Human Factors	Variation in task performance and decision making	Ignorance/carelessness, Rules of Thumb (allowables)
Model	Arises from using simplified relationships; difference between observed and predicted responses	Empirical relationships, imperfections in meshing, mesh size, smear properties
Parameter	Variation in inputs that are not design variables	Material properties (modulus of elasticities across the wing), Flight conditions (pressure, temperature)
Phenomenological	Unimaginable behavior, particularly characteristic for novel projects or advancing the state of the art	Aeroelastic flutter (Tacoma Narrows Bridge)
Statistical	Representing uncertainty using a specific distribution; uncertainty in PDF parameters	Distribution Distribution moments

Phenomenological uncertainty can be removed for two reasons: first, we have scoped our problem down to a conventional wing; and second, it is incredibly difficult to quantify without introducing more uncertainty. As stated by Melchers, this type of uncertainty is most influential when developing new or novel designs. If we were attempting a blended-wing body or truss-braced wing configuration, phenomenological uncertainty would be pertinent because there would almost certainly be phenomenon at stake that we have yet to understand. Still, it would be difficult to model because we do not know what we do not know.

The last category that is removed is the human factors category. It is removed due to the assumption that it is equally effective across all designs such that the absolute value

Table 9: Down-Selection of Uncertainty Sources

Category	Included/Not Included (Y/M/N)	Rationale
Aleatory	N	Transitioning between models, not experiments
Model	Y	Results are entirely dependent on model analysis and assumptions
Phenomenological	N	Application assumed to be conventional
Statistical	M	Included if distributions cannot be rigorously determined
Human Factors	N	Assumed constant across designs
Parametric	M	Parameters required for model execution require assumptions

of the uncertainty is shifted. If we included some configurations (from the analysis of alternatives, for example) that were especially difficult to manufacture, we may be inclined to prescribe the likelihood of human fault to some configurations rather than others. It shifts the expected reliability value evenly across the designs. Therefore, because it is expected to affect all designs equally regardless of value or margin, it is neglected.

The last note is that the "input" category was changed to "parametric" which includes uncertainty about any of the inputs to the model. These parameters are not the variables of interest (such as aspect ratio, wing weight, block fuel, etc.) but the parameters that are required for the model to execute (modulus of elasticity, pressure at cruise, etc.) and have high impact on the final results. The final taxonomy is presented in Table 10.

The development of this taxonomy can be summarized as follows:

Research Result 2.1

If the developed design process is solely dependent on model outputs, then model

Table 10: Uncertainty Taxonomy for Conceptual and Preliminary Structural Wing Design

Category	Definition	Examples
Model	Arises from using simplified relationships; difference between observed and predicted responses	Empirical relationships, imperfections in meshing, mesh size, smear properties
Parametric	Variation in inputs that are not design variables	Material properties (modulus of elasticities across the wing), Flight conditions (pressure, temperature)
Statistical	Representing uncertainty using a specific distribution; uncertainty in PDF parameters	Distribution Distribution moments

uncertainty is the primary source of uncertainty.

The ultimate focus of this thesis will be on model uncertainty. In a way statistical uncertainty and input uncertainty are sub-categories to model uncertainty. For example, the inputs to the model are dependent, well, on the model. Therefore the two are not mutually exclusive. Similarly, the statistical distributions used to describe the uncertainty is dependent on which sources are identified within model uncertainty. Again, these two are dependent. Therefore, model uncertainty is the central focus.

4.2.2 Research Question 2.2: Quantifying Uncertainty

Research Question 2.2 seeks to capture the character of the uncertainty. The end goal is to describe the impact our lack of knowledge may have on design performance. The magnitude and trend of uncertainty directly impacts both the reliability and performance assessments. Therefore uncertainty cannot simply be defined by an arbitrary distribution with arbitrary bounds.

Research Question 2.2

How can the probabilistic description of the uncertainty be derived?

A taxonomy only groups uncertainty sources. It is a structured approach to enumerating

and describing the ways uncertainty can affect results. Developing a method to capture a specified type has already been the subject of much work which will be described here. A special emphasis will be on reliability methods (how uncertainty affects constraints) rather than robustness (how uncertainty affects variance).

Generally, the approaches for reliability-based design can be separated into numerical and analytical approaches. Analytical approaches work to manipulate the mathematical equations that determine feasibility and failure directly. Usually these approaches require an integration such that the result is a probability representing the area under a cumulative distribution function (CDF). These tend to be less computationally expensive than numerical methods given that the mathematical relationships are invertible and differentiable. This is not always the case; or, more generally, this cannot always be guaranteed. The result is that analytical methods are often employed on simplified models. On the other hand, numerical methods are much more computationally expensive. Rather than transforming a function and evaluating it to determine the area, the function is discretized to thousands of points to represent the entire space. This introduces uncertainty of its own which Mahadevan calls discretization error.

Some methods combine both of these approaches: if a given relationship is non-differential, a numerical approach of finite differencing can be used to approximate the derivative at a point (or, usually, thousands of points). On the whole, numerical methods tend to be far more popular with respect to engineering design as the field is moving toward CFD and FEM which are numerical approaches.

Constraint Approximation Methods

Reliability is defined by constraints. If the constraint values can be approximated accurately, then the uncertainty quantification problem is solved. Constraint approximation methods are the most prominent form of an analytical approach to reliability. For reliability calculation, the integrals of the constraints are required [154]. The most popu-

lar constraint approximation methods are first-order and second-order approximations (the acronyms FORM and SORM are frequently use to denote first-order reliability methods and second-order reliability methods, respectively). FORM [152, 155, 156, 157] and SORM [158, 159, 160] have been used in engineering design, and many have worked to improve their efficiency.

Approximating further, the entire integral may not be required but rather a single point that will contribute most to the reliability calculation. This point is called the Most Probable Point (MPP). Because this point is the most significant to determining reliability, some approaches focus the computational resources on increasing accuracy at this point. Methods such as these add an additional optimization formulation to find the MPP. As a result, some separate MPP methods from constraint approximation methods [161].

The question becomes whether analytical approaches are usable for this thesis. There are two main issues with constraint approximation methods (aside from the invertible and differentiable assumption, which is non-trivial). The first issue is that the area is an aggregate of all compliant realizations, and consequently all failed realizations as well. Because the design is assigned a single aggregated value, determining the level of mitigation required to recover the realization becomes troublesome. The second issue is that these methods consider constraints independently of each other. For example, a design may have a 90% change of satisfying a stress constraint and a 75% chance of satisfying a bending constraint. But the design as a whole is not easily given a total reliability metric. Because the entire area is aggregated, determining the union between these two probabilities is not straightforward or perhaps even possible. As observed by Nam, FORM and SORM generally assume that each constraint can be treated independently or that only the most active constraint is relevant, and do not consider joint probability distributions [122].

Because designs are being compared vis-a-vis, a metric representing the design reliability rather than a constraint reliability is preferred. Therefore, we can conclude that constraint approximation methods yield independent constraint reliabilities without infor-

mation regarding the union or extent of constraint violation. Therefore, they cannot be used in a study aimed to demonstrate the impact of mitigation to failed design realizations.

Sampling Techniques

This leads us to numerical approaches. Monte Carlo sampling is by far the most frequently used approach for uncertainty sampling approaches in engineering design [162, 163, 164] and in reliability-based design [165, 166]. Sampling methods are so ubiquitous, in fact, that Helton at Sandia Labs referenced 14 sources reviewing the effectiveness and use of Monte Carlo simulations alone [167] (these are not 14 references of Monte Carlo uses, these are 14 reviews of Monte Carlo uses). Due to the ease of implementation, the computational expense is accepted, though often quite prohibitive [168].

Other than computational expense, other considerations arise with sampling based techniques [169, 170]. A key challenge for a single distribution is ensuring the samples drawn are appropriately representative of the parent distribution. When multiple distributions (random variables) are involved, independently drawn samples can produced unintended correlations. These correlations can be the result of a small sample size or simply by chance. On the opposite side, perhaps the designer desires to sample distributions *dependently*; that is, correlation is intended amongst the random variable samples. Sampling methods such as Latin Hypercube Sampling are not designed to handle both unintended and intended correlation.

Ferson and Oberkampf highlight the challenges of Monte Carlo methods: [91, 171]

- Correlations and dependencies are often ignored
- Input distributions are usually not available (statistical uncertainty)
- Mathematical structure of the model is questionable
- Struggle to represent large epistemic uncertainty of rare events (tail uncertainty)

- Compounding effect of several epistemic uncertainty variables treated as random variables

Ignored Correlations The independent uncertainty assumption runs rampant in the UQ&M community [97]. Ferson describes: "... correlations are commonly omitted from risk analyses and the default assumption of independence is used even when there is no evidence whatever in support of this assumption" [91]. Similar to the difficult of determining PDF distributions, there is such little data to support or refute correlation that it is often ignored altogether.

The works that include correlation require the correlation to be known a priori. Padulo, for example, uses correlation of inputs in aerodynamic design, but seems to have no basis for correlation quantification [172]. Zaidi uses copulas to correlate aircraft technology impact factors, but prescribes the correct copula based on intuition [173].

As a result, uncertainty in aircraft design is often considered to be independent without proof [174]. The inclusion of a correlation algorithm is often considered trivial, as in Green's work: "The assumption of the variables being statistically independent is not required; correlation between the variables can be easily accounted for within the formulation at the cost of more computational work." Green is making the statement that the implementation of the correlation is trivial, though there is no mention of methodology or process by which this correlation can be determined or quantified. Padulo also states that correlation of input variables can be carried out in a straightforward manner using decomposition [172]. Green also states: "Subsequent studies should fully consider any possible statistical correlation between the uncertain variables... the potential number of deterministic and uncertain variables could be significantly more for many cases of interest." In other words, the correlation is considered to be outside the scope of the engineering work. If it is already available, use it; if not, then just assume independence.

However, this issue may be addressed indirectly. For example, if the uncertainty is

applied to the design itself the effect on the constraints will be correlated. On the other hand, if the uncertainty was applied directly to the constraints, then each sample will be independent and most likely inconsistent (a draw increasing weight and a draw decreasing drag, for example). Therefore, if we apply the uncertainty to the design, a portion of the correlation will be accounted.

Unknown Input Distributions This is a characteristic that plagues uncertainty quantification. Using a PDF is a novel approach, but only works well when the parameters of the distribution are known as well as the distribution itself. The throw of the die is the best example of this. If the die has six faces and is perfectly even, the PDF is known as a discrete uniform distribution from 1 to 6. Even if the uncertainty in aircraft conceptual design is aleatory, the PDF is not defined because the sample size required is infeasible. Epistemic is, of course, much worse because it is systematic. This issue will be discussed further when alternative approaches to PDFs are discussed.

A common approach that has developed is to either use a uniform distribution between known bounds or a normal distribution with a defined mean about the expected value and standard deviation that seems appropriate. The uniform distribution approach comes from Laplace's Principle of Insufficient Reason [99], which is to say that applying anything other than uniform would be to introduce additional uncertainty. The normal distribution, however, is derived from the Central Limit Theorem which states that the probability distribution for the sum of a large number of random variables approaches a normal distribution irrespective of the distributions of the individual random variables [175, 176]. This is essentially taking the mean of many samples which will converge on a normal distribution. Of course, a normal distribution is unbounded, which may or may not be desired.

Modeling Rare Events Every day there is an extremely small probability of an extraordinary event occurring. Melchers refers to this as the "tail" effect (the tails of a normal distribution approach negative and positive infinity). Mathematically, the existence of these

events inhibits the performance of the environment because the impacts have such high relative magnitude. For our purposes, because extreme failures cannot be recovered, the extrema should affect each design evenly and therefore more or less cancel itself out. The assumption here is that 100% reliability is not necessarily the goal. This is comparable to what insurance companies refer to as "Acts of God": no amount of preparation could have prevented or mitigated the damage [177].

Compounding Effects of Many Variables This consideration is the child of the previous two considerations. When the number of epistemic uncertainty variables, treated as random variables through PDFs, and the extreme events are included in the PDFs at low probability, the likelihood that an unusual event is selected greatly increases. Moreover, a single draw from any of the uncertainty distributions can cause the extreme value to propagate throughout the analysis. Therefore, the problems of unknown distributions and rare events are magnified when many uncertainty variables are considered. Conversely, if many uncertainty variables are considered with bounded distributions, the realizations are more or less averaged out. This phenomena will be monitored as the results from the uncertainty analysis are presented, though Ferson and Oberkampf do not quantify how many is too many.

Sampling Thought Experiment

We have briefly reviewed two approaches to uncertainty quantification and reliability: analytically (constraint approximation methods) and numerically (sampling methods). We saw that treating each constraint individually and aggregating the reliability of each was unsuitable for a mitigation demonstration. Now let us test the usability of sampling techniques.

We wish to replicate the temporal aspect of the design process moving from conceptual to preliminary design. In many ways we wish to "follow" a design through the process: define design and margin variables, draw a set of uncertainty values, evaluate constraints

to determine compliance, redress with a mitigation action, and re-evaluate to determine recovery. This process can be repeated for a new set of uncertainty conditions. Sutter's wing was just one of many that could have come his way in the development process. Indeed, sampling is very similar to scenario analysis for decision making. Therefore, we can conclude that given a sampling technique is not too computationally expensive, it will be suitable to demonstrate the impact of propagating design knowledge upstream. A Monte Carlo approach will be used as it is the most ubiquitous of the sampling approaches.

Alternatives to PDFs

Other approaches are more intrusive. These approaches attempt to redefine how statistics should be used to quantify uncertainty. A popular example is interval analysis developed by Ferson [98, 91, 89]. Ferson argues that when modeling ignorance (epistemic uncertainty) absolutely no knowledge is known about the distribution between the bounds. Therefore, applying statistics based on PDFs is incorrect. Instead, simply the bounds (or intervals) should be used for the analysis. An interval is not the same as a uniform distribution, as is commonly used as a PDF when no knowledge is known about the distribution. The result is that little known between the bounds.

Many types of uncertainty quantification approaches exist, such as clouds theory, evidence theory, fuzzy theory, imprecise probability theory, interval analysis, and probability theory, to name a few [171, 178, 179, 180]. Unfortunately, most of these methods have not gained significant traction in the uncertainty quantification field since they were developed in the early 2000's, let alone the engineering design field. One reason may be that although these methods more accurately characterize epistemic uncertainty, they shroud the clarity of the results: the associated conclusions are, well, more uncertain. Consequently they may not be as influential to decision makers.

Decomposing Model Uncertainty

The result of the uncertainty taxonomy developed is that model uncertainty will be the focus. However, this category is still too broad to provide insight into uncertainty quantification. Two authors (Thunnissen and Mahadevan) have decomposed model uncertainty into the following sub-categories:

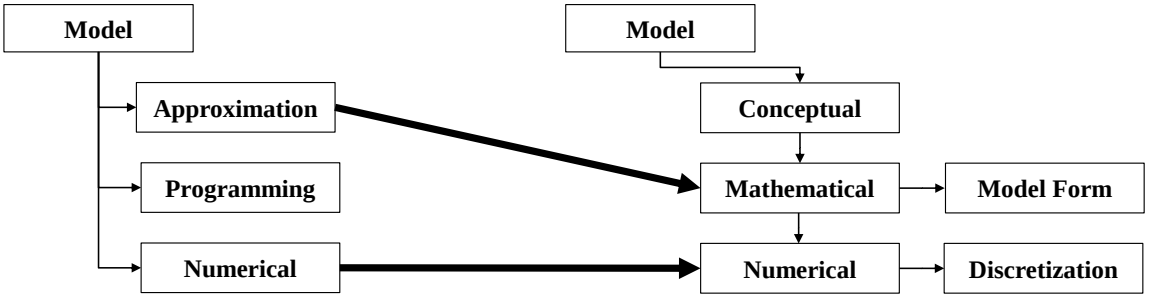

Figure 28: Decomposing Model Uncertainty: Synthesizing Thunnissen's (left) and Mahadevan's (right) Model Uncertainty Decompositions

Thunnissen lists approximation, programming, and numerical error under the umbrella of model uncertainty. Notice the subtle change to "error" rather than uncertainty: here the truth value is assumed to be known. Numerical error, for example, is often a result of truncation. Mahadevan's decomposition is similar, though cascading. Essentially Mahadevan states that the greatest is conceptual uncertainty, or the ability to understand and describe real processes using the model. Beneath that is mathematical uncertainty which is similar to Thunnissen's approximation error. Model form error is the difference between the predicted results of the model and experimental observations, as depicted in Figure 29. The last sub-category is numerical which has a sister category called discretization error.

Due to the absence of experimental results, we cannot use model form error. Therefore we are left with discretization error.

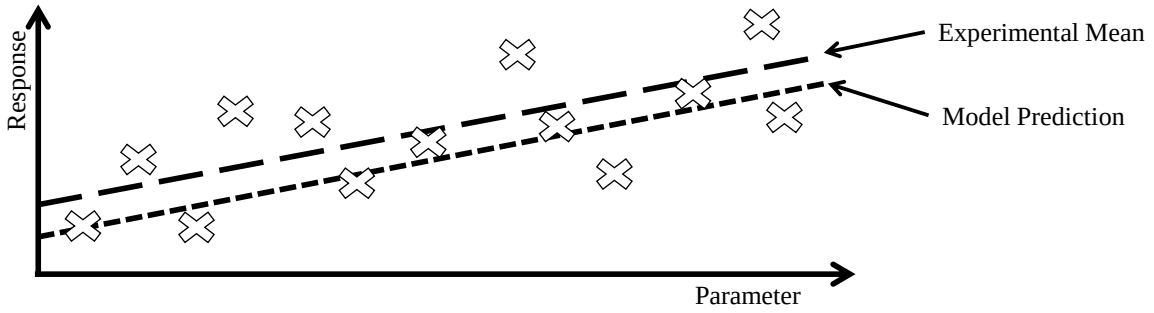

Figure 29: Model Form Error (modified from [53])

Introduction to Richardson's Extrapolation Method

Discretization error arises when "continuum mathematical problems are solved through discretized numerical procedures" [181]. These interstices of the mesh are the points where the analysis is performed. The values between the nodes are either averaged between the nodes or unknown. This is akin to the finite difference relation in calculus where the distance between the points *h* approaches zero in the central difference relation described in Equation 10.

$$\delta_{\mathrm{h}} f(x) = f(x + 0.5h) - f(x - 0.5h) \tag{10}$$

A notional mesh can be described in Figure 30. Data is known (or computed) at the eight nodes that form the mesh while data is unknown or indirectly known at all the points between the nodes (depicted as node $\mathrm{N}_{1,0.5}$). As described by Liu in [131], meshes are often predefined. For our model, the mesh is defined by the number of inches between the nodes such as 6 inches or 10 inches. The larger the distance between the nodes the coarser the mesh (less is known, less resources used) while the smaller the distance the finer the mesh (more is known, more resources used). A one inch mesh is finer than a five inch mesh and so on.

The most common approach to capture discretization error is to use Richardson's Extrapolation method [182]. An important characteristic of this approach is that the error

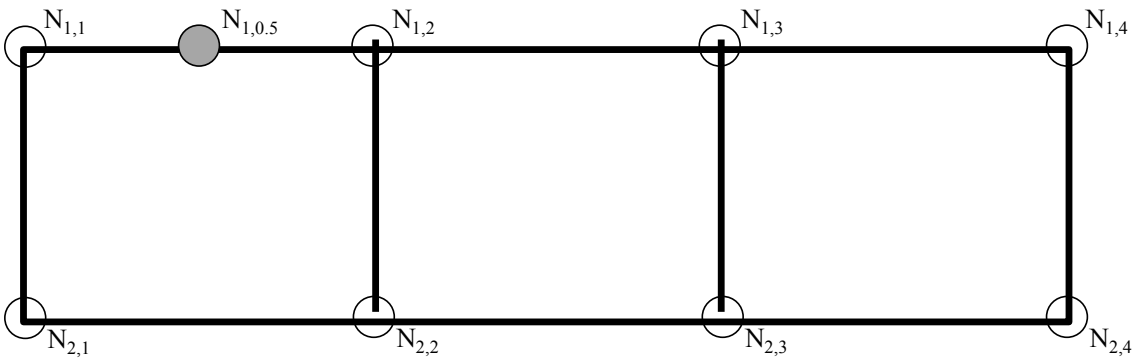

Figure 30: Notion Mesh Defined by 8 Nodes

quantified not only applies to the nodes but to the macro-metrics as well such as lift coefficient or weight. This is highly advantageous for our purposes because we seek to characterize the uncertainty for the wing as a whole rather than at the node-level.

The method works by analyzing a sequence of progressively finer meshes. The finer meshes include more nodes and also changes the information at the original nodes. Consider a mesh that has double the nodes of the notional mesh in Figure 30. The original nodes remain in place while in-between nodes are formed shown in Figure 31. The data at the original nodes now changes due to the presence of more nodes. This step can be repeated for a further finer mesh shown as "Mesh 3" in Figure 31. The difference between the original nodes in the coarse mesh and the finest mesh are compared to determine the error. The finest mesh is assumed to hold the data that is most accurate. The gray nodes depict the nodes that are added due to the mesh refinement.

These three meshes with constant mesh refinement can be used to determine the formal order of accuracy of our model [183]. Its determination is shown in Equation 11.

$$p = \ln(\frac{f_3 - f_2}{f_2 - f_1}) / \ln(r) \tag{11}$$

where f_3 is the coarsest mesh, f_2 is the medium fineness mesh, f_1 is the coarsest mesh, and r is the mesh refinement ratio (here r is 2). The method is called extrapolation because an infinitely fine mesh cannot be used; therefore, the exact solution is guessed. Of course,

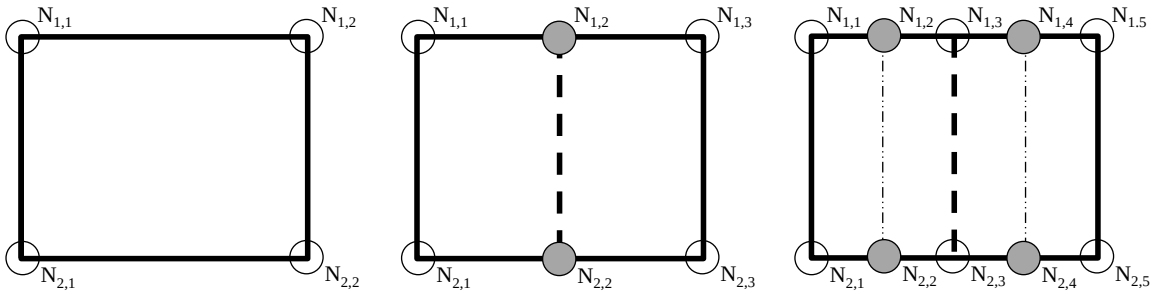

Mesh 1 Mesh 2 Mesh 3

Figure 31: Richardson's Extrapolation Method Illustration of Double Mesh Refinement (r=2)

the infinitely refined mesh is outside the bounds of the given data which makes this error estimation extrapolation. The error can be defined in terms of the fine or the coarse mesh. We will use the fine mesh as the datum to the error.

$$E_{\text{fine}} = \frac{f_2 - f_1}{1 - rp} \tag{12}$$

where f_2 is the coarse mesh and f_1 is the fine mesh. Here f_2 and f_1 are not necessarily the same as f_2 and f_1 in Equation 11.

We have direct control of the mesh size in RADE. Therefore, we can vary mesh size to determine the sensitivity, and, further, utilize Richardson's Extrapolation Method to extrapolate to the ideal solution.

Richardson's Extrapolation Method Requirements

Richardson's method can only apply if a few conditions are met. Hypothesis 2.2 is essentially that these conditions are applicable to the current problem. It is dissected into three key assumptions:

Hypothesis 2.2a

The outputs of the wing-level design environment (e.g. wing weight) are sensitive to mesh size.

While intuitive, the outputs are not guaranteed to be dependent on the fineness or coarseness of the mesh. We can test this by performing a mesh sensitivity (systematically varying mesh size to detect trends in the outputs).

Hypothesis 2.2b

Refining the mesh will result in a more accurate weight estimation with diminishing improvement (i.e. the curve will converge to a finite value).

Richardson's method requires grid convergence: as the mesh size is refined, the output should approach a finite value with diminishing improvement. This can also be tested by a mesh sensitivity, but here the test metric is convergence rather than variation.

If both of these hypotheses are not rejected, then Richardson's Extrapolation Method can be applied to measure the discretization error.

Fitting Error Samples to Parametric Distributions

There is one final step to addressing the characterization of uncertainty. This is fitting the error samples to parametric distributions. If the error samples appear to fit a normal distribution with a defined mean and variance, then they can be replicated using that defined distribution. If not, there will need to be a different approach to implementing the uncertainty. Defining a distribution allows the uncertainty to be described using only a few parameters (distribution type, parameter values). Usually a distribution only requires a couple parameters (normal distribution requires two, for example).

Hypothesis 2.2c

The discretization error distributions can be fit to unbounded, parametric distributions. The best distribution can describe the observed data with 95% confidence.

This hypothesis is distinguished by three aspects: first, unbounded, parametric distributions; second, best fit; and third, 95% confidence. Unbounded distributions were chosen to prevent the definition of bounds. It would be difficult to truncate the error with a high level of certainty. The second piece is defining the "best" fit. A criterion will be needed to determine which among the candidate distributions is represents the data the best. Last, the 95% confidence will also require a test to show that the chosen distribution represents the data accurately.

4.2.3 Research Question 2.3: Quantifying Uncertainty Correlation

If all the hypotheses in Research Question 2.2 are supported by the experimental results, the uncertainty can be accurately captured independently. This is already a contribution to the literature of aircraft design RBDO. However, we can go further by attempting to correlate the errors as well. This is the focus of Research Question 2.3.

Research Question 2.3

Does correlation exist between uncertainty sources? If so, how can it be captured in the RBDO?

There are two parts to this research question: testing for correlation and implementing correlation. Testing should not be an issue due to the plethora of correlation techniques available. Similarly, implementation should be straightforward assuming that error data exists from Research Question 2.2. Should no error dataset be available, correlation may need to be derived using a non-data-based approach such as through heuristics or intuition.

Hypothesis 2.3

Statistically significant (95% confidence) correlations exist between output errors.

Therefore we need to define correlation quantification methods and statistical testing to test Hypothesis 2.3. The null hypothesis is that correlations do not exist ($\rho = 0$) and the alternative hypothesis (which is Hypothesis 2.3) is that non-zero correlations exist ($\rho \neq 0$). Rejecting the null hypothesis will substantiate Hypothesis 2.3.

Approaches can be separated by how they treat uncertainty with respect to the rest of the method. For example, some methods simply just apply additional steps in a predefined methodology to ensure correlation (or, sometimes, to ensure a lack of correlation) [184, 185, 186, 187]. For these methods, the overall process is unchanged, but a step or two are added for the sake of correlation analysis. For example, after randomly sampling five input distributions, the now-filled matrix of values would be analyzed the ensure samples are uncorrelated. Once this step is complete, the rest of the formulation is completed business as usual.

One significant restriction greatly reduces the number of candidates for our purposes, and that restriction is that the approach must be compatible with a sampling method. The Monte Carlo simulation approach is central to the baseline methodology, as each point not only represents the uncertainty distributions but also allows for scenario analysis. These scenarios have henceforth been referred to as realizations. The data tracked by these realizations is an enabler for recourse to be quantified: without specific detail for each specific point (as in, constraint reliability calculations for the entire design cannot be used) the recourse could not be tailored to the non-compliant scenarios.

Correlation Matrix When most people hear the term correlation, they usually think of coefficients and matrices. Indeed, the most traditional approach is to define a matrix where the elements describe the linear relationship between variables. These elements are often

the Pearson correlation coefficient (PCC) or the Spearman rank order correlation (SRCC) [169]. PCC measures the linear relationship on a scale ranging between -1 and 1. The relationships between variables do not affect other relationships; conversely, SRCC is based on ranking. For example, the smallest element in a correlation matrix may be given a rank of 1, the next smallest a rank of 2, and so on until the largest element is reached. In the case of ties, the average rank can be used. The equations defining these coefficients are well known and widely published.

However, the pair of coefficients alone are insufficient for engineering design. A very popular method utilizing the correlation matrix originally developed by Cario [188] is the NORTA method ("NORmal To Anything"). This procedure was developed in order to generate samples from a random variable or vector with a given marginal distribution and correlation matrix [189].

The NORTA method is a very efficient and easy-to-implement sampling method, and has seen use in a variety of contexts [190, 191]. Clemen and Reilly [192] use the NORTA procedure to induce a desired rank correlation in the context of decision and risk analysis. Lurie and Goldberg [193] implement a variant of the NORTA method for use in cost analysis. Henderson et al. adapt the NORTA method to generate samples of dependent quasi-random vectors. The NORTA method is also routinely used in portfolio models in industry. It has also found applications in cost analysis, decision making, and generating test problems [193, 192, 194, 195].

However, the use of correlation matrices has its limits. As an example, a correlation matrix is always symmetric. This is the assumption that variable x has the same effect on y as y has on x. In engineering, this is not always true. Changes in structural weight of the wing may have a higher impact on the landing gear weight than changes in the landing gear weight have on the weight of the wing. In addition, in general the correlation matrix must be positive definite with diagonal elements at positive values. Finally, the elements are usually coefficients of linear relationships or rankings of linear relationships. Indeed,

the classical definition of correlation is restricted to only linear relationships. For these reasons, a correlation matrix approach is unlikely to be suitable for our approach.

Statistically Significant Correlation While improper for implementation, Pearson's correlation coefficient can be used to test Hypothesis 2.3. Because the sample size of the errors will be finite, it is important to introduce a measure of confidence with the correlations. Obviously, the larger the sample size the more confidently we can say that correlations exist. For a sample size of about 50, a Pearson coefficient of 0.3 or greater is statistically significant with 95% confidence. Therefore, this will be the benchmark for Hypothesis 2.3.

Statistical significance can be determined by performing hypothesis testing (independent of Hypothesis 2.3). The null hypothesis is that no correlation exists between the datasets.

$$\begin{aligned} Null\ \ Hypothesis: &\ \ H_0 : \rho = 0 \\ Alternative\ \ Hypothesis: &\ \ H_A : \rho \neq 0 \end{aligned} \tag{13}$$

where ρ is Pearson's correlation coefficient. The test statistic is calculated using Equation 14.

$$t^* = \frac{r\sqrt{n-2}}{\sqrt{1-r^2}} \tag{14}$$

For a defined sample size (say n = 56), we can determine what level of Pearson's correlation coefficient is required for statistically significant correlation.

Table 11 shows various Pearson coefficient values and the resulting test statistic, p-value, and hypothesis test result. The null hypothesis is that the correlation between the two datasets is zero. A p-value less than 0.05 rejects the null hypothesis. Note that rejecting the null hypothesis supports Hypothesis 2.3 (which states that correlations exist).

Table 11: Pearson's Coefficient Test Results to Determine Statistically Significant Correlation with 95% Confidence [196]

Pearson's Coefficient	t*	P-Value	Reject/Fail to Reject
0.9	15.173	0.00	Reject
0.8	9.798	0.00	Reject
0.7	7.203	0.00	Reject
0.6	5.511	0.00	Reject
0.5	4.243	0.00	Reject
0.4	3.207	0.00	Reject
0.3	2.311	0.03	Reject
0.2	1.5	0.13	Fail to Reject
0.1	0.739	0.3	Fail to Reject

Still, Pearson's coefficient needs modification to be directly implemented into the final RBDO methodology.

Copulas The correlation need not be deterministic. Beyond correlation coefficients, a popular approach is the use of joint probability distributions (JPDs). As the name implies, this technique simply joins two PDFs into a single distribution. Inherently, the correlation also becomes probabilistic, capturing the variability in the relationship. Copulas are a common technique based on this concept.

Copulas were introduced formally by Sklar in 1959 [197] with Nelsen writing an entire textbook on the matter [198]. The name "copula" is very general: the word simply means to tie or bond. The broad name has led to many different applications and types of copulas being developed. Similar to the correlation matrix approach, copulas only function under certain assumptions. The first is that the multivariate probability distribution function (the "copula") is composed of marginal uniform distributions. In other words, the input distributions must be uniform and bounded from zero to one. Inversion methods have been developed to disconnect the copula from this requirement, meaning that a triangular distribution can be used with the inversion workaround. Hence, with inversion, the choice of copula is independent of the input distributions, allowing any copula to be chosen as the

JPD. A brief overview of Sklar's theorem is described.

The theorem states that *H* is a joint distribution function with marginals *F* and *G*. Then, a copula C exists for all *x, y* in their domain such that:

$$H(x, y) = C(F(x), G(y)) \tag{15}$$

Recall that *F* and *G* are univariate, uniform distributions (after inversion if otherwise). Thus, Equation 15 expresses *H* as the JPD and *C* as the copula that ties marginal distributions *F* and *G*. Rearranging, copula *C* can be defined in terms of *H, F,* and *G*.

$$C(x, y) = H(F^{-1}(x), G^{-1}(y)) \tag{16}$$

Hence, the copula can be determined from the JPD and the marginal distributions. Rather than mathematically determining the copula using Equation 16, families of copulas have been introduced. For example, the most common family is the Archimedean family which follow the generator function:

$$C(u, v) = \phi_{\theta}^{-1}(\phi_{\theta}(u) + \phi_{\theta}(v)) \tag{17}$$

Using a generator function has many advantages, though its inverse, derivative, and inverse of the derivative must exist. Many types of these copula families exist which capture different types of correlations, including non-linear correlation.

Copulas have found a home particularly in the field of finance and economics to track correlations, such as bond pricing and valuation [173]. Copulas have also been used in engineering design and reliability-based engineering design [157, 199]. Noh compares the performance of copulas with the traditional techniques of the Rosenblatt and Nataf transformations.

Most notably, copulas have been used in the aerospace domain by Zaidi [200]. Zaidi argues that copulas are ideal for simulating dependencies between uncertainty variables in

aircraft design because: “It is likely that these dependent relationships are not known exactly... However experts in the field can provide notional or qualitative understandings of these dependence relationships.” Zaidi implemented the use of copulas to capture technology impact uncertainties in aircraft design using intuition. He conducted three experiments with copulas: the first was a simulation to that coupled the multiple effects of a single technology; the second was a simulation to compare the PDFs of outputs for two correlated technology impact factors; and, the third was a simulation to analyze the results of coupling a technology impact factor with a design variable. The second simulation demonstrated that copulas reduce the standard deviation of objective probability distributions. This is because the full PDF space of each variable is no longer sampled, but only the points that satisfy the coupling relationship specified by the copulas. For this experiment, the two technologies selected were a hybrid laminar flow technology and riblets. These two technologies both facilitate a decrease in the zero-lift drag coefficient. However, there is a perceived limit (diminishing return) to how much the zero-lift drag coefficient can be decreased by technology addition. Consequently, Zaidi chose a copula prescribing an exponential inverse relationship between the technologies, such that a both technologies could not perform exceedingly well: a high impact factor for riblets was correlated with a low impact factor for hybrid laminar flow. This decreased the effective sampling area for both variables, reducing the variability in the objective space compared to a simulation when the technologies are sampled independently from each other.

Therefore, copulas can capture the correlations between all the uncertainty variables and be easily sampled. Although they require marginal distributions as inputs, inversion methods are available to overcome this obstacle.

Research Result 2.3

If correlations exist amongst output errors, an n-dimensional copula can be used to

draw correlated samples. The copula that will allow the correlation to be performed outside the RBDO process and maintain the observed correlations.

4.3 Research Question 3: Developing an Integrated Environment

Before a full methodology can be proposed, incongruities between the conceptual and preliminary models must be resolved. The two tools are not guaranteed to always predict the same outcome, so a resolution process needs to be determined, which is described in Research Question 3.1. Then, assuming that an integration is possible, Research Question 3.2 investigates what new behavior has emerged from this new environment. A research question is not asked to how to incorporate the quantified uncertainty because the baseline method used Monte Carlo sampling from distributions to capture the uncertainty. Because the uncertainty will either be described by new parametric distributions or a copula, a new process is not required since no change to the implementation is necessary.

4.3.1 Research Question 3.1: Bridging Models of Varying Fidelity

Consider the following thought experiment. A given conceptual design is under consideration by a conceptual design team. Using FLOPS, the team estimates the wing weight to be about 40,000 lbs. Assume this design is selected and it moves towards the beginning of preliminary design. Using physics-based tools, the same wing is analyzed, but this analysis yields a structural weight of 42,000 lbs. The wing is 5% heaver that estimated in conceptual design, and that is only the structural portion of the total wing weight. So, which approach is correct?

If the preliminary design tool is assumed to be correct, then uncertainty was realized without being simulation. The baseline method explicitly modeled uncertainty: input variables were changed to simulate an uncertainty realization. Here, no uncertainty sources, variables, or distributions have been defined. There is simply a difference between model output. Still, uncertainty is being realized, but it was not due to a taxonomy or distribution

sample.

This thought experiment motivates Research Question 3.1:

Research Question 3.1

How can two design environments of varying fidelity be integrated to agree on performance estimation?

On one hand, FLOPS uses actual historical data to estimate the wing weight. RADE, on the other hand, uses physics to determine the structural wing weight. They are likely to disagree. There are three options: choose FLOPS' value, choose RADE's value, or integrate the two. If either of the first two options are selected, the value of an integrated environment is diminished. Why integrated two models if one simply trumps the other? Instead we would like to bridge the models using common variables.

Hypothesis 3.1a

The two models can be bridged to agree on a unique set of input and output variables.

Examples of common variables between FLOPS and RADE are aspect ratio, sweep, take-off gross weight, wing skin weight, wing ribs and spars weight, fuel weight, and engine weight. These values must agree in order for an integrated environment to be trustworthy. A process will be developed in Chapter 7 to attempt to converge on take-off gross weight.

Because the two environments share inputs and outputs, we can expect a fixed-point iteration to be attempted as the bridge to form a unique solution. A fixed-point iteration requires initial guesses for the changing values. In this case, these values would probably include the weights (wing weights and take-off gross weight). Therefore, the convergence will need to be tested against various initial guess to show robustness. Otherwise, the a process to select initial guess values will need to be determined.

Hypothesis 3.1b

If the two models converge on a solution, this convergence is robust to the initial guess values.

This hypothesis can easily be tested by an initial guess sensitivity test. Hopefully the convergence will be robust; if not, then a process will need to be developed. This would result in Research Question 3.1b: How can the initial guesses to the fixed-point iteration be determined to result in the most correct solution? This will only be formalized if Hypothesis 3.1b is rejected.

4.3.2 Research Question 3.2: Effect of Wing-Level Constraints on Vehicle-Level Optimums

Once the integrated environment has been completed, we would like to explore any new insights it reveals. Put plainly, the question that needs to be answered is: how does the integrated environment yield better results than the baseline environment? This question is at the forefront of Research Question 3.2:

Research Question 3.2

What impact does the integrated environment have on conceptual design selection relative to the baseline method?

The new environment includes wing-level analysis and constraints. There are new variables that FLOPS does not comprehend. Therefore, we assume that including these constraints will have a significant impact on conceptual design selection. To demonstrate this fully, we can first find a Pareto Front using vehicle-level considerations only. This represents the results of the previous method. Then, we evaluate all the designs along the Front against wing-level constraints. The expectation is that most of these designs will fail because they were optimized without knowledge of these constraints. Finally, wing-level mitigation will be applied to the failed designs to see what percentage can be recovered.

If the most the designs are compliant and recoverable, then the integrated environment provides marginal utility. If, on the other hand, the vast majority of the designs are non-compliant and unrecoverable, then this environment greatly enhances conceptual design selection.

Hypothesis 3.2

If an optimal point is found using an optimization formulation restricted to vehicle-level constraints only, then this point will have no (0%) probability of satisfying wing-level constraints.

This hypothesis will be tested in Chapter 7 using two experiments. The first is a single-design experiment where the aspect ratio of the design point will be varied to measure the effect on span and tip deflection. If the tip deflection constraint is violated before the span constraint, this indicted the optimal vehicle-level designs will violate wing-level constraints. Then, a design selection experiment will be performed where a Pareto Front will be found using a vehicle-only formulation. The designs along this Front will then be evaluated against wing-level constraints to determine reliability. Hypothesis 3.2 states that these designs will have no probability whatsoever of satisfying all wing-level constraints.

4.4 Chapter Summary

Figure 32 summarizes the research questions and hypotheses developed in this chapter. The following Chapters 5, 6, and 7 are devoted to the three subsection shown in the figure: capturing physical design changes, uncertainty quantification, and developing an integrated environment. These three categories represent the three research objectives of this work. The next level shows the sub-research questions poised for each section. Each research question has three sub-categories, though the first has been answered by the literature review. Therefore the two sub-categories form the sections of the following chapters.

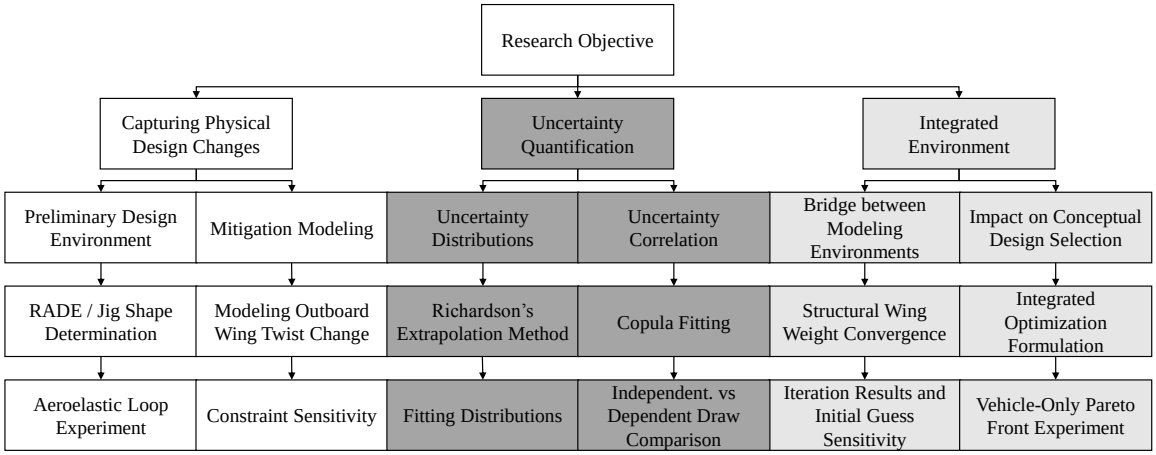

Figure 32: Research Objective Decomposition with Sub-Research Question Proposed Methods and Experiments

CHAPTER 5

PHYSICS-BASED MODELING ENVIRONMENT

Capability Gap 1 found that the benchmark method does not incorporate any physics-based tools. This is a problem because the uncertainty is realized as the model fidelities are increased and mitigation, being a physical design change, must be captured within a physical design environment because transformation functions to propagate physical changes to the conceptual level do not exist.

Research Question 1.1 dealt with enumerating the necessary tools for physics-based wing design and analysis. A series of steps are needed, from defining the geometry to generating a mesh to conducting aerodynamics analysis to finally sizing the structure. The literature review found an integrated environment called RADE that integrated the necessary pieces: VSP for geometry input and manipulation, AFEM for automated mesh generation, AVL for approximating aerodynamics, and Nastran for structural analysis and sizing. This is the environment that will be used to answer Research Question 1.

The first section of this chapter is dedicated to testing Research Question 1.2:

Research Question 1.2
How does the sizing algorithm affect final jig shape and size?

The assumption here is that the known shape is the flight shape. This is not always the case: if the jig shape is already known, it can be used directly. However, in the case that the jig shape is unknown but the flight shape is known, a process is required to determine the jig shape. The shape will be taken from NASA's Common Research Model which is given in the flight shape [201]. Therefore, this process is necessary.

The jig shape determination algorithm in Figure 24 given by RADE documentation was untested as to convergence and stability. Other algorithms will be developed to test against

the proposed jig determination loop to test Hypothesis 1.2. Once a jig shape determination loop is finished, the next step is to study the effect of mitigation actions on the wing design.

Research Question 1.3
How can physical design changes to the wing be captured in the model?

Hypothesis 1.3 addressed this research question by suggesting VSP be used to geometrically scale the wing. This functionality will be tested by comparing a nominal jig shape against a mitigated (altered) jig shape. This will be completed by performing a sensitivity study: the mitigation variables will be systematically varied to study the impact on defined constraints. The expectation is that the applied mitigation will shift the constraint values towards the feasible region.

5.1 Research Question 1.2: Jig Shape Determination Loop

There are two experiments that need to be performed to answer this research question. The first is to test the current implementation of the default algorithm. We expect the jig shape and size to converge without issue for the baseline design point, though we do not know how quickly. Then, a second experiment can be performed to test the single loop process against double-loop processes. This will directly test Hypothesis 1.2. If an RBDO is to be performed using this process, the solution needs to be deterministic: one flight shape should not have multiple jig shapes. If the default process is shown to be probabilistic (multi-modal, divergent, etc.) then a new process will need to be developed to isolate the "correct" jig shape (or at least one for consistency).

5.1.1 Experiment 1.2a: Jig Shape Determination Loop

Experimental Design

This experiments tests the default jig shape determination loop in the RADE environment [139]. Note that this experiment is only required if the input shape is different than the jig

shape. If the jig shape is the input shape, then it can be sized directly. The wing used for this experiment is NASA's Common Research Model wing [201]. Figures 33 and 34 show the wing as described in VSP.

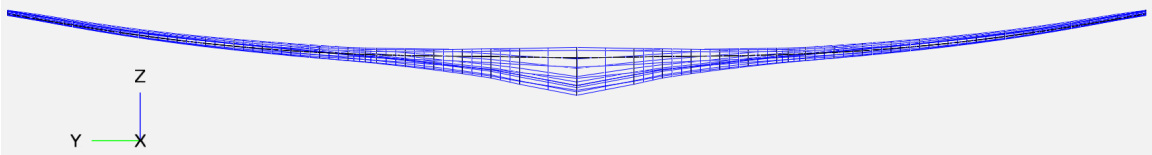

Figure 33: NASA's Common Research Model: Front View

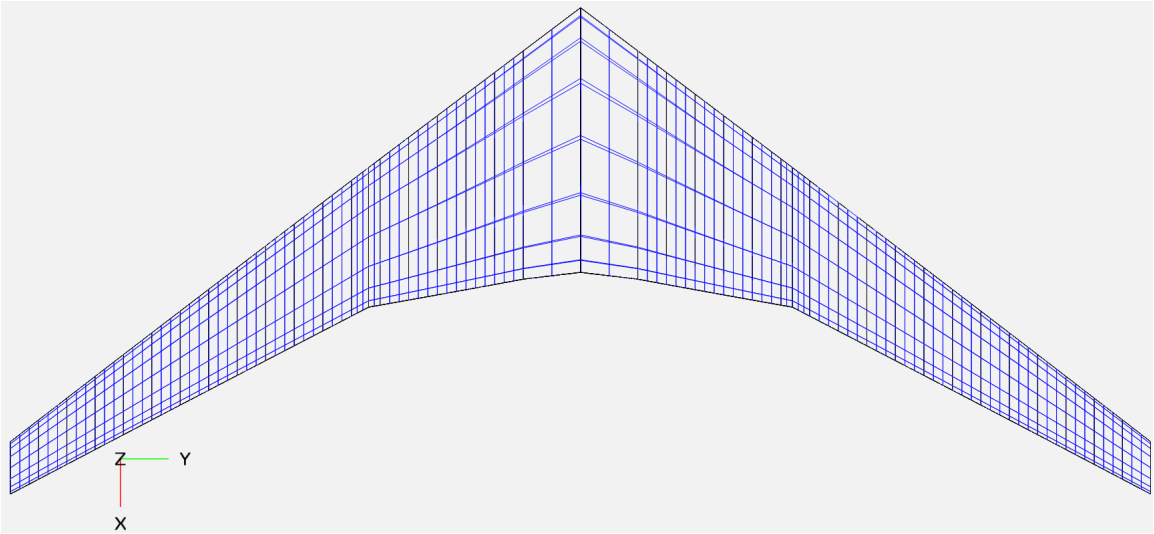

Figure 34: NASA's Common Research Model: Top View

This shape *could* be assumed to be the jig shape. However, the tip deflection is quite high for a jig shape, as shown in Figure 33. This leads us to believe that it is actually the flight shape rather than the jig shape.

The default process in RADE can be described as a single loop that converges on wing weight and shape simultaneously. The tolerance is set between successive iterations to calculate the difference in structural wing weight. Table 12 describes the different calls to Nastran throughout the algorithm.

The shape is initialized and sized based on the flight shape. This weight estimation will have a level of error because the initial structural analysis is completed with guess weights.

Table 12: Effects of Nastran Calls on Wing Weight, Shape, and Type of Loads

	Initial Analysis	Cruise Analysis	Aeroelastic Analysis	Structural Sizing
Weight	Changing	Constant	Constant	Changing
Shape	Changing	Changing	Constant	Constant
Type of Loads	Load Cases	Cruise Case	Load Cases	Load Cases

Table 13: Wing-Level Design Point for Jig Shape Determination Test

Wing Area (ft^2)	Aspect Ratio	Sweep	TOGW (lbs)
4927.29	9.207	37°	657,000
Incidence (°)	Wing Twist (°)	Rib Spacing (in)	Knockdown Factor
6.0	-0.50	30	0.10

The sizing is performed after the aeroelastic analysis (which in turn requires the component thicknesses). There are two different types of loads: load cases are maneuvers used to sizing, and the cruise case is used for jig shape determination. For this experiment, two load cases will be used: a 2.5G maneuver and a -1.0G maneuver. For the cruise analysis, however, the load case is the cruise condition (load factor is 1.0).

For the cruise analysis the weight of the wing is constant, meaning that Nastran is analyzing rather than sizing. The shape deflects during this analysis which is then recorded. A new shape is created by subtracting this displacement from the original shape. Hence, the shape changes during this stage.

The aeroelastic analysis is performed next. This is an analysis call to Nastran with a constant shape under the load cases. The results of this analysis are passed to the sizing call to Nastran. Here the shape remains constant but the wing weight changes. The new weight is recorded and compared to the previous iteration's weight (or initial weight for the first iteration).

This process was completed for the design point described in Table 13. The wing characteristics are described in detail in Table 44.

Table 14: Wing Weight and Tip Deflection by Jig Shape Determination Loop Iteration

Iteration	Tip Deflection (ft, % change)		Wing Weight (lbs, % change)	
Initial	-	-	47,099	-
1	21.91	-	47,706	1.29%
2	21.39	-2.39%	48,233	1.10%
3	21.29	-0.44%	48,614	0.79%
4	21.25	-0.20%	48,850	0.49%
5	21.22	-0.14%	49,007	0.32%
6	21.20	-0.10%	49,127	0.25%
7	21.18	-0.09%	49,233	0.22%
8	21.16	-0.08%	49,327	0.19%
9	21.15	-0.07%	49,407	0.16%
10	21.13	-0.06%	49,477	0.14%
11	21.12	-0.06%	49,530	0.11%
12	21.11	-0.04%	49,539	0.02%
13	21.11	-0.01%	49,568	0.06%
14	21.10	-0.02%	49,577	0.02%
15	21.10	-0.01%	49,590	0.03%
16	21.10	-0.01%	49,601	0.02%

Experimental Results

The results of the experiment are presented in Table 14. For each iteration (including the initial sizing), the tip deflection at cruise (1g load) in the z-direction is given along with the wing weight.

The main result is that the single loop process converges on a solution. The convergence was executed for 16 runs regardless of convergence. In practice, the stopping criterion would be a tolerance in wing weight. If this tolerance was set to 0.5%, the iteration would exit after about 4 iterations. This would result in an output of 48,850 lbs whereas 16 iterations would result in 49,601 lbs for an error of 751 lbs, or about 1.5%. The changes in shape are depicted in Figure 35.

Experiment 1.2a Results

The default jig shape determination process monotonically converges on a shape and

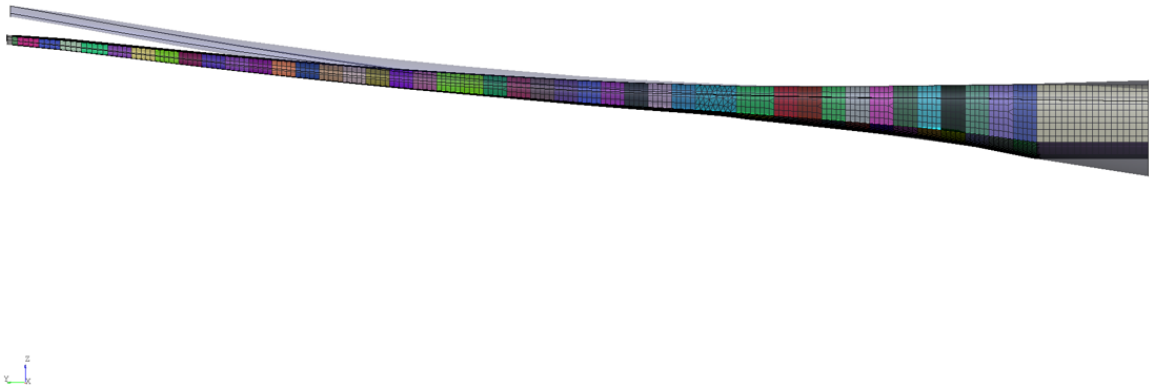

Figure 35: Front View of Flight Shape (Top) and Jig Shape (Bottom)

weight.

5.1.2 Experiment 1.2b: Jig Shape Determination Loop Comparison

Experimental Design

The jig shape has been determined for the design point; however, both the shape and the weight were changing with each iteration. We can first perform a repeatability experiment. This is where the exact same case is executed again (repeated) to test if the results are the same. This test was completed and the results were identical (within 0.01%). The results are not reported because they are virtually the exact same as the results presented in Table 14.

So, we conclude that the process is repeatable (at least for the design point). Now we wish to test how it compares to alternatives. This comparison will provide a number of insights. First, and most important, it will show if the jig shape is dependent on the fixed-point iteration process. If dependence exists, then we will need to determine which process is the "right" process. Second, it will show convergence trends. The single loop process

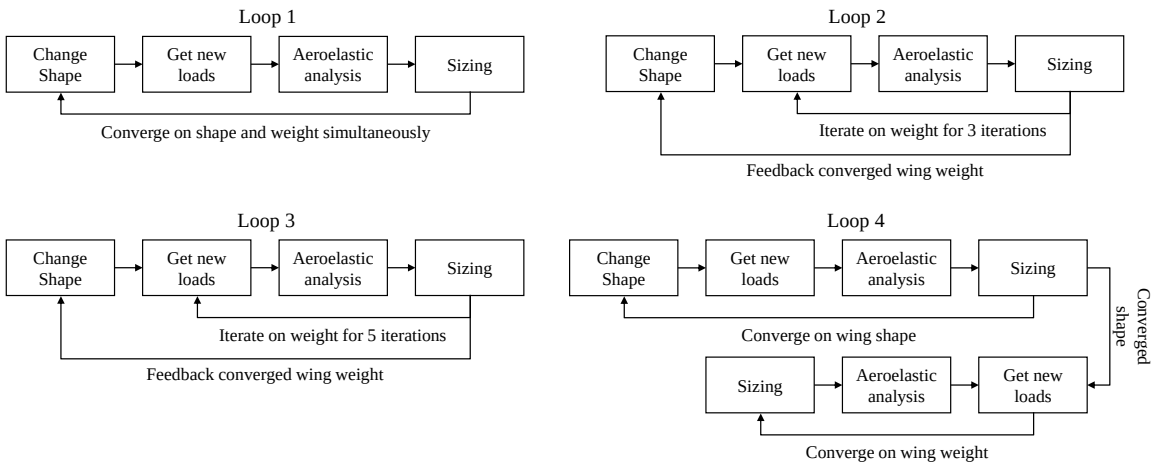

Figure 36: Design Loop Depictions for Aeroelastic Convergence Test

showed to monotonically converge on a solution quickly: if the threshold weight change was about 0.5%, the process would have taken three iterations. Last, it will show efficiencies. Geometrically restructuring the wing takes about two minutes in the computational environment. Alternative approaches that change the shape every three or five iterations will be more efficient than changing the shape every iteration. So, if these approaches prove more accurate, they will also prove to be more efficient over the same number of iterations.

Now we look to see how changing the frequency of weight or shape updating affects the final converged solution. Four loops were used to test Hypothesis 1.2. These loops are depicted in Figure 36.

The first loop is the loop that was used in the prior solution. The second and third loops "pause" the shape of the wing for three and five sizing iterations, respectively. This allows the design to converge on a weight for the given shape. The last loop is similar to the first for ten iterations. Then, the shape is constant while the weight converges.

Experimental Results

Each of the four loops were executed for the same number of iterations as Experiment 1.2a. The results given for the default case are the exact same as presented in Table 14. The

Table 15: Wing Weight and Tip Deflection by Jig Shape Determination Loop Iteration

	Tip Deflection (ft)				Wing Weight (lbs)			
Iteration	1	2	3	4	1	2	3	4
Initial	-	-	-	-	-	-	-	-
0	-	-	-	-	1.29%	1.29%	1.29%	1.29%
1	-2.39%	-	-	-2.39%	1.10%	0.67%	0.67%	1.10%
2	-0.44%	-	-	-0.44%	0.79%	0.60%	0.60%	0.79%
3	-0.20%	-2.10%	-	-0.20%	0.49%	0.95%	0.42%	0.49%
4	-0.14%	-	-	0.14%	-0.32%	0.49%	0.30%	0.32%
5	-0.10%	-	-2.23%	-0.10%	0.25%	0.30%	0.77%	0.25%
6	-0.09%	-1.32%	-	-0.09%	0.22%	0.18%	0.41%	0.22%
7	-0.08%	-	-	-0.08%	0.19%	0.18%	0.25%	0.19%
8	-0.07%	-	-	-0.07%	0.16%	0.16%	0.18%	0.16%
9	-0.06%	-0.15%	-	-0.06%	0.14%	0.15%	0.14%	0.14%
10	-0.06%	-	-1.50%	-0.06%	0.11%	0.10%	0.06%	0.10%
11	-0.04%	-	-	-	0.02%	0.02%	0.00%	0.02%
12	-0.01%	-0.12%	-	-	0.06%	0.03%	0.02%	0.03%
13	-0.02%	-	-	-	0.02%	0.03%	0.02%	0.03%
14	-0.01%	-	-	-	0.03%	0.02%	0.02%	0.02%
15	-0.01%	-0.03%	-0.01%	-	0.02%	0.02%	0.03%	0.02%
Final	21.10	21.01	21.10	21.12	49,601	49,590	49,598	49,590

results of each loop are described in Table 15.

The evidence reported in Table 15 supports the hypothesis that the first loop is an effective convergence method. In fact, when comparing the results of the four loops, all of them converge regardless of loop construction. This shows that the jig shape determination itself is robust.

Experiment 1.2b Results

The four algorithms converge to similar solutions within the ~1% threshold. Therefore, Experiment 1.2b substantiates Hypothesis 1.2.

Table 16: 2nd Wing-Level Design Point for Jig Shape Determination Test

Wing Area (ft^2)	Aspect Ratio	Sweep	TOGW (lbs)
3,500	8.5	35°	575,000
Incidence (°)	Wing Twist (°)	Rib Spacing (in)	Knockdown Factor
6.0	-0.45	25	0.10

Repeated Experiment for a Different Design Point

Ideally this experiment would be repeated for a representative sample of the design space. Because the execution time of this experiment is so large (2-3 days), a design of experiments will not be completed. Though, as a consolation, another design point will be used for the repeated experiment to ensure that the original design point is not an anomaly. The new design point is described in Tabled 16.

As demonstrated by Table 17, the four loops demonstrate similar convergence regardless of construction. Therefore, this result further substantiates Hypothesis 1.2 that the single loop is a reliable convergence algorithm.

Experiment 1.2b Results

The four algorithms converge to similar solutions within the 1% threshold for a two different design points. Therefore, Experiment 1.2b substantiates Hypothesis 1.2.

5.1.3 Answering Research Question 1.2

Research Question 1.2 was derived from a curiosity about the approach to determine jig shape and weight from a given aerodynamic (cruise) shape. The jig shape is required for mitigation analysis because, as noted in Section 4.1.2, the jig shape is the manufactured shape and therefore it is the desired shape to apply mitigation. Further, because it is the 0g shape, load cases can be applied to it to examine aeroelastic effects. Therefore, it is the required shape for mitigation modeling.

Table 17: Wing Weight and Tip Deflection by Jig Shape Determination Loop Iteration for Design Point 2

	Tip Deflection (ft)				Wing Weight (lbs)			
Iteration	1	2	3	4	1	2	3	4
Initial	-	-	-	-	-	-	-	-
0	-	-	-	-	7.88%	7.88%	7.88%	7.88%
1	-8.12%	-	-	-8.12%	2.24%	2.33%	2.33%	2.24%
2	-1.41%	-	-	-1.41%	1.71%	1.73%	1.73%	1.71%
3	-0.62%	-9.98%	-	-0.62%	0.85%	0.75%	0.85%	0.85%
4	-0.29%	-	-	-0.29%	0.52%	0.51%	0.52%	0.52%
5	-0.20%	-	-10.42%	-0.20%	0.44%	0.43%	0.33%	0.44%
6	-0.19%	-0.64%	-	-0.19%	0.42%	0.44%	0.41%	0.42%
7	-0.20%	-	-	-0.20%	0.39%	0.39%	0.38%	0.39%
8	-0.19%	-	-	-0.19%	0.33%	0.33%	0.33%	0.33%
9	-0.15%	-0.54%	-	-0.15%	0.26%	0.27%	0.26%	0.26%
10	-0.11%	-	-0.78%	-0.11%	0.22%	0.22%	0.24%	0.22%
11	-0.08%	-	-	-	0.13%	0.13%	0.13%	0.13%
12	-0.05%	-0.25%	-	-	0.08%	0.09%	0.08%	0.08%
13	-0.03%	-	-	-	0.04%	0.04%	0.04%	0.04%
14	-0.02%	-	-	-	0.04%	0.04%	0.04%	0.04%
15	-0.01%	-0.07%	-0.22%	-	0.03%	0.03%	0.04%	0.03%
Final	16.32	16.32	16.32	16.35	46,225	46,223	46,223	46,223

However, this shape is not guaranteed as an input. Indeed, the input file used for this work is a flight shape rather than a jig shape. Therefore, a transformation process is required. If the jig shape is readily available, this process is unnecessary.

Experiments 1.2a and 1.2b showed that the results of the default process are stable and consistent. It provides fantastically similar results as compared to other processes and converges more quickly in the case of iteration truncation. Therefore it will be used as the jig shape determination process going forward.

5.2 Research Question 1.3: Mitigation Modeling and Testing

Now that the jig shape is determined, we can apply mitigation directly to it. There are many forms of mitigation actions that can be selected for modeling and application. A brief list of

mitigation actions is included in Section 8.2.3. It includes increasing component thickness, adding/subtracting components, and swapping component materials (metallic for composite). While all of these options are available, the focus here is to develop a process that demonstrates the effect of mitigation. In other words, the process and environment are emphasized over the actions themselves. As a result, a single action is selected for this work.

The historical example of the Sutter twist is selected due to the historical evidence of occurrence.

In the jig shape determination loop, the flight shape was considered fixed. Now, if mitigation is applied, the jig shape has been modified, which will in turn modify the flight conditions to cause a new flight shape. The reverse process required to determine jig shape is used to determine the new flight shape. An abbreviated process is shown in Figure 37.

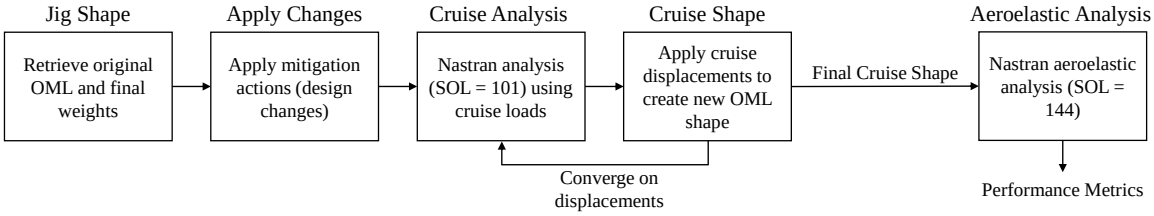

Figure 37: Cruise Shape Convergence Loop: Reverse of Jig Shape Determination Loop without Sizing

A key detail to the new process is that weight remains constant (or, more specifically, there is no sizing step). This means that the number, material, and thickness of the wing components remains constant.

The complete wing-level design process is laid out in Figure 38. The process is present as a "vee" because each step downward (on left side) has a corresponding step upward (on the right side). The left half is taking the flight shape and determining a jig shape. The right half is taking the new jig shape and determining a new flight shape. The center of the "vee" is where the uncertainty and mitigation are applied. During the first half of the process the wing undergoes sizing whereas the weight remains constant in the second half.

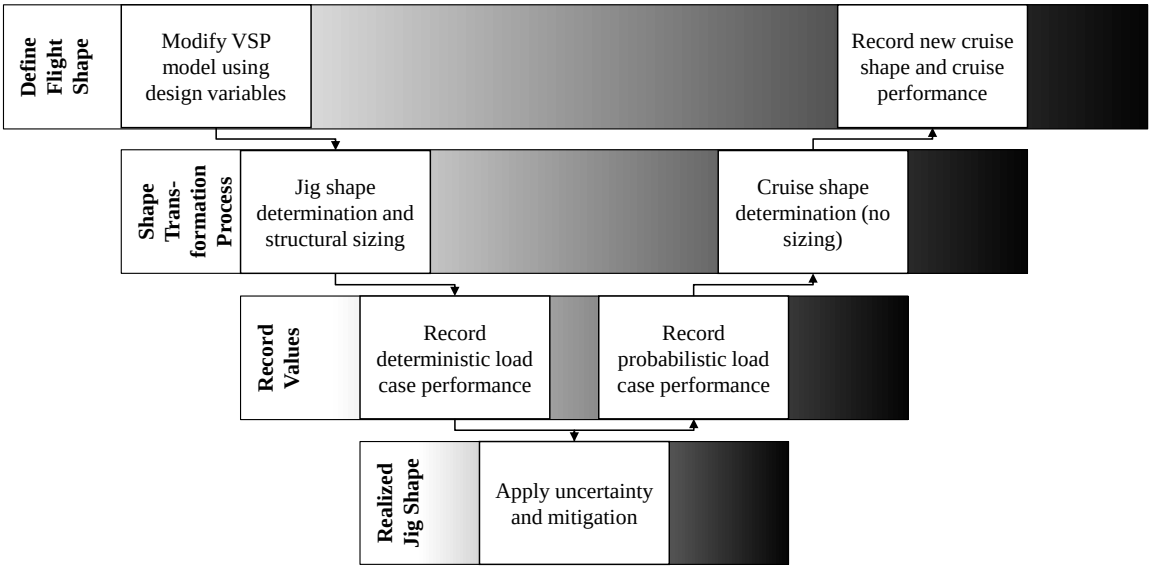

Figure 38: Wing-Level Sizing and Uncertainty Analysis "Vee"

5.2.1 Experiment 1.3a: No Mitigation Applied to Jig Shape (Verification Case)

Experimental Design

Figure 38 shows that if no mitigation is applied then the output of the process should be identical to the input. We would like to test this to verify both the jig shape determination loop as well as the flight shape determination loop. If the output shape is the same as the input shape, then the developed platform is reliable: the flight shape process yields the same shape as the input to the jig shape process.

We can test this by repeating Experiment 1.2a again except now the final jig shape will be used to determine a new flight shape. This is going down the left-hand side of the "vee" depicted in Figure 38. For this experiment, no uncertainty or mitigation is applied. Here, uncertainty is referring to capturing uncertainty via a source variable and distribution (such as load factor or modulus of elasticity). The modeled mitigation is set to zero. We expect the resulting flight shape to be identical to the initial flight shape. Figure 39 shows the difference between the initial flight shape and determined jig shape.

When comparing shapes we can use two tools. The first is visual inspection. Pictures can be taken of the front of the wing to compare the initial and final shapes. These two

Figure 39: Initial Flight Shape (top) and Un-Mitigated Jig Shape (bottom)

shapes should overlap exactly. Secondly, we can compare tip deflection at cruise. This is a quantified metric of the z-direction tip displacement using the center wing as a datum. We would expect this value to be the exact same for the jig shape and the final shape. This is because the jig shape, by definition, is the shape that will deform to the cruise shape under cruise conditions. Therefore, when the jig shape is under cruise conditions (the 1g load), the tip deflection should be the same as the final shape deflection at cruise (because the final shape deflection at cruise *is* the final shape; applying a 1g load will not displace it). In other words, the final shape is the shape that will not deform under a 1g load.

There is a very small detail here that is included for fullness. Because the input shape is the flight shape, the aerodynamics are known for that shape at the onset of the process. Therefore, the cruise conditions are not updated during the jig shape determination even though the 1g shape is changing. This is done to hold the flight shape constant. Recall that the aerodynamics and structures analysis are decoupled. This means that the loads do not update with deformation internally. In other words, AVL determines the loads which are used for Nastran to determine deformation due to the loads. Since the shape has now

changed, the loads estimation has now changed. Therefore, AVL is now used to evaluate new loads. This process iterates until convergence.

This is the process that is used to determine the new flight shape for the mitigated jig shape. However, this process of updating the cruise aerodynamics is not required for the jig shape determination loop because the flight shape conditions are fixed (constant). Therefore they are not updated.

Experimental Results

The results from this experiment are given in Table 18 and Figure 40. Because no mitigation was applied, we would expect the final shape to overlay exactly to the flight shape. Figure 40 shows this to be the case.

Figure 40: Initial Flight Shape and Final Flight Shape for Un-Mitigated Jig Shape (overlaid)

Table 18 shows that the deflections are almost exactly equal. Further, because the flight shape loop does not perform sizing, the tip deflection is reached within four iterations. Clearly this loop is much more efficient than the sizing loop which required 10-15 iterations to reach 21.1 feet tip deflection.

Table 18: Z-Direction Cruise Tip Deflection: Comparison between Flight Shape to Jig Shape and Jig Shape (without Mitigation) to Flight Shape

Iteration	Flight Shape to Jig Shape (ft)	Jig Shape to Flight Shape (ft)
1	21.91	29.94
2	21.39	21.65
3	21.29	21.09
4	21.25	21.11
Final	21.10	21.11

Of course, there are six degrees of freedom that describe deformation (three displacement, three rotation for every point). The z-direction is reported here because it aligns with the visual test presented in Figures 39 and 40. The performance metric of interest for the final flight shape is the span efficiency (e).

Experiment 1.3a Results

The results of this experiment found that the final flight shape is approximately equal to the initial flight shape. This verifies both the jig shape and flight shape determination processes.

5.2.2 Experiment 1.3b: Applying Mitigation

Experimental Design

Because the jig shape is known, the wing twist can be applied directly via the VSP file. VSP records the wing geometry of the jig shape as well as the wing twist at each wing section. This way the mitigation is treated as a design variable, but only affects the right-side of the wing design "vee."

Because the change is assumed to be small, the number of wing components does not change such that the wing configuration remains constant. Since the number of components and the thickness and material of each component has remained constant, the wing weight has remained constant.

Figure 41 compares an un-mitigated and a mitigated wing. The wing twist that has been applied is an increase in washout (or a decrease in wing twist) by 0.20° linearly. To keep in accordance with Sutter's testimony, only the outboard wing has been modified (specifically at wing section six). The twist at the root remains constant.

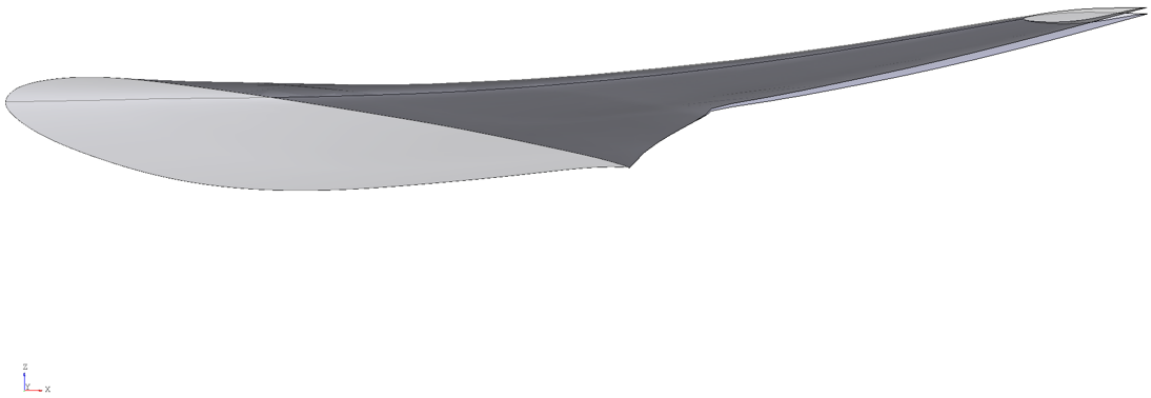

Figure 41: Left Wing View Comparison of a Mitigated (top) and Un-Mitigated (bottom) Wing

Figure 41 shows that at the root, the two wings overlay perfectly. This is because the root twist has not been affected. At the tip, however, the two wings diverge. The top is the un-mitigated wing. The twist for this wing has remained constant to the design value of -0.5° (note: the default CRM wing does not have a constant twist slope; the slope has been made constant so that it can be a design variable in the overall optimization). The lower wing, however, has had a decrease in twist starting about 25% down the span. Here the trailing edges of the wings begin to diverge (near the Yehudi station). Each sequential wing section decreases in twist in accordance with the -0.20° mitigation action shown in Table 19. Because the view is behind the wing, the mitigated wing is on top: as the twist becomes more negative, the leading edge moves downward and the trailing edge moves upward.

Note that the angle of attack between the two wings is not held constant. The total

Table 19: Wing Twist by Section for Un-Mitigated and Mitigation Wing

Wing	1	2	3	4	5	6	7	8	9	10
Default	5.5°	5°	4.5°	4°	3.5°	3°	2.5°	2°	1.5°	1°
Mitigated	5.5°	5°	4.5°	4°	3.5°	2.8°	2.1°	1.4°	0.7°	0°
	11	12	13	14	15	16	17	18	19	20
Default	0.5°	0°	-0.5°	-1°	-1.5°	-2°	-2.5°	-3°	-3.5°	-4°
Mitigated	-0.7°	-1.4°	-2.1°	-2.8°	-3.5°	-4.2°	-4.9°	-5.6°	-6.3°	-7°

weight of the aircraft is constant between the two wings such that both wings must produce the same amount of lift. Therefore, the angle of attack is higher for the mitigated wing because the average twist is more negative. In this way, outboard wing twist has a tangible effect on span efficiency. The angle of attack may be too high or too low for any given combination of wing area and take-off gross weight. Therefore, decreasing or increasing the twist could be either beneficial or detrimental to induced drag. The effect is not ubiquitous for all combinations of design variables.

Experimental Results

We now apply mitigation to the jig shape to determine if the final flight shape changes. The expectation is that the final shape will be measurably different than the initial flight shape. Figure 42 shows the initial flight shape and final flight shape for a mitigated jig shape.

Figure 42: Difference in Initial Flight Shape and Mitigated Flight Shape

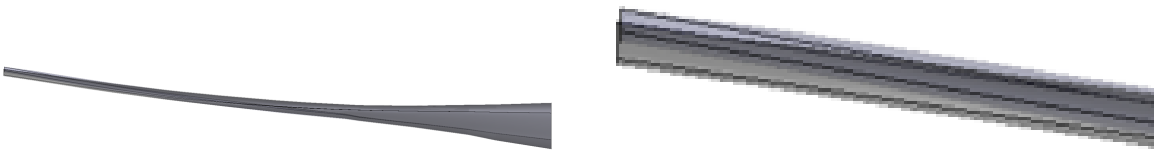

(a) Initial Flight Shape and Final Flight Shape for Mitigated Jig Shape (overlaid)

(b) Initial Flight Shape and Final Flight Shape for Mitigated Jig Shape (zoomed)

Table 20: Z-Direction Cruise Tip Deflection: Comparison between Flight Shape to Jig Shape and Jig Shape (with Mitigation) to Flight Shape

Iteration	Flight Shape to Jig Shape (ft)	Jig Shape to Flight Shape (ft)
1	21.91	17.50
2	21.39	11.39
3	21.29	11.00
4	21.25	11.09
Final	21.10	11.09

Unfortunately the change is difficult to visually observe due to poor visualization techniques. Thankfully, the cruise tip deflection is quantified in Table 20.

The table of the z-direction deflections shows that the two values are not equal. Increasing the washout of the wing has decreased the tip deflection at cruise. This matches the expectation that increasing washout would shift the lift distribution inboard thereby decreasing the load on the outboard wing. As a result, the tip deflection decreases relative to the initial flight shape. This will result in differing cruise characteristics such as span efficiency. It is also important to note that the mitigation did not affect wing weight.

Experiment 1.3b Results

The results from Experiment 1.3b show that the mitigated jig shape deforms to a different flight shape than the un-mitigated jig shape; therefore, mitigation can be physically modeled, and its effect on cruise shape and performance can be determined.

5.2.3 Experiment 1.3c: Constraint Sensitivity to Mitigation

Experimental Design

The last task to perform is a sensitivity study on various responses due to a mitigation action. Formal constraints other than stress have not yet been defined (Nastran sizes to maximum stress internally), but we can use some nominal constraints for the time being.

The vehicle-level design environment is mostly interested in the cruise condition. The aerodynamics at cruise directly affect range and block fuel, for example. Therefore a metric of interest will be an aerodynamic cruise metric which will change will flight shape and (by extension) mitigation. The span efficiency metric is chosen because it is calculated by AVL and is also an input the vehicle-level environment. The second and third will be the tip deflections at each of the load cases (2.5G maneuver and -1.0G maneuver). These are chosen because we expect that the constraint violation that necessitated the Sutter Twist was a tip deflection constraint. The final output for this sensitivity study will be the maximum Von Mises stress to test if twisting the wing has had any effect on structural constraints. Because Nastran is no longer sizing, the stress constraint can be violated.

We can test for sensitivity by setting three values for the wing twist and three values for the twist start location. The start location is the wing section number out of a possible 20 sections (the wing tip existing at section 20). The second mitigation variable is the magnitude of the change in linear wing twist slope. Note that this is not simple addition: the magnitude of the change becomes larger the greater number of sections that are affected as shown in Table 19. The design variable values are identical to the design point described in Table 13.

The wing sections selected are 1, 7, and 15. Even though altering the wing twist at the first section cannot qualify as the "outboard" wing, it is selected to show the sensitivity of the constraints. The values selected for the change in linear twist slope are between -1.0°and 1.0°. Because the design twist is -0.5°, modifying the twist by ± 1°should have a measurable effect on the performance.

Experimental Results

The results shown in Figure 43 show the higher the mitigation, the higher the effect. This trend was expected and desired. The black triangles show the twist enforced at section 15 (out of 20 possible), and it appears to have much less effect than the other section

Figure 43: Mitigation Sensitivity Study: Span Efficiency and Maximum Von Mises Stress

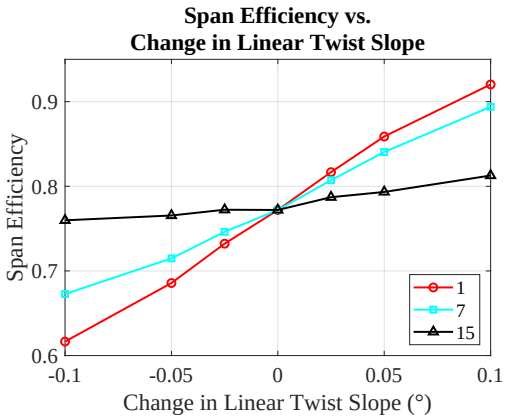

(a) Effect of Outboard Change in Linear Wing Twist Slope on Span Efficiency

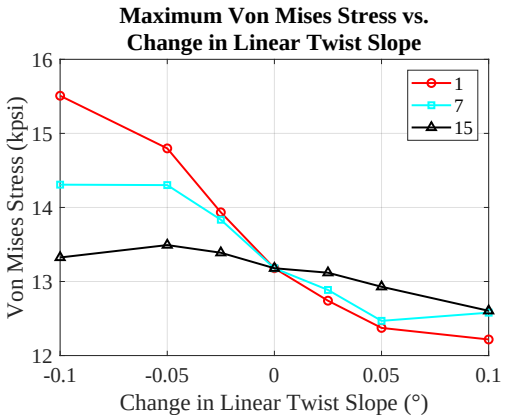

(b) Effect of Outboard Change in Linear Wing Twist Slope on Maximum Von Mises Stress

settings. Increasing the washout (decreasing linear twist slope) has a negative effect on these constraints: a decrease in span efficiency and an increase in maximum Von Mises stress. This is an interesting finding: both appear to be penalty functions for the applied mitigation. In the case of the Sutter Twist, which we are mimicking, where the outboard wing was "carrying too much load," we would expect the mitigation action to increase washout (change in twist slope to be negative). This has an inherent penalty with respect to drag (span efficiency) and stress. Decreasing the washout, on the other hand, has the opposite trend.

The trends for the tip deflections are exactly mirrored between the two maneuver load cases. This presents somewhat of a quandary when applying mitigation: changing the wing to recover one constraint may result in violating the other. A lower maximum tip deflection is desired but so is a higher minimum tip deflection. It seems that the mitigation space available that will help one without hurting the other will be small.

Experiment 1.3c Results

The results of Experiment 1.3c show that mitigation (wing twist) measurably affects

Figure 44: Mitigation Sensitivity Study: Tip Deflection at 2.5G and -1.0G Maneuver Load Cases

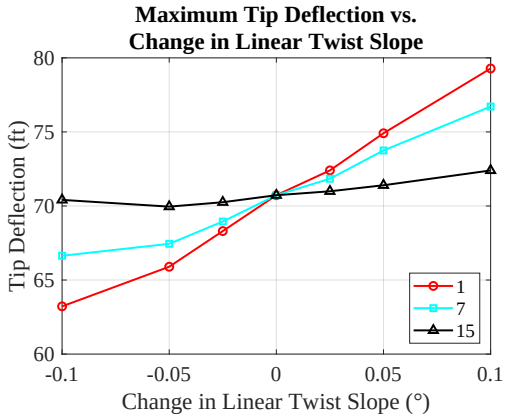

(a) Effect of Outboard Change in Linear Wing Twist Slope on 2.5G Maneuver Tip Deflection

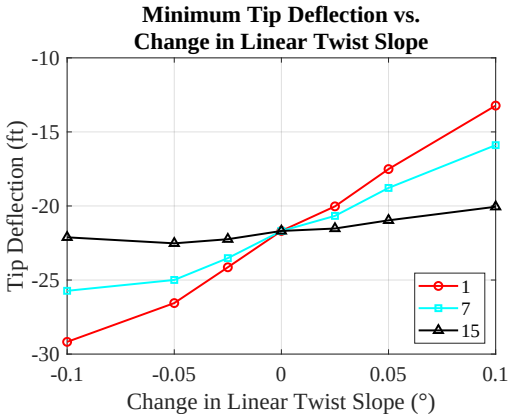

(b) Effect of Outboard Change in Linear Wing Twist Slope on -1.0G Maneuver Tip Deflection

the constraints. Varying levels of mitigation can be used to recover varying levels of constraint violation.

5.2.4 Answering Research Question 1.3

Research Question 1.3 is a central focus to this work. While the ARMOUR (benchmark) method did include mitigation modeling, it was entirely done on the conceptual level by k-factors: no specific *physical* design changes were implemented. Therefore, this is the first time mitigation has been modeled to this level of fidelity. In fact, the physics-based model was required explicitly for this purpose.

Therefore, a majority of the effort in answering Research Question 1.3 was developing this new capability. The RADE environment offered the tools necessary for structural sizing (Nastran), aerodynamic evaluation (AVL), and geometry modification (VSP), but they needed to be reorganized to perform mitigation application and testing. Experiment 1.3a verified both the jig and flight shape determination processes. Experiment 1.3b showed that mitigation will affect and result in a new flight shape relative to the un-mitigated shape. Finally, Experiment 1.3c showed that the constraints can be affected through mitigation.

While wing twist was the only demonstrated mitigation action, this process can be

used as a testbed for other mitigation actions: adding components, increasing component thickness, exchanging component material, and much more.

CHAPTER 6
UNCERTAINTY QUANTIFICATION

The first research question dealt solely with creating a higher fidelity model. Moving from low-fidelity to high-fidelity models will most likely reduce uncertainty: variable values that were previously unknown are now defined and quantified (stress, for example). Research Question 2 deals with capturing the uncertainty explicitly; that is, including uncertainty explicitly as variables in the mathematical formulation. The first step towards quantifying uncertainty was investigating common types and categorizations. This was the first research question of this area:

Research Question 2.1

What are typical categorizations of uncertainty, and which are most prevalent to design uncertainty?

This led to a synthesized taxonomy (Table 7) as well as a developed taxonomy (Table 8) taken from the fields of design, structural engineering, and wing design. Model uncertainty was selected as the focus because the decision-making criteria is entirely dependent on model analysis (even if the models are based on empirical data). Two other categories to keep in mind are statistical uncertainty and parametric uncertainty. We will implement statistical uncertainty should we find no suitable method to describe our uncertainty types as probability distributions.

As described by Chapters 3 and 4, uncertainty tends to be described as a uniform distribution between two set bounds without justification. The only justification for this approach is that a better one is unavailable. However, there is no guarantee that this is true. This led to the development of Research Question 2.2:

Research Question 2.2

How can the probabilistic description of the uncertainty be derived?

The term "derived" here is taken to mean supported by analysis of the uncertainty versus prescribed by the user. We would like the distributions to be outputs of an approach rather than inputs to an approach. The third piece of Research Question 2 is formalized as follows:

Research Question 2.3

Does correlation exist between uncertainty sources? If so, how can it be captured in the RBDO?

Chapter 3 showed that uncertainty sources are often assumed to be independent of each other when no evidence to support this assumption exists; indeed, the only evidence is the lack of contrarian evidence. Similar to the descriptions of the uncertainty sources, we would like the correlations to be outputs of analysis rather than inputs.

Answering these two research questions (2.2 and 2.3) is the focus of this chapter which will follow the approach described in Figure 26.

We propose to describe the model uncertainty via discretization error (Section 4.2.2). In order to do so, a number of sub-research questions must be answered. This series of sub-research questions are summarized in Figure 45. Each question requires a step in the process of determining the discretization error. The process begins with a mesh size sensitivity and convergence test to quantify the formal order of accuracy. Then, using this value, a series of points taken from the design space can be evaluated at two levels of mesh size. The result will be an associated error for each output metric. This process is complete when each output metric has a corresponding, parametric distribution that can represent the discretization error with 95% confidence.

Figure 46 shows the overall process to answer Research Question 2.3. This question is predicated on answering Research Question 2.2 to the extent that data samples can be

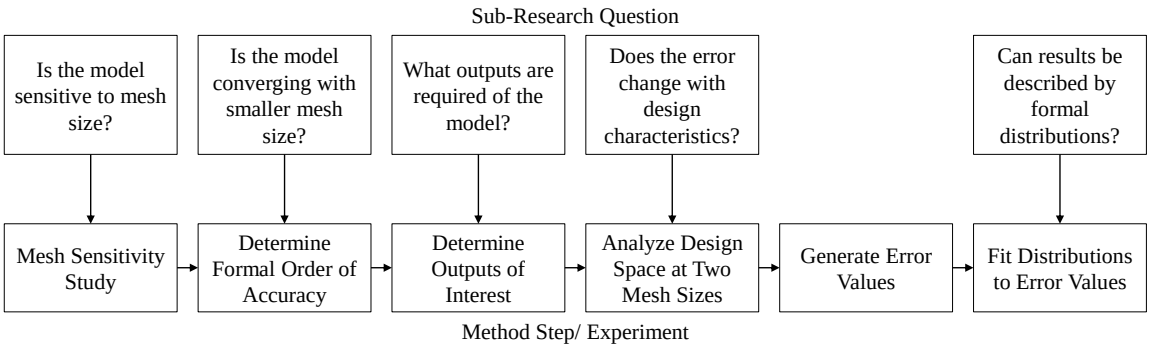

Figure 45: Quantifying Discretization Error Approach

generated. If no samples are generated, then another approach to generate error data is needed. This process begins with testing for correlation using visual inspection and Pearson's Correlation Coefficient. Recall that a magnitude above 0.3 shows correlation with 95% confidence for a sample size of over 50 samples. The second half of the process describes the fitting of a copula, or joint probability distribution. Essentially this integrates each of the individual distributions into a single, n-variate distribution. A sample taken from the copula will be n-dimensional, where n is the number of output metrics (wing weight, max stress, etc.).

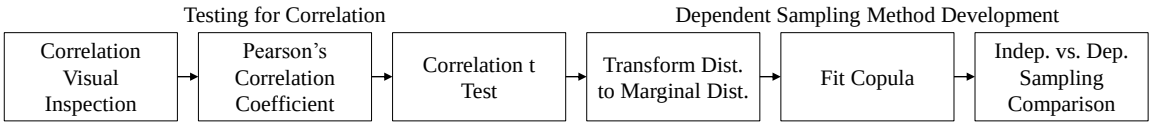

Figure 46: Correlated Sampling Approach

6.1 Research Question 2.2: Determining Uncertainty Distributions

As stated in Chapter 4, the proposed approach is to use Richardson's Extrapolation Method to described discretization error in the FEM used for wing-level design and analysis. Figure 45 depicted the overall process both in terms of sub-research questions and methodology steps. This process will be followed here.

6.1.1 Experiment 2.2a and 2.2b: Mesh Size Sensitivity

Experimental Design

For Richard's Extrapolation Method to be used, two criteria have to be met: the mesh size has to have a measurable impact on the output (wing weight), and the output has to converge to finite value as the mesh is refined. Richardson's Method is predicated on these two characteristics: it forecasts (extrapolates) this finite value and compares the calculated value to the ideal solution.

This experiment can be easily completed with a mesh sensitivity: the same wing-level design point used in Section 5.1 is sized at varying levels of mesh size. The output of interest here is wing weight, with an associated assumption that the other outputs would be affected similarly. In fact, the other outputs are all directly affected by weight (e.g. stress).

Richardson's Method only requires three mesh sizes of constant mesh refinement ratio to calculate the formal order of accuracy (Section 4.2.2). The mesh refinement ratio is the quotient of coarse mesh size over the fine mesh size. For example, if a mesh size of 10 inches is used as the coarse mesh, an accompanying mesh size of 5 inches would result in a mesh refinement ratio of 2. A third mesh is required, which can either be 2.5 inches or 20 inches. This is required in order to calculate the formal order of accuracy defined in Equation 11.

While only three executions are required to computationally calculate the formal order of accuracy, a wide range of mesh sizes will be used to form an overall mesh size trend. The default mesh size in RADE for Nastran is 7 inches. Mesh sizes between a refinement ratio of 2 (3.5 to 14) will be used for the sensitivity. Note that the computation time increases by orders of magnitude for the finest meshes relative to the coarsest meshes.

Experimental Results

The results of the mesh sensitivity are given in Figure 47. Clearly the final weight output is dependent on mesh size. The wing weight changes from about 47,000 pounds to almost 52,500 pounds. This is an increase of over 11% from the coarse meshes to the finest meshes.

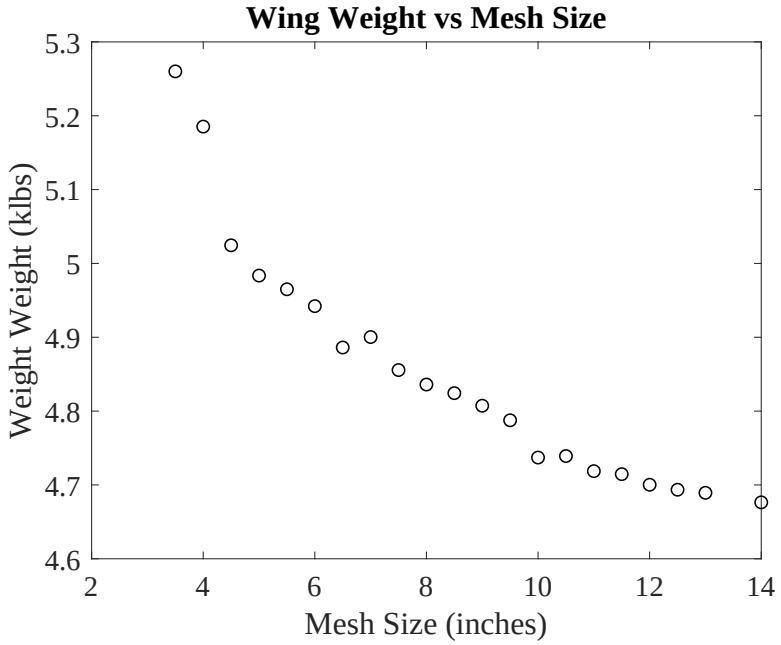

Figure 47: Wing Weight Sensitivity to Mesh Size

Experiment 2.2a Results

The mesh size sensitivity shows that the wing weight is dependent on mesh size. Therefore the modeling environment meets the first criterion required for Richardson's Extrapolation Method.

We now look to see if the trend is diverging or converging. As demonstrated by Figure 47, the wing weight result is *diverging* (approaching infinity) as the mesh size approaches zero. This is the opposite desired trend: the weight should converge on a finite value as the mesh size approaches continuity. Instead, it approaches infinity. In reality infinite stress

does not exist. Therefore, Hypothesis 2.2b is rejected as originally written in Section 4.2.2. This means that Richardson's Extrapolation cannot be used for this model. Practically, this is an issue because the formal order of accuracy is negative rather than positive. Thus, Hypothesis 2.2b is restated, or qualified.

Experiment 2.2b Results

The wing weight appears to approach infinity as the mesh is refined. This result qualifies Hypothesis 2.2b which now states that *some* of the mesh sensitivity will exhibit convergent behavior.

Formal Order of Accuracy

The divergence exhibited in Figure 47 results in a negative p (formal order of accuracy) value and yields the opposite error sign (negative instead of positive). Notional p values are depicted in Figure 48. The red line with the circular points represents the desired converging trend. This occurs when the difference in wing weight between the fine and medium mesh is smaller than the difference in wing weight between the medium and coarse mesh. This change in difference signifies an approach to a finite value and therefore a positive p value and positive error. When the change in wing weight does not change from the difference between fine and medium and medium and coarse, the trend is said to be "linear" because the change is constant. The resulting p value is zero and the error is negative infinity. This trend is demonstrated by the cyan plus-sign points. The last notional trend depicted is the diverging trend shown by the blue x-sign points. The change in wing weight between the medium and coarse mesh is much smaller than the change between fine and medium meshes. Here the p value is negative and the error is negative as well.

There are two trends in Figure 48 that represent actual values from Figure 47 which are the black square points and the green triangle points. The black square points show the general trend shown in Figure 47 using mesh sizes of 3.5, 7, and 14 inches. The trend

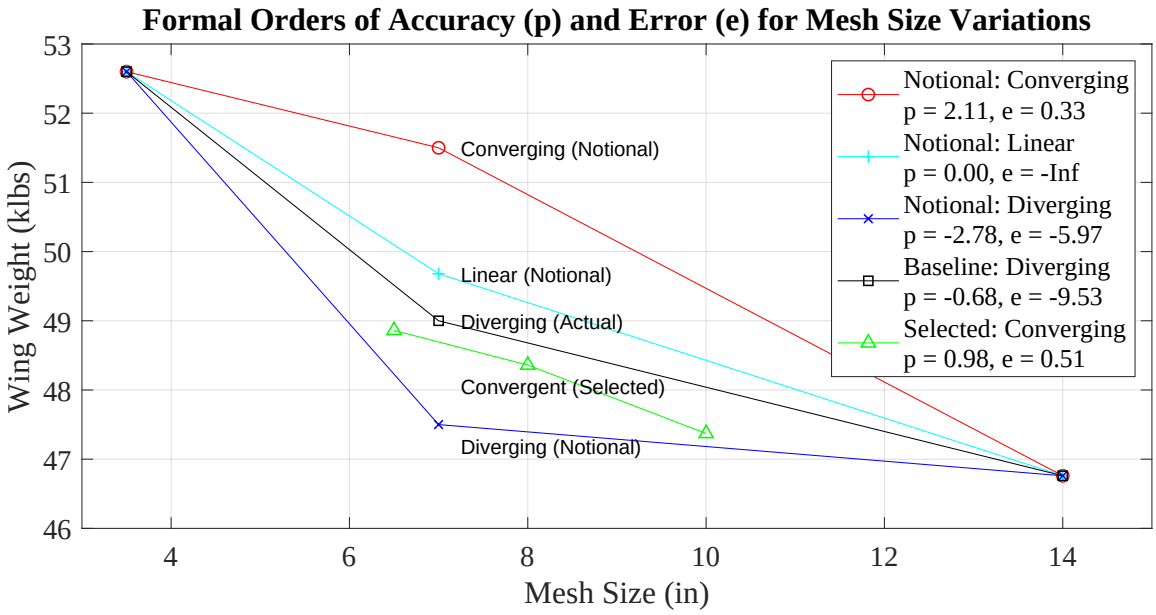

Figure 48: Formal Orders of Accuracy and Error for Mesh Size Variations

is diverging with a p value of -0.68 and error of -9,530 pounds. The values are negative because the extrapolation assumes the values are switched (the user meant the coarse mesh to be the fine mesh) such that the wing weight converges as the mesh size increases. If this were true, the model would converge on a finite value as the mesh size approaches infinity.

There does exist, however, a set of points that exhibit convergent behavior at mesh sizes 6.5, 8, and 10 (recall that the three values must have the same mesh refinement ratio; the ratio here is approximately 0.805). The wing weights are 48,861, 48,359, and 47,370 pounds, respectively. Utilizing Equation 11, this results in a formal order of accuracy of 0.98 using a mesh refinement ratio of 2.

$$p = \ln(\frac{f_3 - f_2}{f_2 - f_1}) / \ln(r) = \ln(\frac{47,370 - 48,359}{48,359 - 48,861}) / \ln(2) = 0.98 \tag{18}$$

Note that two is not the proper mesh refinement ratio here. The correct mesh refinement number is 6.5/8 which is about 1.25. This would result in a p value greater than three, which means the model is extremely convergent.

These points are represented in green in Figure 48. The resulting wing weight error is

510 pounds, or about 1%.

A Crossroads: Stress Singularities

Here we come to a choice: continue with Richardson's Extrapolation or abandon it altogether because the trend is divergent rather than convergent. Before we make this decision, we need to know why the model diverges with diminishing mesh size when we expected the model to converge.

The reason lies in the assumptions formed when developing the model and running Nastran. As aforesaid, the model is designed to be an early stage preliminary design tool based on physics rather than empirical data. It is not, however, a detailed design tool which considers *all* the components that will be used in the final design. Connection components (nuts and bolts) have been ignored. This choice was made to decrease the modeling effort requirement and computational expense (the number of parts to model, generate, and analyze would drastically increase). Instead, the connections between the components were modeled as point forces. A point force is a force that acts on a single, infinitesimal point rather than an area. Physically, point forces do not exist: all forces are distributive forces. Other names for point forces are stress concentrations or stress singularities. Figure 49 shows why the wing weight approaches infinity as the mesh size decreases.

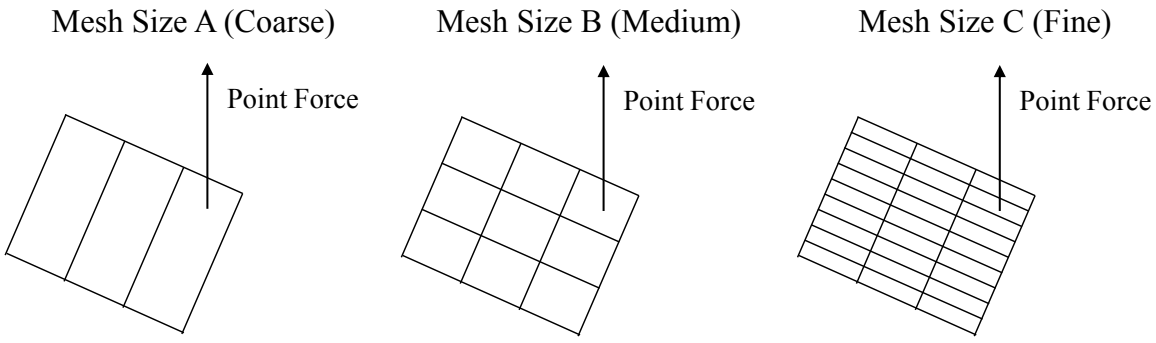

Figure 49: Point Force Acting on Variable Mesh Sized Elements

Meshes A, B, and C represent three different mesh sizes (coarse, medium, and fine,

respectively). The mesh refinement ratio is three as the number of elements is tripling between the meshes (3, 9, and 27 elements). Consequently, the mesh area is dividing into thirds as well. Assume that the magnitude of the point force remains constants for each mesh size. The finite element model will compute a single stress value for each individual element. Then, the stress of the element which holds the point force is tripling every time the area is divided.

$$Stress_{\mathrm{A}} = \frac{Force}{Area_{\mathrm{A}}} \tag{19}$$

$$Stress_{\mathrm{B}} = \frac{Force}{Area_{\mathrm{B}}} \tag{20}$$

$$Stress_{\mathrm{C}} = \frac{Force}{Area_{\mathrm{C}}} \tag{21}$$

If the force remains constant while the area is changing between the meshes then the resulting stress value changes as well.

$$Area_{\mathrm{A}} = 3(Area_{\mathrm{B}}) = 9(Area_{\mathrm{C}}) \tag{22}$$

Then, by changing the mesh size only and not the actual force, the stress in the fine mesh is now nine times the stress in the coarse mesh.

$$\frac{Stress_{\mathrm{C}}}{Stress_{\mathrm{A}}} = \frac{\frac{Force}{Area_{\mathrm{C}}}}{\frac{Force}{Area_{\mathrm{A}}}} = \frac{Area_A}{Area_C} = \frac{9(Area_C)}{Area_C} = 9 \tag{23}$$

This step is completed during the model synthesis step of the wing environment. To resolve this issue we would need a new model. This option is not pursued for two reasons. The first is that the effort would be non-trivial and is beyond the scope of this work. The second is that a finite element model which includes all the structural component pieces is further down the design process (detailed design). As a result, the current model may

be representative of a design tool which makes assumptions to simplify analysis. In other words, a tool that integrated the entire wing parts may be unusable in this context due to the complexity to automatically generate and analysis wing designs. For these reasons, this option is not pursued.

The other option is to define the formal order of accuracy with the points that exhibit convergent behavior. While this is a bit cheeky, it will allow us to demonstrate the process of quantifying the discretization error and test for error correlation.

6.1.2 Generating Error Values

Now that a formal order of accuracy is defined, the design space can be sampled to generate a dataset of errors. Each design will have an associated error for each defined output (wing weights, max stress, tip deflection constraints, etc. taken from Section 2.2.3). The design space was sampled to gather a set of errors to fit distributions. The variables and their ranges are defined identically to the surrogate ranges defined in Section 8.2.6. 56 cases were completed. These cases were taken from the Latin-Hypercube design of experiments and also from the additional randomly sampled designs. These designs were chosen to save on computation time: the seven inch mesh was already needed for surrogate modeling fitting for the case study in Chapter 8.

6.1.3 Fitting Distributions to Error Values

Once the dataset was built, the results for each metric were fit to number of candidate distributions. Each distribution was evaluated using Bayesian Information Criterion (BIC) [202]. There are a number of criterion that could be considered. Akaike Information Criterion (AIC) [203] could also be used (though the results showed the same ranking among candidate distributions). The candidate distributions evaluated were: Beta, Birnbaum-Saunders, Exponential, Extreme Value, Gamma, Generalized Extreme Value, Generalized Pareto, Inverse Gaussian, Logistic, Log-logistic, Lognormal, Nakagami, Normal, Rayleigh, Rician,

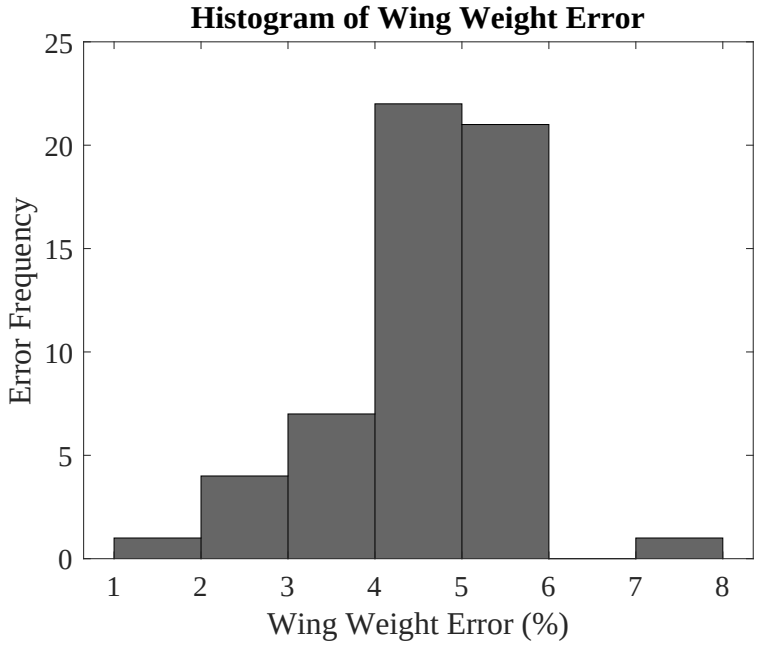

Figure 50: Histogram of Wing Weight Error

T Location-scale, and Weibull.

The results of the candidate distributions for wing weight are described in Table 21. The parameters for each of the distributions are also shown along with the BIC values.

Table 21: Top Candidate Distributions for Wing Weight Discretization Error as Determined by BIC

Distribution Type	BIC Value	Parameters
Logistic	166.70	[4.65, 0.549]
Weibull	168.24	[4.96, 5.17]
t Location-Scale	170.00	[4.70. 0.735, 3.54]
Normal	170.10	[4.57, 1.04]
Rician	170.30	[4.45, 1.04]

Table 21 shows that the top candidates are similar in accurate representation (which is reinforced visually by Figure 51). Unfortunately there is no way to estimate the absolute accuracy of each of the candidate models (the absolute magnitude of BIC has no intrinsic meaning) [204]. Therefore, we cannot say how *well* each of these candidate distributions

the wing weight error. This follows the aphorism in statistics that "all models are wrong, but some are useful" [205]. The Anderson-Darling test will can show if the distribution is accurate with 95% confidence, but the accuracy cannot be quantified beyond this level.

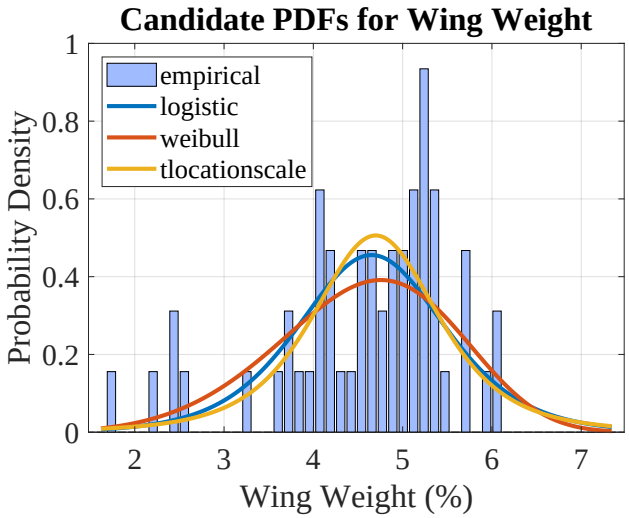

Figure 51: Candidate Distribution Comparison for Wing Weight Error

The distributions of discretization error and the top candidate distributions are shown in Figures 52, 53, and 54. As will be described in Chapter 7, the bridge variables between the two design environments will be the wing skin weight and the wing ribs and spars weight. Therefore those two outputs are included in the characterization and correlation approach (whereas total wing weight is neglected).

$$Wing\ Weight = Skin\ Weight + Ribs\ and\ Spars\ Weight \tag{24}$$

The discretization error is divided by the fine mesh value (seven inch mesh) to give the percent error. This way, in the final implementation, the uncertainty can be applied as modifiers or multipliers rather than adders.

Both wing weight outputs exhibit close to normal distribution discretization error, though the best model representations for both is a logistic distribution. It is also important to note that wing skin weight is centered about 5% error whereas the ribs and spars weight error is

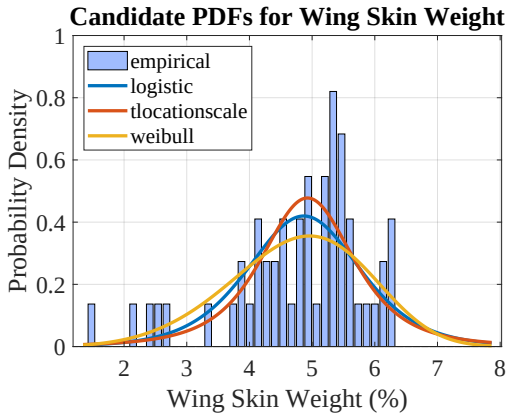

(a) Candidate Distribution Comparison for Describing Wing Skin Weight Error

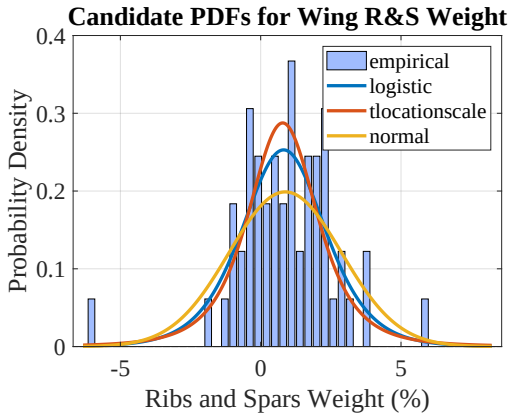

(b) Candidate Distribution Comparison for Describing Ribs and Spars Weight Error

Figure 52: Candidate Distribution Comparison for Wing Skin Weight Error (a) and Ribs and Spars Weight Error (b)

centered about 1%. The magnitude of the skin weight is much great (10x) than that of the ribs and spars weight. Recall Figures 47 and 48: the ideal wing weight is expected to be larger than the fine mesh estimation. Consequently, both error distributions are centered on positive values.

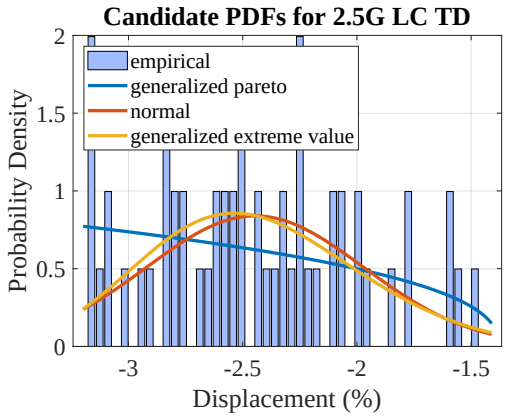

(a) Candidate Distribution Comparison for Describing 2.5G Maneuver Load Case Error

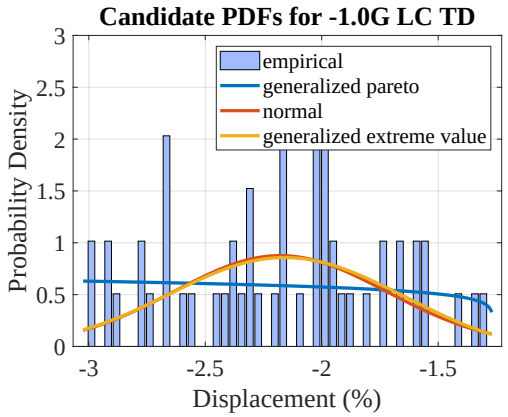

(b) Candidate Distribution Comparison for Describing -1.0G Maneuver Load Case Error

Figure 53: Candidate Distribution Comparison for Tip Deflection Errors

Both tip deflection error distributions appear to be almost uniform between about -1% and -3%. This means that the values are *overestimated* rather than underestimated. With epistemic uncertainty, we would not expect the error to have defined bounds; uniform

distributions were not included among the candidate distributions for this reason. Still, these two error distributions could be described using uniform distributions. Though, if this was assumed a priori, the bounds of the uniform distributions would not have been known.

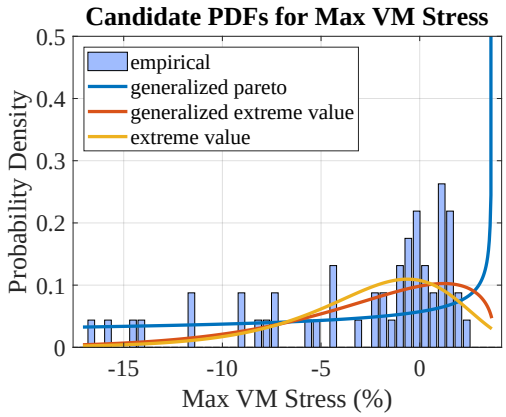

(a) Candidate Distribution Comparison for Describing Max Von Mises Stress Error

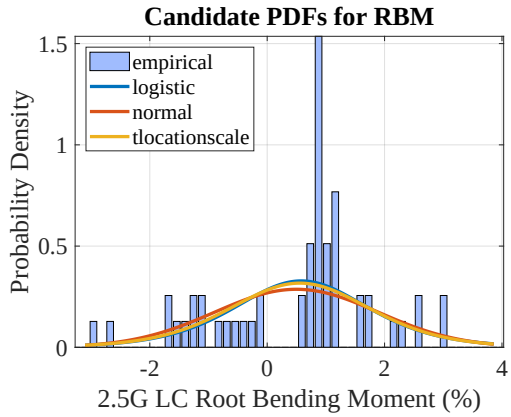

(b) Candidate Distribution Comparison for Describing 2.5G Maneuver Root Bending Moment

Figure 54: Candidate Distributions of Stress Error (a) and Root Bending Moment Error (b)

6.1.4 Experiment 2.2c: Representing Error Sample using Parametric Distributions

Experimental Design

Each of the error samples has a candidate distribution that fit best based on the BIC criterion. Now we would like to test if the candidate distribution can represent the error sample with 95% confidence. This can be completed using an Anderson-Darling test [206]. The null hypothesis is that the error samples are drawn from the given distribution. A p-value greater than 0.05 fails to reject the null hypothesis. Therefore if a p-value less than 0.05 rejects the null hypothesis and Hypothesis 2.2c (which states that the candidate distribution can represent the error sample). The alternative hypothesis is that the error sample is from a different distribution. If a p-value is found to be lower than 0.05, another distribution can be used for the test. However, there is no guarantee that the error sample *can* be represented by an unbounded, parametric distribution. Therefore, there is a chance that some variable

Table 22: Anderson-Darling Test: Best Fit Distributions for Nastran Output Discretization Error

Variable	Distribution	Result	P-Value
Wing Skin Weight	Logistic	Fail to Reject	0.557
Ribs and Spars Weight	Logistic	Fail to Reject	0.857
Max Tip Deflection	Generalized Pareto	Fail to Reject	0.333
Min Tip Deflection	Generalized Pareto	Fail to Reject	0.246
Von Mises Stress	Generalized Pareto	Reject	0.002
Root Bending Moment	Logistic	Fail to Reject	0.157

Table 23: Anderson-Darling Test: Best Fit Distributions for Nastran Output Discretization Error (Second-best Fit for Maximum Von Mises Stress)

Variable	Distribution	Result	P-Value
Wing Skin Weight	Logistic	Fail to Reject	0.557
Ribs and Spars Weight	Logistic	Fail to Reject	0.857
Max Tip Deflection	Generalized Pareto	Fail to Reject	0.333
Min Tip Deflection	Generalized Pareto	Fail to Reject	0.246
Von Mises Stress	Generalized Extreme Value	Fail to Reject	0.310
Root Bending Moment	Logistic	Fail to Reject	0.157

errors cannot be fit to distributions (though they "look" like parametric distributions).

Experimental Results

The results from the test are given in Table 22. Each of the distributions fail to be rejected other than the Von Mises Stress. Upon reviewing the shape of the Generalized Pareto function in Figure 54a, the curve is clearly increasing in probability where the data does not exist. This leads us to believe that the second-best distribution can be tested.

The second-best distribution is the generalized extreme value distribution. This was tested using the Anderson-Darling test and failed to be rejected. Therefore, with the substitution of the generalized Pareto distribution, all the parametric distributions have p-values greater than 0.05. The new results are given in Table 23.

Because the null hypothesis was that the distributions can indeed represent the sampled

Table 24: Distribution Types and Parameters

Output	Distribution Name	BIC	Distribution Parameters
Skin Weight	Logistic	176.3	4.87, 0.596
Ribs & Spars Weight	Logistic	234.0	0.818, 0.989
2.5G Tip Displacement	Generalized Pareto	73.29	-0.711, 1.29, -3.20
-1.0 Tip Displacement	Generalized Pareto	74.73	-0.902, 1.59, -3.02
VM Stress	Generalized Extreme Value	327.97	-0.749, 5.360, -3.392
RBM	Logistic	202.24	0.580, 0.762

error with 95% confidence, the results of the experiment substantiate Hypothesis 2.3b.

Experiment 2.3b Results

While most of the best fit distributions failed to be rejected by the Anderson-Darling test, the null hypothesis was rejected for the best fit Von Mises distribution. Therefore Hypothesis 2.3 is qualified to now state that a distribution can be found for each output variable that represents the error with 95% confidence.

A summary of the distribution types and parameter values is given in Table 24. Though some twenty distributions were evaluated, only Logistic, and Generalized Pareto, and Generalized Extreme Value are needed.

6.1.5 Answering Research Question 2.2

The aircraft conceptual design uncertainty quantification field is plagued by notional distributions with notional bounds. Research Question 2.2 sought to fill this void by deriving uncertainty distributions rather than prescribing them. The results of Research Question 2.1 were that model uncertainty was central due to the reliance on model-based decision-making. Further, model uncertainty was whittled down to discretization error which is known and studied in CFD and FEM. Richardson's Extrapolation Method was used to characterize this error by extrapolating to an ideal solution.

Experiments 2.2a and 2.2b showed that the wing-level analysis tool (Nastran) is dependent on mesh size but also divergent. Even still, some convergent points existed with constant mesh refinement. Further, the error samples found throughout the design space were fit to parametric distributions in Experiment 2.2c. Now, each of the output metrics can be represented by a parametric distribution with 95% confidence. This is a significant result as there is no theoretical guarantee that the error samples could be fit to a distribution. Even without an approach to capture correlation, this already represents a significant contribution to the state-of-the-art in aircraft conceptual design.

6.2 Research Question 2.3: Testing for Error Correlation

Because the distributions passed the Anderson-Darling test, the uncertainty can be sampled from these distributions independently. This already fills the capability gap of uncertainty characterization. Though, the quantification process can be enhanced further by testing for correlation.

6.2.1 Experiment 2.3a: Testing for Correlation via Visual Inspection

Experimental Design

The first and easiest test for correlation is the eye test. This simple experiment is first conducted to provide an overall measure of the expected correlation (or lack thereof). This can be done simply be plotting each variable along one axis with another on the opposite axis. If a pattern presents itself then a correlation exists. If, on the other hand, the points appear to be randomly scattered, then no evidence for correlation is provided.

The key enabler here for correlation testing is the matching between the error samples. Because each design has a unique set of error samples, they can be mapped against each other. For example, Design One has an error value for wing skin weight *and* wing ribs and spars weight. For Design One, the skin weight error may be high whereas the ribs and spars error may be low. Considering a second design (Design Two), the skin weight error may

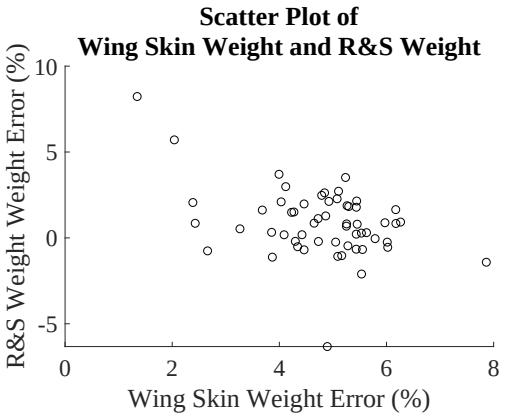

(a) Scatter plot of Wing Skin Weight and Ribs and Spars Weight Errors

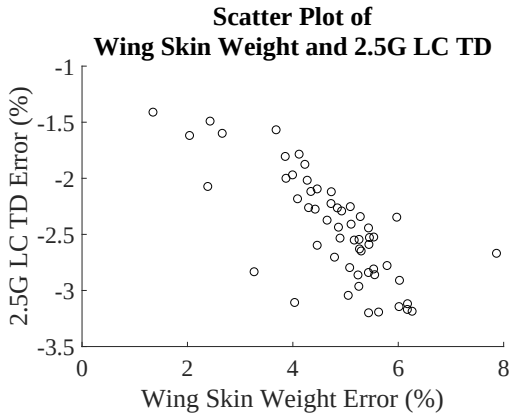

(b) Scatter plot of Wing Skin Weight and -1.0G Maneuver Load Case Tip Displacement Errors

Figure 55: Scatter plots of Wing Weight Errors (a) and Wing Skin and -1.0G Tip Displacement Errors (b)

be low but the ribs and spars weight error may be high. If a series of 50 designs are plotted against each other, the trend may appear that a high error in wing skin weight correlates with a low error in ribs and spars weight. The key is that each error in one variable space has a partner in the other variable space. Because these connections are known, we can test to see if there are correlations.

Experimental Results

Figures 55 and 56 visually depict errors against each other. Some combinations, such as the wing weight errors, do not appear to be strongly correlated if at all. Others, though, do, such as the wing skin weight error and the tip displacement error for the -1.0G maneuver load case shown in sub-figure 55b.

6.2.2 Experiment 2.3b: Testing for Correlation via Pearson's Correlation Coefficient

Experimental Design

Many correlation techniques were enumerated in Section 4.2.3. A common and easy test for perform is to calculate the Pearson Correlation coefficient between each pair of variables.

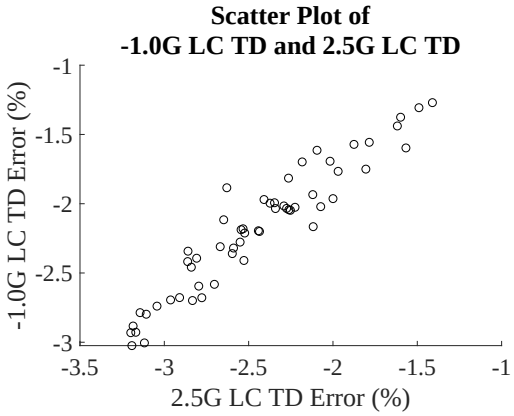

(a) Scatter plot of 2.5G and -1.0G Maneuver Load Case Tip Displacement Errors

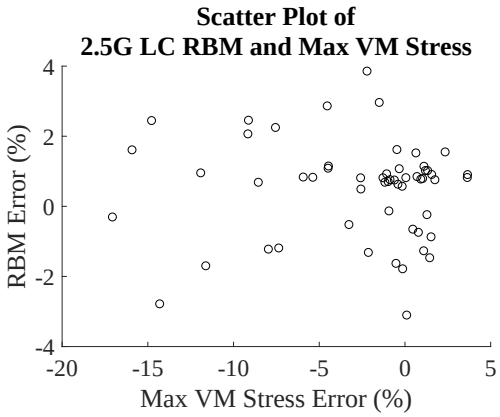

(b) Scatter plot of Max Von Mises Stress and 2.5G Maneuver Load Case Root Bending Moment

Figure 56: Scatter plots of Tip Displacement Errors (a) and Stress and Root Bending Moment Errors (b)

Pearson will provide a value between ± 1 with the degree of linear correlation. The higher the magnitude, the higher the degree of correlation. At this point, we are only interested in the existence of correlation (which is the magnitude) rather than the trend (which is the sign). As denoted in Section 4.2.3, a Pearson coefficient magnitude of 0.3 or higher represents correlation with 95% confidence.

Experimental Results

The experiment was conducted by assimilating all the errors into a matrix and applying MATLAB's "corrcoef" function. This results in a Pearson's coefficient for each possible pair of variable is shown in Table 25.

As expected, the tip displacement errors have the strongest correlation at 0.95. The next strongest correlation exists between wing skin weight error and 2.5G maneuver load case tip displacement at -0.74. The third largest correlation magnitude is between the ribs and spars weight and the -1.0G maneuver load case at -0.66. There are five correlations in all that exceed 0.3 in magnitude. As previously mentioned, with the sample size of 56, a Pearson correlation coefficient above 0.3 shows correlative above the 95% confidence

Table 25: Pearson's Correlation Coefficient for Every Variable Pair

	Skin Weight	R&S Weight	2.5G TD	-1.0 TD	VM Stress	RBM
Skin Weight	1	-0.42	-0.74	-0.66	0.43	0.03
R&S Weight	-0.42	1	0.25	0.24	-0.18	-0.03
2.5G TD	-0.74	0.25	1	0.95	-0.29	0.07
-1.0 TD	-0.66	0.24	0.95	1	-0.17	0.06
VM Stress	0.43	-0.18	-0.29	-0.17	1	-0.03
RBM	0.03	-0.03	0.07	0.06	-0.03	1

threshold.

Experiment 2.3b Results

Experiment 2.3 found that Pearson correlation coefficient magnitudes greater than 0.3 exist amongst the variable errors. Therefore the experiment rejects the null hypothesis that no correlation exists and substantiates Hypothesis 2.3.

Unfortunately we cannot use Pearson's coefficient because it is strictly bi-variate (only assess pairs of variables). We wish to capture dependencies across all six dimensions. Therefore, we need a different approach.

6.2.3 Transforming Distributions into Marginal Distributions

To form a copula the distributions need to be transformed to marginal distributions. A marginal distribution is a uniform distribution between zero and one. This approach is very common and many formulations are possible [207]. This inversion step is performed using MATLAB's ksdensity function. The following figures show that the distributions have been transformed to marginal distributions (uniform from zero to one) while maintaining the correlations.

Figures 57, 58, and 59 show that the correlation between the variables is maintained

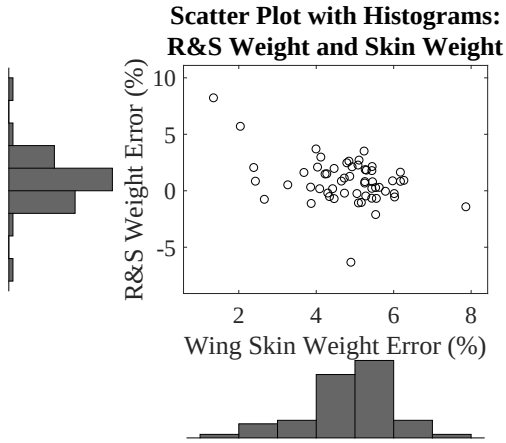

(a) Scatter plot of Observed Error with Histograms

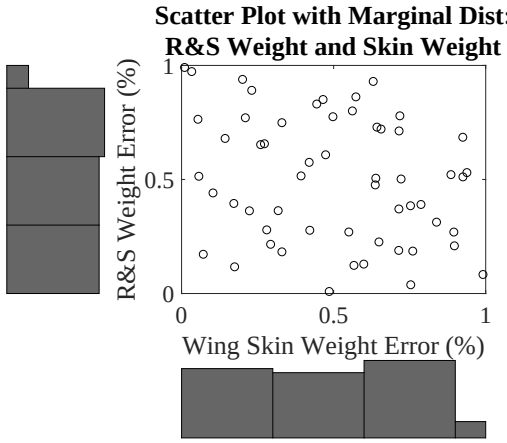

(b) Scatter plot of Error from Transformed Marginal Distribution

Figure 57: Scatter Plots between Wing Skin Weight Error and Ribs and Spars Weight Error from Observed Histograms and Transformed Marginal Distributions

while the histograms have been transformed to represent uniform distributions between zero and one. Now that the observed error is in the marginal space a joint probability distribution can be formed by way of a copula.

6.2.4 Student's *t* Copula

A student's t copula was fit to the six variables using the transformed marginal distributions. This type of copula was selected because it is n-dimensional [208].

Table 26: Rho Values for Student's t Copula

	Skin Weight	R&S Weight	2.5G TD	-1.0 TD	VM Stress	RBM
Skin Weight	1	-0.31	-0.75	-0.70	0.18	-0.04
R&S Weight	-0.31	1	0.15	0.17	0.08	-0.04
2.5G TD	-0.75	0.15	1	0.95	-0.18	0.13
-1.0 TD	-0.70	0.17	0.95	1	-0.05	0.12
VM Stress	0.18	-0.08	-0.18	-0.05	1	-0.13
RBM	0.04	-0.04	0.13	0.12	-0.13	1

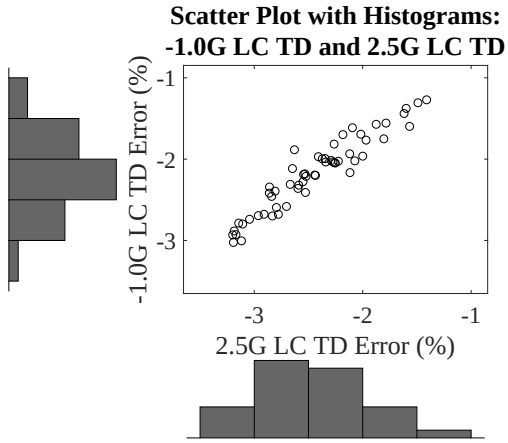

(a) Scatter plot of Observed Error with Histograms

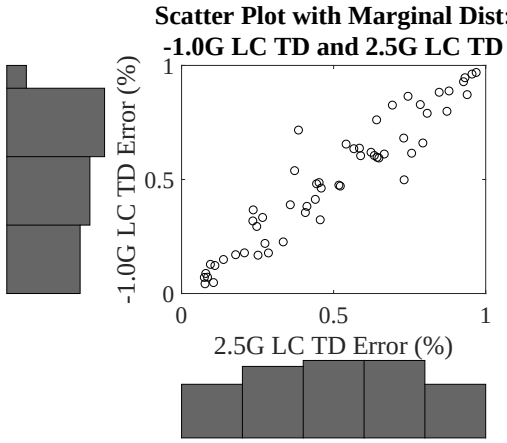

(b) Scatter plot of Error from Transformed Marginal Distribution

Figure 58: Scatter Plots between Tip Displacement Errors from Observed Histograms and Transformed Marginal Distributions

Notice that these values are similar to Pearson's coefficient but not exactly the same (recall Pearson's was strictly bi-variate correlation). There is another value needed to fit a t copula which is the degrees of freedom (ν). The value of ν here is 10.69.

It is important to note that the copula alone is insufficient to produce the proper results. The copula requires marginal distributions as inputs, and likewise produces results as marginal distributions. Therefore, the inverse transform in applied such that the marginal distributions are now transformed to the candidate distributions determined in Section 6.1.3.

6.2.5 Experiment 2.3c: Independent vs. Dependent Sampling

Experimental Design

Finally: the crescendo. After characterizing the discretization error using distributions, testing for uncertainty, inverting the distributions into marginal distributions, fitting a copula, and transforming the distributions back to the original form, we can perform an experiment to test whether the dependence between the samples has been preserved.

We will test this by comparing three sets of data. The first set is the empirical error (or

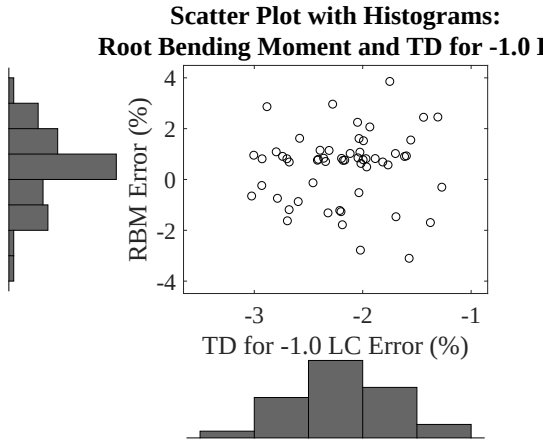

(a) Scatter plot of Observed Error with Histograms

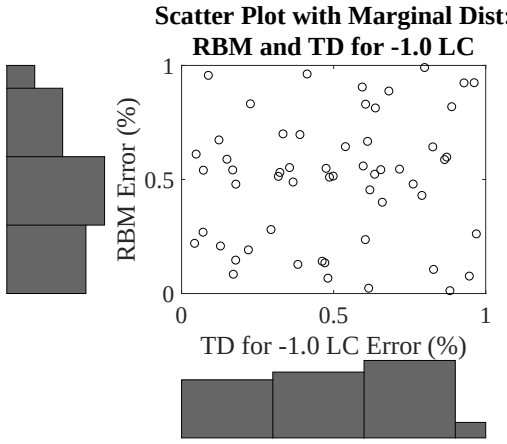

(b) Scatter plot of Error from Transformed Marginal Distribution

Figure 59: Scatter Plots between Max Von Mises Stress Error and 2.5G Maneuver Load Case Root Bending Moment Error from Observed Histograms and Transformed Marginal Distributions

observed error). This is the error for the cases that were executed at the two different mesh sizes. The second set of data is sampled points drawn *independently* from each other. The third and last set of data are sampled points that are drawn dependently; that is, from the copula. If there are trends in the observed error data, then we expect these trends to not be captured in the independent sampling and captured in the dependent sampling.

Experimental Results

The results of this experiment are depicted in Figures 60, 61, 62.

Figure 60 shows the three sets of samples for the wing weight components (skin and ribs/spars). The observed data does show some correlation (Pearson's Coefficient of -0.42) between the two weight estimations. Further recall from Figure 52 that both distributions resembled normal distributions (visually). The dependent sampling on the right shows the negative correlation: for the points sampled at the lower error values for wing skin error, the ribs and spars weight error is higher. Thus, the negative correlation detected in Pearson's correlation has been preserved.

Recall from Figure 53 that both the tip deflection error distributions resembled uniform

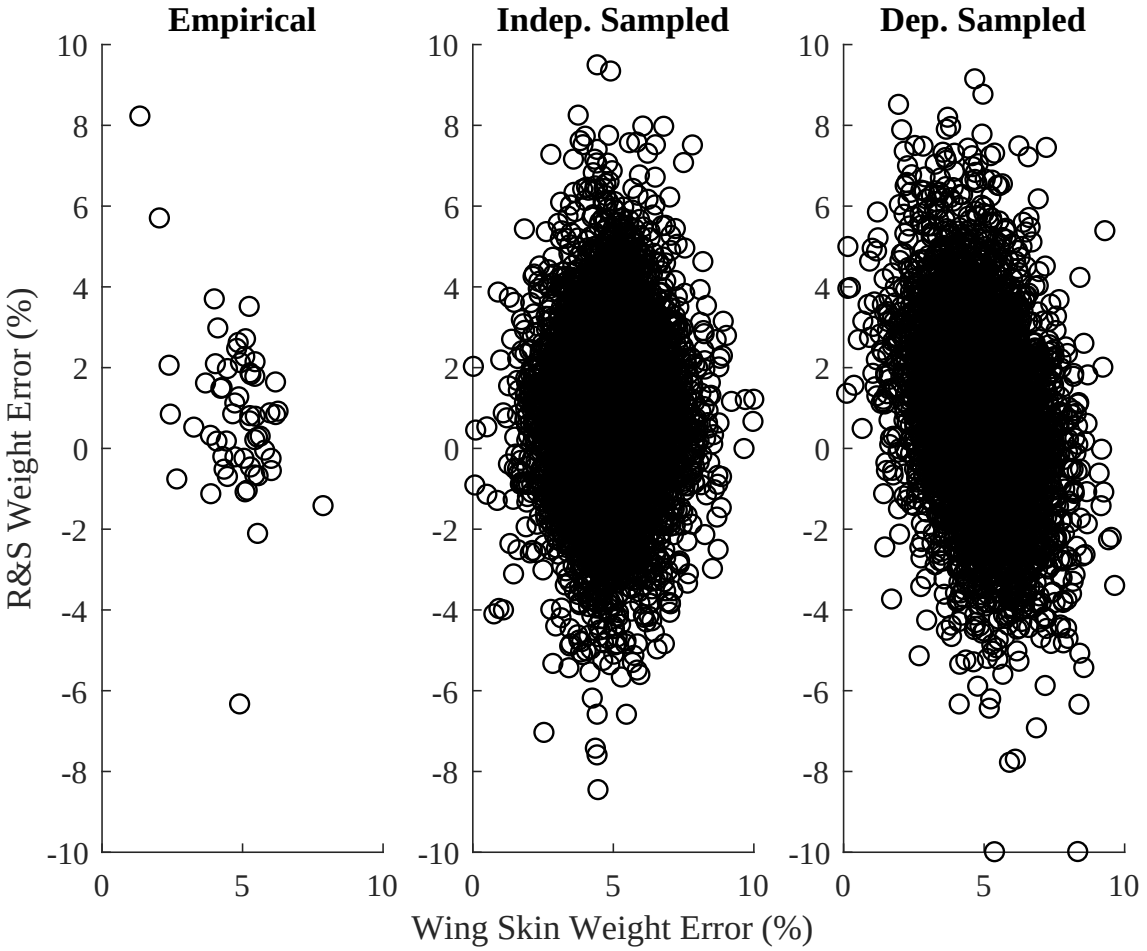

Figure 60: Comparison between Observed, Independent, and Dependent Error Sampling for Wing Skin Weight Error and Ribs and Spars Weight Error

distributions (visually). Therefore, the independent sampling in the middle results in a box: no correlation whatsoever between high and low values of either variable error. The dependent sampling could not be more different: this pair of variables had the highest correlation magnitude of any pair, as reinforced by the scatter plot of the observed error. Drawing from the copula reflects this correlation.

Figure 62 shows the pair between the 2.5G maneuver load case and the wing skin weight errors. This pair repeats the same trend: the dependence that is failed to be captured in the independent sampling is indeed captured in the dependent sampling. This pair was chosen because it appears to capture higher correlation at the tails rather than the linear correlation

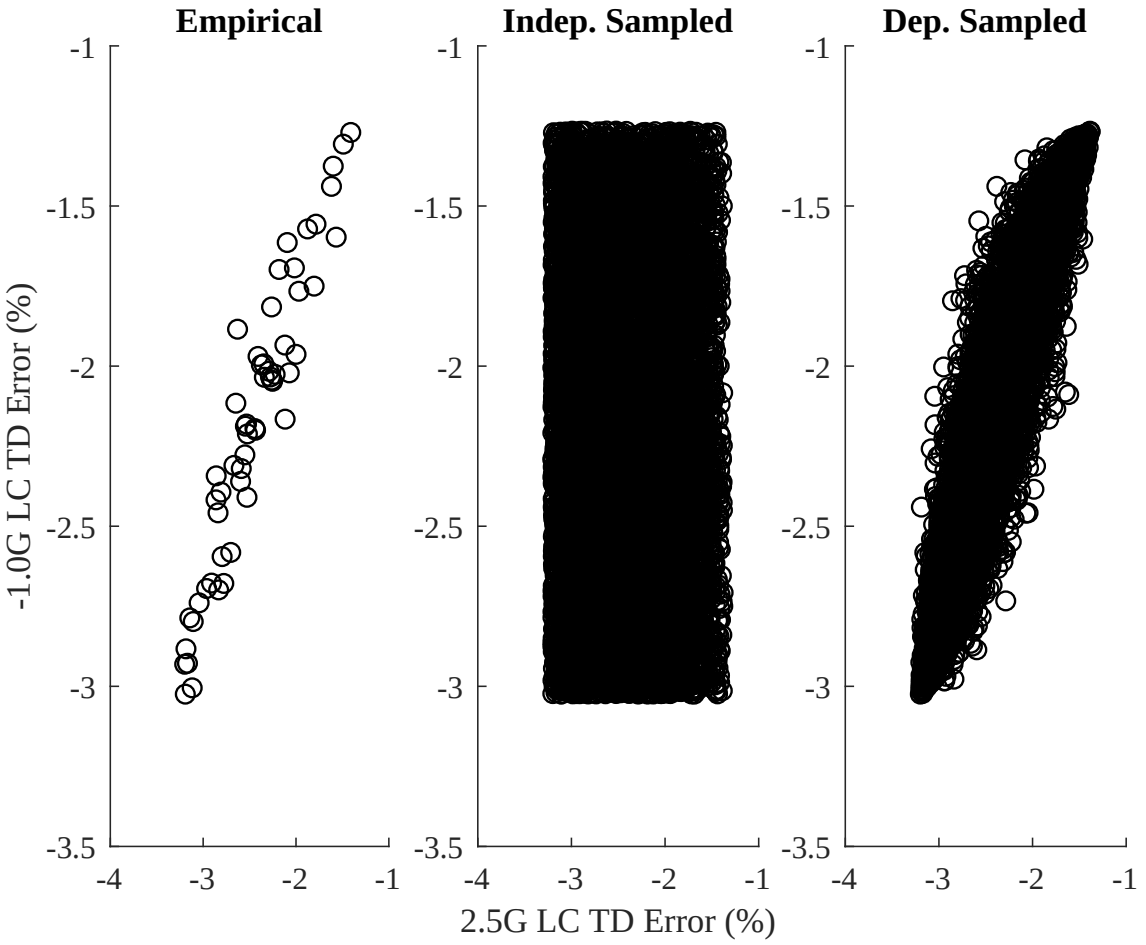

Figure 61: Comparison between Observed, Independent, and Dependent Error Sampling for 2.5G and -1.0G Maneuver Load Case Tip Displacements

shown in Figure 61.

Experiment 2.3c Results

The dependent sampling clearly shows similar correlation to the observed data than the independent sampling. Therefore the results of Experiment 2.3c support the use of the copula to maintain correlations between uncertainty variables within a sampling-based method.

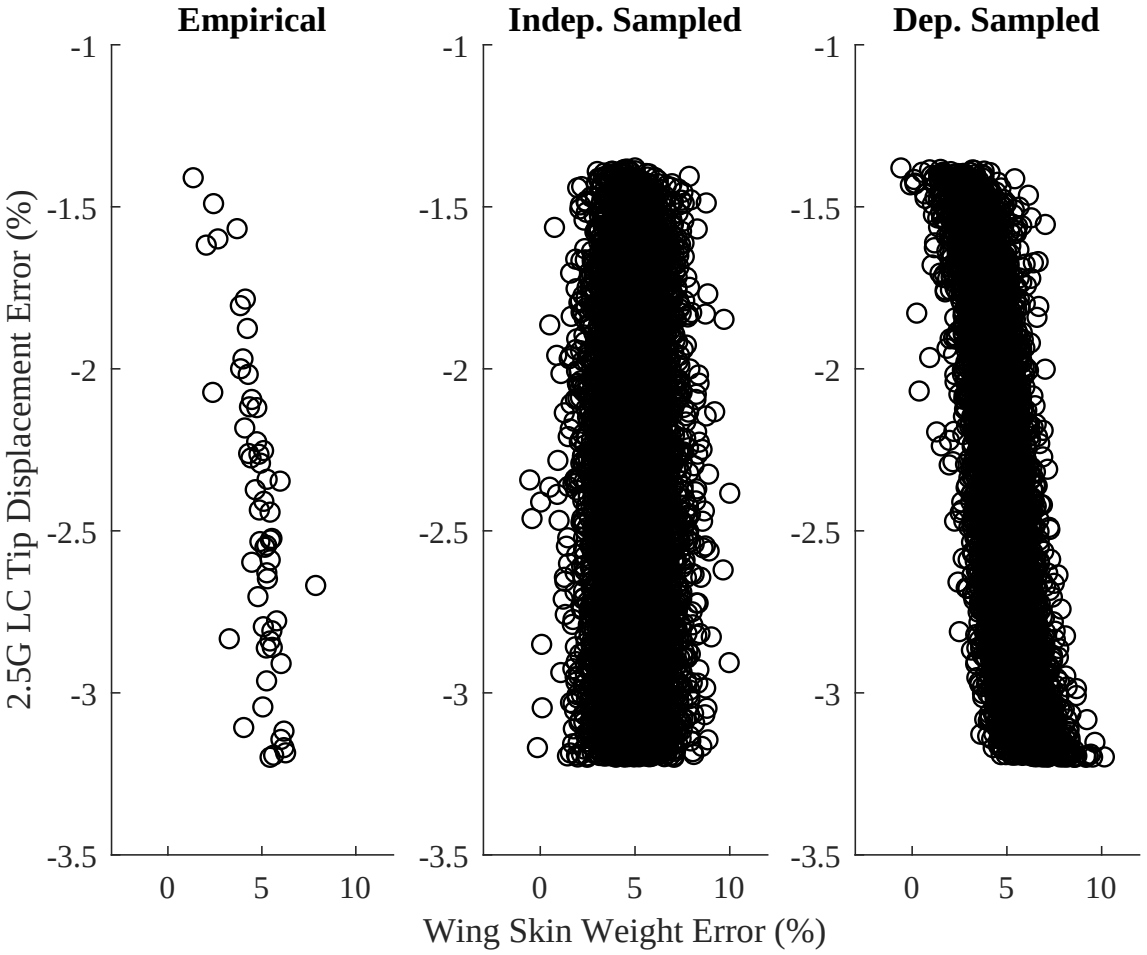

Figure 62: Comparison between Observed, Independent, and Dependent Error Sampling for Wing Skin Weight Error and 2.5G Maneuver Load Case Tip Displacement Error

6.2.6 Experiment 2.3d: Comparison of Independent and Dependent Uncertainty Sampling

Experimental Design

We can go beyond visual inspection to demonstrate the contrast between independent and dependent sampling. Independent and dependent uncertainty distributions can be sampled and applied to a nominal design point. This will result in two different distributions in the constraint space: one distribution with the independence assumption and one distribution without the independence assumption. Because the correlation trims the extremes of the uncertainty space (best demonstrated in Figure 61), we would expect the reliability

estimation of the dependence sampling case to be *higher* relative to the independent sampling case. We would not, however, expect a change in the expect value of the constraint (average) but only the variance (standard deviation).

Experiment Results

Consider a case where a design is sized and evaluated against the wing-level constraint such as tip deflection. The deterministic value of the maximum tip deflection (determined by the 2.5G maneuver load case) is 61.2 feet and the minimum tip deflection (determined during the -1.0G maneuver load case) is -20.35 feet. Now the copula that was fit during the previous experiment is used as the dependent sampling distribution whereas the individual distributions fit in Experiment 2.2c are used as the independent sampling distribution.

If just one of the constraints is examined, the independent and dependent sampling are identical. This result is shown in Figure 63 for a sample of 10,000 points.

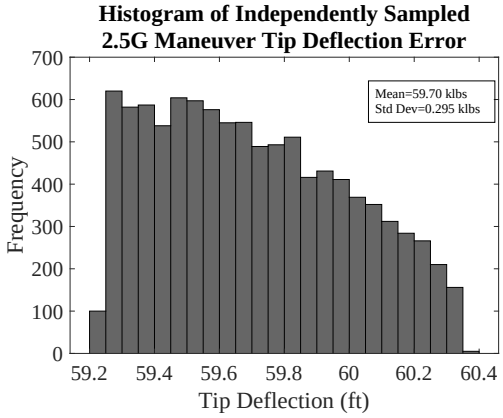

(a) Histogram of Independently Sampled 2.5G Maneuver Load Case Tip Deflection

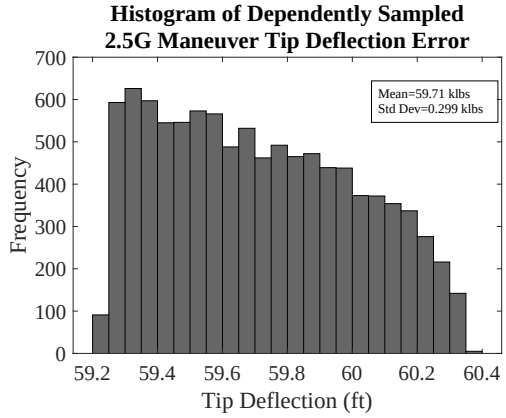

(b) Histogram of Dependently Sampled 2.5G Maneuver Load Case Tip Deflection

Figure 63: Histograms of 2.5G Maneuver Tip Deflection Error: Independently and Dependently Sampled

The histograms are identical because the individual distribution has been preserved. This step acts as a verification for the marginal transformation step performed in Section 6.2.3: each of the individual distributions are maintained. However, if two variables are sampled from the copula the dependency remains (as previously demonstrated by Figure

61).

Each of these samples represents a realization of uncertainty (or possible scenario or future state) of the design. The design remains constant, but the output is uncertain due to the model uncertainty (discretization error). Considering only the tip deflection outputs and constraints, we can calculate the probability of compliance for the design. For comparison, compliance is calculated using the individual distributions (independent sampling) and the copula (dependent sampling). The results are given in Figure 64 for a 10,000 point sample.

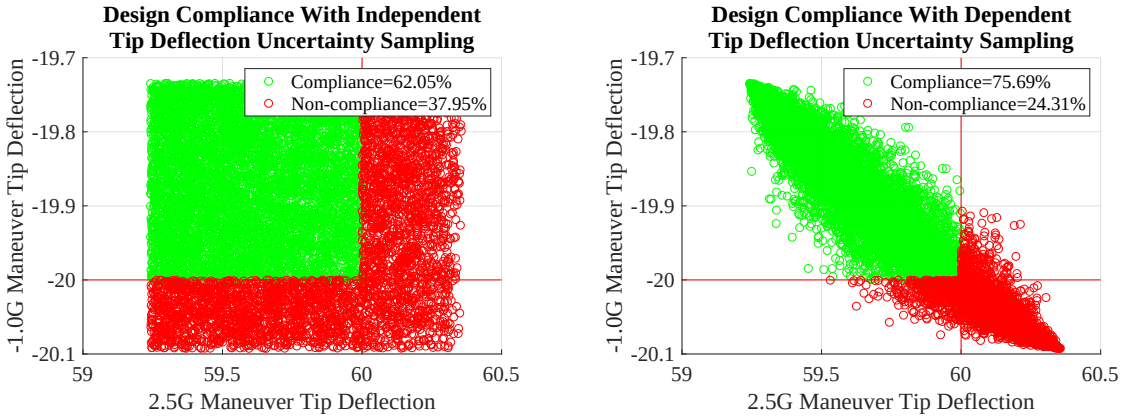

(a) Candidate Distribution Comparison for Describing 2.5G Maneuver Load Case Error

(b) Candidate Distribution Comparison for Describing -1.0G Maneuver Load Case Error

Figure 64: Compliance Estimation of Tip Deflection Constraints Comparing Independent and Dependent Sampling

The independent sampling probability of compliance is about 62% whereas the dependent sampling is about 76%. Clearly the independent sampling case is underestimating the compliance. Consider the variance between the outcomes of the independent versus dependent sampling cases. The correlation decreases the overall uncertainty space compared to the independent sampling. The copula captures just a slice of the independent sampling rectangle. This reduction in uncertainty space increases the compliance estimation. In other words, the independent uncertainty assumption would lead to an underestimated compliance due to overestimated uncertainty. This result matches published trends in the literature when comparing independent sampling against dependent sampling [173].

Experiment 2.3d Results

Independent sampling underestimates compliance because it overestimates the uncertainty space. The existence of correlation decreases the area of uncertainty, which increases the compliance estimation relative to the independent uncertainty case.

We can even go further and propagate these changes to the vehicle-level. Unfortunately, the strongest correlation exists between the wing-level constraint values. The only outputs of Nastran that propagate to the vehicle-level are the wing weight variable estimations. These exhibit weak correlation. Therefore, we would not expect the vehicle-level performance metric to be affected significantly by the sampling method when only weak correlation exists. In fact, Pearson's coefficient between the wing weight variables is -0.31 which is just barely sufficient to say that correlation exists with 95% confidence.

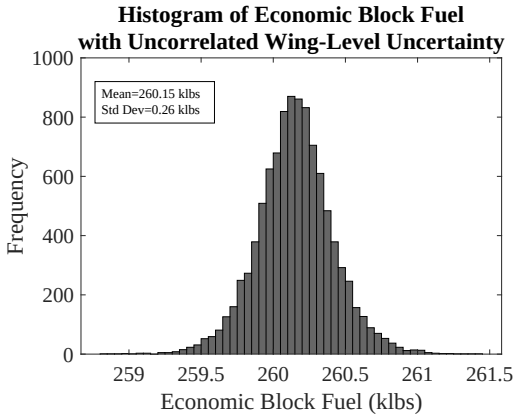

(a) Candidate Distribution Comparison for Describing 2.5G Maneuver Load Case Error

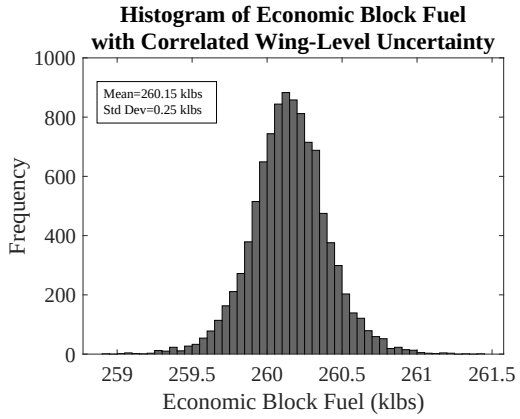

(b) Candidate Distribution Comparison for Describing -1.0G Maneuver Load Case Error

Figure 65: Economic Block Fuel Histogram Comparing Independent and Dependent Sampling

As demonstrated by Figure 65, the average economic block fuel does not change between the independent and dependent sampling cases; however, the standard deviation changes by a little bit. This is a similar trend shown in Figure 64, as the mean tip deflection estimation was not changed but the variance has changed. Again, this is because the uncertainty space has decreased in area resulting in less extreme uncertainty realizations.

6.2.7 Answering Research Question 2.3

Research Question 2.3 depended on finding error values from the results of Research Question 2.2. Thankfully, error samples were produced which could be used for correlation testing. Because each design had a set of error samples, these sets could be used to quantify correlation. Experiment 2.3a and 2.3b showed visually and quantitatively that correlations existed between some of the variable pairs with 95% confidence. These dependencies were captured by integrated the individual distributions into a single joint probability distribution (copula). Comparing the observed sample, independent sample, and dependent sample in Experiment 2.3c illustrated the contrast between independent and dependent sampling. The correlated sampling results in a higher compliance estimation against independent sampling because the uncertainty space is limited.

This Research Question did not delve outside the realm of established correlation techniques. Scatter plots, Pearson's Correlation coefficient, and copulas have all been widely used and published, even in the aircraft conceptual design field. However, similar to the derived candidate distributions in Research Question 2.2, the resulting copula was *derived* rather than *prescribed*. This means that the results of this process were solely dependent on the error quantification process (Richardson's Extrapolation Error) rather than assumed distributions or correlations. These are *actual* results rather than *notional* results. Consequently, the copula was fit using computational data and results rather than intuition or subject matter expertise.

CHAPTER 7

DEVELOPING A BI-LEVEL MODELING ENVIRONMENT

There are a number of difficulties when combing models of varying order and fidelity. The first is that they are almost guaranteed to not agree; that is, the results for identical designs will most likely be different. If this proves to be the case here, we will need a process to decide between the model environments or somehow coalescing the two. This obstacle led to Research Question 3.1:

Research Question 3.1
How can two design environments of varying fidelity be integrated to agree on performance estimation?

We expect to be able to integrate the two environments. We hypothesize that this can be performed by reconciling the key difference between the two models: that is, structural wing weight. By conducting a fixed-point iteration on the structural wing weight we can get the environments to agree on aircraft and wing design results (Hypothesis 3.1a in Section 4.3.1).

Assuming that process can be developed to reconcile the modeling environments, the next goal is to investigate what additional value the integrated environment provides by comparing it to the current benchmark method which is a vehicle-only environment. In short, the optimization process only considers vehicle-level design, margin, uncertainty, and constraint variables. If we perform an optimization solely using this environment the result is a vehicle-only Pareto Front: a set of points that are non-dominated with respect to all the vehicle-level designs considered. These points represent the "best" vehicle designs, and they are non-comparable with respect to the objectives (economic block fuel and reliability). These points can then be evaluated using the integrated environment; that is, against

wing-level constraints to determine how they would have fared had they progressed to the preliminary design phase. This reasoning led to the formulation of Research Question 3.2:

Research Question 3.2

What impact does the integrated environment have on conceptual design selection relative to the baseline method?

The expectation is that the vehicle-only Pareto Front will not fare well if wing-level constraints are not included in the optimization formulation. This will be explored further in a thought experiment.

7.1 Research Question 3.1: Bridging Models of Differing Fidelity

7.1.1 Vehicle-Level and Wing-Level Variables

The first question is whether the models yield the same results for a given aircraft design. To that end we need to determine which inputs are similar to both models (e.g. aspect ratio) and which inputs are mutually exclusive (e.g. fan pressure ratio, rib spacing) which is described in Table 27.

Table 27: Vehicle-Level and Wing-Level Input Variable Comparison

Variable	TWR	WSR	FPR	HPCPR	TOC Thrust	EWMARG	FCDSUB
Vehicle	✓	✓	✓	✓	✓	✓	✓
Wing							
Variable	Range	Payload	AR	Sweep	Twist Slope	Rib Spacing	KDF
Vehicle	✓	✓	✓	✓			
Wing			✓	✓	✓	✓	✓

where TWR is thrust-to-weight ratio, WSR is wing loading ratio, FPR is fan pressure ratio, HPCPR is high pressure compressor pressure ratio, TOC Thrust is top of climb thrust, EWMARG is empty weight margin, FCDSUB is total drag factor, AR is aspect ratio, Twist Slope is the linearized span-wise linear twist slope, and KDF is knockdown factor.

Recall that the preliminary design phase is dependent on the outputs of the conceptual design phase. So even though variables such as fan pressure ratio and range are not explicitly modeled within the wing-level environment, the effects are propagated downstream through variables such as take-off gross weight.

Some of the inputs to the wing-level analysis are outputs from the vehicle-level analysis. These outputs include take-off gross weight, engine weight, fuel weight, and others. This forms an opportunity to match the two environments through these "bridge" variables. Continuing further, there are inputs to EDS that are assumptions or estimations of future analysis results. These come in the form of efficiency factors such as span efficiency and wing weight. Therefore are bi-lateral connections between these two environments.

The explicit weight components of the wing can be defined as inputs. Left undefined, FLOPS will internally calculate a wing weight. The inputs to affect wing weight directly are summarized in Table 28.

Table 28: FLOPS Wing Weight Input Variables [126]

Variable	Definition
FRWI	Entire wing weight
FRWI1	Wing ending material weight
FRWI2	Wing ribs and spars weight
FRWI3	Miscellaneous systems weight

From Table 28 we see that the entire wing weight can be defined by the user or in portions: FRWI controls the entire wing weight, FRWI1 and FRWI2 affect structural weights, and FRWI3 affects additional systems weights. RADE, being a wing structural sizing environment, cannot, however, estimate the *total* wing weight. FLOPS includes additional and ancillary weights that are non-structural. Therefore, the structural wing weight can be affected directly while the total wing weight can still be calculated by FLOPS. Therefore, Nastran will be used to determine structural wing weight and FLOPS will be used to determine total wing weight.

It is worth noting that a subtle assumption has been made with this approach: the wing-level analysis is more trustworthy than vehicle-level analysis in the structural wing weight estimation. In truth, this assumption is most likely incorrect as FLOPS is based on actual wing weights whereas Nastran is based on simplified physics. In other words, Nastran has higher uncertainty than FLOPS because physical data is more certain than simplified theory. This assumption is made for two reasons. Fist, wing weights are outputs of Nastran but inputs to FLOPS. Therefore, algorithmically, the integration is straightforward to choose Nastran's structural wing weights over FLOPS'. The second reason is that the paradigm moving forward in the design process will increasingly rely physics-based tools rather than empirically based tools. For example, FLOPS cannot be used to perform a rib spacing sensitivity, but Nastran can. As a result, while the FLOPS value may be useful for final comparison, the rest of the design phase will need physics-based accounting. Thus, going forward in the design process, the models the highest granularity would be used.

To conclude, we can use the output weights from wing-level analysis as inputs to vehicle-level analysis to reconcile the environments. However, other dependent variables such as take-off gross weight and span efficiency form connections as well. As these values are not known a priori, we will need to perform a convergence.

7.1.2 Experiment 3.1a: Design Point Structural Wing Weight Convergence

Experimental Design

The discrepancy between the empirical and physics-based prediction values must be reconciled. Here, FLOPS uses historical data to estimate wing weight (and all the other weights) while Nastran uses FEM. Further, FLOPS estimates *total* wing weight while Nastran only estimates structural wing weight.

Recall that wing loading (WSR) is a design variable. For this convergence, it will be fixed (constant). Takeoff gross weight (TOGW) and wing area (S), though, will be varying based on the weight estimations. When the wing area changes, the lift distribution on the

Table 29: Selected Design Point for Structural Wing Weight Convergence

Range	Payload	TWR	WSR	TO Thrust	TOC Thrust
7,530 nmi	64,050 lbs	0.30	134	78,400 lbs	19,600 lbs
FPR	HPCPR	Mach	Altitude	EWMARG	FCDSUB
1.6	20	0.85	35,000 ft	0.00	0.95
Aspect Ratio	Aspect Ratio (VSP)	Sweep	Rib Spacing	KDF	Twist
10	9.14	35°	30 in	0.10	-0.5°

wing changes as well (i.e. angle of attack) which will affect the span efficiency. A single evaluation of FLOPS and Nastran is depicted in Figure 66:

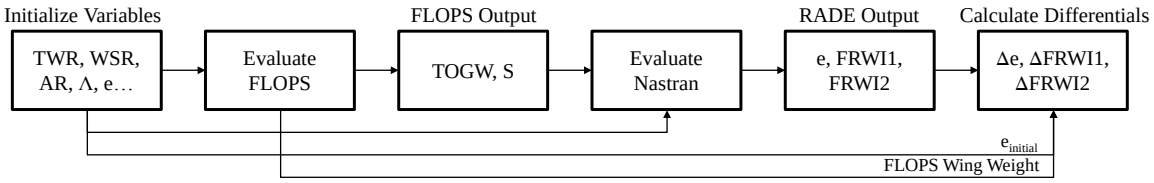

Figure 66: Calculating Differential between FLOPS and Nastran Wing Weight Calculations

Now that we have a process that determines the difference between FLOPS and RADE, we can iterate on this difference to attempt convergence. Using fixed-point iteration (FPI) we will converge on a set of structural wing weight values (FRWI1 and FRWI2), wing area, span efficiency, and take-off gross weight.

We start by testing whether a single point will converge. Note that this test uses the sizing solution from the jig shape determination process formulated in Research Question 1.2. A point is selected arbitrarily for testing, given in Table 29.

The process described in Figure 66 can be looped to form a FPI to converge on a structural wing weight. This process is shown in Figure 67.

There are a series of possible outcomes when performing the convergence. These outcomes are described in Table 30.

Out of all the possible outcomes, there is only one that is desirable, which is to converge on a realistic solution quickly. There are many others that are not preferable. The iteration may be divergent. In this case it would continue forever without finding a result. Or,

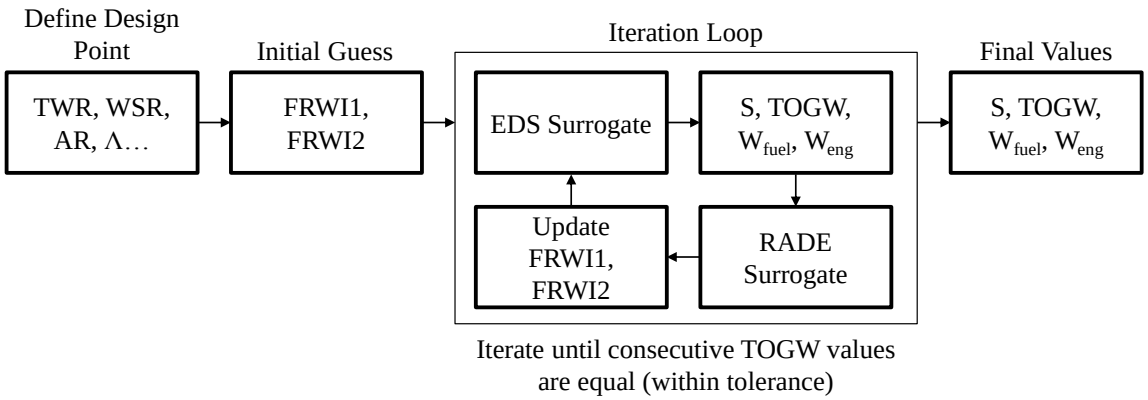

Figure 67: Structural Wing Weight Convergence Loop

Table 30: Possible Outcomes of Structural Wing Weight Convergence

Type	Outcome
Divergent	Continually executes
Convergent: Unrealistic	Result is very different than initial results
Convergent: Realistic	Result is similar to initial results
Convergent: Expensive	Convergence is too computationally expensive for RBDO

the iteration may converge to an unrealistic solution, such as a final take-off gross weight of 10,000 pounds. Or, similarly, a span efficiency below 0.4 would be unrealistic. The iteration could converge but take too long. Because this step will be performed for every design in the RBDO, this process needs to take less than a minute (preferably less than a second). So, the best result is a quick convergence with a final solution that is realistic.

The term "realistic" is ambiguous. Its use is to distinguish a result that is believable versus one that is not. It can be quantified by, say, $\pm 10\%$ of the first evaluation of FLOPS; however, the first evaluation is dependent on the initial guesses of the wing weights and span efficiency. Therefore the threshold is broadened to 20%.

Experimental Results

The results for the design point described in Table 29 are given by iteration in Figures 68 and 69. They are broken down by the variable values that are changing between iterations,

namely: take-off gross weight, wing area, span efficiency, and wing weight values (FRWI1 and FRWI2). The iteration only required five iterations which shows applicability to large-scale optimization problems. The tolerance (as shown by Figure 68a) is set to 0.01% change in take-off gross weight between successive iterations.

Figure 68: Structural Wing Weight Convergence Takeoff-Gross Weight Results by Iteration

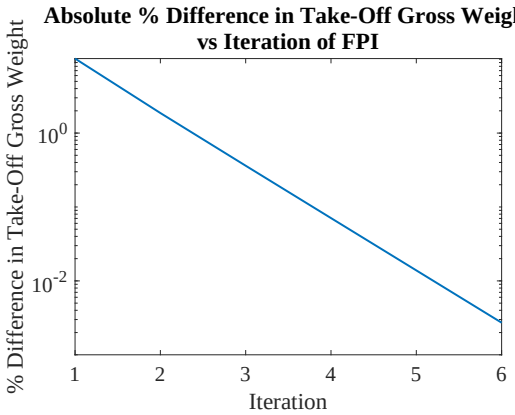

(a) Absolute Difference in TOGW between EDS and RADE Estimation by Iteration, %

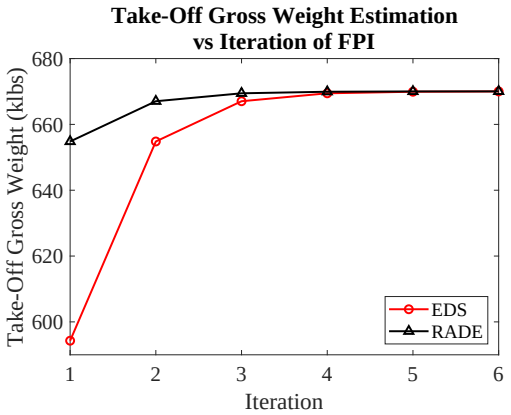

(b) Magnitude of TOGW Estimated by EDS and RADE by Iteration, klbs

Figure 68 shows the change in take-off gross weight estimations and the percent difference between FLOPS and RADE (Nastran) estimations. The take-off gross weight converges rather quickly to a value of about 670,000 pounds and changes by over 10% (which is within the 20% believability threshold). The first Nastran value is within a couple percent of the final solution.

The wing weights, wing area, and span efficiency results by iteration are shown in Figure 69. The first iteration of FRWI1 and FRWI2 are the initial guesses which were defined without preparation (generic values). The bending material weight (FRWI1) is must larger than the ribs and spars weight (FRWI2) so we can see a lag between the two values. The initial FRWI1 value is low, so the value for FRWI2 for iteration two is much lower. After FRWI1 jumps during the second iteration, FRWI2 jumps in iteration three. This is why the lines appear to converge: the scales of the axes match the trends of each which are mirrors.

Figure 69: Structural Wing Weight Convergence Wing-Level Results by Iteration

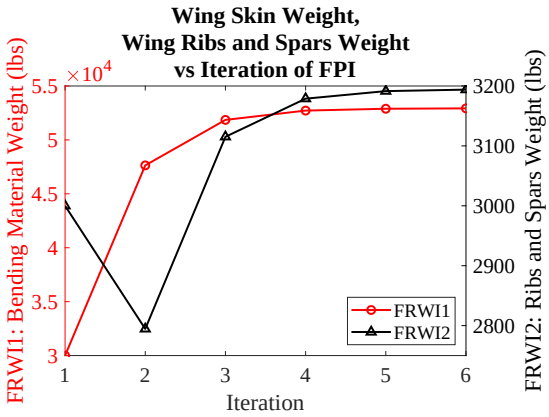

(a) Bending Material and Ribs and Spars Weight vs Iteration of FPI

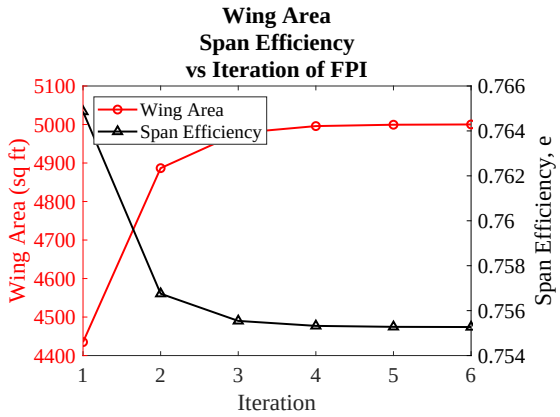

(b) Wing Area and Span Efficiency Convergence vs Iteration of FPI

The wing area changes as the take-off gross weight changes (due to constant wing loading). The span efficiency changes with angle of attack which changes with take-off gross weight and wing area. The magnitude of the span efficiency is highly dependent on the design wing twist. Note that the original span-wise wing twist distribution from NASA's CRM was changed to a single linearized slope. This decreased the estimated span efficiency from 0.85 (original) to 0.755 (modified).

The initial and final results of the iteration are given in Table 31. The final values represent the final solution; in order words, if these values were given to EDS and RADE at the beginning of the convergence, it would have converged in one iteration. This exercise was completed but no plots are shown because there were only values (one iteration is insufficient to form a graph).

Table 31: Initial and Final Values of FRWI1, FRWI2, Wing Area, and Span Efficiency

Variable	Initial Guess	Final Result
FRWI1 (lbs)	30,000	52,930
FRWI2 (lbs)	3,000	3,194
Span Efficiency	0.90	0.755
Wing Area (ft^2)	-	5,000
TOGW (lbs)	-	670,015

Experiment 3.1a Results

The results of Experiment 3.1a show that the two environments of differing fidelity converge on a solution using the defined intermediate variables. This result substantiates Hypothesis 3.1a.

7.1.3 Experiment 3.1b: Structural Wing Weight Convergence Design Space Exploration

Experimental Design

The previous section demonstrated that, for a single point, the devised structural wing weight convergence loop will provide a solution that would match the inputs and outputs of both EDS and RADE. However, there are a couple of potential problems with using fixed-point iteration. First, there is no guarantee that a solution will be found. Second, there many be multiple solutions in the space (the solution is non-unique). Lastly, as a corollary to the second problem, the found solution may be dependent on the initial guesses such that the answer is dependent on the initial conditions.

The first problem is addressed by Experiment 3.1b. The central question here is whether there are designs within the design space that will result in divergence or unrealistic results. This can be investigated by sampling the design space and performing the structural wing weight convergence. To test for convergence, the computation time itself is the test statistic: clearly the loop diverges if the loop never exits (assuming the only stopping criterion is based on take-off gross weight). For this loop, there is no limit to the maximum number of iterations, so the existence of divergence will become evident. To test for realistic result, all the solutions for the sampled designs can be aggregated to show whether outliers exist. We expect to find a distribution of results that is continuous.

The designs chosen for this experiment are at the bounds of the design space. This space is identical to the space defined in Section 8.2.6 of the Case Study sans the margin, uncertainty, mitigation, and constraint variables. Table 32 shows bounds of the vehicle-

Table 32: Vehicle-level Design Variables

Variable	Thrust-to-Weight	Wing Loading	Fan Pressure Ratio	HPC Pressure Ratio	TOC Thrust (lbs)
Min	0.26	128	1.5	18	17,000
Max	0.35	137	1.75	23	22,000

Table 33: Wing-level Design Variables

Variable	Aspect Ratio	Sweep (°)	Rib Spacing (in)	Twist Slope (°)
Min	8	33	20	-0.2°
Max	11	40	35	-0.6°

level design space and Table 33 shows the bounds of the wing-level design space. Aspect ratio and sweep are shared (intermediate) variables, so they can be displayed in either (both) tables.

Rather than perform an exhaustive Monte Carlo simulation, only the bounds of the design space are evaluated for this experiment. A two-level, full factorial design using the low and high levels of each of the nine design variables was used, resulting in 512 cases ($2^9 = 512$).

Experimental Results

The results of Experiment 3.1b are shown in Figures 70, 71, and 72.

The convergence is iterating on take-off gross weight specifically, so its results are highlighted in Figure 70. The design point used in Experiment 3.1a converged to a take-off gross weight of about 670,000 pounds. This value seems to about average for the full factorial design of experiments. As expected, there are no major outliers and all the cases converged.

Similar results for the wing weights (FRWI1 and FRWI2) as well as the wing characteristics (wing area and span efficiency) are shown in Figures 70 and 71. The overall

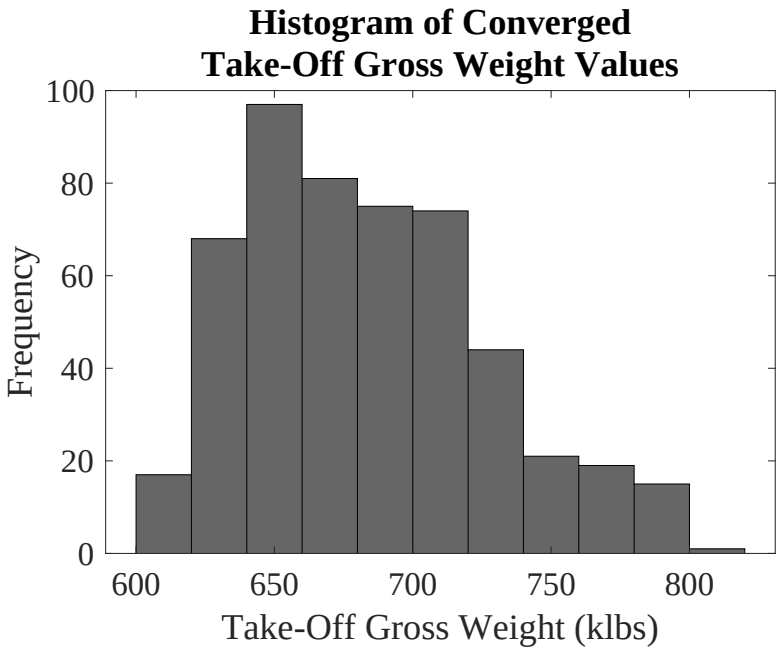

Figure 70: Histogram of Converged Take-Off Gross Weight Values from Design Space Exploration

distributions are functions of the defined design space. Because the design of experiments only considered extremes, the distributions are not representative of expected results (such as averages). The extremes were chosen to determine whether the edges of the space would cause problems for the structural wing weight convergence.

Of the solutions, the span efficiency (Figure 72a) is the only metric to have a few of the cases exceed realistic bounds: a few solutions have values above one. This is unrealistic because the theoretical bound for span efficiency is less than or equal to one. This appears to only occur on a few instances and a constraint can enforce values less than one.

The last convergence metric to check is the rate of convergence. Figures 68 showed logarithmic convergence for the design point, reaching the tolerance of 0.01% change in take-off gross weight within six iterations. The number of iterations for each design in the full factorial design of experiments are shown in Figure 73. The entire set required about 0.6 seconds of run all 512 cases. Even for the designs at the boundary, the convergence loop requires less than ten iterations to complete.

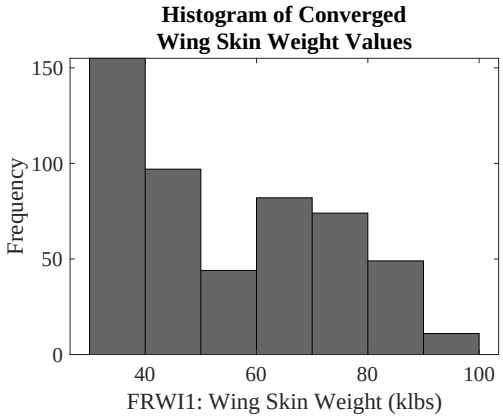

(a) Histogram of Converged Wing Skin Weight Values from Design Space Exploration

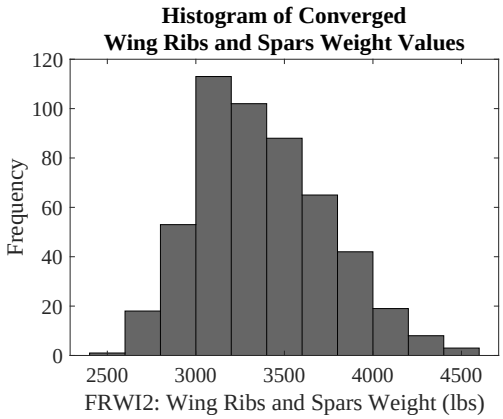

(b) Histogram of Converged Wing Ribs and Spars Weight Values from Design Space Exploration

Figure 71: Histogram of Converged Wing Skin Weight and Ribs and Spars Weight Values from Design Space Exploration

Experiment 3.1b Results

The results of Experiment 3.1b show that the structural wing weight convergence loop results in realistic solutions are the edges of the design space. It is therefore assumed that the interior of the design space will result in realistic solutions as well. This result substantiates Hypothesis 3.1a.

7.1.4 Experiment 3.1c: Structural Wing Weight Convergence Sensitivity Experiment

Experimental Design

The second and third issues mentioned in Section 7.1.3 (namely, multi-modality and robustness to initial guesses) are addressed here. They go to together: if multiple solutions exist, the initial guesses would determine which local set would be found. If, however, there is only one solution, then the convergence should be robust to the initial guess values. Because the change in take-off gross weight monotonically decreased in Experiment 3.1a, we expect that the convergence is insensitive to varying initial guesses (Hypothesis 3.1b).

We can test this by performing the convergence multiple times with many different

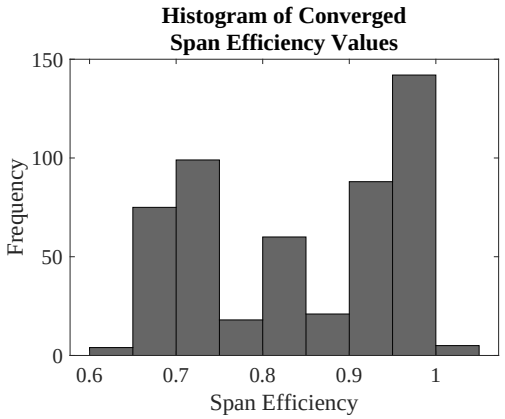

(a) Histogram of Converged Wing Area Values from Design Space Exploration

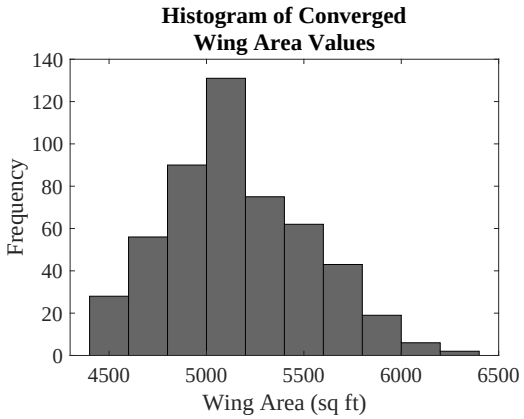

(b) Histogram of Converged Span Efficiency Values from Design Space Exploration

Figure 72: Histogram of Converged Wing Area and Span Efficiency Values from Design Space Exploration

Table 34: TOGW Sensitivity to a Wide Range of FRWI1 & FRWI2 Initial Guesses

FRWI1/FRWI2	2,000	3,000	4,000	5,000	6,000	7,000
30,000	670,030	670,030	670,030	670,030	670,030	670,030
40,000	670,020	670,020	670,020	670,020	670,020	670,030
50,000	670,030	670,030	670,030	670,030	670,030	670,030
60,000	670,030	670,030	670,030	670,030	670,030	670,050
70,000	670,040	670,040	670,040	670,040	670,040	670,050

combinations of inputs. There are only three initial guesses required for the convergence: FRWI1, FRWI2, and span efficiency. Wing area and take-off gross weight are outputs of the first function call (vehicle-level sizing). The experiment will test various weight combinations between FRWI1 and FRWI2.

Experimental Results

Table 34 shows the take-off gross weight solutions for various initial guesses of FRWI1 and FRWI2. All values are in pounds. FRWI1 values are displayed in the vertical column whereas FRWI2 values are displayed in the horizontal top row.

The final results for FRWI1, FRWI2, wing area, and span efficiency can be found in the

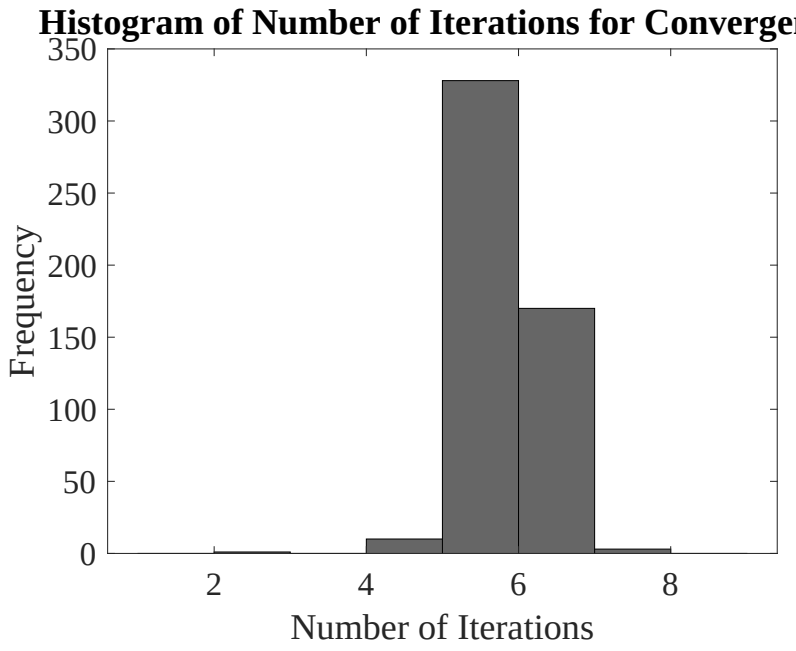

Figure 73: Histogram of Number of Iterations for Convergence from Design Space Exploration

appendix Chapter A. They show a similar trend with TOGW in that the results are robust to the initial guess of FRWI1 and FRWI2.

Experiment 3.1c Results
The results of Experiment 3.1c show that the structural wing weight convergence is robust to a variety of initial guess values. This result substantiates Hypothesis 3.1b.

An informal test was completed for varying span efficiency in the same manner the wing weights have been varied. While not formally included in this document, the trends were identical to the experiment performed here.

7.1.5 Answering Research Question 3.1

Two modeling environments of varying order/fidelity have been integrated into a single environment. Though the outputs are initially unequal (because their approaches are inequivalent), they can be "bridged" using intermediate variables (take-off gross weight, wing

weights, and span efficiency). The EDS environment is first evaluated with initial guesses of the wing weights and span efficiency, which outputs an estimated take-off gross weight and wing area. These are inputs to RADE which then outputs span efficiency and wing weights. This process is repeated until the take-off gross weight does not change between iterations beyond a defined threshold (set to 0.01%).

This process was shown to converge on a solution and be robust to the initial guesses. The initial guess values do no appreciably change the results of the weight, wing area, or span efficiency values. This implies that there is only one feasible solution for each design point. Many other points will be tested during the full case study in Chapter 8, but for now we will assume that these trends are repeatable for all design points within the design space. Therefore, we conclude that these two environments can be integrated into a single environment, overcoming a major obstacle in developing a bi-level design analysis approach

7.2 Research Question 3.2: Effect of Wing-Level Constraints on Conceptual Design Selection

Now that a bi-level environment has been developed, we would like to measure the impact of the wing-level considerations on the conceptual design point selection. The benchmark method only considered the vehicle-level variable spaces in the conceptual design environment (EDS). We can compare the results by optimizing for vehicle-level performance and reliability (same formulation as the benchmark method); then, evaluate the optimal designs against wing-level constraints. The goal here is to test how the optimal set of designs shifts with the newly acquired design knowledge.

7.2.1 Experiment 3.2: Aspect Ratio Thought Experiment

Consider a fixed conceptual design with only one design variable: aspect ratio. Aspect ratio is usually maximized because it has an inverse relationship with induced drag (Equations

25 and 26, where b is span, S is wing area, e is Oswald efficiency factor, and C_L is lift coefficient). Maximizing aspect ratio results in a larger span (for a given wing area). Therefore, for an optimization where the only design variable is aspect ratio, the optimal designs will be at the highest levels of aspect ratio (assuming the performance metric is correlated with lower drag).

$$AR = \frac{b^2}{S} \tag{25}$$

$$CD_i = \frac{C_L^2}{\pi ARe} \tag{26}$$

In practice, however, the span is limited to a given length. Then, if the optimization formulation is now modified to include a span constraint, the aspect ratio will be increased until the border of feasibility is reached.

Notional Numerical Example

Using values similar to the design point, consider a design point with a defined wing-loading of 130 and take-off gross weight of 650,000 pounds. This would result in a wing area of 5,000 square feet. If we consider two different aspect ratios, say 8 and 10, then the two resulting spans would be 200 feet and 223.6 feet, respectively, for a un-swept, rectangular wing. Assuming constant values of lift coefficient (C_L) and span efficiency (e), the induced drag would be 25% lower for the higher aspect ratio wing. Therefore, without a span constraint, the higher aspect ratio wing would be preferred. However, if a span constraint of 215 feet was enforced, the lower aspect ratio design would be selected.

7.2.2 Experiment 3.2a: Single Design Aspect Ratio Sensitivity

Experimental Design

We can apply the same logic to a design evaluated in the new integrated environment. A sample design point is selected as the baseline point. The aforementioned constraints (span, tip deflection) are recorded as well as a sample performance metric (economic block fuel, which is the fuel required to go from gate to gate for the design mission).

We expect higher aspect ratio to be preferable with respect to the performance metric but eventually to violate one or more constraints. The span constraint for this experiment will be the same as the benchmark method which is 215 feet. The tip deflection constraint will be set to 80 feet for the 2.5G maneuver load case and -30 feet for the -1.0G maneuver load case. We are looking to see if an increase in aspect ratio would violate wing-level constraints before violating vehicle-level constraints. If this is true, then we would expect an optimizer to prefer vehicle-level designs that are actually infeasible with respect to downstream constraints.

Experimental Results

The design is frozen for all design variables except the aspect ratio value (the frozen values are equal the design point's values found in Table 13). Both environments were evaluated for these points (including structural wing weight convergence and jig shape determination). The results for this design with only varying aspect ratio are displayed in Table 35.

Four outputs are of interest: span, tip deflections, and economic block fuel. Here, the span and tip deflections act as constraints whereas economic block fuel is the performance metric. As expected, higher aspect ratio values result in higher span values and lower economic block fuel. The higher the span the higher the tip deflection during the 2.5G maneuver load case (Max TD) as well as lower tip deflection during the -1.0G maneuver load case (Min TD). These represent the wing-level constraints that are not considered

Table 35: Effect of Aspect Ratio on Span, Tip Deflections, and Economic Block Fuel

Aspect Ratio	Span (ft)	Max TD (ft)	Min TD (ft)	Block Fuel (klbs)
8	195.5	57.6	-15.1	272.3
9	202.8	68.1	-20.4	261.4
10	210.2	80.2	-28.2	252.4
11	217.2	92.7	-36.9	243.2
Aspect Ratio	Span (ft)	Max TD (ft)	Min TD (ft)	Block Fuel (klbs)
8	-5.3%	-22.8%	-39.8%	5.8%
9	-1.7%	-8.8%	-18.8%	1.6%
10	1.8%	7.5%	12.1%	-1.9%
11	5.2%	24.1%	46.5%	-5.5%

during a vehicle-only optimization.

The percentage change is provided in Table 35 to show the steepest effects of changing aspect ratio. These values are relative to the average of the four cases. Clearly, the tip deflections are affected more than span or economic block fuel. If a span constraint of 215 ft. was applied to this design space, the aspect ratio would be constrained somewhere between 10 and 11. If the constraint value was at 80 feet, the design with aspect ratio at 10 would be infeasible, but the vehicle-only formulation would not know this. Therefore, a higher aspect ratio wing (~10) would be preferred to decrease economic block fuel when the span constraint is not more restrictive than the tip deflection constraint. However, because the vehicle-level formulation does not know when stop increasing aspect ratio, an infeasible wing is likely to be described as optimal and therefore selected as the chosen conceptual design.

Experiment 3.2a Results

The results of Experiment 3.2a show that preferable vehicle-level designs can fail wing-level constraints without failing vehicle-level constraints. This supports Hypothesis 3.2 that the optimization process will result in high-performing, compliant designs with respect to the vehicle-level constraint space but non-compliant designs

with respect to the wing-level constraint space.

Capturing Tip Deflection Via Span

Because FLOPS has no awareness of tip deflection, the proposal could be made to form a sort of surrogate of tip deflection using a vehicle-level metric. Perhaps span could be used as a surrogate for tip deflection: a relationship between tip deflection and span could be formulated to determine a new, restrictive span constraint. Unfortunately, span is insufficient to capture the complexity of the tip deflection constraint as demonstrated by Table 36.

Table 36: Effect of Sweep on Span and Maximum Tip Deflections

Aspect Ratio	Span (ft) at 37°Sweep	Span (ft) at 33°Sweep	% Difference
8	195.57	195.03	-0.3%
9	202.89	202.40	-0.2%
10	210.20	209.77	-0.2%
11	217.27	216.93	-0.2%
Aspect Ratio	Max TD (ft) at 37°Sweep	Max TD (ft) at 33°Sweep	% Difference
8	57.65	51.95	-9.9%
9	68.11	60.57	-11.1%
10	80.24	71.31	-11.1%
11	92.70	84.12	-9.3%

The span is largely unchanged by the variation in sweep (in fact, by definition in FLOPS, the span should not change at all: the small change seen here is due to numerical changes in glove area calculation) whereas the tip deflection has about a 10% change. This shows that span itself can remain unchanged whereas tip deflection can change significantly. In other words, the two metrics are sometimes independent. Therefore, a span constraint cannot be used as a substitute for a tip deflection constraint.

Recovering Designs with Mitigation

If we assume a span constraint of 215 feet and a maximum tip deflection constraint at 80 feet then the design with an aspect ratio of 10 satisfies the vehicle-level constraint but

not the wing-level constraint. Now the question becomes whether or not we can recover this design using wing-level mitigation. The mitigation that we apply is derived from the historical example of the Sutter twist: outboard wing twisting. Twisting the wing should shift the wing distribution inward and therefore decrease the lifting load on the outboard wing, thereby decreasing the maximum tip deflection. We would expect the alteration to decrease the maximum tip deflection and increase the minimum tip deflection. Table 37 shows the effect of both positive and negative changes to the linearized wing twist at wing section 6.

Table 37: Effect of Wing Twist Mitigation on Span, Tip Deflections, and Economic Block Fuel

Change in Twist Slope	Span	TD_{max}	TD_{min}	BF_{econ}
-0.05°	210.2	78.0	-30.3	260.3
0°	210.2	80.2	-28.2	252.4
0.05°	210.2	82.5	-25.6	246.0
Change in Twist Slope	Span	TD_{max}	TD_{min}	BF_{econ}
-0.05°	0.0%	-2.7%	-7.3%	3.1%
0.00°	0.0%	0.0%	0.0%	0.0%
0.05°	0.0%	2.8%	9.4%	-2.5%

We can see from Table 37 that increasing washout (decreasing wing twist by -0.05°) decreases the maximum tip deflection. The value dropped from 80.2 feet to 78.0 feet meaning that now the point is recovered. For this case, the wing-level mitigation was sufficient to satisfy the previously violated maximum tip deflection constraint.

However, notice that the minimum tip deflection is now -30.3 feet which exceeds the constraint of -30 feet. For this design to be recovered, the mitigation then must be sufficient to recover the maximum tip deflection violation without violating the minimum tip deflection constraint. This value would be about -0.02°. This example illustrates that mitigation has the potential to recover a design but also to cause a violation in a previously satisfied constraint.

We can also investigate the trends of this mitigation action by varying the design wing

twist. As demonstrated by Table 38, the trend of this mitigation action does not change with the design twist.

Table 38: Effect of Wing Twist Mitigation (-0.05, 0, 0.05 respectively) on Tip Deflections and Economic Block Fuel

Mitigation Twist (°)	Design Twist (°)	TD_{max} (ft)	TD_{min} (ft)	BF_{econ} (klbs)
-0.05	-0.6	77.7	-43.5	293.8
	-0.5	78.0	-30.3	260.3
	-0.4	78.2	-16.1	238.7
Mitigation Twist	Design Twist	TD_{max}	TD_{min}	BF_{econ}
0.00	-0.6	79.8	-42.4	283.22
	-0.5	80.2	-28.26	252.4
	-0.4	80.4	-12.45	234.2
Mitigation Twist	Design Twist	TD_{max}	TD_{min}	BF_{econ}
0.05	-0.6	82.0	-40.9	272.5
	-0.5	82.5	-25.6	246.0
	-0.4	82.8	-9.20	231.1

Failing Constraints Deterministically

It is important to note here that the design failed the wing-level constraint without the presence of modeled uncertainty variables. Unlike Research Question 2, there are no uncertainty variables or probability density functions. There are no sampling methods or noise factors. The design failed the tip deflection constraint in the same manner that it failed the span constraint: deterministically. This was not a case where the margin was insufficient to cover an unfavorable uncertainty realization; indeed, there need not be *any* uncertainty realizations at all. The constraint violation came from the design space itself and the lack of knowledge of wing-level constraints. This leads us to believe that even in the absence of uncertainty realizations, conceptual designs can still fail wing-level constraints.

Here the definition of uncertainty has changed. Before, the definition was simply the potential difference between a predicted value and a realized value. The difference itself is called error once the "truth" has been realized. This definition is different. EDS did not

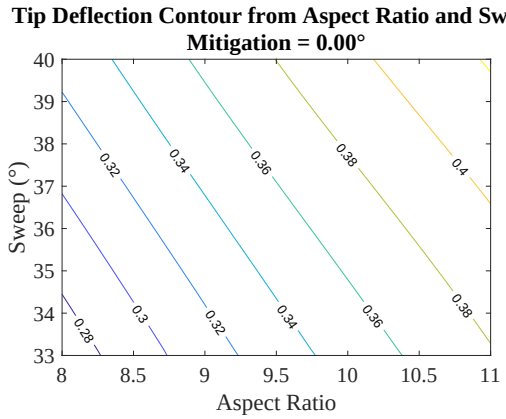

(a) Change in Linear Twist Slope = 0.0°

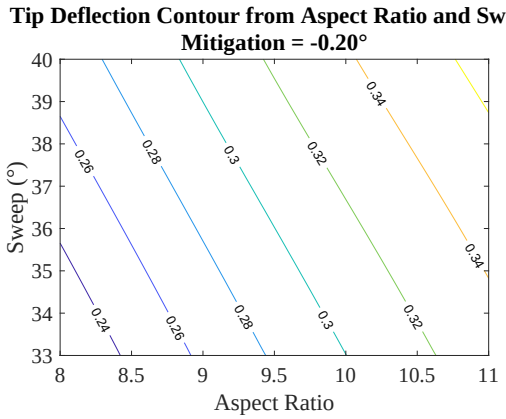

(b) Change in Linear Twist Slope = -0.20°

Figure 74: 2.5G Maneuver Load Case Tip Deflection Contour Plot Against Aspect Ratio and Sweep: Comparison between no mitigation 74a and maximum washout mitigation 74b

incorrectly estimate tip deflection: it cannot estimate tip deflection. The definition of uncertainty here is a null or empty set. EDS has no awareness of tip deflection and therefore it is unknown (uncertainty). Consequently, designs, in the total absence of uncertainty, can fail wing-level constraints because the vehicle-level environments do not take these constraints into consideration. In other words, the designs fail the constraints *deterministically* due to the design values rather than *probabilistically* due to uncertainty realizations (sampling from probability density functions).

This trend can be represented graphically by using contour plots. Figure 74 shows lines constant maximum tip deflection for the 2.5G maneuver load case against aspect ratio and sweep. Note that the constraint has changed to be non-dimensional as defined by tip deflection divided by span. The constraint value will be about 30% (TD_{max}/Span ≤ 0.3).

Figure 74 shows that this constraint shifts from left to right when negative wing twist mitigation is applied. Essentially, mitigation is expanding the feasible design space: more combinations of aspect ratio and sweep are now feasible.

To conclude, this experiment shows that, for a single design such as the baseline design, wing-level mitigation actions can recover designs that failed one or more constraints deterministically (rather than just probabilistically). In other words, the presence of miti-

gation actions here expands the feasible design space rather than solely safeguards against probabilistic uncertainties.

Experiment 3.2a Results (continued)

Because the wing-level constraints can be failed deterministically (due to design variable values) rather than probabilistically (due to uncertainty sources), Hypothesis 3.2 is substantiated in that vehicle-level optima will have a probability of compliance of exactly zero with respect to wing-level constraints.

7.2.3 Experiment 3.2b: Evaluating Vehicle-Level Optima Against Wing-Level Constraints

We would like to take this trend to the optimization level for conceptual design selection. As the thought experiment and tip deflection experiment demonstrated, the vehicle-only environment will probably push the design space towards infeasible designs with respect to the wing-level constraints. We can test this hypothesis by first finding a Pareto Front in a vehicle-only optimization formulation. Then, we can take the Pareto Front and evaluate them against wing-level constraints to determine feasibility. Finally, we can apply wing-level mitigation to see if any of the failed cases can be recovered.

A Quick Note on Pareto Fronts

A Pareto Front (or Frontier) is the set of points that are non-dominated relative to all considered points and non-comparable relative to each other [209]. It is used when two or more objective variables are defined but a preference between the objectives is unknown. If only one objective is used, then a single design will result as the optimum. If two objectives are defined and no preferences is prescribed, then two or more points may be non-comparable. This means that one design (Design A, for example) is better than the second design (Design B) with respect to one objective but worse with respect to the other objective. Because we do not which objective is valued more highly, we cannot choose one of these points

over the other. They are non-comparable. For our formulation, consider three designs: A, B, and C, where:

$$\begin{aligned} A_{Rel} &> B_{Rel} \\ A_{Rel} &> C_{Rel} \\ A_{EBF} &> B_{EBF} \\ A_{EBF} &< C_{EBF} \end{aligned} \tag{27}$$

where Rel is reliability and EBF is economic block fuel. We wish to maximize reliability while minimizing economic block fuel (representing operating cost and efficiency). Design A is preferable to Design B with respect to reliability but inferior with respect to block fuel. Regardless of *how much* different these values may be, we cannot say which is superior. Therefore, we record both points. Design C, however, is *dominated* by Design A because it is inferior to both objective metrics. Designs A and B would be recored in the Pareto Front but Design C would be excluded as depicted in Figure 75a.

If, however, Design C had lower economic block fuel than Design A, it would be a non-dominated design because it would be better than A and in one metric but worse in the other.

$$A_{EBF} > C_{EBF} \tag{28}$$

Thus, it would be along the Pareto Front as illustrated by Figure 75b.

Experimental Design

To perform this experiment, the first step is to generate a Pareto Front with the vehicle-only formulation as described in Table 40. Table 40 also shows the wing-level constraints that

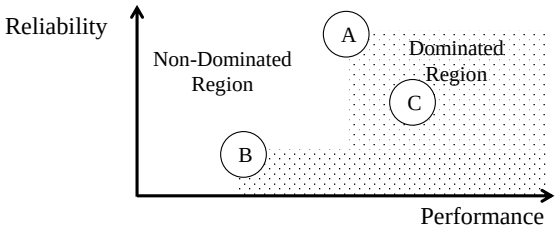

(a) Two Dominant Designs, One Dominated Design

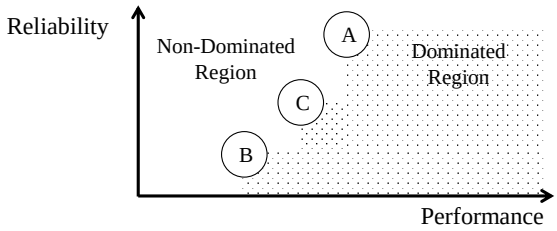

(b) Three Non-Dominated Designs

Figure 75: Pareto Front Illustration: Dominated and Non-Dominated Designs with Respect to Reliability and Performance

will be used after the Pareto Front has been found. Table 39 shows the design and margin variables used to determine the Front. In order to compare "apples-to-apples" later on, the wing-level design space will be included in the vehicle-level Pareto Front. Similarly, the designs will undergo structural wing weight convergence. This will allow the designs to be unique in both the vehicle and wing spaces. Later, when we evaluate these designs via the wing-level environment, we will not need to re-define wing-level design variables.

Table 39: Design and Margin Variables Comparison between Vehicle-Only and Integrated (Vehicle and Wing) Environments

Design Variable	Vehicle-Only	Integrated
TWR	✓	✓
WSR	✓	✓
AR	✓	✓
Sweep	✓	✓
FPR	✓	✓
HPCPR	✓	✓
TOC Thrust	✓	✓
Rib Spacing	✓	✓
Wing Twist	✓	✓

The wing-level uncertainty variables are not shown. However, the copula that was fit in Section 6.2.4 is used for wing-level uncertainty. The reason it is included for this formulation (even though the focus is on the vehicle-level) is that the uncertainty characterizes the physics-based model's prediction power. Because the tool itself is included in this

Table 40: Uncertainty and Constraint Values Comparison between Vehicle-Only and Integrated (Vehicle and Wing) Environments

Vehicle-Level Uncertainty	Vehicle-Only	Integrated
Profile Drag	0-5%	0-5%
Fuel Flow	0-5%	0-5%
Fuselage Weight	0-5%	0-5%
Engine Weight	0-5%	0-5%
Constraint	Vehicle-Only	Integrated
Range	7,530 nmi	7,530 nmi
Span	215 ft	215 ft
Span Efficiency	0.5	0.5
Max TD/Span	-	0.3
Min TD/Span	-	-0.2
Max Von Mises Stress	-	15,395 MPa
Root Bending Moment	-	8e8 ft-lbs

formulation, its associated uncertainty is as well.

An optimization using a genetic algorithm was run for 50 generations and 200 individuals per generation. Admittedly, this optimization is not meant to be a rigorous demonstration of the final Pareto Front of the vehicle-only environment, but it will be sufficient to show the overall direction that the optimization was moving towards with respect to the design variables.

Experimental Results

The results of this optimization are depicted in Figures 76 and 77. Similar plots can be made for the entire design space (and more will be shown for the Case Study), but our focus here remains on the wing space: specifically aspect ratio and sweep.

As expected, Figure 76 shows that the highest performing designs (lowest economic block fuel) have the highest aspect ratio. The aspect ratio stops abruptly at about 10.5, which is where we would expect the span constraint to start becoming active (recall that there are no wing-level constraints included in this formulation; as a result, the tip deflection

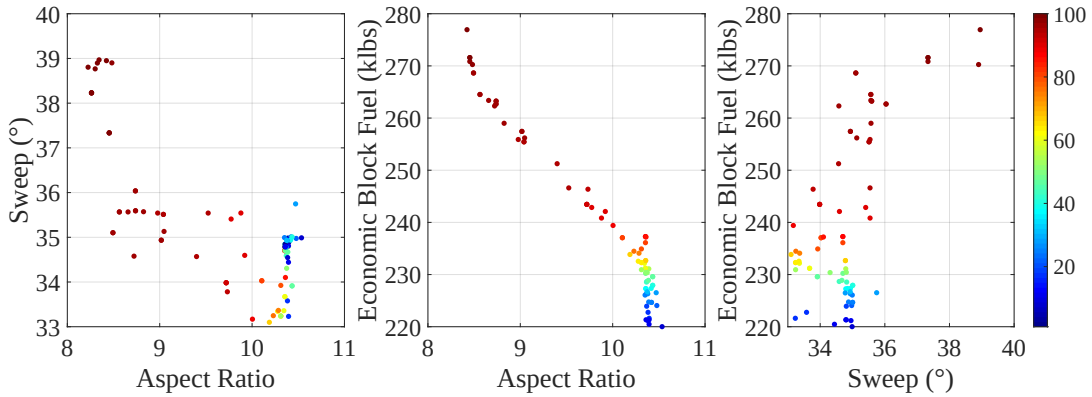

Figure 76: Vehicle-Only Optima in Aspect Ratio and Sweep Space

constraint is not enforced). As also shown by the though experiment in Section 7.2.2, decreasing the sweep allows for higher aspect ratios. One final trend to observe is that higher aspect ratios result in lower economic block fuels, which was also expected.

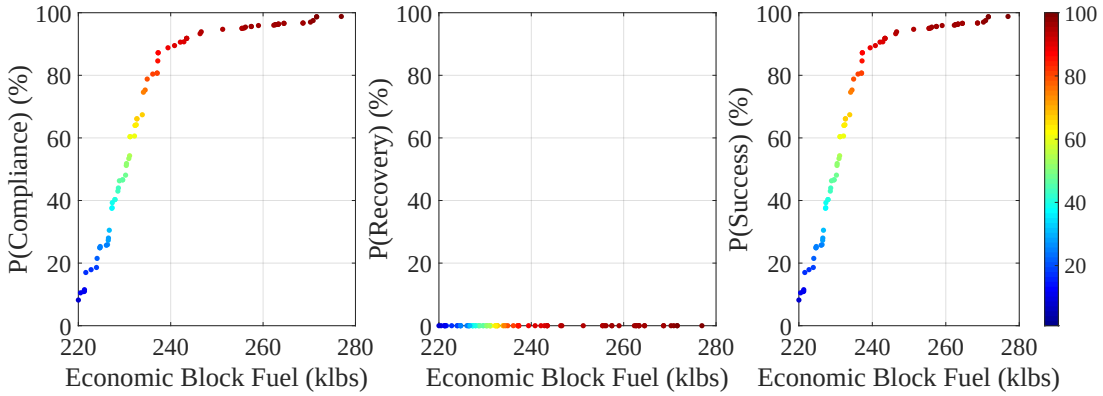

Figure 77: Vehicle-Only Optima in Objective Space

Looking at the objective space in Figure 77 shows that the probability of compliance is equal to the probability of success. This is expected because no mitigation is included in the formulation. This figure also shows that 100% reliability is achieved, meaning that design and margin variable combinations exist that satisfy all the vehicle-level constraints under uncertainty. The range of the economic block fuel is between about 220,000 and 280,000 pounds, a change of about 30%, meaning that there is a significant trade between

reliability and performance.

Experimental Results: Evaluating the Vehicle-Level Pareto Front against Wing-Level Constraints

Now we take the set of designs along the Pareto Front and evaluate them against wing-level constraints. There are 103 design points along the Pareto Front: each was evaluated now with the same uncertainty as before but now with wing-level constraints. As described in Section 7.2.2, if the constraint fails due to the design variables rather than the uncertainty variables, the reliability will fall to zero. All the realizations will fail because the constraint is violated by the design variable combinations rather than the margin variable values. The results of this experiment are shown in Figures 78 and 79.

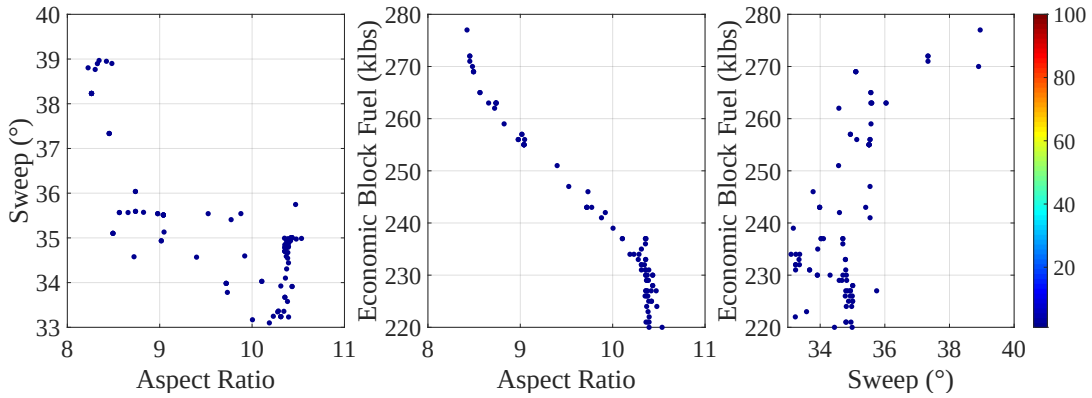

Figure 78: Vehicle-Only Optima with Wing-Level Constraints in Aspect Ratio and Sweep Space

The color bar in Figure 78 shows the probability of success for each of the designs. They are all dark blue because they are all zero. This result is reinforced by Figure 79: all probabilities are zero. If *any* of these points had been selected as the design to freeze as the design process progressed from conceptual to preliminary design, the program would be stopped. In the absence of mitigation, the process would require redesign or cancellation: the worst possible outcomes. The constraint violations are aggregated, so we do not know *which* constraints are violated, but we can surmise from the thought experiment that the tip

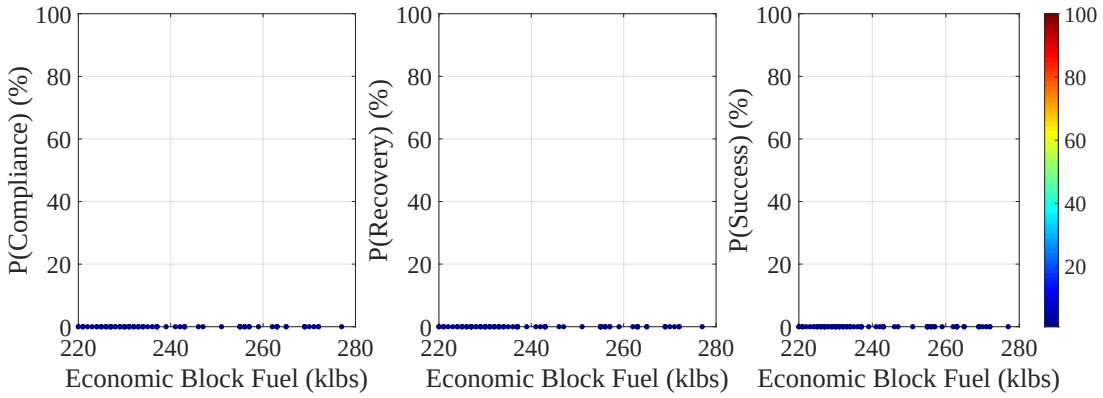

Figure 79: Vehicle-Only Optima with Wing-Level Constraints in Objective Space Space

deflection constraint is significant.

Experiment 3.2b Results

The results of Experiment 3.2b show that the vehicle-level optima selected via Pareto Front have zero probability of satisfying wing-level constraints. This result substantiates Hypothesis 3.2.

The results shown in Figures 78 and 79 show the danger in selecting a conceptual design without considering downstream constraints. Until now, downstream constraints could not be considered in a conceptual design environment because the tools to do so were not integrated into a single environment.

Experimental Results: Evaluating the Vehicle-Level Pareto Front against Wing-Level Constraints and Mitigation

To avoid redesign or cancellation we can attempt to apply mitigation to recover these failed designs. Because these points are drawn from a vehicle-only environment yet failed after implementing wing-level constraints, we can conclude that the designs are failing the wing-level constraints rather than the vehicle-level constraints. Therefore, we would expect wing-level mitigation to have some effect when recovering the designs. The definition of

the applied mitigation space is described in Table 41.

Table 41: Wing-Level Mitigation Variables and Ranges

Change in Twist Linear Slope		Wing Section	
Minimum	Maximum	Minimum	Maximum
-0.20°	0.20°	6	12

The change in reliability is demonstrated in Figures 80 and 81. Thankfully some of the designs can be recovered (as shown by the variety of color in Figure 80 and non-zero P(Recovery) in Figure 81). 31 out of the 103 designs were able to have some level of recovery. Figure 80 shows that these 31 designs are the ones with the lower aspect ratios whereas the higher aspect ratios were unrecoverable. The average reliability of the recovered designs was about 33.5%. This means that, average across the entire set, the reliability of the vehicle-only Pareto Front is only about 10.4%. If one design from the Pareto Front (which is an *optimized* set) was randomly selected, there would be an 89.6% chance that redesign would be necessary.

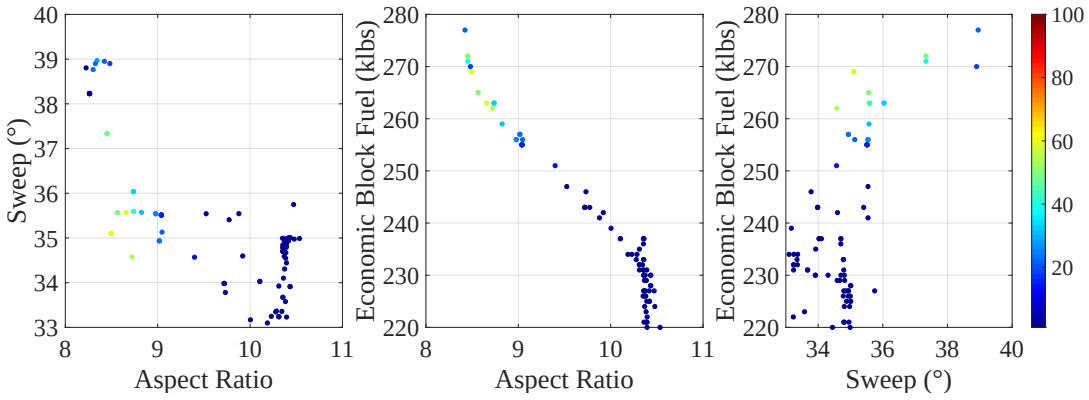

Figure 80: Vehicle-Only Optima with Wing-Level Constraints and Mitigation in Aspect Ratio and Sweep Space

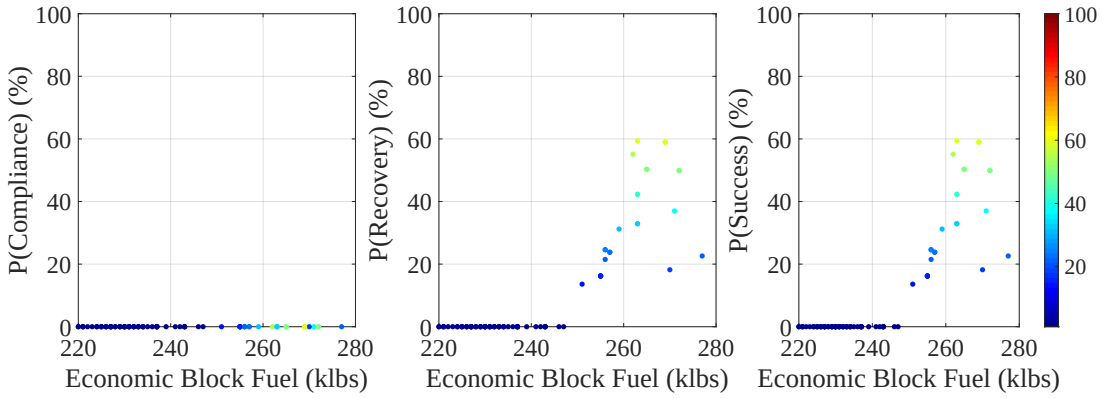

Figure 81: Vehicle-Only Optima with Wing-Level Constraints and Mitigation in Objective Space

Experiment 3.2b Results (continued)

The results of Experiment 3.2b show that the vehicle-level optima selected via Pareto Front have non-zero probability of satisfying wing-level constraints when mitigation is considered. Therefore, Hypothesis 3.2 does not hold when wing-level mitigation is considered. This result qualifies Hypothesis 3.2 to now state that the probability of success is only non-zero when wing-level mitigation is not considered.

7.2.4 Answering Research Question 3.2

Research Question 3.2 highlighted the impact of a wing-level design formulation in addition to the benchmark vehicle-only formulation. Note that the current state-of-the-art in aircraft conceptual design methods only consider the vehicle-level formulation. All the experiments performed in this section reinforced the danger in performing optimization without knowledge of downstream constraints. Because higher aspect ratio reduces block fuel, the vehicle-level optimizer will prefer these designs. However, these are the designs that are likely to fail downstream constraints without modeled uncertainty (noise factors). Therefore, the non-compliance was a result of the design space only. In the case the constraints are said to be failed deterministically rather than probabilistically. Consequently,

they have a zero percent chance of satisfying downstream constraints. Again, this is because the failure is not due to noise factors or possible future states. It is due to the design space selection.

In other words, designers could be shooting themselves in the foot when they use optimization formulations without all the applicable constraints. This is just one example of aspect ratio and tip deflection on the wing level, but this trend is possibly occurring on the other major systems as well (engine, fuselage, etc). To answer Research Question 3.2, the impact of the bi-level environment is highly consequential. Integrating downstream constraints is paramount to a successful design. Otherwise, optimization may be rendered futile by future redesign and complications downstream.

CHAPTER 8
CASE STUDY

This chapter presents a case study based on a new conceptual design RBDO framework. A more in-depth discussion of the framework will first be provided such that no sidebar is required when the results are discussed. A case study is then presented from start to finish using the new framework. The developed process is called a framework because it is a general approach rather than a specific methodology.

8.1 RABiDA Framework Overview

Section 3.3.1 described the need for a new overall approach to conceptual design selection under uncertainty, calling for a two-stage design process such that uncertainty can be realized and mitigation can be performed in response to uncertainty. The framework that has been developed to fill this gap is called the Reliability Assessment using Bi-level Design Analysis (RABiDA) framework. The goal of the method is to perform conceptual design selection based on both performance and reliability. A two-stage approach is taken where the first level is an empirically-based, vehicle-level conceptual design tool and the second level is a physics-based, wing-level design tool. Using two tools of differing fidelity results in two different problem formulations (variables particular to each design level) though some variables are shared.

Figure 19 depicted the ARMOUR method which has been used as the benchmark for this work. The opportunities for improvement are thus: the addition of a higher fidelity model, uncertainty quantification and correlation, and a bridge between the modeling environments. These opportunities have formed the backbone of the three posed research questions. The results form the RABiDA framework. For example, the wing was selected as the major component of focus. This need not be the case: an engine environment could

easily replace the wing environment. Further, Richardson's Extrapolation Method is not required either: the requirement is *any* process to quantify uncertainty within the modeling environments. Because the result is so general, it is called a framework rather than a methodology.

The overall framework is given in Figure 82.

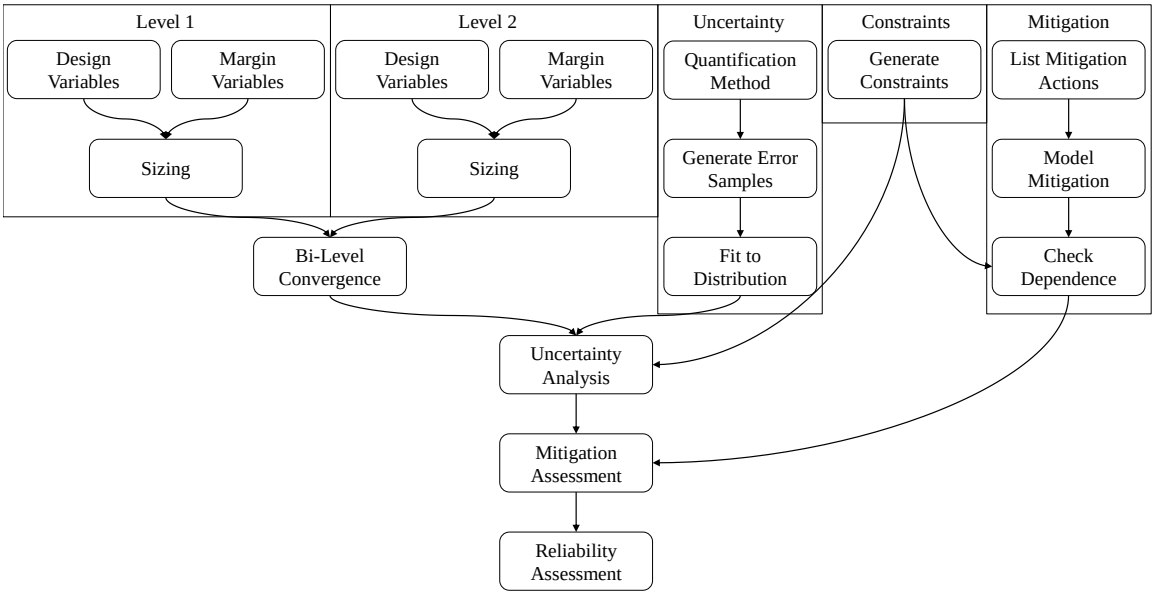

Figure 82: Overall Reliability Assessment using Bi-level Design Analysis (RABiDA) Framework

The RABiDA framework starts with defining the two model design and margin spaces before sizing via model execution. The outputs are used to converge to a solution via the bi-level convergence (though this process need not be restricted to only two levels; this process can be used for n number of sizing environments). Aside from the design side, an uncertainty quantification method is required. It needs to capture or estimate the uncertainty caused by the selected modeling environments. The quantification method is executed with a sampling across the design space to create a dataset for each metric of interest which are then fit to parametric distributions or a copula if correlations exist. Of course, constraints are required to reliability analysis so they must be defined. With these in mind, a list of mitigation actions is created with the degrees of freedom available on the downstream level

(Level 2, or wing-level for the case study). These actions are then modeled and tested for constraint sensitivity. Obviously a mitigation action that does not affect constraints will not improve reliability and should therefore be discarded.

These steps complete the problem formulation portion of the framework and represent the majority of the effort required to perform bi-level conceptual design RBDO. Only the optimization is left to be completed, which is described extensively in Section 8.1.1 but is essentially composed of three main parts: uncertainty analysis, mitigation assessment, and reliability assessment. The uncertainty analysis applies the number of realizations of scenarios under investigation to the (previously) deterministic design point. The realizations are then separated into compliant and non-compliant with the non-compliant realizations undergoing mitigation assessment. The final step is to determine the reliability (total number of compliant and recovered realizations) and expected performance of the design.

8.1.1 Optimization Process

The optimization process to determine the performance and reliability is depicted in Figure 83. It begins by sampling the design and margin space. The design spaces of both levels are combined such that a design is described by both levels. The first step is to perform sizing and synthesis at both levels (using a structural wing weight convergence loop, for example, as completed in Section 7.1.2). The output of this is a consistent design at both levels. This completes the deterministic sizing process.

The next step is to apply the uncertainty. Typically uncertainty is modeled by probability density functions. The sampling of these distributions can be independent or dependent depending on which is approach is selected. The deterministic design now transforms from a single design to thousands possibilities. Each future state is characterized by one draw from the uncertainty distributions. Each possible future state is evaluated against wing-level constraints to determine feasibility. For all the infeasible possible future states, a sampling of mitigation is applied to see if any set of mitigation actions is available for recovery.

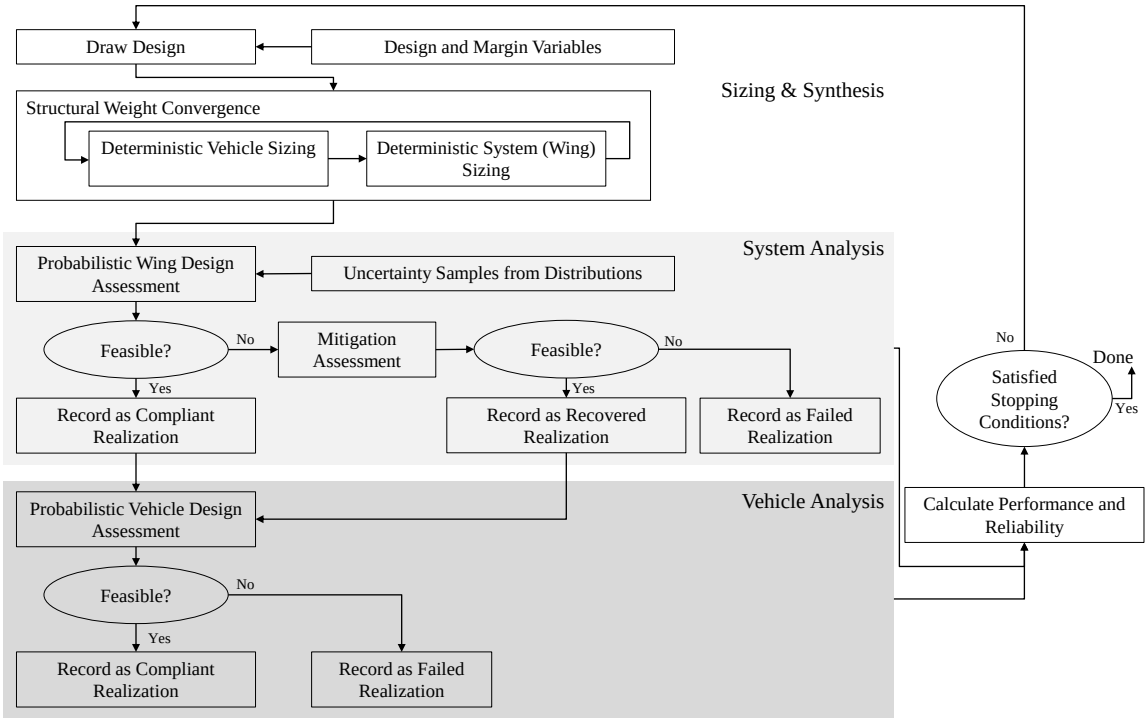

Figure 83: RABiDA Optimization Process

If a realization is compliant (passed all constraints) or recovered (required mitigation to pass the constraints), it progresses to the vehicle analysis where the modified design is evaluated to test against vehicle-level constraints to ensure that mitigation has not caused a constraint violation. The reliability of the design is the percentage of all possible future states that are feasible against the total number of future states.

8.1.2 Mathematical Formulation of Reliability

The flowchart given in Figure 83 is described here mathematically. An optimization algorithm will be used to determine the Pareto Front. It will require a process to produce the two objective metrics (economic block fuel and reliability). The algorithm will be a genetic algorithm.

Determine Individual

The process begins with the algorithm drawing an individual from the population. The initial population is intentionally spread across the design and margin space. An individual is defined by a unique set of design and margin variable values. The values are defined for both the vehicle and wing levels.

$$X = [x_v, h_v, x_w, h_w] \tag{29}$$

Perform Structural Wing Weight Convergence

The individual then undergoes the structural wing weight convergence loop to converge on a reconciled point between the two environments. The convergence requires the design and margin values to return the take-off gross weight, wing area, span efficiency, and wing weight components.

$$[TOGW, S, e, FRWI1, FRWI2] = SWW(x_v, h_v, x_c, h_c) \tag{30}$$

The new values are appended to the individual such that they can be used in later steps. The individual is now a sized design.

$$x := [x_v, h_v, x_c, h_c] \cup [S, e, FRWI1, FRWI2] \tag{31}$$

Sample Uncertainty and Evaluate Performance and Constraints

An uncertainty matrix is defined by sampling the copula. The surrogates are then evaluated using the design and uncertainty samples. The output is a matrix with the dimensions of the number of responses by the number of uncertainty realizations (r representing responses, g representing constraints). The single design is now represented by several possible future

states. The outputs are defined with subscript *h* to denote that only margin has been applied.

$$[[r_h], [g_h]] = f(x_v, h_v, x_w, h_w, [u]) \tag{32}$$

Determine Compliance

Compliance is calculated by adding the total number of designs that satisfy all constraints. Compliance is typically presented as a fraction of the total number of possible future states, but for now it is purely the sum of feasible points.

$$Compliance = \sum_{i=1}^{1{,}000} q(g_{h,i}, g) \quad where \quad q = \begin{cases} 1 & \text{if } g_{h,i} <= g \\ 0 & \text{if } g_{h,i} > g \end{cases} \quad \forall g \tag{33}$$

Apply Mitigation to Non-Compliant Realizations

Only the non-compliant realizations undergo mitigation assessment. The non-compliant uncertainty scenarios are denoted by u_m. A new set of responses and constraints are yielded by the mitigation analysis. It is important to note that the mitigation matrix is applied to each uncertainty scenario. If one or more sets of mitigation actions are found to satisfy all constraints, the set will the most desirable performance metric will be chosen.

$$[r_m], [g_m] = f(x, [u_m], [m]) \tag{34}$$

Calculate Recovery

The new constraint values due to the presence of mitigation are now evaluated against the constraints. The total number of cases considered is the total number of uncertainty scenarios less the number of compliant realizations. If a design is 100% compliant, no

mitigation assessment is completed.

$$Recovery = \sum_{i=1}^{1{,}000-Compliance} q(g_{m,i}, g) \quad where \quad q = \begin{cases} 1 & \text{if } g_{m,i} <= g \\ 0 & \text{if } g_{m,i} > g \end{cases} \quad \forall g \tag{35}$$

Calculate Reliability and Performance

The total reliability is found by adding the number of compliant realizations to the number of recovered realizations then dividing by the total number of uncertainty scenarios. These equations were given in Chapter 3 but are repeated for convenience.

$$Compliance = Number\, of\, feasibility\, realizations \tag{36}$$

$$Recovery = Number\, of\, recoverable\, realizations\, due\, to\, mitigation \tag{37}$$

$$Reliability = \frac{Compliance + Recovery}{Total\ Number\ of\ Uncertainty\ Scenarios} \tag{38}$$

Only the reliable points are used for calculating performance. The performance values of the infeasible scenarios are not of interest because they would result in redesign or cancellation. Therefore the performance value is a weighted average of the compliant and recovered scenarios.

$$r = \frac{r_h * Compliance + r_m * Recovery}{Compliance + Recovery} \tag{39}$$

8.1.3 Step-by-Step Process for Aircraft Conceptual Design

The prior research and results have laid the foundation to demonstrate the impact of a new design framework. The goal is to determine which designs are the best with respect to performance and reliability on *both* the vehicle-level and wing-level analyses. The overall process is as follows (metrics or tools specific to this case study are given in parentheses):

1. Determine application
    1.1. Define requirements (PAX class, range, payload) and overall configuration (number of engines, tail wing type)
    1.2. Determine design generation and analysis tools (FLOPS, NPSS, VSP)
    1.3. Configure baseline model input files (.in, .npss, .vsp) for vehicle, engine, and wing
2. Formulate optimization problem
    2.1. Select performance objective metric (economic block fuel) and reliability metric (P(Success))
    2.2. Define design (TWR, WSR, AR, etc.) and margin (empty weight, drag, etc.) variable spaces
    2.3. Define failure modes and constraint values at both vehicle and wing levels (take-off field length, maximum Von Mises stress, etc.)
    2.4. Describe wing-level load cases and conditions (2.5G maneuver, -1.0G maneuver)
3. Define and model mitigation actions
    3.1. Generate list of physical design changes that will affect constraints (outboard wing twist)

3.2. Model selected actions within lower-level environment (VSP and FEM)

3.3. Test for mitigation-constraint dependence (variation in tip deflection)

4. Characterize uncertainty

4.1. Determine most relevant sources of uncertainty (model uncertainty)

4.2. Determine method to describe uncertainty sources (Richardson's Extrapolation Method)

4.3. Fit results to parametric distributions and to copula if correlations are present (Student's t Copula)

5. Determine vehicle- and wing-level design point

5.1. Determine bridge variables between environments (take-off gross weight, span efficiency, wing area, wing component weights)

5.2. Translate common input variable definitions (aspect ratio)

5.3. Evaluate both environments at design point

5.4. Calibrate drag factor to match mission take-off gross weight (drag factor FCD-SUB)

6. Generate surrogate models

6.1. Determine list of input, output, and intermediate variables and associated ranges

6.2. Build design of experiments and run cases (Latin Hypercube)

6.3. Ensure that outputs are within variable ranges

6.4. Check goodness of fit metric for surrogate equations

7. Perform optimization

7.1. Select optimization algorithm and uncertainty sampling method

7.2. Vary sizing (design and margin) variables to determine optimal set using optimization algorithm

7.3. Report out Pareto Front of performance and reliability

This process is generic enough for any two-phase design environments, though the definition for what constitutes a "phase" is fluid. Here, the conceptual design phase is represented by the vehicle design environment while the preliminary design phase is represented by the wing design environment. The environments at different levels of fidelity, which is necessary to simulate the change in design knowledge throughout the design process.

8.2 Case Study

A detailed application of RABiDA will now be completed from beginning to end. The subsection numbers match the steps described in Section 8.1.3. This study is a single realization of the many possible applications of a bi-level design analysis framework.

8.2.1 Step 1: Select Application

Consider a start-up company (Rabid Raccoons Inc., RRI) that seeks to enter the aircraft design and manufacturing space. It lacks the capital or subject matter expertise that the legacy players (Boeing and Airbus) maintain. Therefore, it would like to start gaining distinction by performing conceptual design selection using advanced tools and environments rather than subject matter expertise (which it does not have). Their value proposition is that they can provide traceable, verified design selection using industry standard tools. Its hope is to gain enough momentum to become the premier design provider for aerospace concepts or be acquired by one of the aerospace giants.

For its first product, it wants to demonstrate the impact of its advanced methodologies on an established aircraft design concept: the Boeing 777-200ER vehicle and mission, due the abundance of publicly available data. The mission profile is detailed in Table 42 [210].

Table 42: Boeing 777-200ER-Like Mission

Range	Payload	Mach	Altitude
7,530 nmi	64,050 lbs	0.84	35,000 ft

Table 43: Boeing 777-200ER-Like Design Point

Thrust-to-Weight	Wing Loading	Take-off Gross Weight
0.296	133.34	657,000 lbs

The conceptual design environment will also perform propulsion analysis and engine sizing. The engine paired with the Boeing 777-200ER notional aircraft is an engine similar to the GE90-94B-like with 78,400 pounds of takeoff thrust. The design point and size of the 777-200ER-like aircraft will be set as follows in Table 43.

For this application to be analyzed in an FEM environment, much more detailed information is required. Consequently, a Boeing 777-200ER-like wing FEM is difficult to gather. So, the wing will be replaced by a wing from NASA's Common Research Model [201].

CAD level data is available on NASA's website which can be easily translated into usable VSP files. Characteristics of the CRM VSP wing are given in Table 44.

While the VSP file for the entire vehicle is available, the CRM does not have a defined mission or take-off gross weight. Therefore, the Boeing 777-200ER values are used instead. Section 8.2.5 is devoted to reconciling these two configurations.

Table 44: Wing Characteristics of NASA's Common Research Model Wing

Span	Area	Aspect Ratio	Sweep	Taper Ratio	Incidence Angle
191.4 ft.	4,464 ft^2	8.41	37°	0.197	6.00°

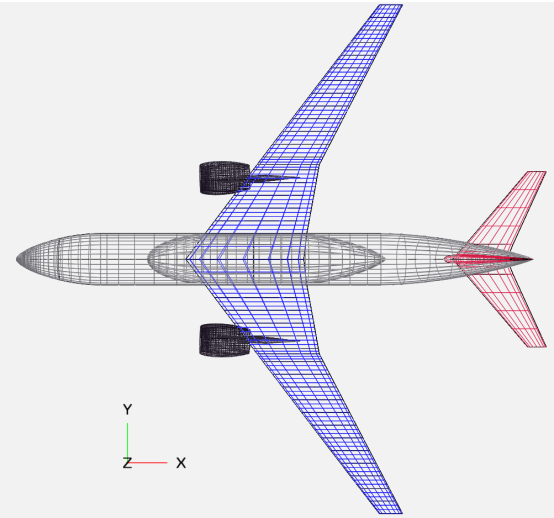

Figure 84: CRM VSP Vehicle-Level Model

8.2.2 Step 2: Formulate Optimization Problem

Select Optimization Objective Metric

By nature of uncertainty quantification and management, one objective metric will be reliability. If this was the only objective metric, we would assume to converge on a highly conservative design with respect to the design and margin variables. Therefore, a performance objective is used as well, making this formulation multi-objective.

Recalling the economic introduction given in Chapter 1, the ideal optimization formulation would only have one metric: profit. Profit would consider the expected income (revenue) generated by the design and aggregate the cost. Because revenue is difficult to forecast and cost is proprietary, only the technical side of the problem with reliability and performance will be considered. The analogy here is that a higher performing aircraft would be more desirable (competitive) and higher reliability would mean less cost (program delays). Because RRI does not have the historical cost data to attribute to mitigation, the economic analysis is excluded. Instead, RRI provides a strictly technical comparison between the designs.

One key characteristic that would make an aircraft desirable is low operating costs,

Table 45: Case Study Formulation: Design and Margin Variables

Vehicle-Level Design	Vehicle-Level Margin	Wing-Level Design	Wing-Level Margin
Thrust-to-Weight	Empty Weight Margin	Aspect Ratio	Knockdown Factor
Wing Loading	Drag Margin	Sweep	-
Fan Pressure Ratio	-	Rib Spacing	-
HPC Pressure Ratio	-	Wing Twist	-
Lapse Ratio	-	-	-
Aspect Ratio	-	-	-
Sweep	-	-	-

such as low fuel cost. If an aircraft is cheap to operate, then perhaps customers would be willing to pay a higher price to the manufacturer. Therefore, the objective metric used here is economic block fuel which is defined as the amount of fuel required for the aircraft to go from gate to gate when performing the design mission.

Note that this case is different than the maximum range case. For maximum range the aircraft will be carrying the maximum level of fuel. For the economic mission, the aircraft may not need to carry as much fuel as possible. Therefore, for the economic mission, the take-off gross weight is less than the maximum take-off gross weight. The design take-off gross weight (the values given in this work) is the maximum take-off gross weight: once the vehicle has been sized to this weight, this value is considered fixed (or frozen). Therefore, it may decrease but it may not increase. This is why range is also a constraint.

Select Design and Margin Space

The design and margin variables are selected to be similar to the ones used in the baseline method [23]. They are described in Table 45. These variables (along with all the variables included in the formulation) are included in Figure 85.

Note that the wing design space could have been much greater but has been simplified for this process. Though the number of variables vastly increases as the level of fidelity increases, the overall impact of a single variable diminishes. Therefore the most influential

Table 46: Case Study Formulation: Constraint Variables

Vehicle-Level Constraint	Value	Units
Span	215	ft
Range	7,530	nmi
Take-off Field Length	11,000	ft
Approach Velocity	140	ft/sec
Wing-Level Constraint	Value	Units
Max Tip Deflection/Span	0.30	-
Min Tip Deflection/Span	-0.20	-
Max Von Mises Stress	15,395	psi
Root Bending Moment	8,000,000	ft-lbs
Span Efficiency	0.60	-

variables have been selected.

Define Constraint Values and Failure Modes at Vehicle- and Wing-Levels

Constraints will be enforced at both the vehicle- and wing-levels. They are summarized in Table 46. Both FLOPS and Nastran will size the design to satisfy the sizing criteria (range for FLOPS, stress for Nastran). The sizing constraints (range and stress) need to be re-evaluated post-sizing (after uncertainty has been realized and/or mitigation has been applied).

The tip deflection constraint has been normalized against span. For example, a wing with span 200 feet will satisfy the constraint value of 30% if it has a tip deflection constraint of 60 feet or less. This allows wings with greater span to have greater tip deflection.

The Von Mises stress was calculated using the component strengths of aluminum as described in Table 47 and Equation 40.

$$\sigma_v = \sqrt{\frac{(\sigma_1 - \sigma_2)^2 + (\sigma_2 - \sigma_3)^2 + (\sigma_3 - \sigma_1)^2}{2}} \tag{40}$$

Table 47: Case Study Formulation: Aluminum Strength Characteristics

Strength	Value (psi)
Tensile	47,000
Compression	43,000
Shear	30,000

Table 48: Case Study Formulation: Load Case Conditions

Case	Type	Load Factor	Mach	Altitude	Static Margin
1	Pull-up	2.5	0.88	35,000 ft	0.1
2	Push-down	-1	0.88	35,000 ft	0.1

Describe Wing-Level Load Cases and Conditions

As described in Section 2.2.3, there are various types of load cases an aircraft will undergo. For this work, we only need to demonstrate their importance, so we will select two of the most common: a pull-up maneuver and a push-down maneuver. The conditions of each maneuver are defined in Table 48.

Formulation Summary

Here we include additional information about the formulation for the sake of clarity. The formulation is quite large, so it has been decomposed in a number of different ways. Table 49 shows all the variables by their type: design, margin, uncertainty, mitigation, constraint, intermediate, and objective.

Because we are using two separate design environments, a new category of variable has been created, termed "intermediate." This type are the "go-betweens" of the two environments. For example, in this formulation, the intermediate variables are wing skin weight, wing ribs and spars weight, span efficiency, take-off gross weight, and wing area. Span efficiency is actually double-counted because it is intermediate during the structural wing weight convergence and also intermediate during uncertainty analysis. To make this clear,

Table 49: Case Study Formulation: Variable by Type

Type	Vehicle	Wing	Total (Unique)
Design	7	4	9
Margin	2	1	3
Uncertainty	4	6	10
Mitigation	0	2	2
Constraints	4	5	9
Intermediate	6	6	6
Objectives	2	0	2
Total	25	24	41

Table 50: Case Study Formulation: Variable by Model Usage

Model	Quantity
EDS Inputs	19
EDS Outputs	7
RADE Inputs	7
RADE Outputs	9
Total	42

it has been repeated in Figure 85 as both “e” in the Sizing & Synthesis step and “ue” in the Wing Analysis step.

The intermediate variables are also the bridge variables. They complicate the enumeration of variables because they are double-counted: they are outputs of one environment and inputs to the other. This also means that they are inputs to some surrogate equations and outputs of other surrogate equations, as described by Tables 50 and 51. Aspect ratio and sweep are double-counted inputs because they are inputs to the vehicle-level environment as well as the wing-level environment.

While the uncertainty and mitigation variables are yet to be defined, here we include a comprehensive variable listing, detailing the name, symbol, units, type, surrogate ranges (if applicable), and usage of each variable in Figure 85.

Table 51: Case Study Formulation: Variable by Surrogate Usage

Variable	Quantity
Inputs	26
Outputs	16
Total	42

Step	Category	Name	Symbol	Units	Type	Surrogate Ranges		Determined by:	Input to:
Sizing & Synthesis	Vehicle Design	Aspect Ratio	AR	-	Design	8	11	DoE Table	EDS, RADE
		Sweep	Λ	Degrees	Design	33	40	DoE Table	EDS, RADE
		Thrust-to-Weight Ratio	TWR	-	Design	0.26	0.35	DoE Table	EDS
		Wing Loading	WSR	-	Design	128	137	DoE Table	EDS
		Fan Pressure Ratio	FPR	-	Design	1.5	1.75	DoE Table	EDS
		HPC Pressure Ratio	HPCPR	-	Design	18	23	DoE Table	EDS
		Lapse Rate	LR	-	Design	0.18	0.22	DoE Table	EDS
	Vehicle Margin	Drag Margin	FCDSUB	%	Margin	0	0.03	DoE Table	EDS
		Empty Weight Margin	EWMARG	%	Margin	0.94	0.98	DoE Table	EDS
	Structural Wing Weight Convergence	Wing Weight, Bending Material	FRWI1	lbs	Intermediate	10000	95000	Weight Convergence FPI	EDS
		Wing Weight, Spars and Ribs	FRWI2	lbs	Intermediate	2000	11000	Weight Convergence FPI	EDS
		Span Efficiency	e	-	Intermediate	0.6	1	Weight Convergence FPI	EDS
	Vehicle-to-Wing Intermediate	Takeoff Gross Weight	TOGW	lbs	Intermediate	500000	900000	EDS	RADE
		Wing Area	S	ft^2	Intermediate	3000	6000	EDS	RADE
Wing Analysis	Wing Design	Rib Spacing	RS	in	Design	25	35	DoE Table	RADE
		Wing Twist Linear Slope	TwistSlope	Degrees	Design	-0.6	-0.2	DoE Table	RADE
	Wing Margin	Knockdown Factor	KDF	-	Margin	0.01	0.2	DoE Table	RADE
	Wing Uncertainty	Wing Weight, Bending Material	uFRWI1	%	Uncertainty	10000	95000	Sample Distribution	EDS
		Wing Weight, Spars and Ribs	uFRWI2	%	Uncertainty	2000	11000	Sample Distribution	EDS
		2.5G Tip Deflection	uTDmax	%	Uncertainty	-	-	Sample Distribution	Reliability Analysis
		-1.0 Tip Deflection	uTDmin	%	Uncertainty	-	-	Sample Distribution	Reliability Analysis
		Max Von Mises Stress	uVM	%	Uncertainty	-	-	Sample Distribution	Reliability Analysis
		Root Bending Moment	uRBM	%	Uncertainty	-	-	Sample Distribution	Reliability Analysis
	Wing Mitigation Actions	Linear Delta Wing Twist	mTwist	Degrees	Mitigation	-0.2	0.2	Sample Distribution	RADE
		Delta Wing Twist Section	mSect	-	Mitigation	6	12	Sample Distribution	RADE
	Wing Constraints	Root Bending Moment	gRBM		Constraint	-	-	RADE	Reliability Analysis
		Maximum von Mises Stress	gVM	psi	Constraint	-	-	RADE	Reliability Analysis
		Max Tip Deflection	gTDx	in	Constraint	-	-	RADE	Reliability Analysis
		Min Tip Deflection	gTDn	in	Constraint	-	-	RADE	Reliability Analysis
		Span Efficiency	ge	-	Constraint	-	-	RADE	Reliability Analysis
	Wing-to-Vehicle Intermediate	Span Efficiency	ue	-	Intermediate	0.6	1	RADE	EDS
Performance Analysis	Vehicle Uncertainty	Engine Uncertainty, Fuel Flow	uFACT	%	Uncertainty	1	1.05	Sample Distribution	EDS
		Engine Uncertainty, Weight	uWeng	%	Uncertainty	1	1.05	Sample Distribution	EDS
		Fuselage, Weight	uFRFU	%	Uncertainty	1	1.05	Sample Distribution	EDS
		Vehicle, Parasitic Drag	uFCDO	%	Uncertainty	1	1.05	Sample Distribution	EDS
	Vehicle Constraints	Range at MTOW	Range	nmi	Constraint	-	-	EDS	Reliability Analysis
		Take-off Field Length	TOFL	ft	Constraint	-	-	EDS	Reliability Analysis
		Span	Span	ft	Constraint	-	-	EDS	Reliability Analysis
		Approach Velocity	Vapp	ft/s	Constraint	-	-	EDS	Reliability Analysis
	Objective	Reliability	Rel	-	Objective	-	-	Reliability Analysis	Optimizer
		Block Fuel for Economic Mission	Bfecon	lbs	Objective	-	-	EDS	Optimizer

Figure 85: Case Study Complete List of Variables

8.2.3 Step 3: Define and Model Mitigation Actions

Generate List of Physics Design Changes That Will Affect Constraints

We now need to brainstorm which design changes could be implemented that affect the constraints given in Table 46. For the vehicle-level constraints, some actions are given in the baseline method. These are summarized in Table 52.

We generate a list of potential wing actions from scratch. Of course, we include the historical example of outboard wing twist. While outboard wing twist was not selected to affect span efficiency (and also stress), it will have the secondary effects of doing so (see figures from Section 5.2.

Table 52: Case Study Formulation: List of Potential Vehicle-Level Mitigation Actions

Design Change	Constraint Affected
Additional Take-off Gross Weight	Range
Throttle Push	Take-off Field Length
Advanced High-Lift Device	Approach Velocity

Table 53: Case Study Formulation: List of Potential Wing-Level Mitigation Actions

Design Change	Constraint Affected
Wing Twist	Tip Deflection, Span Efficiency
Increase Component Thickness	Von Mises Stress
Composite Materials	Wing Weight
Adding a Component	Wing Stiffness, Induced Twist

Considering the stress constraint, there are two main factors: force and area. Decreasing the force or increasing the area would decrease the stress. Consequently a straightforward mitigation action would be to increase the component or part thickness that is under maximum stress. This is much less complicated than addressing the force distribution along the wing components.

The last constraint is root bending moment. This constraint will be affected some by the outboard wing twist, but the main factor is actually take-off gross weight. This is because there is not a take-off gross weight constraint on the vehicle level. As a result, the magnitudes vary wildly across the design and margin space (especially between minimum and maximum margin). Therefore the most effective mitigation would be to decrease weight, either on the vehicle-level or wing-level. A way to decrease weight is to use a composite material rather than a metallic material.

Model Selected Actions within FEM Environment

The details of this section are largely covered in Section 5.2. Keeping in accordance with the historical account, we would like to use outboard wing twist as our mitigation actions.

We would also like to isolate the effect of wing-level mitigation on the overall optimization process. Therefore, it will be the only mitigation action included in this formulation.

Test for Mitigation-Constraint Dependence

Refer to Figures 43 and 44 for the sensitivity analysis of the mitigation actions.

8.2.4 Step 4: Characterize Uncertainty

Refer to Research Question 2 in Chapter 6 for greater detail into this process.

To recap, a uncertainty taxonomy was developed to determine the most relevant sources of uncertainty. For this problem, model uncertainty was declared the most significant as the two sources of knowledge for this method are models. Within model uncertainty we selected discretization error because the physics-based model is based on mesh size. To characterize the uncertainty we used Richardson's Extrapolation Method and a mesh size sensitivity to determine mesh size dependence. The design space was then sampled to generate a distribution of errors for each output. These distributions were fit to parametric distributions and tested for correlation. Because correlations existed with 95% confidence, a t copula was fit using the parametric distributions. Accounting the for correlation is important because, as demonstrated by Experiment 2.3d in Section 6.2.6, the independence assumption underestimates compliance.

8.2.5 Step 5: Determine Vehicle- and Wing-Level Design Point

Determine Bridge Variables between Environments

These values are different on the vehicle-level than the notional Boeing 777-200ER wing. Therefore, a process is needed to match the two such that the final design matches the notional Boeing 777-200ER mission at the designated take-off gross weight. This process is outlined in Figure 86.

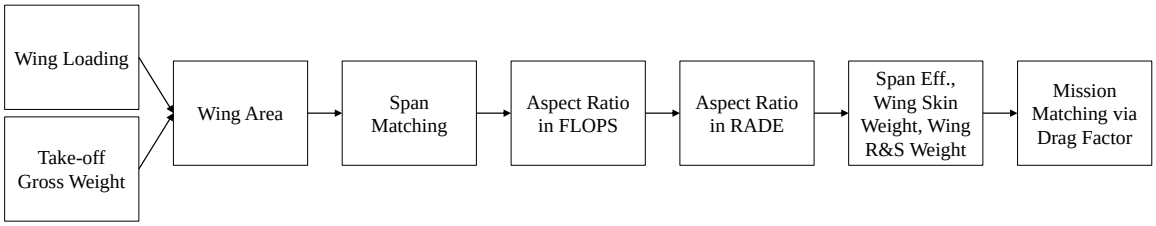

Figure 86: Resolving Vehicle and Wing Input Configuration

Translate Common Input Variable Definitions

Because the wing loading and the take-off gross weight are defined by the Boeing 777-200ER, the wing area is already known.

$$WingArea = \frac{Take - Off\ Gross\ Weight}{Wing\ Loading} = \frac{657,000\ lbs}{133.34\ lbs/ft^2} = 4927.29 ft^2 \tag{41}$$

The new wing can be scaled via VSP to fit the new wing area. The resulting span is 203.58 ft. Unfortunately the two environments define aspect ratio differently. RADE uses VSP which defines aspect ratio traditionally with Equation 25 defined in Section 7.2. FLOPS, on the other hand, takes into account the glove area of the wing:

$$Aspect\ Ratio_{FLOPS} = \frac{Span^2}{(Wing\ Area) * (1 - PGLOV)} \tag{42}$$

where PGLOV is the percent of the wing area devoted to the glove area. Therefore, aspect ratio is calculated only using the non-glove wing area. This will need to be taken into account when translating between the two models. Combining Equations 25 and 42 yields:

$$Aspect\ Ratio_{FLOPS} = AspectRatio_{VSP} * (1 - PGLOV) \tag{43}$$

So, the next step is determining this "PGLOV" value. The aspect ratio of the CRM wing was given in the VSP model as 8.411. The Boeing 777-200ER-like wing had an

Table 54: FLOPS Settings to Verify Aspect Ratio

IRW	MYWTS	GW	PGLOV	SW	FIXSPN
2	1	657,000 lbs	0.08644	4,927.29 ft^2	203.58 ft

aspect ratio of 9.207. This would result in a PGLOV value of 0.08644.

We would like to test this relationship another way. We can ensure congruency by running FLOPS in "analysis" mode (i.e. non-sizing mode). The settings in FLOPS are changed to the values shown in Table 54.

IRW changes FLOPS from sizing to analysis. MYWTS sets the weight of the vehicle to be an input rather than output (GW, or take-off gross weight, is set to 657,000 pounds). SW is the wing area which has been fixed to 4,927.29 square feet as defined by Equation 41. Finally, the span was fixed using FIXSPN to the scaled value in VSP which is 203.58 feet.

When running in this mode, FLOPS outputs an aspect ratio of exactly 9.207, a span of 203.58 feet, and a wing area of 4927.29 square feet. This shows the relation in Equation 43 was correct.

Evaluate Both Environments at Design Point

Initial values for the bridge variables need to be determined. This can only be done be evaluating each model once. Due to the nature of our problem formulation, though, we need only evaluate the wing-level environment. This is because we are trying to match a known take-off gross weight of 657,000 pounds.

For a complete connection, more bridge variables could be included that connect from the vehicle-level environment to the wing-level environment. These variables are fuel weight and engine weight. They cannot be know beforehand and would therefore require an execution of the vehicle-level environment (though ultimately determined by the structural wing weight convergence). They have been excluded here because during initial testing

Table 55: RADE Environment Sing-Pass at Design Point

Wing Skin Weight	Wing Ribs and Spars Weight	Span Efficiency
44,686 lbs	3,207 lbs	0.77

Table 56: Mission Take-off Gross Weight Matching via Drag Factor

Drag Factor	Take-off Gross Weight
0.9	637,181 lbs
0.91	641,801 lbs
0.92	646,592 lbs
0.93	651,207 lbs
0.94	656,066 lbs
0.95	661,021 lbs
0.94186	657,000 lbs

they did not show to have a significant impact on the wing-level results. It is not that these values do not matter; indeed, they are required for execution of RADE. They are excluded because their range of values is insufficient to measurably affect the results. In other words, the engine weight does not vary enough to warrant its inclusion into the problem formulation.

Executing the RADE environment at the design point yields the results given in Table 55. The wing component weights are determined using the jig shape and sizing determination while the span efficiency is taken from the flight shape.

Calibrate Drag Factor to Match Take-Off Gross Weight

The last factor to be determine is the drag factor FCDSUB. We use it as a fudge factor the match the mission to the take-off gross weight by performing a simple interpolation. The results are given in Table 56.

This concludes the process of matching the vehicle- and wing-level design point. The numerical results are summarized in Figure 87. The final design point is fully described

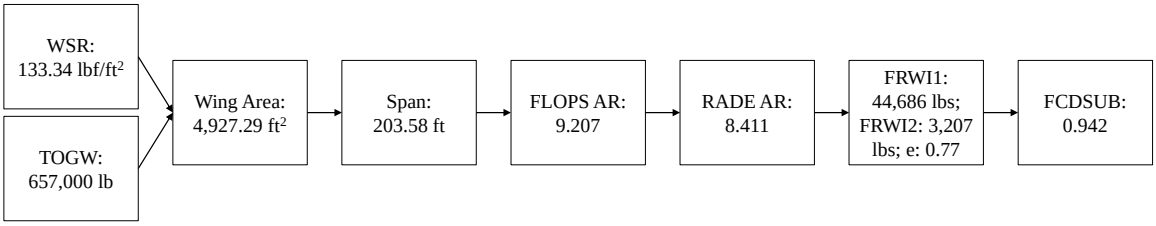

Figure 87: Resolved Vehicle and Wing Input Configuration

Table 57: Final Design Point

Range	Payload	TWR	WSR	TO Thrust	TOC Thrust
7,530 nmi	64,050 lbs	0.296	133.34	78,400 lbs	19,600 lbs
FPR	HPCPR	Mach	Altitude	EWMARG	FCDSUB
1.58	20.03	0.84	35,000 ft	0.00	0.942
AR_{FLOPS}	AR_{VSP}	Sweep	Rib Spacing	KDF	Twist
9.207	8.411	37°	30 in	0.10	-0.5°

(on both levels) in Table 57.

Demonstrating Design Point Congruency: Structural Wing Weight Convergence

We can quickly check the results to make sure that our design point is congruent in both environments by showing that the structural wing weight convergence, which takes into account both environments, will indeed converge on a value almost identical to the initial value. The results of the convergence are given in Figures 88 and 89.

While the convergence requires three iterations, we can see from the y-axis in Figure 88b that the final result is not far from the initial guess. The target take-off gross weight is 657,000 pounds, but the convergence shows about 660,100 pounds. This is an error of about 0.47% which is introduced by the use of the surrogate models. The FLOPS initial guess of take-off gross weight was 661,000 pounds. So, the difference between the final value and the initial value is less than 1,000 pounds, or 0.13%. Therefore, we can conclude that we have found a design point that will approximately yield the same result between the two environments.

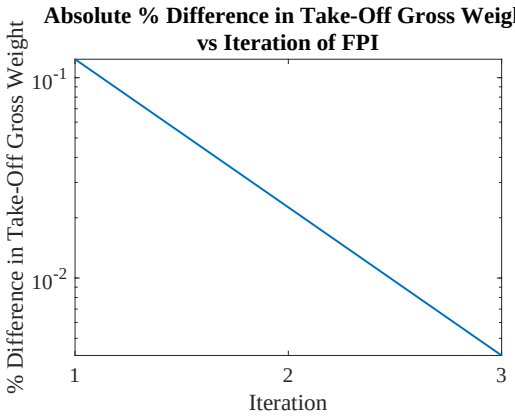

(a) Absolute Difference between EDS and RADE TOGW Estimations vs Iteration of FPI, %

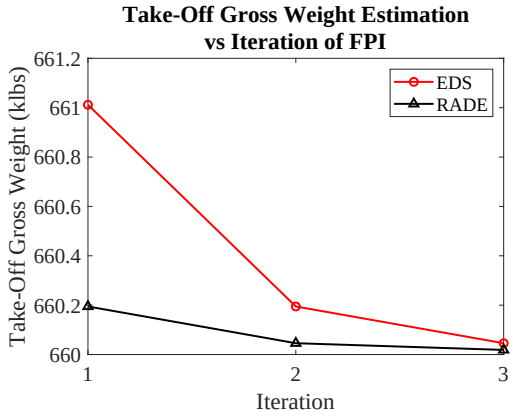

(b) EDS and RADE TOGW Convergence vs Iteration of FPI, %

Figure 88: Case Study Take-off Gross Weight Convergence at Design Point

Figures 89a and 89b show similar trends. The values vary throughout the convergence, but the y-axes show that the variation is small. The largest change is with respect to the ribs and spars weight, which changes about 140 pounds or about 4%. This is the largest change but will have the smallest effect because the magnitude of the ribs and spars weight is small compared to the bending material weight.

8.2.6 Step 6: Generate Surrogate Models

To perform optimization the behavior of the environments need to be captured by surrogate models for faster estimation. A surrogate is a representative model that performs similarly to the actual model within a defined space. The advantage of using surrogate models is a vastly decreased execution time (especially for the physics-based model).

Determine List of Input, Output, and Intermediate Variables and Associated Ranges

Figure 85 already described all the variables used in this case study as well as their ranges for the design of experiments. Each type of variable (design, margin, uncertainty, mitigation) and their ranges are included in Tables 58 and 59. The design and margin variables affect sizing whereas the uncertainty and mitigation variables do not.

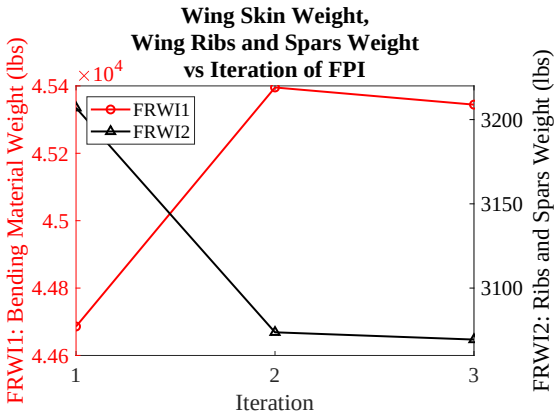

(a) Bending Material and Ribs and Spars Weight vs Iteration of FPI

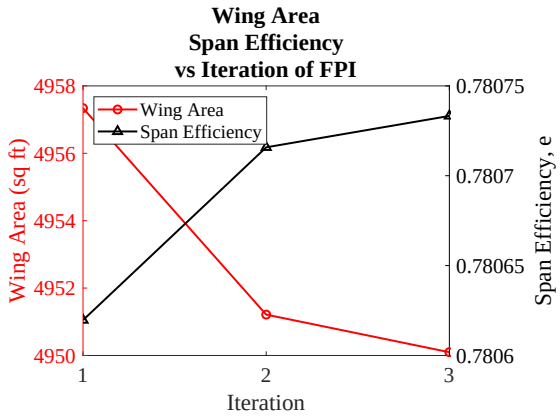

(b) Wing Area and Span Efficiency Convergence vs Iteration of FPI

Figure 89: Case Study Wing Weights, Area, and Span Efficiency at Design Point

Table 58: EDS Environment Surrogate Ranges: Sizing Variables

Variable	Thrust-to-Weight	Wing Loading	Fan Pressure Ratio	HPC Pressure Ratio	TOC Thrust
Min	0.26	128	1.5	18	17,000
Max	0.35	137	1.75	23	22,000
Variable	Empty Weight Margin	Drag Margin	Wing Skin Weight	Ribs and Spars Weight	Span Efficiency
Min	0	0.94	10,000	2,000	0.6
Max	0.03	0.98	95,000	11,000	1

The uncertainties in the vehicle-level were inspired by the baseline method but are not exactly the same. There are two weight uncertainties (fuselage and engine). The idea is that those disciplines performed their own physics-based analysis and returned different values than expected (in a similar process that was done with the wing). To capture this process multipliers have been added to their respective weights, up to 5%. The profile drag was selected rather than total drag because RADE is using AVL to approximate induced drag. Adding a factor on induced drag would require a connection to RADE. Finally fuel flow is used as another engine-level uncertainty representing the difference between estimated and actual fuel consumption of the engine at the required thrust.

Table 59: EDS Environment Surrogate Modeling Ranges: Post-Sizing Variables

Variable	Profile Drag	Fuel Flow	Fuselage Weight	Engine Weight
Min	1	1	1	1
Max	1.05	1.05	1.05	1.05
Variable	Span Efficiency	Engine Throttle	Wing Skin Weight	Ribs and Spars Weight
Min	0.6	0.99	10,000	2,000
Max	1	1.05	95,000	11,000

Table 60: RADE Environment Surrogate Modeling Ranges: Sizing Variables

Variable	Wing Area	Take-off Weight	Aspect Ratio	Sweep
Min	3,000	500,000	8	33
Max	6,000	900,000	11	40
Variable	Rib Spacing	Knockdown Factor	Twist Slope	
Min	20	0.01	-0.2°	
Max	35	0.2	-0.6°	

The EDS environment was evaluated first to determine how the outputs are distributed (namely, take-off gross weight). This range of values was used to determine the range of inputs to the RADE environment.

Build Design of Experiments and Run Cases

A design of experiments is used to extract the most amount of information with the least amount of computational effort. A space filling design (Latin Hypercube) was used for both

Table 61: RADE Environment Surrogate Modeling Ranges: Post-Sizing Variables

Variable	Wing Twist	Wing Section
Min	-0.2	6
Max	0.2	12

Table 62: Design of Experiments: Vehicle- and Wing-Level Summaries

Level	Design of Experiments	Finished Cases
Vehicle-Level	Latin Hypercube	166
Wing-Level	Latin Hypercube, Random	126

environments. There was not a design of experiments used for the boundaries or corners of the variable space (such as central composite) because these points tend to fail. For example, consider a design with the lowest wing area, lowest aspect ratios, highest washout, and highest take-off gross weight. The angle-of-attack required to match lift to weight would be incredibly high. Usually the case fails or the span efficiency is tremendously low.

For the design of experiments, 10 cases were counted for each variable, which is standard for Latin Hypercube designs. So, the vehicle-level design was 190 case. The wing-level environment was estimated to be more difficult to represent, so 20 cases per variable were counted for each variable (140 total). The number of failures was much higher for the wing-level environment so additional random cases were run. A summary of the design of experiments can be found in Table 62.

Check Goodness of Fit Metrics for Surrogate Equations

Feed-forward neural networks were used as the surrogate models. The topologies differ between the environments. Because FLOPS is based on historical regressions, we assume that the neural network topology does not need to be complex. Hence, the vehicle-level surrogates were fit using a single hidden layer of five nodes. The wing-level environment surrogates were fit using two hidden layers with five nodes in the first hidden layer and ten nodes in the second hidden layer. Both networks used hyperbolic tangent as the activation

Table 63: Surrogate Equations Goodness of Fit: Vehicle-Level Environment

Variable	Validation RMSE	Validation R^2
Economic Block Fuel	4,574	0.97
Take-off Gross Weight	8,000	0.98
Take-off Field Length	560	0.89
Range	107	0.99
Approach Velocity	0.33	0.99
Span	0.99	0.99

Table 64: Surrogate Equations Goodness of Fit: Wing-Level Environment

Variable	Validation RMSE	Validation R^2
Skin Weight	2,214	0.99
Ribs and Spars	103	0.96
SWW Span Eff.	0.02	0.98
Design Span Eff.	0.03	0.97
Max TD	22.78	0.95
Min TD	1.75	0.97
Max VM	504	0.89
RBM	387,602	0.97

function. A summary of the goodness of fit metrics is given in Table 63 for the vehicle-level surrogates and Table 64 for the wing-level surrogates. Detailed information about each variable's goodness of fit can be found in the appendix in Chapter B.

8.2.7 Step 7: Perform Optimization

Now that the variables are defined and the surrogates have been fit, we may proceed to the optimization.

Select Optimization Algorithm

Many optimization algorithms exist that can perform this optimization. We are using both continuous variables and discrete variables (wing section can only be integer values). The optimization terminology uses "design" variable to refer to the variable or variables that

the algorithm varies to find an optimum. This clashes with the terminology we have developed: here, design variable means sizing variable, which are the design and margin variable spaces. Note that the final result is a unique set of design and margin variables. The uncertainty and the mitigation are used in the process but they are not designs but rather conditions applied to the designs. Therefore, the final result will be a unique set of design (wing loading, aspect ratio, sweep, etc.) and margin (empty weight, drag, etc.) variable values.

A genetic algorithm is selected because it was shown to perform well for the baseline method. It is straightforward and built-in to MATLAB which was the environment used for this optimization. It can also handle more than one objective metric.

Uncertainty Sampling Method

As described in Section 4.2.2, a Monte Carlo approach will be used as the sampling method for the uncertainty. The sampling approach allows us to analyze the uncertainty conditions as possible future states and perform scenario analysis on each (apply a series of mitigation strategies to a single future state). Predefining a copula allows to sample it directly at the onset of the optimization process such that the correlations are included without any changes to the process itself. Changing between independent and dependent sampling is simply changing between sampling the copula or sampling each parametric distribution individually.

A Note on Computational Expense

The baseline method was able to use 10,000 uncertainty samples. This method will only allow for 1,000 due to computational expense. The reason is due to the increase caused by the trend discussed in Section 7.2. When the probability of compliance of a given design was zero for the baseline method, the design failed a constraint deterministically (such as span). Because no mitigation was available to address the span constraint, there was no

need to apply a mitigation assessment. This saved computation time: 10,000 uncertainty conditions did not need to be evaluated with mitigation for each. For this work, however, mitigation *does* affect some of the deterministic constraints (e.g. tip deflection). Consequently, in the case that a design fails a tip deflection constraint, every one of the possible future states would fail, but these scenarios will still need to undergo a mitigation assessment. Furthermore, the baseline method required a level of compliance to be 70%. This further decreases the load of mitigation assessment and therefore computation time. That condition is not enforced in this thesis because of the deterministic wing-level constraints.

Report Out Pareto Front of Performance and Reliability

The optimization was run for 1,000 uncertainty points, 1,000 mitigation strategies, 200 individuals, and 250 generations. A fuller optimization (with more uncertainty and mitigation) will be provided in Section 8.4.

All the designs recorded during the optimization are filtered in a Pareto Front filter such that only the dominant designs remain. A design is dominant if it is better in some way than every other point (see Section 7.2.3). While the Front can be n-dimensional, the objective space is only two dimensional (reliability and economic block fuel). The Pareto Front results of the optimization are given in Figures 90, 93, 94, and 95.

Two populations described by Figure 90 are illuminated. The first cluster (or population in genetic algorithm terms) is characterized by low compliance, high recovery, and a wide range of reliability. The second cluster is characterized by high compliance, low recovery, and highest reliability.

It may seem peculiar that the majority of the Pareto Front relies on mitigation to be reliable. This result is caused by two sources. The first and more obvious source is that mitigation is not accompanied by a performance penalty. Therefore, the better performing designs will prefer to rely on mitigation rather than margin. The second source is that the decision-making criteria are based on the technical aspects of margin and mitigation. The

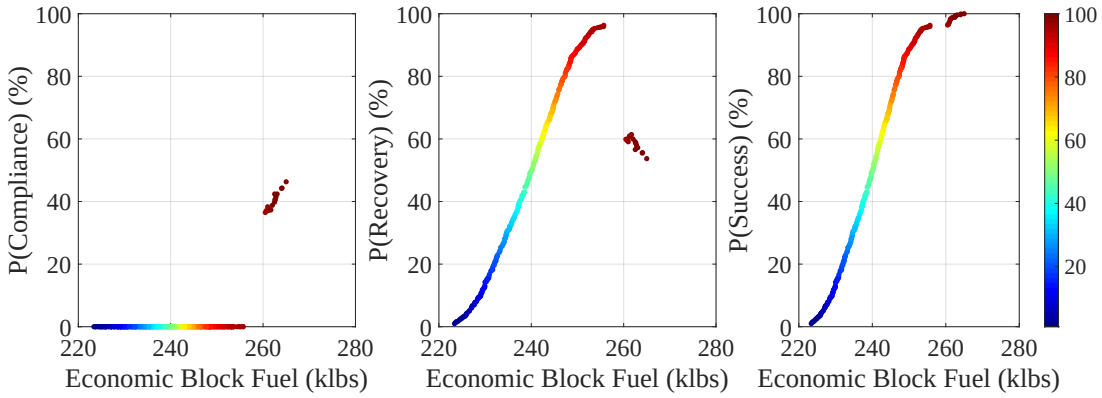

Figure 90: Pareto Front Design Points in Objective Space

largest aspect of mitigation that was neglected was the programmatic delay caused by the constraint violation. Mitigation is expensive and stressful. The program must be delayed to determine which constraint was failed and by how much. Then, a design change must be determined and to what extent. After the change is made, the design is re-tested to ensure constraint satisfaction. This entire process is foregone if the design is compliant. Because this aspect of mitigation is ignored, mitigation is preferred over margin.

The two clusters are highlighted in Figure 91.

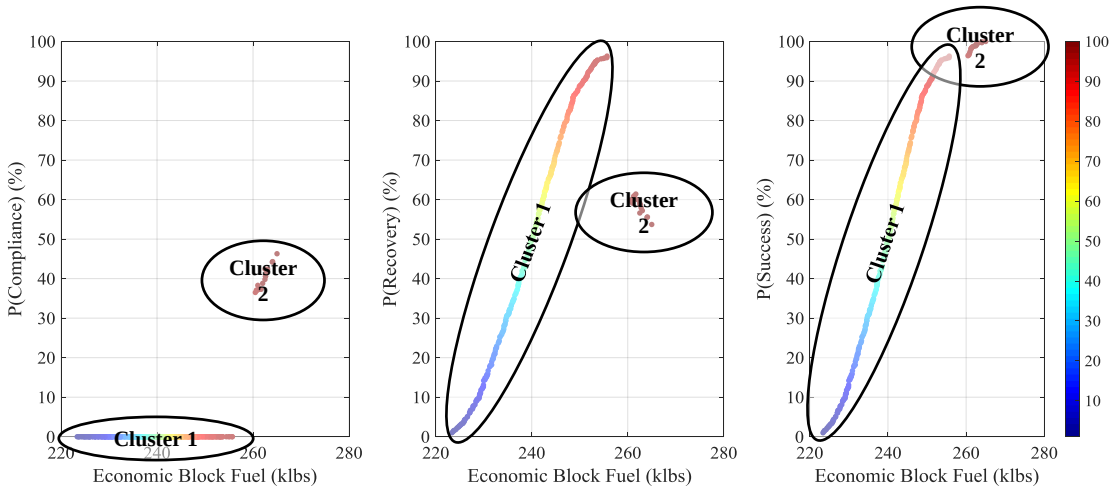

Figure 91: Pareto Front Design Points in Objective Space with Cluster Designation

Due to the cost of redesign, designers may only consider possibilities with a high level of reliability. Therefore the central focus of the Pareto Front would be, say, between 90%

and 100% reliability (as shown in Figure 92). Recall that 100% less the reliability is equal to the probability of failure, or redesign. Thus, if a design has a reliability of 95%, then it has a 5% chance of redesign. Isolating the Front between 90% ad 100% assumes the designers have a appetite for probability of failure up to 10%.

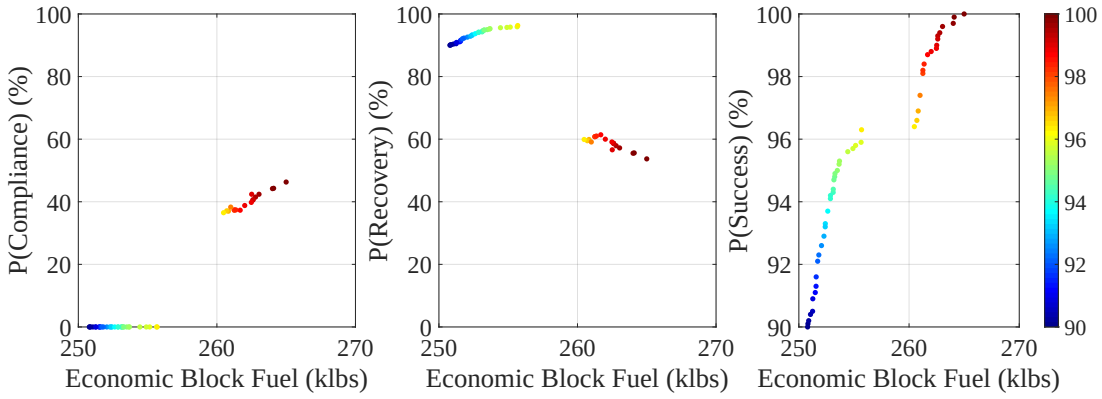

Figure 92: Pareto Front Design Points in Objective Space with At Least 90% Reliability

The discontinuity in this regime of reliability accentuates the distinction between the two clusters. The highest reliability designs (Cluster 2) accounts for the Front above 96% reliability. This jump occurs at about 5,000 pounds between economic block fuel estimates. Cluster 1, which relies heavily on recovery, can only get so high in probability of success: if the management elects to choose from the most reliable designs, then a drop in performance is expected.

It is also important to note that reliability cannot exceed 100%. Therefore, Cluster 2 has lower recovery than Cluster 1 because compliance is relatively higher. For a given probability of success, a high compliance results in a low recovery.

Now we will see if the cluster trend continues throughout the design space. The discontinuity in the objective space suggests discontinuities elsewhere. If so, management will need to make a definitive decision between a Cluster 1 design and a Cluster 2 design.

These next plots show the *design* space. Recall that for each design 1,000 uncertainty scenarios were evaluated with 1,000 possible mitigation strategies. Thus, the result of each

point is an aggregation of the uncertainty and mitigation analyses. Because each point is a design, it has a unique set of design and margin variables on the vehicle- and wing-levels. Each plot in the figures views the designs from a different lens, but the designs themselves do not change. Said another way, every point in the thrust-to-weight ratio and wing loading plot is present in the fan pressure ratio and high pressure compressor pressure ratio plot with the exact same color shade.

Figure 93 shows the dominant points in the vehicle-level design space. Clearly there are trends in the Pareto Front translate to the vehicle-level design space. The middle plot shows that the weight penalty of higher engine weight is insufficient to drive towards highest overall pressure ratios. Typically, the higher the overall pressure ratio the higher the efficiency but also the engine weight. While the left and middle plots do not show a distinction between the clusters shown in Figure 91, the margin plot (right) most certainly does. This plot suggests that Cluster 1 is hitting maximum margin for its most reliable designs. This implies that the reliability had room to improve if the margin bounds were expanded. This is not true for Cluster 2, however: it did not need the maximum levels of margin to reach the highest levels of reliability.

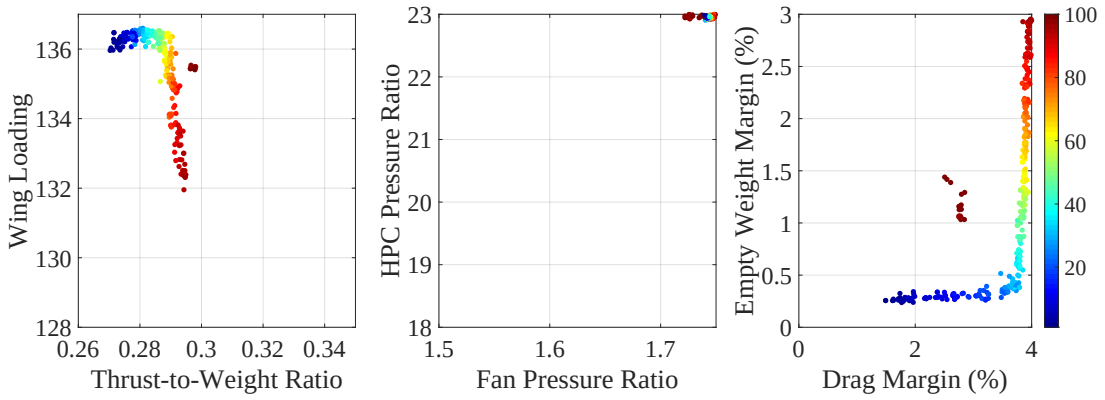

Figure 93: Pareto Front Design Points in Vehicle Space with Reliability

This is an interesting trend that supports the conclusions of Research Question 3.2 in Section 7.2.2: *the most reliable designs do not have the highest margin*. Cluster 2 (the most

reliable designs) are not characterized by larger margin. Margin is not the characteristic which gives it the increase in reliability: it is the design space. This result is counter-intuitive because we know that margin is inversely related with performance. The worst-performing designs along the Pareto Front should have the highest margin, but they do not. Cluster 1 does exhibit this trend, however: its worst-performing designs *do* have the highest margin but lowest levels of compliance

If this observation holds true, then in the wing-level design space there should be two distinct clusters. We expect this because the mitigation is on the wing-level (and is used to overcome deterministic constraints). Figure 94 focuses on the wing dimensions of aspect ratio and sweep. Clearly, lower sweep values are preferable across the entire Front. This is most likely due to the trend shown in Table 36 that lower sweep values decrease tip deflection. The highest aspect ratio along the Pareto Front is less than 9.5, meaning that half of the aspect ratio range is infeasible.

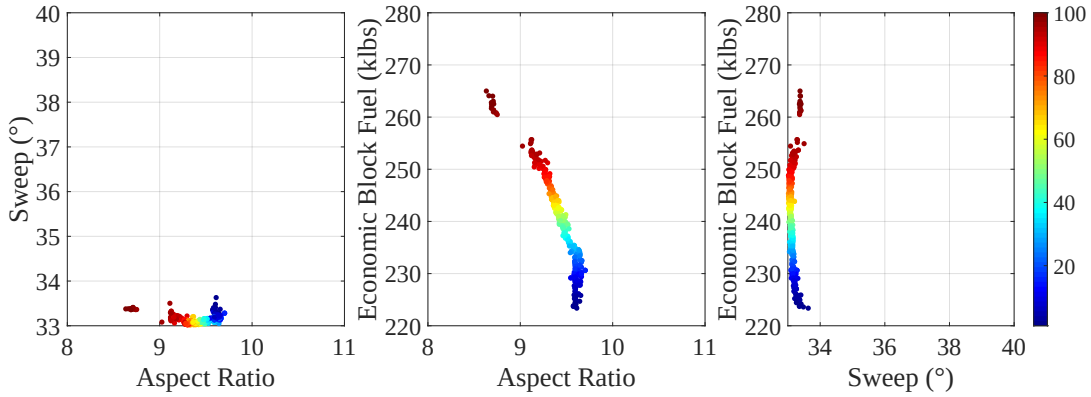

Figure 94: Pareto Front Design Points in Aspect Ratio and Sweep Spaces with Performance Objective

Still, the two clusters are present. Further, Cluster 2 (the more reliable cluster denoted by the darkest red color) is at lower aspect ratios. This will lead to decreased performance but also to feasibility with respect to the wing-level deterministic constraints.

Figure 95 *again* shows two main clusters along the Pareto Front.

This is a new finding that has not yet been reported. The two-cluster phenomena is

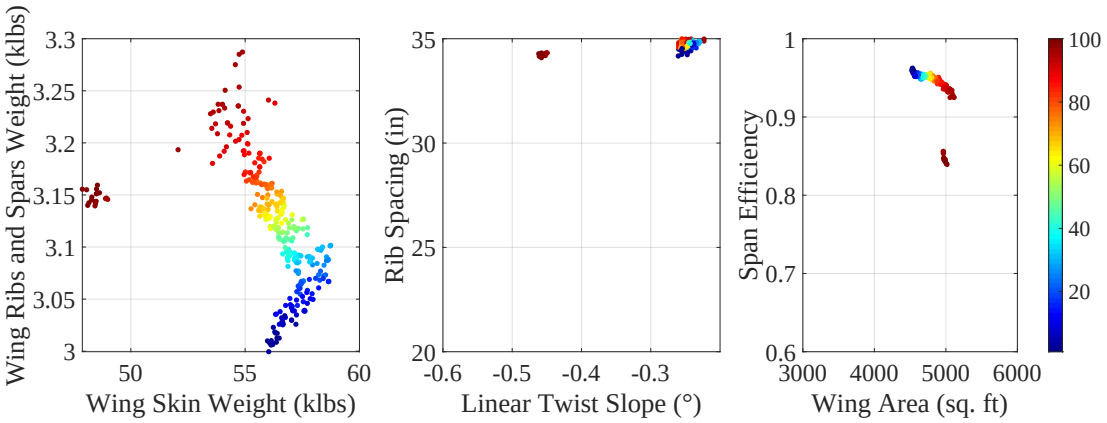

Figure 95: Pareto Front Design Points in Wing Space with Reliability

Table 65: Comparison of Pareto Front Clusters

Variable	Cluster 1 (Performance)	Cluster 2 (Reliability)
Margin	Low to High	Medium
Aspect Ratio	High	Low
Wing Skin Weight	Low	High
Twist Slope	High	Low
Span Efficiency	High	Low
Compliance	None	Low

summarized in Table 65. These seem to be the two areas that produce the best designs.

The impact of this finding management must make a decision up front: high reliability or high performance? Because the two clusters form in two separate design spaces, one cluster must be chosen. Within each cluster, the design and margin values vary gradually, so picking a cluster is much more consequential than picking a design. A design may be tweaked downstream, such as through a mitigation action. But, the two clusters represent very different design spaces: one cluster cannot be tweaked to fit into another cluster.

This is the value proposition Rabid Raccoons Inc. was looking for: the advanced process has brought about new insights communicate to their clients. Rather than providing a single deterministic result or even a single group of results, RRI provides two clusters of close performance and reliability. Their clients can choose one of the clusters on which to

focus, then a design within that cluster.

One final note is that the results of the case study are a direct consequence of the problem formulation. Adjusting the bounds of the uncertainty or mitigation variables or constraint values may result in a starkly different result. In other words, the two-cluster phenomenon may just be an artifact of this particular problem. In fact, with higher margin bounds, Cluster 1 would have composed the entire Pareto Front. The result do, however, reinforce the findings of Research Question 3.2 in Section 7.2 that the highest levels of reliability occur in a different *design* space rather than just the *margin* space.

8.3 Comparison between Max(P(Compliance)) and Max(P(Success))

Rabid Raccoons Inc. would like to demonstrate the power of including mitigation in the optimization process. To demonstrate their prowess, they perform a second optimization with the probability of compliance as the objective metric rather than the probability of success. This difference is the probability of recovery, or the impact of mitigation. Maximizing the compliance will not favor designs that have higher sensitivity to mitigation.

8.3.1 Optimization Formulation

The previous case study was completed to maximize the probability of success. However, the results showed a high reliance on mitigation to recover non-compliant designs rather than a balance between compliance and recovery. Due to the hidden costs of mitigation, management's current paradigm may be to still maximize for compliance rather than success. Or, mitigation may simply be considered too expensive and only used if absolutely necessary.

We would expect there to be a large difference in performance between the two optimization formulations. Because there is a much greater performance penalty to margin relative to mitigation, we expect the higher probability of compliance to result with a higher economic block fuel.

8.3.2 Results Comparison

The comparison of these two optimization formulations is analogous to the vehicle-only Pareto Front discussed in Section 7.2.3. The designs from the previous formulation have retained their shape and color. The new formulation results are designated by an unfilled hexagon. Results are given in Figures 96, 97, 98, and 99.

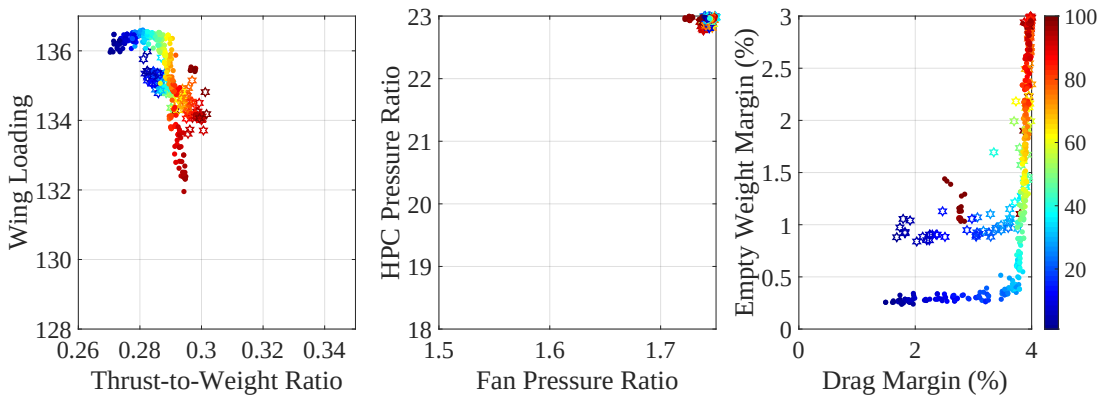

Figure 96: Pareto Front Comparison between Compliance and Success Maximizations in Vehicle Space

As expected, Figure 97 shows that the circles reach higher aspect ratios than the hexagons. The circles also have lower sweep relative to the hexagons and lower economic block fuel. Again, we expect this to be the influence of deterministically failing the tip deflection constraint.

Figure 98 shows an interesting result: the maximum probability of compliance results seem to fill the gap between Cluster 1 and Cluster 2 in the maximum probability of success results in the linear twist slope space. This is the variable which distinguished the clusters the most. Further, the maximum compliance case does not seem to show a two-cluster phenomenon.

Figure 99 shows a drastic difference in the utility of mitigation. As aforesaid, the filled circles rely heavily on mitigation to recover the non-compliant designs. The hexagons, on the other hand, does not utilize mitigation hardly at all. Still, they are able to reach about

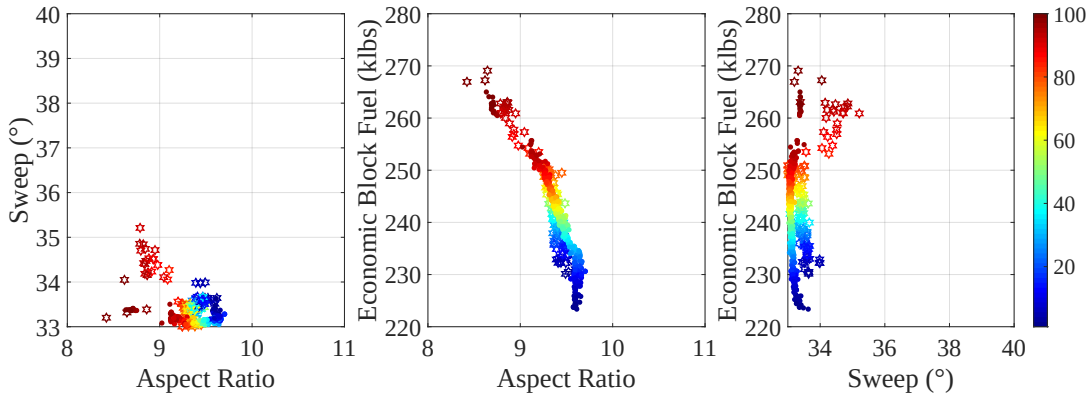

Figure 97: Pareto Front Comparison between Compliance and Success Maximizations in Aspect Ratio and Sweep Space

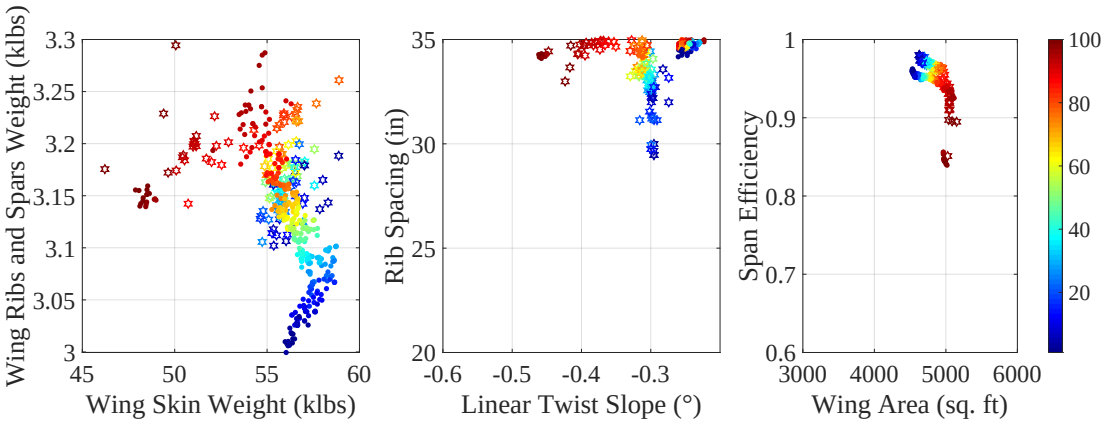

Figure 98: Pareto Front Comparison between Compliance and Success Maximizations in Wing Space

90% compliance. To reach 100% reliability, however, some mitigation is required.

This comparison may lead us to believe that maximizing compliance is actually more preferable when the program delay caused by mitigation is taken into account because the decrease in block fuel does not appear to be substantial along the Front (approximately 10,000 of economic block fuel, or about 3-4%). Further, at the highest levels of reliability, the two Pareto Fronts converge. However, the maximum compliance cases are completely Pareto dominated by the maximum success cases. Therefore, if mitigation is technically trusted and financially manageable, optimizing with it included is absolutely essential to determining the best conceptual design.

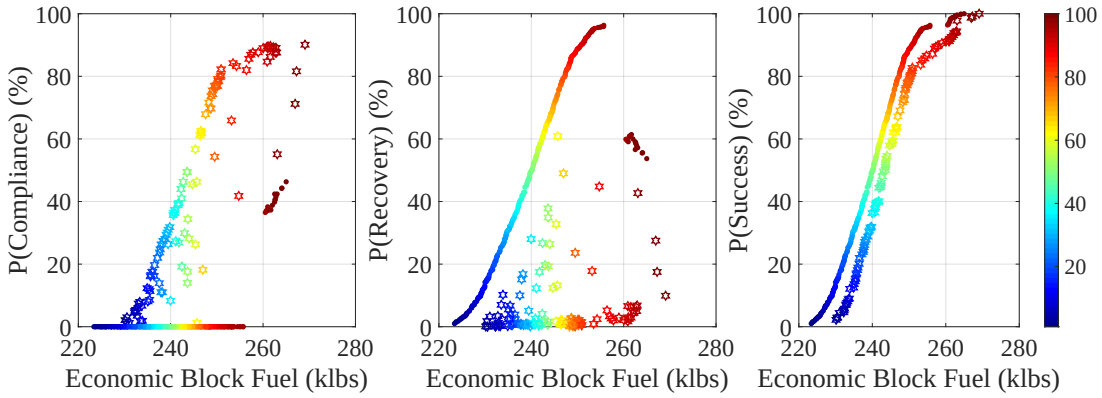

Figure 99: Pareto Front Comparison between Compliance and Success Maximizations in Objective Space

8.4 Optimization Results with Vehicle-Level Mitigation and Wing-Level Parametric Uncertainty

For the sake of fullness, we wish to finish this section with an optimization formulation complete with non-wing-level mitigation and parametric uncertainty.

Now that a bi-level conceptual design RBDO framework has been established, it can be extended to major components other than just the wing. Ideally, this process would be replicated for the engine, fuselage, and landing gear teams as well: each group would have a set of higher fidelity tools as well as sources of uncertainties, constraints, and possible mitigation actions. Everything that has been completed for the wing can be indeed be replicated for these other systems. Then, the lower-level (higher fidelity) analysis has been completed, the new information is propagated back upstream to perform a more intelligent conceptual design selection process.

While integrating these other systems is beyond the scope of this work, we can simulate this effect by using the same method that the benchmark method used (conceptual design level k-factors). The first variable that is added for the full formulation is an engine-level mitigation variable called throttle push. It increases the engine rating to cause it to run hotter to produce more thrust, which will affect any constraints that are sensitive to thrust

Table 66: RADE Environment Surrogate Modeling Ranges: Additional Variables

Variable	Throttle Push	Modulus of Elasticity	Jig Shape Displacement
Type	Mitigation	Uncertainty	Uncertainty
Min	0.99	0.95	0.9
Max	1.05	1.05	1.1

(such as take-off field length). Obviously burning the engine hotter would have operational and financial consequences, which would be an interesting study for future work.

The next two variables that are included for the final formulation are parametric uncertainty variables. Section 4.2 described the possible need to incorporate parametric uncertainty (which is essentially a sub-category to model uncertainty). A wide range of variables could be used here as the number of variables required to execute the higher fidelity analysis is high. The first parametric uncertainty variable is the modulus of elasticity for aluminum. This will affect the structural responses of the wing to loads. An increase in the modulus of elasticity will increase the stiffness of the wing (lower maximum stress, tip deflection, etc.).

The second uncertainty variable is the jig shape displacement. This is assuming there is some error either with the input aerodynamic shape or the final jig shape result. This is a parametric uncertainty because the flight shape is an input to the jig shape determination algorithm and the jig shape is an input to the constraint analysis and new flight shape determination algorithm. The variable itself is a scalar multiplied to the displacement vector between flight shape to jig shape. A positive value implies the displacement is underestimated relative to the true displacement.

To summarize, the additional variables are a throttle push, modulus of elasticity uncertainty, and jig shape uncertainty. The ranges of these variables used to develop surrogate models are recorded in Table 66. Note that an entirely new design of experiments is required, as well as re-fitting all the other surrogates to incorporate these input variables.

The throttle push will affect the take-off field length constraint, though this constraint is not affected by the uncertainty because the take-off gross weight is fixed. The modulus of elasticity will affect the tip deflection and stress constraints. The jig shape displacement uncertainty is a scalar multiplied by the six degree-of-freedom vector between the original flight shape and the final jig shape. Unlike the other uncertainty variables, the sign of this variable is not explicitly beneficial or detrimental to constraint satisfaction. A positive modulus of elasticity, on the other hand, will always move the design towards constraint satisfaction.

Figures 100, 101, 102 and 103 show the results for the full optimization; that is, vehicle-level and wing-level design, margin, uncertainty, and constraint variables. The difference between these results and the case study results is the presence of three additional variables (modulus of elasticity uncertainty, jig shape uncertainty, and throttle push, as described by Table 66). It was run for 250 generations with 200 individual (same optimization settings as prior two optimizations).

Figure 100 shows the results for the full optimization in the objective space. Clearly, the two cluster phenomenon still exists shown by the disconnect along the Pareto Front. Here, the jump occurs more towards the center of the Front (~85%) compared to before (~95%). Essentially this means that if management prefers 90% reliability or higher, the second cluster is exclusively chosen (Cluster 1 is disregarded). The performance overall is improved: the Front has shifted leftwards due to the new variables. This is most likely due to the mitigation action and positive uncertainty values of modulus of elasticity.

The highest pressure ratios are again favored, which is expected because the variables did not affect engine sizing. The vehicle-level margin plot (right) is interesting: similar trend as before, except the highest levels of margin are not utilized. This means that the reliability is not bounded by the levels of margin available.

Figure 102 shows a similar story as before: lowest levels of sweep, and lower levels of aspect ratio correlate with higher reliability. The lower levels of sweep are most likely

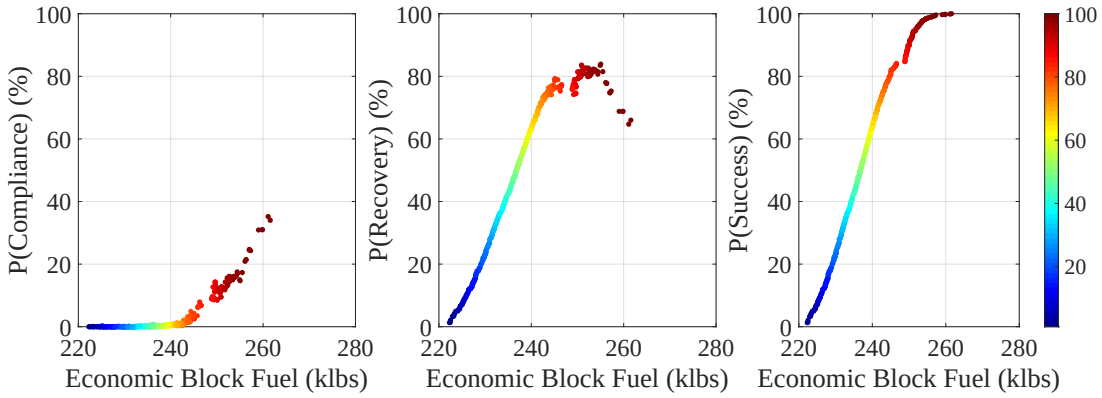

Figure 100: Full Optimization: Pareto Front Design Points in Objective Space

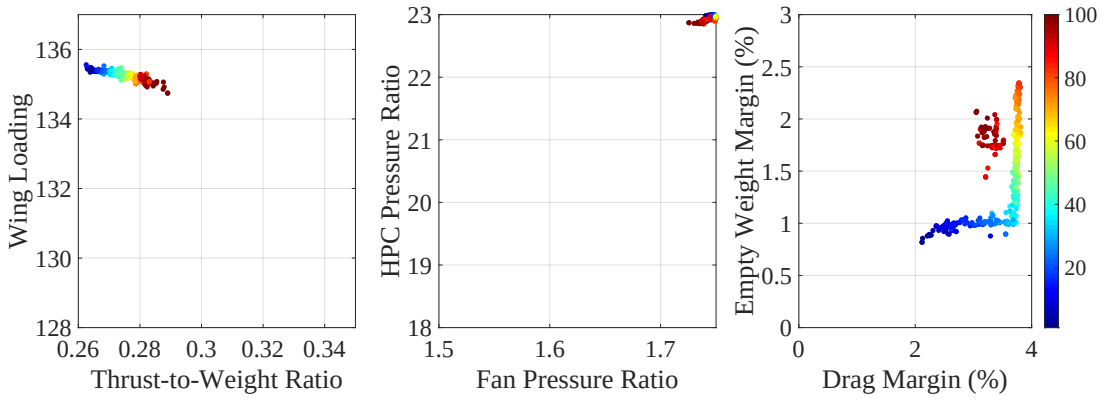

Figure 101: Full Optimization: Pareto Front Design Points in Vehicle Space with Reliability

most preferable because they enable higher levels of aspect ratio (as shown in Experiment 3.2a in Section 7.2.2).

The difference between the clusters is amplified in Figure 103. Higher wing skin weight is associated with the lower reliability cluster whereas lower wing bending weight is associated with the higher reliability cluster. A similar trend is present with respect to wing area and wing twist slope.

The two cluster effect is even more pronounced in this optimization than in the prior optimizations. This implies that as the formulation includes more variables, multiple populations may present themselves as along the Pareto Front. Of course, this is a function of

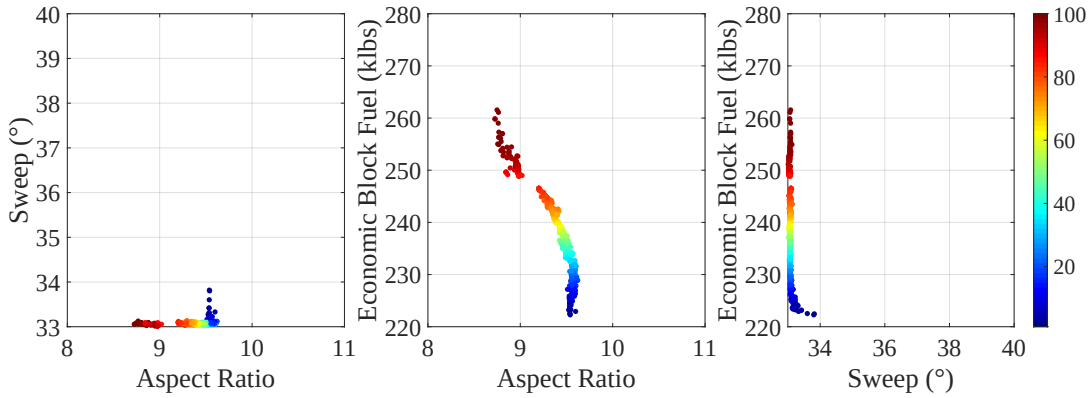

Figure 102: Full Optimization: Pareto Front Design Points in Aspect Ratio and Sweep Space with Reliability

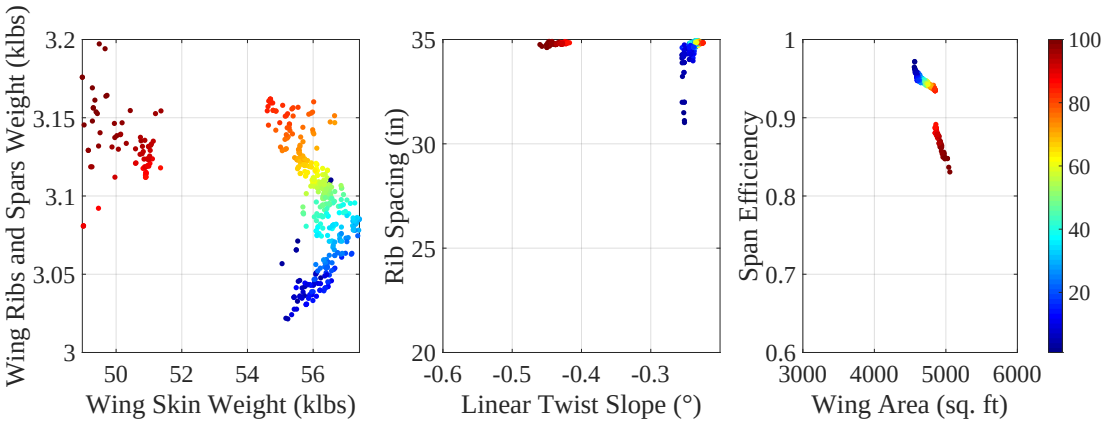

Figure 103: Full Optimization: Pareto Front Design Points in Wing Space with Reliability

the variable bounds and constraint values, which is why characterizing the uncertainty (and constraints) is of absolute importance.

CHAPTER 9

CONCLUSIONS

This work began with a brief history of engineering design and the inherent risk involved in innovation. Very quickly the inherent uncertainty emerged as a major obstacle still facing aircraft designers and manufacturers. A literature review revealed that some reliability-based optimization methods do exist, but capability gaps prevent the level of risk from being addressed. This prompted a focused literature review on the specific gaps which revealed models and methods available to fill the capability gaps. The most relevant candidates from the literature review were applied to the benchmark method through a series of research questions, hypotheses, experiments, and results. Filling the capability gaps resulted in the development of a new framework termed Reliability Assessment using Bi-level Design Analysis (RABiDA) framework.

The overarching Research Objective was to develop this method, as was formalized in Chapter 3:

Research Objective
Develop an integrated vehicle- and wing-level design environment with uncertainty characterization and correlation to perform reliability-based design optimization.

This objective was decomposed into three sub-objectives as depicted in Figure 20: determining a physics-based environment, quantifying the relevant uncertainty, and integrating the two levels into a single bi-level analysis environment. Each sub-objective was designated a corresponding research question.

9.1 Summary of Research Questions

A summary of the capability gaps, research questions, hypothesis, experiments, and results is given in Figure 104.

Capability Gap	Research Question	Topic	Hypothesis/Response	Test	Result
1	1.1	Physics-based tools	RADE (VSP, AFEM, Nastran, AVL)	-	-
	1.2	Jig shape determination algorithm	Similar (~1%) solutions if monotonically converging	Sizing loop comparison	Substantiated
	1.3	Mitigation modeling	VSP	Constraint sensitivity	Substantiated
2	2.1	Uncertainty taxonomy	Model Uncertainty	Lit. Review	-
	2.2	Describing uncertainty	Dependent on mesh size	Mesh sensitivity	Substantiated
			Converging with refinement	Mesh sensitivity	Qualified
			Fit to distributions with 95% CI	Anderson-Darling	Qualified
	2.3	Uncertainty correlation	Correlations exist	Pearson coefficient	Substantiated
			Impact of dependent uncertainty sampling	Compliance comparison	Substantiated
3	3.1	Bridging tools of differing fidelity	Converges on unique solution	Structural wing weight convergence	Substantiated
			Robust across design space	Design space exploration convergence test	Substantiated
			Robust to initial guess	Initial guess sensitivity	Substantiated
	3.2	Effect of wing-level constraints	Reliability of single vehicle design	Aspect ratio sensitivity	Substantiated
			Reliability of vehicle-level optima	Vehicle-only Pareto Front	Qualified

Figure 104: Reliability Assessment using Bi-level Design Analysis (RABiDA)

9.1.1 Research Question 1: Capturing Physical Design Changes

The first research question was prompted by the discretization of the design process. To account for downstream effects, the benchmark method simulated changed at the vehicle level. This inhibited both the uncertainty quantification and the mitigation modeling: both were reduced to vehicle-level multipliers. This prompted the pursuit of finding or developing a physics-based environment that can be a testbed for mitigation modeling and assessment and uncertainty realization.

Research Question 1.1 sought an enumeration of candidate physics-based models. This question was answered with a literature review given in Section 4.1.1.

Research Question 1.1

What tools are needed to perform physics-based, structural wing-level design and

analysis? If more than one is required, how can these tools be integrated to form a single wing-level design environment?

The review revealed that RADE overcame a number of the obstacles to using a physics-based analysis as a design environment. An associated hypothesis was stated that RADE would suffice as a physics-based, wing-level design and analysis environment.

Research Result 1.1

The Rapid Airframe Design Environment can be used as a testbed to model physical design changes to the wing because it integrates the necessary tools (VSP, AFEM, AVL, Nastran) to perform physics-based wing design.

NASA's Common Research Model was used as a notional wing geometry. Due to the tip deflection of the model, it was assumed to represent the flight shape, while the jig shape is required for mitigation modeling. RADE described a default loop to translate the flight shape into the jig shape which used a fixed-point iteration and the flight shape as the initial guess. The convergence loop structure was questioned in Research Question 1.2:

Research Question 1.2

How does the sizing algorithm affect final jig shape and size?

An experiment was designed to test the default loop structure against three other alternatives, two of which were characterized by a double-loop iteration rather than default single-loop iteration. The hypothesis was that as long as the convergence occurs monotonically, the loop structure will not affect the convergence. This hypothesis was formalized as Hypothesis 1.2:

Hypothesis 1.2

If a single loop convergence that simultaneously alters both weight and shape mono-

tonically converges on a solution, then adding additional loops will converge on a similar (~1%) solution.

This hypothesis was tested and the result given in Section 5.1.2, which substantiated Hypothesis 1.2. Therefore, the default loop structure remain unchanged. This experiment was repeated for a separate design point in Section 5.1.2 which continued to support the hypothesis.

After the model process was solidified, the task of mitigation modeling was completed. As noted by Capability Gap 1, the prior methods did not explicitly model mitigation. Therefore, a process needed to be developed.

Research Question 1.3

How can physical design changes to the wing be captured in the model?

The mitigation was implemented by utilizing the VSP model and applying the change in wing twist directly to the geometry. The resulting change in wing-level outputs was given in a sensitivity study in Section 5.2.3. The results from this test supported the hypothesis that the implementation was working correctly: the trends of the modified wings matched expectations.

Research Result 1.3

If a parametric tool was used to generate a wing shape from a set of variables and VSP file, then the same tool can be used to parametrically affect the wing geometry without re-sizing.

Therefore, Research Question 1 was concluded as answered by the RADE environment, jig shape determination loop study, and the mitigation-constraint sensitivity experiment.

9.1.2 Research Question 2: Uncertainty Quantification and Correlation

The second capability gap found was a plethora of unsupported uncertainty assumptions throughout the reliability-based design optimization aerospace field. First, many methods did not include a formal categorization of the various applicable uncertainty sources. Second, the sources were assumed to be characterized by prescribed parametric distributions. This assumption probably introduced more uncertainty than it captured. Finally, the sources of uncertainty were assumed to be independent of each other. These shortcomings were described in Capability Gap 2.

Before uncertainty can be captured, it needs to be understood by the modeler. So, the first order of business was to gather a list of uncertainty sources that apply to aircraft design, as directed in Research Question 2.1:

Research Question 2.1

What are typical categorizations of uncertainty, and which are most prevalent to design uncertainty?

This research question was answered by a literature review, synthesis, and development of uncertainty taxonomies. The final result was presented in Section 4.2.1. After the sources of uncertainty were labeled, the spotlight shifted to model uncertainty which was further filtered to discretization error. Highlighting a highly specific type of uncertainty was beneficial to characterizing it.

Research Question 2.2

How can the probabilistic description of the uncertainty be derived?

The literature review revealed a common technique to quantify discretization error cause by mesh size in finite element methods called Richardson's Extrapolation Method. However, the model must satisfy two requirements, which led to the first two parts of Hypothesis 2.2:

Hypothesis 2.2

a) The outputs of the wing-level design environment (e.g. wing weight) are sensitive to mesh size.

b) Refining the mesh will result in a more accurate weight estimation with diminishing improvement (i.e. the curve will converge to a finite value).

c) The discretization error distributions can be fit to unbounded, parametric distributions. The best distribution can describe the observed data with 95% confidence.

Testing this hypothesis was the central focus of Section 6.1. Wing weight (and others) was found to be dependent on mesh size, and REM was used to determine the error between a seven inch mesh and a continuous mesh. However, Hypothesis 2.2b was qualified because Nastran did not exhibit converging behavior with mesh refinement. Three convergent points of constant mesh refinement (6.5, 8, and 10) did exhibit convergence, however. Therefore, Hypothesis 2.2b was qualified. Errors were sampled across the design space to produce a distribution of discretization errors, which were fit to parametric distributions with 95% confidence in Section 6.1.3. Hypothesis 2.2c was qualified to state that *a* distribution could be found rather than the *best* distribution (as defined by BIC) will pass the Anderson-Darling test. If correlations were not found, then these distributions could be used to quantify the uncertainty.

Qualified Hypothesis 2.2b, 2.2c

b) A set of wing-level outputs with a constant mesh refinement ratio exists that exhibits convergent behavior.

c) The discretization error distributions can be fit to unbounded, parametric distributions with 95% confidence.

Because the discretization error was caused by mesh size, and the mesh affected the analysis of the design itself, we expected the errors to be correlated. However, we wanted

to test for this directly, as described in Research Question 2.3:

Research Question 2.3
Does correlation exist between uncertainty sources? If so, how can it be captured in the RBDO?

If correlations exist, we want to maintain it within the RBDO. The error set created in Section 6.1.2 was used to test for correlations visually by scatter plot and quantitatively by Pearson's Correlation Coefficient. Because correlation magnitudes were found above the 0.3 threshold for a sample size of 50, Hypothesis 2.3 was substantiated.

Hypothesis 2.3
Statistically significant (95% confidence) correlations exist between output errors.

A Student's t copula was used because it is n-dimensional, so all output errors could be captured in a single copula. The copula was tested against independent sampling of the distributions in the experiment given in Section 6.2.5. A compliance comparison was conducted between the independent and dependent uncertainty cases in Section 6.2.6. This comparison showed that the independent case underestimated compliance (by about 10%) due to its overestimation of the uncertainty space, showing that the independence assumption has a measurable impact on the decision-making criteria.

9.1.3 Research Question 3: Bi-Level Environment

The last capability gap was a default gap caused by the previous two gaps. Filling this gap required a new, integrated environment that could account for a bi-level approach to reliability-based design optimization with correlated uncertainty. Fortunately, a copula can be sampled just like a distribution; therefore, no major changes to the methodology were required to implemented the correlated uncertainty. Integrating the vehicle- and wing-level environments, however, was much more involved.

Two environments at different levels of fidelity are not guaranteed to agree. This motivated Research Question 3.1:

Research Question 3.1

How can two design environments of varying fidelity be integrated to agree on performance estimation?

Because the vehicle- and wing-level environments share common variables, it was hypothesized that these variables could be used to converge on a consistent solution between the environments:

Hypothesis 3.1

The two models can be bridged to agree on a unique set of input and output variables.

This convergence loop was developed and tested in Section 7.1.2. It was shown to converge quickly and reliably. The convergence was also shown to be robust against a wide variety of initial guesses for a single design as well as across the design space. The completion of this convergence showed that the environment could produce consistent designs at both the vehicle- and wing-levels.

The final research question sought to demonstrate the new insight illuminated by the integrated environment:

Research Question 3.2

What impact does the integrated environment have on conceptual design selection relative to the baseline method?

The best way to show the new knowledge is to compare a set of optimums under the old paradigm and evaluate them under the new paradigm, as described in Hypothesis 3.2:

Hypothesis 3.2

If optimal points are found using an optimization formulation restricted to vehicle-level constraints only, then these points will have no probability of satisfying wing-level constraints.

This experiment was conducted in Section 7.2. The vehicle-level Pareto Front had an approximately a 10.4% (given in Section 7.2.3) probability of satisfying the wing-level constraints with wing-level mitigation. Without mitigation, the Pareto Front had a 0% probability of success. As discussed in Section 7.2.3, this was most likely a result of optimizing towards economic block fuel which pushed the Pareto Front towards higher levels of aspect ratio. The experiments in Sections 7.2.1 and 7.2.2 showed that the wing-level constraints can fail before the vehicle-level constraints. Hypothesis 3.2 is clarified to exclude mitigation because outboard wing twist allowed some probability of success to exist. Without wing-level mitigation, however, the results support the hypothesis that the reliability is zero percent.

The entire breakdown of the research objective, research questions, experiments, and results is given in Figure 105.

9.1.4 Case Study

A full implementation of RABiDA was given in Chapter 8. A Boeing 777-200ER-like mission was combined with a NASA's Common Research Model wing to perform the reliability-based design optimization. The results were given in Section 8.2.7 which showed a two cluster phenomenon: the Pareto Front was dominated by two distinct groupings within the design space. One group relied heavily on mitigation (no compliance at all) while the other group reached the highest levels of reliability.

A comparison between maximizing for probability of compliance versus probability of success is given in Section 8.3. The former optimization reflects the vehicle-level

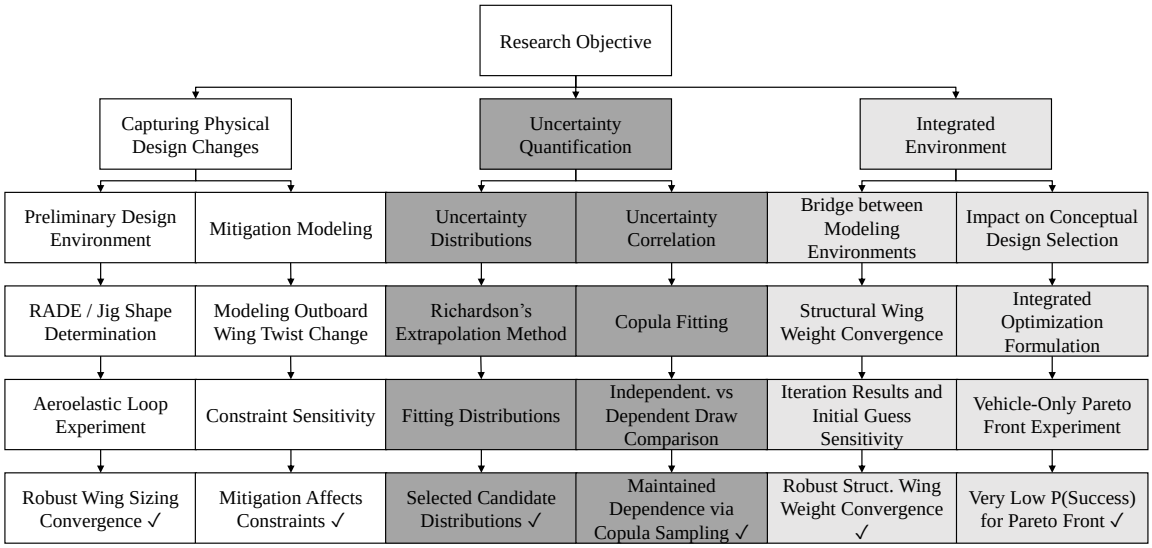

Figure 105: Final Research Objective Decomposition with Proposed Methods and Experiments

only Pareto Front from Experiment 3.2. A final optimization is performed, complete with vehicle-level mitigation and wing-level parametric uncertainty, in Section 8.4.

9.2 Contributions

The Motivational Problem for this work was to address the high level of risk facing aircraft designers and manufacturers. By definition, risk is defined as the product of severity and likelihood. This thesis addressed the latter under the mindset that reducing the likelihood of a catastrophic event (redesign, cancellation) would reduce the risk of the aircraft design process. Because the uncertainty (and therefore likelihood of an unfavorable event) was highest during conceptual design, conceptual design selection was the focal point of this work.

The additional research has resulted in improvements to the benchmark method. Figure 106 shows the changes relative to the benchmark in Figure 19.

The changes to the ARMOUR method were motivated by three capability gaps. These gaps were turned into research questions and ultimately answered with processes, experimentation, and testing. The changes to the benchmark method are highlighted in Figure

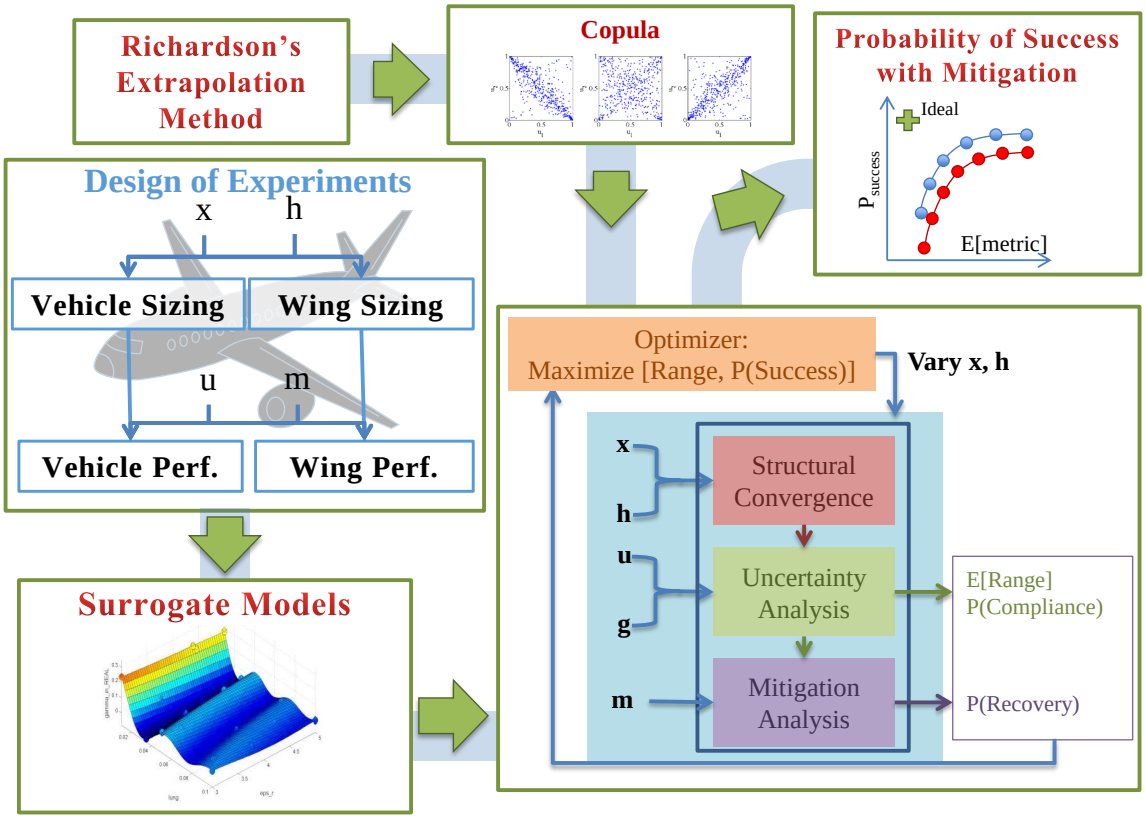

Figure 106: Improved ARMOUR Methodology

107.

There are three main contributions of this work: developing a mitigation modeling process, characterizing model uncertainty computationally rather than heuristically, and developing a bi-level RBDO conceptual design selection framework.

9.2.1 Mitigation Modeling Process and Development

Until now, mitigation has not been explicitly modeled. Indeed, the benchmark method was the first to designate a unique variable space to mitigation. Still, the mitigation was vaguely defined in terms of actions and implemented as multipliers on vehicle-level variables. Now, mitigation can be applied directly to a physical model and the effects can be determined computationally. The majority of this effort was the implementation of an accurate but efficient physics-based modeling environment. Wing twist was demonstrated, but the over-

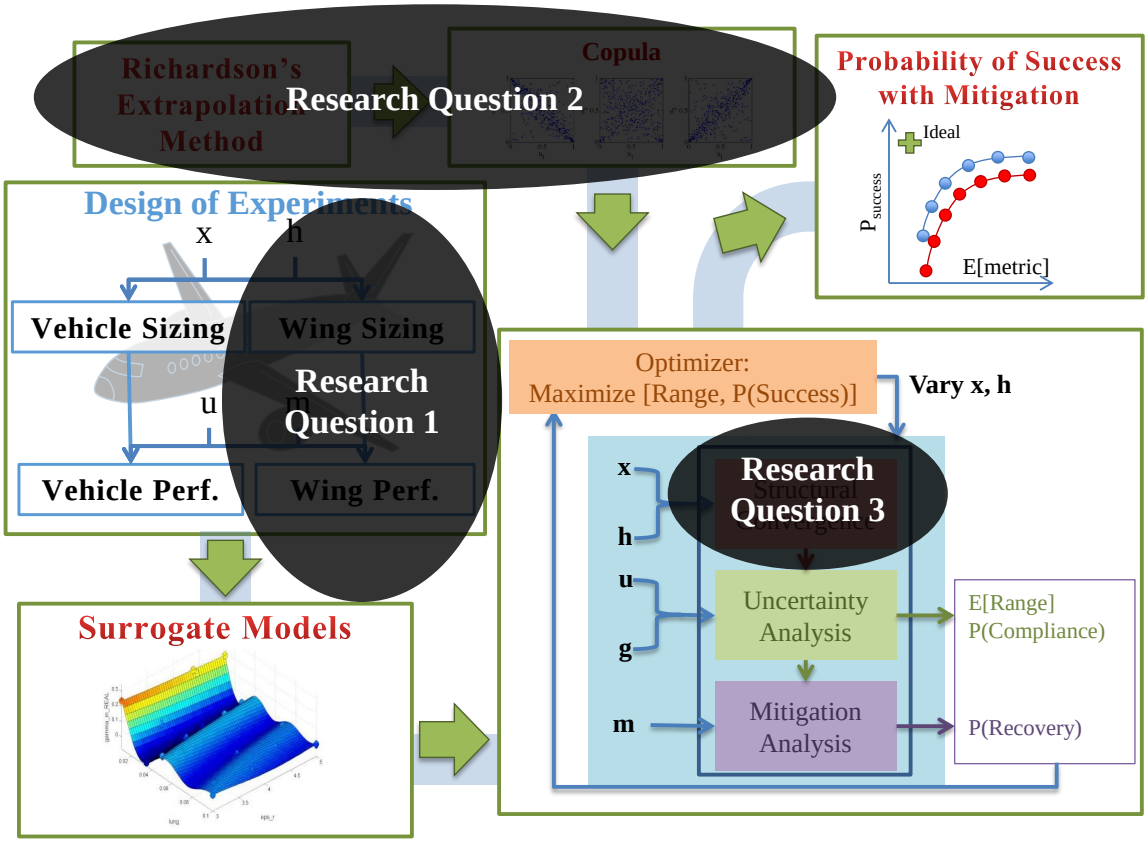

Figure 107: Improved ARMOUR Methodology as a Result of Answered Research Questions

all process provides capability for all kinds of mitigation actions (increasing number of components, adding or decreasing weight, testing new material properties, etc.).

9.2.2 Model Uncertainty Characterization in Aircraft Design

The contribution here is a cross-pollination of the fields of aircraft design selection and uncertainty quantification. The methods of discretization error quantification, error samples fitting with parametric distributions at 95% confidence, testing for correlation, and copula fitting are widely used outside of aircraft conceptual design selection: the baseline methods required limiting assumptions (uniform, independent distributions) and used intuition and subject matter expertise rather than data-based approaches. Here, the uncertainty has been determined experimentally using the models themselves. A major finding was the ability

to fit the discretization error dataset to parametric distributions with 95%. There was no theoretical guarantee that these error values would resemble parametric distributions.

9.2.3 Bi-Level Design Environment

The call for a bi-level approach was initially prompted by the mitigation modeling: in order to model mitigation without a transformation function, it had to be captured explicitly. However, a major contribution of this work was the capturing of *natural* uncertainty. The term "natural" is used here because the bi-level approach revealed that the vehicle-only formulation would fail wing-level constraints without the presence of simulated uncertainty (i.e. noise variables, distributions, etc.). The constraints were failed *deterministically* rather than *probabilistically*. The non-compliance was due to a lack of knowledge: the vehicle-level design environment did not include wing-level constraints into its formulation; as a result, when optimization was performed, the optimal points were in an infeasible region when wing-level constraints were enforced. In other words, vehicle-level only optimization reduced reliability rather than optimized it. Thus, a bi-level environment reduced uncertainty of the benchmark method.

While RADE may introduce new sources of uncertainty due to simplifying assumptions, there is now an estimated value rather than a null value. Further, the uncertainty sources can be named, whether it be smear properties, approximated aerodynamics, uniform component thickness, etc. Future work can characterize the uncertainty caused by the simplifying assumptions because the sources are known.

9.3 Future Work

While RABiDA presents the current state-of-the-art with respect to aircraft conceptual design with uncertainty quantification and mitigation actions, there are several opportunities for improvement. Suggestions for continued work are provided here.

9.3.1 Extending Model Uncertainty

There is an opportunity to extend the model uncertainty category beyond just discretization error. While RADE provides an estimation of wing-level parameters, there are a number of significant assumptions made in order to simplify the physics-based analysis. Capturing the uncertainty caused by these assumptions would extend the uncertainty quantification to approximation error as well as discretization error.

A key assumption, for example, is that aluminum is used as the material and that it is isotropic. This affects the stiffness matrix and ultimately the tip deflection constraint. Further, AVL is an approximate aerodynamics tool. Future work could include comparing its performance to an actual CFD code to compare the results. Similar to discretization error, there may be a trend throughout the design space on the difference between the two results. Because the CFD model would be of higher order and fidelity, it would be considered the "truth" value for this case.

Finally, a "goodness of fit" metric for the mesh would be advantageous to characterizing the quality of the meshing process. Highly tapered wings, for example, are more difficult to mesh than rectangular wings. As a result, the mesh can be worse and therefore affect stress and weight calculations. This can even be added to Richardson's Extrapolation Method: the error can be accompanies by a mesh goodness factor. The error used for the extrapolation should take into account the quality of the mesh. Otherwise, the extrapolation is confounding the effects of mesh size with mesh quality.

9.3.2 Capture Non-Technical Attributes of Margin and Mitigation

The final results demonstrated a high reliance on mitigation to maximize performance. This trend was not surprising because the non-technical aspects of mitigation were not included in the creation of this framework. As stated in Chapter 2, mitigation includes a delay in the development program which greatly decreases the appeal of mitigation actions. This stoppage time is assumed to be expensive and stressful. Including this attribute of mitigation

would bring back balance to the margin versus mitigation discussion. However, developing a "cost" function for mitigation is academically elusive. Mitigation tends to be highly proprietary, notwithstanding the cost of mitigation as well. The withheld information creates a challenge for academic work to capture all aspects of mitigation.

9.3.3 Nastran Convergence

As demonstrated by Figure 47, Nastran diverges as mesh size decreases. This is the antithesis of the desired behavior. As noted, the principal reason is the point force connections between components versus distributive force connections. Therefore, an approach could be developed to transform these forces or redefine maximum stresses for the elements. Maximum stress does not have to be used, but what measure should be used in its stead? The maximum stress could be removed for each component at the connection, but there is no guarantee how many elements will be in a given part or component. Therefore, it is impossible to generically determine a stress vale that is "far enough" away to be used via Saint Venant's Principle [183].

9.3.4 Extend Wing-Level Constraint Space

There are two ways to expand the wing-level constraint space. The first is to include a larger number of constraints, such as buckling and flutter. These are some of the most common wing-level constraints and could have been included in this methodology. Of course, to be included in a RBDO method requires that uncertainty, margin, and mitigation variables are also present that affect these constraints. This is an area for this method to be extended. For this work, Nastran required about five minutes to size a wing, which was sized about five times for each sizing (jig shape convergence iterations). Including buckling did not show to increase computation time dramatically, but the results became probabilistic due to a more sensitive convergence algorithm in Nastran. Flutter, on the other hand, greatly increased the Nastran computation time. This is an area that would require an approximate

flutter analysis or more efficient surrogate production to be a feasible approach to capturing the flutter constraint within the greater RBDO method.

The second way to expand the constraint space is to remove the constraint aggregations. The aggregate used in this thesis was maximum Von Mises stress. A straightforward mitigation action for violating a stress constraint is to simply increase the thickness ("beef up") of the component. However, if only the *maximum* value is recorded, there is no evidence that the second highest stress value also violates the stress constraint. If so, how many elements are in constraint violation? A way to improve this method could be to capture the stress field rather than a single stress value. If the entire field is known or predicted, then exactly how many components violated the constraint and by how much would be known. If only one stress is known and it represents the maximum stress throughout the entire wing, then *every* part of the wing would need to be modified to ensure constraint satisfaction. This is no good: mitigation should be tailored to the specific piece of the design that fails the constraint. Therefore, it was excluded for this work but should be considered for future work.

9.3.5 Extend Wing-Level Mitigation Space

There are two clear mitigation actions that were not included in this work. While they were neglected mostly to isolate the effect of outboard wing twist, they are also more difficult to implement. They are increasing wing thickness and substituting metallic material for composite.

Component thickness can be modified directly in the physics-based model. However, what rules govern this process? If a rib is thickened, should all the ribs be thickened as well? Research is needed to determine a structured approach to modify component thicknesses and manage the effects.

Modeling composites is already gaining steam in the community. Composite materials present strong strengths over metallic materials, and their popularity will only grow as the

industry becomes more comfortable working with and maintaining composites in aircraft. In this work the use of composite materials was suggested as a weight mitigation action, but the impact of composites in general offers many opportunities to mitigate uncertainty (maximum stress, for example). Therefore an interesting study would be the effect of mixing and matching metallic and composite materials during sizing and post-sizing. What rules govern which material can be used where? Further, historical regressions (such as those used by FLOPS and EDS) tend to not have accurate composite estimations. Therefore adding composites would require an assessment to both the vehicle- and wing-level environments

Appendices

APPENDIX A

STRUCTURAL WING WEIGHT CONVERGENCE RESULTS

Figure 34 showed the take-off gross weight results for the structural wing weight convergence robustness experiment performed in Section 7.1.4. Take-off gross weight is just one of the five convergence variables: the others are wing skin weight, wing ribs and spars weight, wing area, and span efficiency. Because the take-off gross weight converges on a single solution despite a wide variety of initial guesses, we can assume that the other variables do as well. But, for completeness, the results of the other four variables are presented here.

As demonstrated by Tables 67, 68, 69, and 70, the conclusion drawn in Section 70 that the solution is robust to initial guess is substantiated.

Table 67: FRWI1 (lbs) Sensitivity to a Wide Range of FRWI1 & FRWI2 Initial Guesses

FRWI1/FRWI1	2,000	3,000	4,000	5,000	6,000	7,000
30,000	52,930	52,930	52,930	52,930	52,930	52,930
40,000	52,926	52,926	52,927	52,927	52,927	52,927
50,000	52,929	52,929	52,929	52,929	52,929	52,930
60,000	52,927	52,928	52,929	52,930	52,930	52,926
70,000	52,933	52,933	52,934	52,934	52,934	52,934

Table 68: FRWI2 (lbs) Sensitivity to a Wide Range of FRWI1 & FRWI2 Initial Guesses

FRWI1/FRWI1	2,000	3,000	4,000	5,000	6,000	7,000
30,000	3,194.4	3,194.4	3,194.4	3,194.4	3,194.4	3,194.4
40,000	3,194.1	3,194.1	3,194.1	3,194.2	3,194.2	3,194.2
50,000	3,194.3	3,194.3	3,194.3	3,194.3	3,194.4	3,194.4
60,000	3,194.2	3,194.3	3,194.4	3,194.4	3,194.4	3,194.8
70,000	3,194.6	3,194.7	3,194.7	3,194.7	3,194.7	3,194.7

Table 69: Wing Area (ft^2) Sensitivity to a Wide Range of FRWI1 & FRWI2 Initial Guesses

FRWI1/FRWI1	2,000	3,000	4,000	5,000	6,000	7,000
30,000	5,000.1	5,000.1	5,000.1	5,000.1	5,000.1	5,000.1
40,000	4,999.7	4,999.7	4,999.7	4,999.8	4,999.8	4,999.8
50,000	4,999.9	5,000.0	5,000.0	5,000.0	5,000.0	5,000.1
60,000	4,999.8	4,999.9	5,000.0	5,000.1	5,000.1	5,000.7
70,000	5,000.4	5,000.5	5,000.5	5,000.5	5,000.5	5,000.5

Table 70: Span Efficiency Sensitivity to a Wide Range of FRWI1 & FRWI2 Initial Guesses

FRWI1/FRWI1	2,000	3,000	4,000	5,000	6,000	7,000
30,000	0.7553	0.7553	0.7553	0.7553	0.7553	0.7553
40,000	0.7553	0.7553	0.7553	0.7553	0.7553	0.7553
50,000	0.7553	0.7553	0.7553	0.7553	0.7553	0.7553
60,000	0.7553	0.7553	0.7553	0.7553	0.7553	0.7553
70,000	0.7553	0.7553	0.7553	0.7553	0.7553	0.7553

APPENDIX B

NEURAL NETWORK GOODNESS OF FIT METRICS

Step 6 of the developed framework necessitated the fitting of surrogate models. These models allow optimization to be performed by significantly (several orders of magnitude) decreasing the computation time of model execution. However, the cost is an introduction of error: the representative model is slightly different in prediction than the imitated model. A summary of the surrogate fits was given in Section 8.2.6 in Figures 63 and 64. Here, all of the surrogate fit outputs are provided. Each output includes fit characteristics such as the root mean squared error (RMSE) and R^2 values, as well as plots of the actual values versus predicted values and residual values by predicted values.

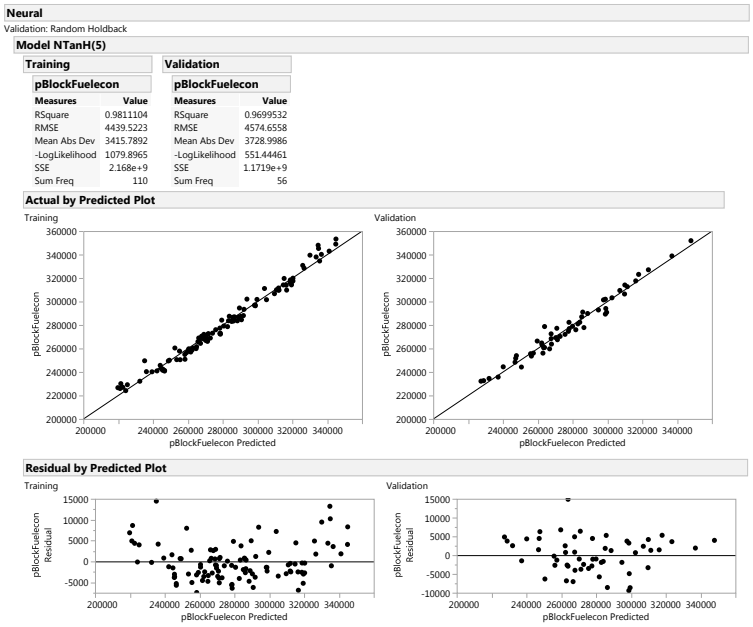

Figure 108: Neural Network Fit for Economic Block Fuel

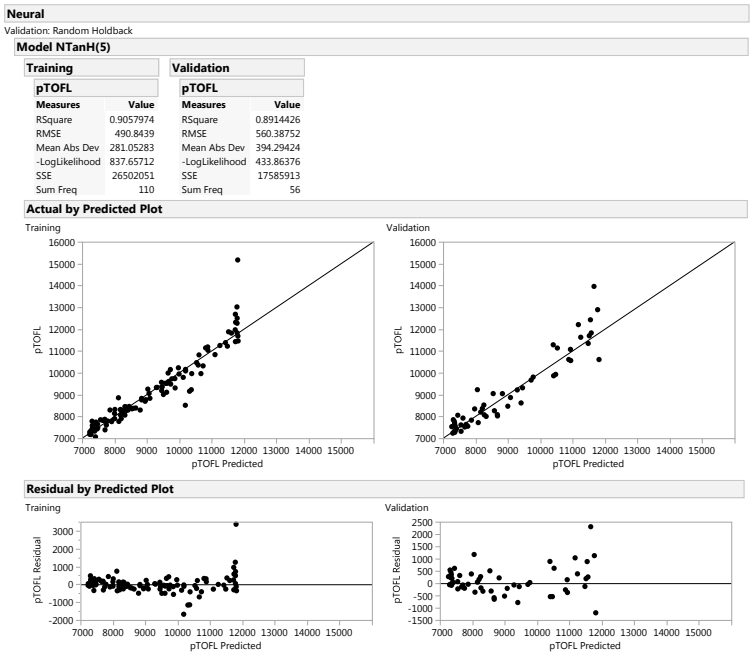

Figure 109: Neural Network Fit for Takeoff Field Length

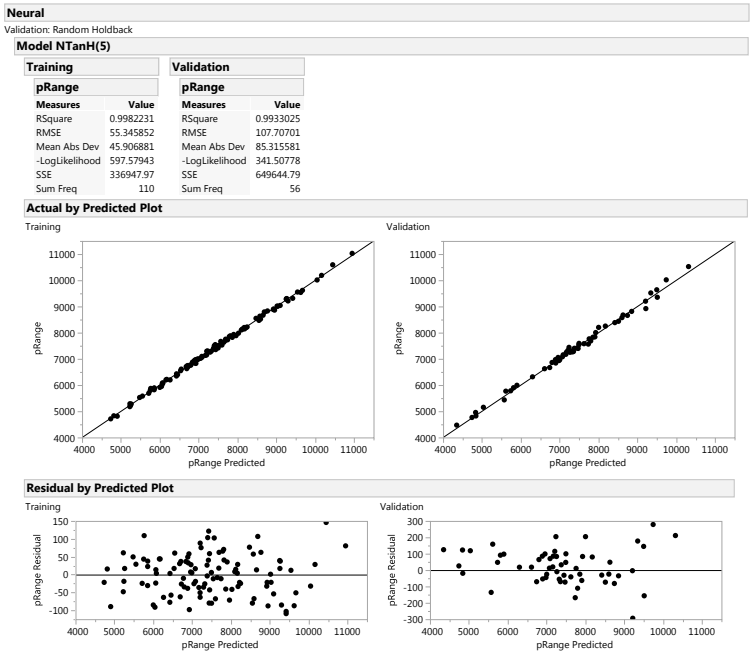

Figure 110: Neural Network Fit for Maximum Range

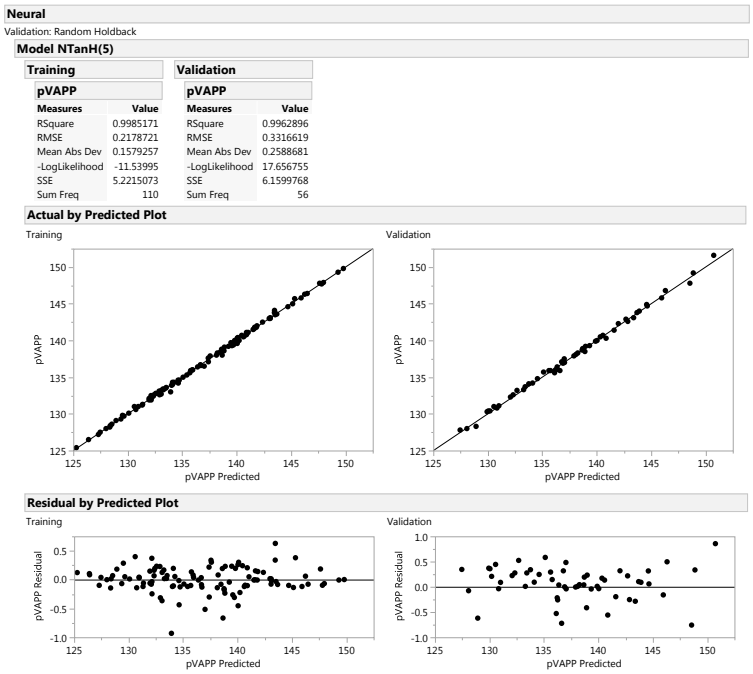

Figure 111: Neural Network Fit for Approach Velocity

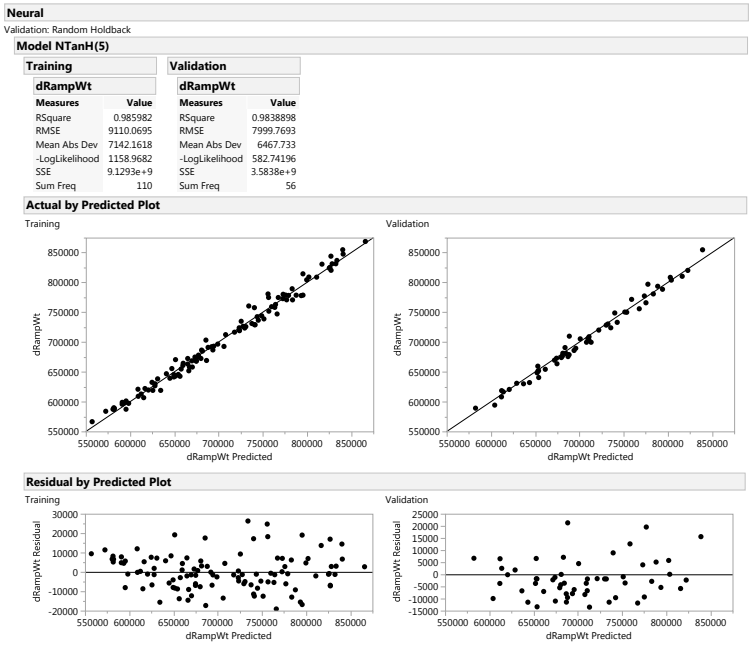

Figure 112: Neural Network Fit for Takeoff Gross Weight

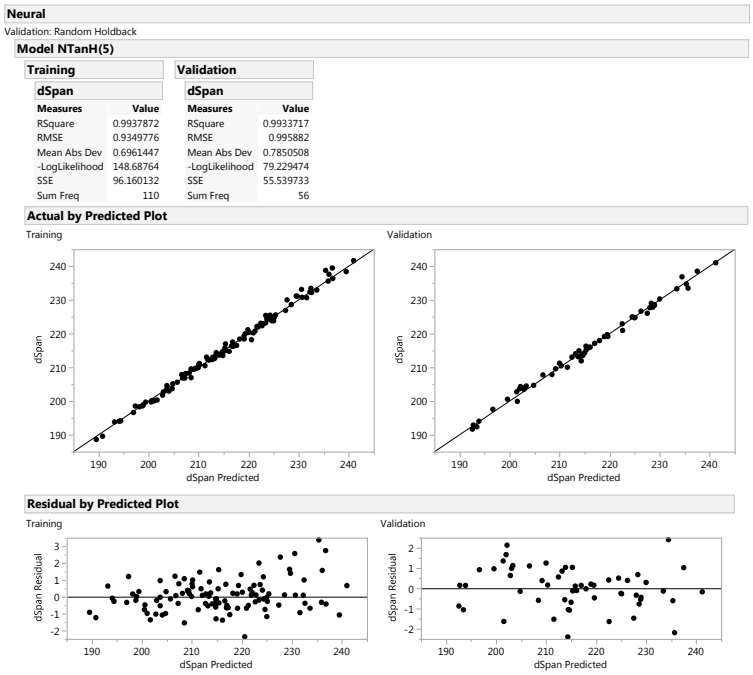

Figure 113: Neural Network Fit for Wing Span

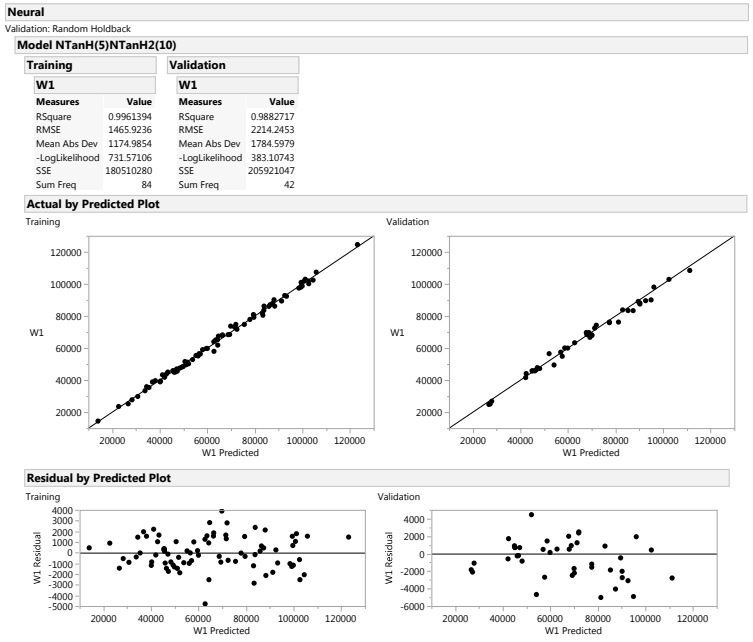

Figure 114: Neural Network Fit for Bending Material Weight (FRWI1)

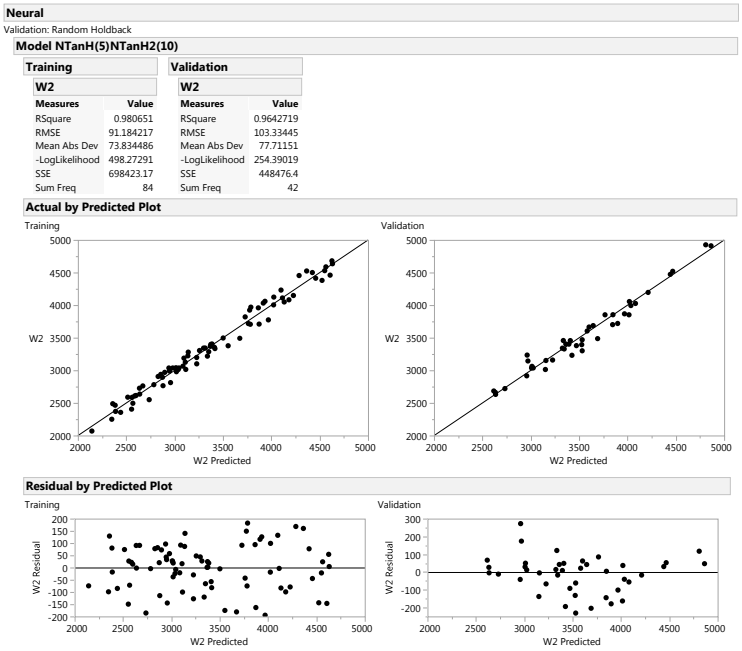

Figure 115: Neural Network Fit for Ribs and Spars Weight (FRWI2)

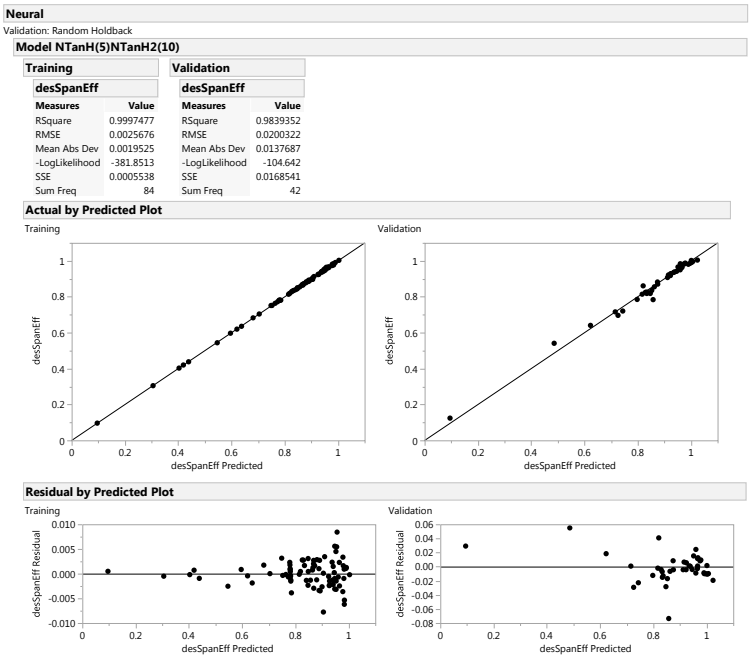

Figure 116: Neural Network Fit for Design Span Efficiency

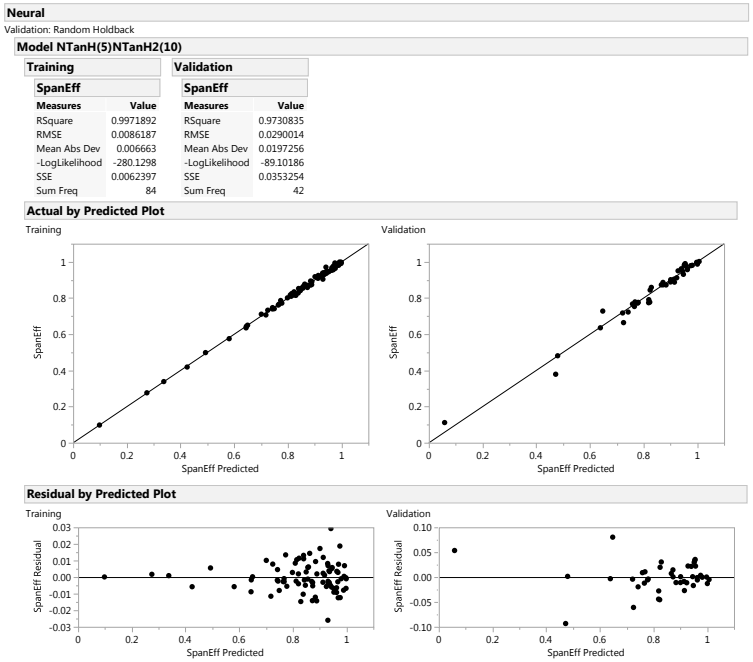

Figure 117: Neural Network Fit for Span Efficiency (post-mitigation)

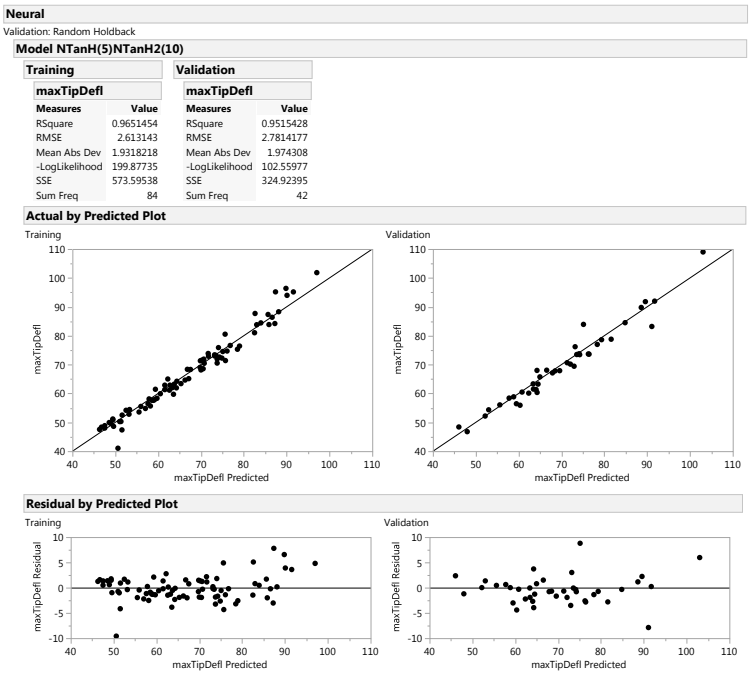

Figure 118: Neural Network Fit for 2.5G Maneuver Tip Deflection

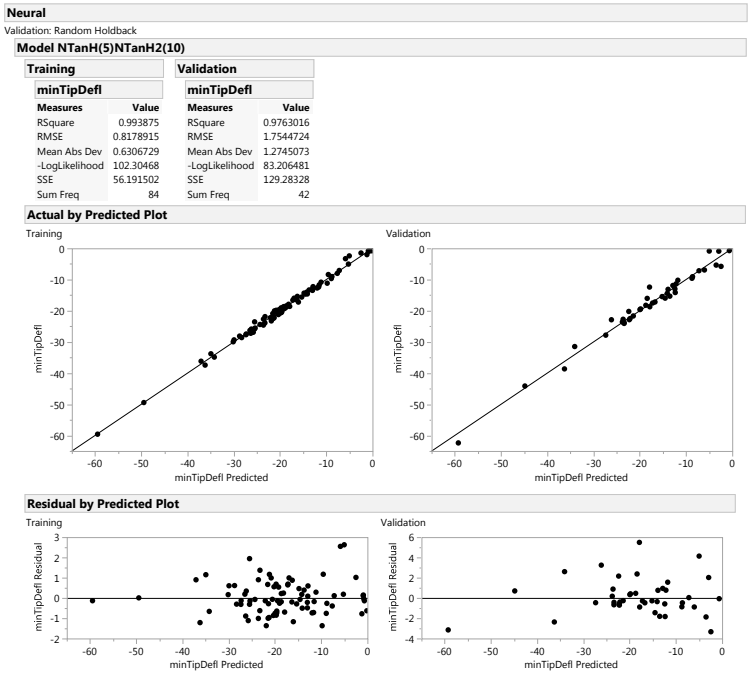

Figure 119: Neural Network Fit for -1.0G Maneuver Tip Deflection

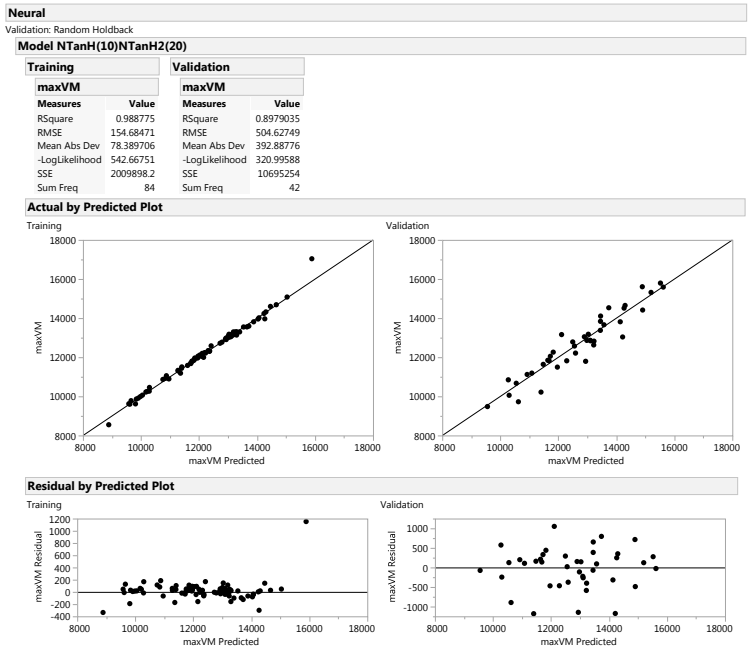

Figure 120: Neural Network Fit for Maximum Von Mises Stress

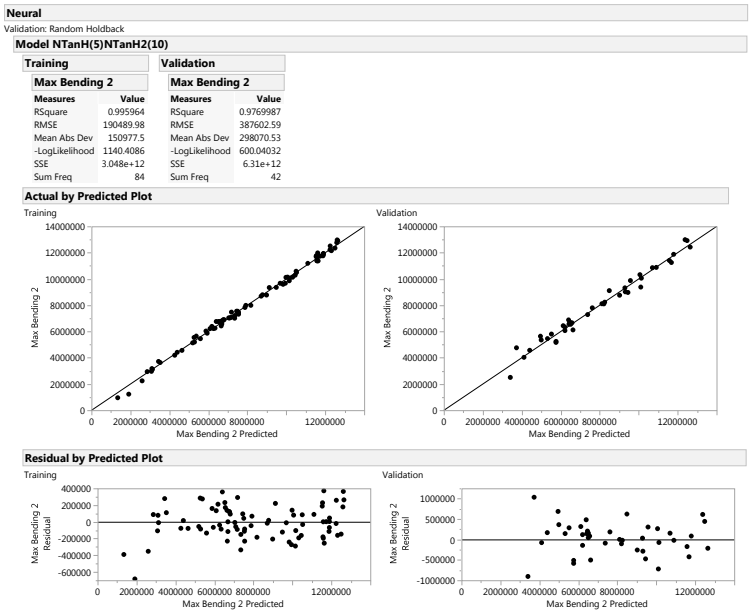

Figure 121: Neural Network Fit for 2.5G Maneuver Root Bending Moment

BIBLIOGRAPHY

[1] D. P. Raymer, "Aircraft design: A conceptual approach, american institute of aeronautics and astronautics," *Inc., Reston, VA*, p. 21, 1999.

[2] A. M.D.O. T. Committee *et al.*, "Current state of the art on multidisciplinary design optimization (mdo)," *An AIAA White Paper. AIAA*, 1991.

[3] G. E. Dieter, L. C. Schmidt, and S. AZARM, *Engineering design*, 2009.

[4] M. Asimow, *Introduction to design*. Prentice-Hall, 1962.

[5] D. N. Mavris, D. A. DeLaurentis, O. Bandte, and M. A. Hale, "A stochastic approach to multi-disciplinary aircraft analysis and design," in *36th Aerospace Sciences Meeting & Exhibit, Reno, NV*, 1998.

[6] A. Keane and P. Nair, *Computational approaches for aerospace design: The pursuit of excellence*. John Wiley & Sons, 2005.

[7] T. Paynter, Ed., *Northrop grumman to acquire orbital atk for $9.2 billion*, 2017.

[8] L. Whiteman, "2017 was a record year for aerospace m&a. could 2018 be even better?" *Motley Fool*, 2017.

[9] D. P. Schrage, "Technology for rotorcraft affordability through integrated product/process development (ippd)," 1999.

[10] K. A. Khan and G. D. Houston, "Design optimization using life cycle cost analysis for low operating costs," BOMBARDIER AEROSPACE DOWNSVIEW (ONTARIO), Tech. Rep., 2000.

[11] W. Spitz, F. Berardino, R. Golaszewski, and J. Johnson, "Development cycle time simulation for civil aircraft," 2001.

[12] D. N. Mavris and D. A. DeLaurentis, "Methodology for examining the simultaneous impact of requirements, vehicle characteristics, and technologies on military aircraft design," 2000.

[13] J Shah and H Hazelrigg, "Research opportunities in engineering design," in *NSF Strategic Planning Workshop, Final Report*, 1996.

[14] K. Hoeg and R. P. Murarka, "Probabilistic analysis and design of a retaining wall," *Journal of Geotechnical and Geoenvironmental Engineering*, vol. 100, no. Proc. Paper 10436, 1974.

[15] O. E. Dictionary, *Oxford english dictionary online*, 2007.

[16] T. Nam, D. Soban, and D. Mavris, "A non-deterministic aircraft sizing method under probabilistic design constraints," in *47th AIAA/ASME/ASCE/AHS/ASC Structures, Structural Dynamics, and Materials Conference 14th AIAA/ASME/AHS Adaptive Structures Conference 7th*, 2006, p. 2062.

[17] J. D. Anderson, *Aircraft performance and design*. McGraw-Hill Science/Engineering/Math, 1999.

[18] Z. Jiang, S. Chen, D. W. Apley, and W. Chen, "Resource allocation for reduction of epistemic uncertainty in simulation-based multidisciplinary design," in *ASME 2015 International Design Engineering Technical Conferences and Computers and Information in Engineering Conference*, American Society of Mechanical Engineers, 2015, V02BT03A036–V02BT03A036.

[19] D. P. Thunnissen, "Propagating and mitigating uncertainty in the design of complex multidisciplinary systems," PhD thesis, California Institute of Technology, 2005.

[20] A. Urbina, S. Mahadevan, and T. L. Paez, "Quantification of margins and uncertainties of complex systems in the presence of aleatoric and epistemic uncertainty," *Reliability Engineering & System Safety*, vol. 96, no. 9, pp. 1114–1125, 2011.

[21] T.-L. Zhu, "A reliability-based safety factor for aircraft composite structures," *Computers & Structures*, vol. 48, no. 4, pp. 745–748, 1993.

[22] T. P. Choi, "A recourse-based solution approach to the design of fuel cell aeropropulsion systems," PhD thesis, Georgia Institute of Technology, 2008.

[23] J. S. Wilson, "Uncertainty quantifiation with mitigation actions for aircraft conceptual design," PhD thesis, Georgia Institute of Technology, 2015.

[24] R. Shishko and R. Aster, "Nasa systems engineering handbook," *NASA Special Publication*, vol. 6105, 1995.

[25] D. Gates. (2011). Boeing projects break-even on 787 manufacturing in 10 years, The Seattle Times.

[26] J. Sutter and J. Spenser, *747: Creating the world's first jumbo jet and other adventures from a life in aviation*. Harper Collins, 2010.

[27] J. Hawk, "The boeing 787 dreamliner: More than an airplane," in *Presentation to AIAA/AAAF Aircraft Noise and Emissions Reduction Symposium, American Institute of Aeronautics and Astronautics and Association Aéronautique et Astronautique de France*, 2005.

[28] C Murray, "Boeing 787 dreamliner rolls out smoother ride with gust suppression," *Design News. Retrieved April*, 2009.

[29] C. S. Tang, J. D. Zimmerman, and J. I. Nelson, "Managing new product development and supply chain risks: The boeing 787 case," in *Supply Chain Forum: An International Journal*, Taylor & Francis, vol. 10, 2009, pp. 74–86.

[30] J. Johnsson, "Boeing 787 dreamliner turns into rainmaker, and shares soar," 2017.

[31] Domini. (2015). Will 787 program ever show an overall profit? analysts grow more skeptical, The Seattle Times.

[32] J. Gertler, "F-35 joint strike fighter (jsf) program," Congressional Research Service, Tech. Rep. 7-5700, 2018.

[33] A. Drusch. (2014). Fighter plane cost overruns detailed, Politico.

[34] A. Capaccio, "F35 program costs jump to 406.5 billion in latest estimate," 2017.

[35] J. C. Helton, "Conceptual and computational basis for the quantification of margins and uncertainty," Sandia National Laboratories (United States). Funding organisation: US Department of Energy (United States), Tech. Rep., 2009.

[36] L. Jaulin, *Applied interval analysis: With examples in parameter and state estimation, robust control and robotics*. Springer Science & Business Media, 2001, vol. 1.

[37] (2018). Orders & deliveries summary, Airbus.

[38] (2018). Boeing 787: Orders and deliveries (updated monthly), The Boeing Company.

[39] M. Schwartz. (2019). Airbus to stop production of a380 superjumbo jet, NPR.

[40] J. Roskam, "Airplane design: Part i: Preliminary sizing of airplanes," vol. 1, 1985.

[41] M. J. Hughes, C. Perullo, and D. N. Mavris, "Common core engine design for multiple applications using a concurrent multi-design point approach," in *AIAA Propulsion and Energy Forum*, 2014.

[42] J. Schutte, J. Tai, J. Sands, and D. Mavris, "Cycle design exploration using multi-design point approach," in *ASME Turbo Expo 2012: Turbine Technical Conference and Exposition*, American Society of Mechanical Engineers, 2012, pp. 271–281.

[43] D. P. Thunnissen, "Method for determining margins in conceptual design," *Journal of spacecraft and rockets*, vol. 41, no. 1, pp. 85–92, 2004.

[44] M. D. Griffin, *Space vehicle design*. AIAA, 2004.

[45] D. N. Mavris, O. Bandte, and D. A. DeLaurentis, "Robust design simulation: A probabilistic approach to multidisciplinary design," *Journal of Aircraft*, vol. 36, no. 1, pp. 298–307, 1999.

[46] I. Kroo, S. Altus, R. Braun, P. Gage, and I. Sobieski, "Multidisciplinary optimization methods for aircraft preliminary design," in *5th Symposium on Multidisciplinary Analysis and Optimization*, 1994, p. 4325.

[47] B Wujek, J. E. Renaud, and S Batill, "A concurrent engineering approach for multidisciplinary design in a distributed computing environment," *Multidisciplinary Design Optimization: State of the Art*, pp. 13–16, 1997.

[48] A. Giunta, O Golividov, D. Knill, B Grossman, W. Mason, L. Watson, and R. Haftka, "Multidisciplinary design optimization of advanced aircraft configurations," in *Fifteenth International Conference on Numerical Methods in Fluid Dynamics*, Springer, 1997, pp. 14–34.

[49] D. Dubois, H. Fargier, and H. Prade, "Fuzzy constraints in job-shop scheduling," *Journal of intelligent Manufacturing*, vol. 6, no. 4, pp. 215–234, 1995.

[50] J. Ramík *et al.*, "Inequality relation between fuzzy numbers and its use in fuzzy optimization," *Fuzzy sets and systems*, vol. 16, no. 2, pp. 123–138, 1985.

[51] Z. Ruttkay, "Fuzzy constraint satisfaction," in *Fuzzy Systems, 1994. IEEE World Congress on Computational Intelligence., Proceedings of the Third IEEE Conference on*, IEEE, 1994, pp. 1263–1268.

[52] M. H. Sadraey, *Aircraft design: A systems engineering approach*. John Wiley & Sons, 2012.

[53] R. E. Melchers and A. T. Beck, *Structural reliability analysis and prediction*. John Wiley & Sons, 2018.

[54] C. L. Pettit, "Uncertainty quantification in aeroelasticity: Recent results and research challenges," *Journal of Aircraft*, vol. 41, no. 5, pp. 1217–1229, 2004.

[55] J. H. Starnes Jr and R. T. Haftka, "Preliminary design of composite wings for buckling, strength, and displacement constraints," *Journal of Aircraft*, vol. 16, no. 8, pp. 564–570, 1979.

[56] F. Beer, E. Johnston, and J DeWolf, "Mechanics of materials, 2002," *McGraw-Hill, New York*, 2002.

[57] A. B. Lambe, G. J. Kennedy, and J. R. Martins, "An evaluation of constraint aggregation strategies for wing box mass minimization," *Structural and Multidisciplinary Optimization*, vol. 55, no. 1, pp. 257–277, 2017.

[58] G Kreisselmeier and R Steinhauser, "Systematic control design by optimizing a vector performance index," in *Computer aided design of control systems*, Elsevier, 1980, pp. 113–117.

[59] G. Kreisselmeier and R. Steinhauser, "Application of vector performance optimization to a robust control loop design for a fighter aircraft," *International Journal of Control*, vol. 37, no. 2, pp. 251–284, 1983.

[60] L. Krog, A. Tucker, M. Kemp, and R. Boyd, "Topology optimisation of aircraft wing box ribs," in *10th AIAA/ISSMO multidisciplinary analysis and optimization conference*, 2004, p. 4481.

[61] P. Duysinx and O. Sigmund, "New developments in handling stress constraints in optimal material distribution," in *7th AIAA/USAF/NASA/ISSMO symposium on multidisciplinary analysis and optimization*, 1998, p. 4906.

[62] G. Qiu and X. Li, "A note on the derivation of global stress constraints," *Structural and Multidisciplinary Optimization*, vol. 40, no. 1-6, p. 625, 2010.

[63] J París, F Navarrina, I Colominas, and M Casteleiro, "Topology optimization of continuum structures with local and global stress constraints," *Structural and Multidisciplinary Optimization*, vol. 39, no. 4, pp. 419–437, 2009.

[64] J Paris, F Navarrina, I Colominas, and M Casteleiro, "Block aggregation of stress constraints in topology optimization of structures," *Advances in Engineering Software*, vol. 41, no. 3, pp. 433–441, 2010.

[65] C. Le, J. Norato, T. Bruns, C. Ha, and D. Tortorelli, "Stress-based topology optimization for continua," *Structural and Multidisciplinary Optimization*, vol. 41, no. 4, pp. 605–620, 2010.

[66] R. H. Myers, D. C. Montgomery, *et al.*, *Response surface methodology: Process and product optimization using designed experiments*. Wiley New York, 1995, vol. 4.

[67] W. Yao, X. Chen, W. Luo, M. van Tooren, and J. Guo, "Review of uncertainty-based multidisciplinary design optimization methods for aerospace vehicles," *Progress in Aerospace Sciences*, vol. 47, no. 6, pp. 450–479, 2011.

[68] R. Rackwitz, "Reliability analysisa review and some perspectives," *Structural safety*, vol. 23, no. 4, pp. 365–395, 2001.

[69] T. Matsumura and R. T. Haftka, "Reliability based design optimization modeling future redesign with different epistemic uncertainty treatments," *Journal of Mechanical Design*, vol. 135, no. 9, p. 091 006, 2013.

[70] M McDonald and S Mahadevan, "Design optimization with system-level reliability constraints," *Journal of Mechanical Design*, vol. 130, no. 2, p. 021 403, 2008.

[71] S. Sankararaman and S. Mahadevan, "Likelihood-based approach to multidisciplinary analysis under uncertainty," *Journal of Mechanical Design*, vol. 134, no. 3, p. 031 008, 2012.

[72] S. Rangavajhala, C. Liang, and S. Mahadevan, "Design optimization under aleatory and epistemic uncertainties," in *12th AIAA Aviation Technology, Integration, and Operations (ATIO) Conference and 14th AIAA/ISSMO Multidisciplinary Analysis and Optimization Conference*, 2012, p. 5665.

[73] E. J. Cramer, J. E. Dennis Jr, P. D. Frank, R. M. Lewis, and G. R. Shubin, "Problem formulation for multidisciplinary optimization," *SIAM Journal on Optimization*, vol. 4, no. 4, pp. 754–776, 1994.

[74] G. Taguchi, *Introduction to quality engineering: Designing quality into products and processes*. 1986.

[75] H.-G. Beyer and B. Sendhoff, "Robust optimization–a comprehensive survey," *Computer methods in applied mechanics and engineering*, vol. 196, no. 33, pp. 3190–3218, 2007.

[76] A. Haldar and S. Mahadevan, *Probability, reliability, and statistical methods in engineering design*. John Wiley, 2000.

[77] L. Huyse, "Solving problems of optimization under uncertainty as statistical decision problems," in *19th AIAA Applied Aerodynamics Conference*, 2001, p. 1519.

[78] I. Enevoldsen and J. D. Sørensen, "Reliability-based optimization of series systems of parallel systems," *Journal of structural engineering*, vol. 119, no. 4, pp. 1069–1084, 1993.

[79] S. Mahadevan, "Stochastic finite element based structural reliability analysis and optimization.," 1989.

[80] X. Chen, T. Hasselman, D. Neill, X. Chen, T. Hasselman, and D. Neill, "Reliability based structural design optimization for practical applications," in *38th Structures, structural dynamics, and materials conference*, 1997, p. 1403.

[81] L. Wang, R. V. Grandhi, and D. A. Hopkins, "Structural reliability optimization using an efficient safety index calculation procedure," *International Journal for Numerical Methods in Engineering*, vol. 38, no. 10, pp. 1721–1738, 1995.

[82] S. W. Kandebo, "Putting f 135 to the test.," *Aviation week and space technology*, vol. 160, no. 12, pp. 52–54, 2004.

[83] C. E. Howard, "Technical and supply chain issues cause delays, cost airbus 1.5b," *Intelligent Aerospace*, 2016.

[84] J. Flottau, "Airbus plans to increase a350 production rate to 13 per month," *HAviation Week*, 2015.

[85] P. L. Bernstein and P. L. Bernstein, *Against the gods: The remarkable story of risk*. Wiley New York, 1996.

[86] I. Hacking, *The emergence of probability: A philosophical study of early ideas about probability, induction and statistical inference*. Cambridge University Press, 2006.

[87] W. L. Oberkampf, J. C. Helton, C. A. Joslyn, S. F. Wojtkiewicz, and S. Ferson, "Challenge problems: Uncertainty in system response given uncertain parameters," *Reliability Engineering & System Safety*, vol. 85, no. 1-3, pp. 11–19, 2004.

[88] S. Ferson and K. Sentz, "Epistemic uncertainty in agent-based modeling," 2016.

[89] S. Ferson and L. R. Ginzburg, "Different methods are needed to propagate ignorance and variability," *Reliability Engineering & System Safety*, vol. 54, no. 2-3, pp. 133–144, 1996.

[90] J. M. Keynes, "The general theory of employment," *The quarterly journal of economics*, vol. 51, no. 2, pp. 209–223, 1937.

[91] S. Ferson, "Quality assurance for monte carlo risk assessment," in *Uncertainty Modeling and Analysis, 1995, and Annual Conference of the North American Fuzzy Information Processing Society. Proceedings of ISUMA-NAFIPS'95., Third International Symposium on*, IEEE, 1995, pp. 14–19.

[92] D. Dequech, "Fundamental uncertainty and ambiguity," *Eastern Economic Journal*, vol. 26, no. 1, pp. 41–60, 2000.

[93] W. Heisenberg, "Über den anschaulichen inhalt der quantentheoretischen kinematik und mechanik," in *Original Scientific Papers Wissenschaftliche Originalarbeiten*, Springer, 1927, pp. 478–504.

[94] N. Bohr, *The quantum postulate and the recent development of atomic theory*, 1928.

[95] R. V. Hogg and A. T. Craig, "Introduction to mathematical statistics.(5"" edition)," *Englewood Hills, New Jersey*, 1995.

[96] L. DeLaurentis and D. Mavris, "Uncertainty modeling and management in multidisciplinary analysis and synthesis," in *38th Aerospace sciences meeting and exhibit*, 2000, p. 422.

[97] J. Bukowski, L. Korn, and D. Wartenberg, "Correlated inputs in quantitative risk assessment: The effects of distributional shape," *Risk Analysis*, vol. 15, no. 2, pp. 215–219, 1995.

[98] S. Ferson and M. A. Burgman, "Correlations, dependency bounds and extinction risks," *Biological Conservation*, vol. 73, no. 2, pp. 101–105, 1995.

[99] P. S. marquis de Laplace, *Essai philosophique sur les probabilités*. Bachelier, 1825.

[100] P. Cheeseman, "An inquiry into computer understanding," *Computational Intelligence*, vol. 4, no. 2, pp. 58–66, 1988.

[101] R. T. Cox, "Probability, frequency and reasonable expectation," *American journal of physics*, vol. 14, no. 1, pp. 1–13, 1946.

[102] D. V. Lindley, "Scoring rules and the inevitability of probability," *International Statistical Review/Revue Internationale de Statistique*, pp. 1–11, 1982.

[103] R. E. Neapolitan, "A survey of uncertain and approximate inference," in *Fuzzy logic for the management of uncertainty*, John Wiley & Sons, Inc., 1992, pp. 55–82.

[104] D. P. Thunnissen, "Uncertainty classification for the design and development of complex systems," in *3rd annual predictive methods conference*, 2003, pp. 16–17.

[105] D. A. Delaurentis, *A probabilistic approach to aircraft design emphasizing stability and control uncertainties*. 1998.

[106] W. Oberkampf, S. DeLand, B. Rutherford, K. Diegert, and K. Alvin, "A new methodology for the estimation of total uncertainty in computational simulation," in *40th Structures, Structural Dynamics, and Materials Conference and Exhibit*, 1999, p. 1612.

[107] M. J. Daskilewicz, B. J. German, T. T. Takahashi, S. Donovan, and A. Shajanian, "Effects of disciplinary uncertainty on multi-objective optimization in aircraft conceptual design," *Structural and Multidisciplinary Optimization*, vol. 44, no. 6, pp. 831–846, 2011.

[108] A. J. Ramirez, A. C. Jensen, and B. H. Cheng, "A taxonomy of uncertainty for dynamically adaptive systems," in *Proceedings of the 7th International Symposium on Software Engineering for Adaptive and Self-Managing Systems*, IEEE Press, 2012, pp. 99–108.

[109] D. Thunnissen, "Balancing cost, risk, and performance under uncertainty in preliminary mission design," in *Space 2004 Conference and Exhibit*, 2004, p. 5878.

[110] M. R. Kirby, "A methodology for technology identification, evaluation, and selection in conceptual and preliminary aircraft design," PhD thesis, School of Aerospace Engineering, Georgia Institute of Technology, 2001.

[111] G. A. Hazelrigg, *Systems engineering: An approach to information-based design*. Pearson College Division, 1996.

[112] P Wersching and J Wu, "Probabilistic methods," *7th Annual Short Course on Probabilistic Analysis and Design, Southwest Research Institute, San Antonio, TX*, 1996.

[113] K. Zhou, J. C. Doyle, K. Glover, *et al.*, *Robust and optimal control*. Prentice hall New Jersey, 1996, vol. 40.

[114] D. N. Mavris, N. I. Macsotai, and B. A. Roth, "A probabilistic design methodology for commercial aircraft engine cycle selection," 1998.

[115] J. Tan, K. Otto, and K. Wood, "Concept design trade-offs considering performance margins," *DS 85-1: Proceedings of NordDesign 2016, Volume 1, Trondheim, Norway, 10th-12th August 2016*, 2016.

[116] T. A. Zang, S. Mahadevan, J. C. Tai, and D. N. Mavris, "A strategy for probabilistic margin allocation in aircraft conceptual design," in *16th AIAA/ISSMO Multidisciplinary Analysis and Optimization Conference*, 2015, p. 3443.

[117] T. A. Zang, M. J. Hemsch, M. W. Hilburger, S. P. Kenny, J. M. Luckring, P. Maghami, S. L. Padula, and W. J. Stroud, "Needs and opportunities for uncertainty-based multidisciplinary design methods for aerospace vehicles," 2002.

[118] B. E. Robertson, "A hybrid probabilistic method to estimate design margin," PhD thesis, Georgia Institute of Technology, 2013.

[119] J. K. Hollmann and P. CEP, "Recommended practices for risk analysis and cost contingency estimating," *Association for the Advancement of Cost Engineering (AACE), Working Maual*, 2009.

[120] S. E. Burroughs and G. Juntima, "Exploring techniques for contingency setting," *AACE International Transactions*, ES31, 2004.

[121] T. Nam and D. Mavris, "Multi-stage reliability-based design optimization for aerospace system conceptual design," in *49th AIAA/ASME/ASCE/AHS/ASC Structures, Structural Dynamics, and Materials Conference, 16th AIAA/ASME/AHS Adaptive Structures Conference, 10th AIAA Non-Deterministic Approaches Conference, 9th AIAA Gossamer Spacecraft Forum, 4th AIAA Multidisciplinary Design Optimization Specialists Conference*, 2008, p. 2073.

[122] T. Nam, "A generalized sizing method for revolutionary concepts under probabilistic design constraints," PhD thesis, Georgia Institute of Technology, 2007.

[123] E. J. Paulson and R. P. Starkey, "Development of a multistage reliability-based design optimization method," *Journal of Mechanical Design*, vol. 136, no. 1, p. 011 007, 2014.

[124] G. B. Dantzig, "Linear programming under uncertainty," in *Stochastic Programming*, Springer, 2010, pp. 1–11.

[125] J. R. Martins and A. B. Lambe, "Multidisciplinary design optimization: A survey of architectures," *AIAA journal*, vol. 51, no. 9, pp. 2049–2075, 2013.

[126] L. McCullers, "Aircraft configuration optimization including optimized flight profiles," 1984.

[127] J. K. Lytle, "The numerical propulsion system simulation: An overview," *NASA TM*, vol. 209915, 2000.

[128] P. Barros, M. R. Kirby, and D. N. Mavris, "An approach for verification and validation of the environmental design space," in *26th international congress of the aeronautical sciences*, 2008.

[129] J. C. Tai, J. M. Mines, E. J. Inclan, and S. Y. Zhu, "Uncertainty quantification and management in engine conceptual design," in *52nd AIAA/SAE/ASEE Joint Propulsion Conference*, 2016, p. 5064.

[130] Langley Research Center, *Vehicle sketch pad (vsp)*, https://software.nasa.gov/software/LAR-17491-1.

[131] G.-R. Liu, *Mesh free methods: Moving beyond the finite element method*. CRC press, 2002.

[132] K Ho-Le, "Finite element mesh generation methods: A review and classification," *Computer-aided design*, vol. 20, no. 1, pp. 27–38, 1988.

[133] Siemens, *Star-ccm+*, https://mdx.plm.automation.siemens.com/star-ccm-plus.

[134] Langley Research Center, *Fun3d*, https://fun3d.larc.nasa.gov/.

[135] Livermore Software Technology Corporation, *Ls-dyna*, https://www.oasys-software.com/dyna/soft dyna/.

[136] ANSYS Inc., *Structural analysis software*, https://www.ansys.com/products/structures.

[137] S. M. (2001). Nasa releases classic software to public domain.

[138] J. A. Corman, N. Weston, C. Friedland, D. N. Mavris, and T. W. Laughlin, "A parametric multi-fidelity approach to conceptual airframe design," in *2018 AIAA Modeling and Simulation Technologies Conference*, 2018, p. 1930.

[139] J. A. Corman, D. Sarojini, A. Gharbi, and D. N. Mavris, "Estimating jig shape for an aircraft wing determined through aerodynamic shape optimization with rigid body assumptions," in *AIAA Scitech 2019 Forum*, 2019, p. 0418.

[140] T. Laughlin, J. Corman, and D. Mavris, "A parametric and physics-based approach to structural weight estimation of the hybrid wing body aircraft," in *51st AIAA Aerospace Sciences Meeting including the New Horizons Forum and Aerospace Exposition*, 2013, p. 1082.

[141] M. Drela and H. Youngren, "Avl 3.36 user primer," *Department of Aeronautics and Astronautics, Massachusetts Institute of Technology, Cambridge, MA*, 2017.

[142] K Maute and M Allen, "Conceptual design of aeroelastic structures by topology optimization," *Structural and Multidisciplinary Optimization*, vol. 27, no. 1-2, pp. 27–42, 2004.

[143] S. Aly, M. Ogot, R. Pelz, and M. Siclari, "Jig-shape static aeroelastic wing design problem: A decoupled approach," *Journal of aircraft*, vol. 39, no. 6, pp. 1061–1066, 2002.

[144] Z. Wan, L. Liang, and C. Yang, "Method of the jig shape design for a flexible wing," *Journal of Aircraft*, vol. 51, no. 1, pp. 327–330, 2013.

[145] K. Holloway. (2018). Southwest airline engine accident, National Transportation Safety Board.

[146] A. Walker, "Study and analysis of the first 120 failure cases," *Structural Failures in Buildings, the Institution of Structural Engineers, London, July*, pp. 15–40, 1981.

[147] J Schneider and M Matousek, "Untersuchungen zur struktur des sicherheitsproblems bei bauwerken," *Zürich Institut für Baustatik und Konstruktion, ETHZ*, 1976.

[148] J. Kuttenkeuler and U. Ringertz, "Aeroelastic tailoring considering uncertainties in material properties," *Structural optimization*, vol. 15, no. 3-4, pp. 157–162, 1998.

[149] W Stroud, T Krishnamurthy, B. Mason, S. Smith, and A. Naser, "Probabilistic design of a plate-like wing to meet flutter and strength requirements," in *43rd AIAA/ASME/ASCE/AHS/ASC Structures, Structural Dynamics, and Materials Conference*, 2002, p. 1464.

[150] A. Manan and J. Cooper, "Design of composite wings including uncertainties: A probabilistic approach," *Journal of Aircraft*, vol. 46, no. 2, pp. 601–607, 2009.

[151] V. Garzon and D. Darmofal, "Using computational fluid dynamics in probabilistic engineering design," in *15th AIAA Computational Fluid Dynamics Conference*, 2001, p. 2526.

[152] S. Mahadevan and N. Smith, "Efficient first-order reliability analysis of multidisciplinary systems," *International Journal of Reliability and Safety*, vol. 1, no. 1-2, pp. 137–154, 2006.

[153] R. Zhang and S. Mahadevan, "Model uncertainty and bayesian updating in reliability-based inspection," *Structural Safety*, vol. 22, no. 2, pp. 145–160, 2000.

[154] X. Du, "First order and second reliability methods," *Probabilistic engineering design*, pp. 1–33, 2005.

[155] F. Hui and L. Weiji, "An efficient method for reliability-based multidisciplinary design optimization," *Chinese Journal of Aeronautics*, vol. 21, no. 4, pp. 335–340, 2008.

[156] X. Du and W. Chen, "Collaborative reliability analysis under the framework of multidisciplinary systems design," *Optimization and Engineering*, vol. 6, no. 1, pp. 63–84, 2005.

[157] Y. Noh, K. Choi, I. Lee, D. Gorsich, and D. Lamb, "Reliability-based design optimization with confidence level under input model uncertainty due to limited test data," *Structural and Multidisciplinary Optimization*, vol. 43, no. 4, pp. 443–458, 2011.

[158] A. Der Kiureghian, H.-Z. Lin, and S.-J. Hwang, "Second-order reliability approximations," *Journal of Engineering mechanics*, vol. 113, no. 8, pp. 1208–1225, 1987.

[159] M. Hohenbichler and R. Rackwitz, "Improvement of second-order reliability estimates by importance sampling," *Journal of Engineering Mechanics*, vol. 114, no. 12, pp. 2195–2199, 1988.

[160] J. Liang, Z. P. Mourelatos, and J. Tu, "A single-loop method for reliability-based design optimization," in *ASME 2004 International Design Engineering Technical Conferences and Computers and Information in Engineering Conference*, American Society of Mechanical Engineers, 2004, pp. 419–430.

[161] B.-L. Choi, J.-H. Choi, and D.-H. Choi, "Reliability-based design optimization using enhanced initial design and two-point approximation technique," in *proceedings of 10th AIAA/ISSMO MAO conference*, vol. 4518, 2004.

[162] J. Hurtado and A. H. Barbat, "Monte carlo techniques in computational stochastic mechanics," *Archives of Computational Methods in Engineering*, vol. 5, no. 1, p. 3, 1998.

[163] D. Padmanabhan, R. Tappeta, and S. Batill, "Monte carlo simulation in reliability based optimization applied to multidisciplinary system design," in *44th AIAA/ASME/ASCE/AHS/ASC Structures, Structural Dynamics, and Materials Conference*, 2003, p. 1503.

[164] X. Gu, J. E. Renaud, S. M. Batill, R. M. Brach, and A. S. Budhiraja, "Worst case propagated uncertainty of multidisciplinary systems in robust design optimization," *Structural and Multidisciplinary Optimization*, vol. 20, no. 3, pp. 190–213, 2000.

[165] H. Liu, W. Chen, and A. Sudjianto, "Relative entropy based method for probabilistic sensitivity analysis in engineering design," *Journal of Mechanical Design*, vol. 128, no. 2, pp. 326–336, 2006.

[166] J. D. Martin and T. W. Simpson, "A methodology to manage system-level uncertainty during conceptual design," *Journal of Mechanical Design*, vol. 128, no. 4, pp. 959–968, 2006.

[167] J. C. Helton, J. D. Johnson, C. J. Sallaberry, and C. B. Storlie, "Survey of sampling-based methods for uncertainty and sensitivity analysis," *Reliability Engineering & System Safety*, vol. 91, no. 10, pp. 1175–1209, 2006.

[168] X. Du and W. Chen, "Sequential optimization and reliability assessment method for efficient probabilistic design," in *ASME 2002 International Design Engineering Technical Conferences and Computers and Information in Engineering Conference*, American Society of Mechanical Engineers, 2002, pp. 871–880.

[169] M Vorechovsky and D Novak, "Correlation control in small-sample monte carlo type simulations i: A simulated annealing approach," *Probabilistic Engineering Mechanics*, vol. 24, no. 3, pp. 452–462, 2009.

[170] M Vorechovsky, "Correlation control in small sample monte carlo type simulations ii: Analysis of estimation formulas, random correlation and perfect uncorrelatedness," *Probabilistic Engineering Mechanics*, vol. 29, pp. 105–120, 2012.

[171] W. Oberkampf, J. Helton, and K. Sentz, "Mathematical representation of uncertainty," in *19th AIAA Applied Aerodynamics Conference*, 2001, p. 1645.

[172] M. Padulo, M. S. Campobasso, and M. D. Guenov, "Novel uncertainty propagation method for robust aerodynamic design," *AIAA journal*, vol. 49, no. 3, pp. 530–543, 2011.

[173] T. Zaidi, H. Jimenez, and D. Mavris, "Copulas theory for probabilistic assessment: Overview with application to airplane performance analysis," *Journal of Aircraft*, vol. 52, no. 6, pp. 1802–1820, 2015.

[174] L. Green, H.-Z. Lin, and M Khalessi, "Probabilistic methods for uncertainty propagation applied to aircraft design," in *20th AIAA Applied Aerodynamics Conference*, 2002, p. 3140.

[175] J. R. Benjamin, "Cornell ca. probability," *Statistics, and decision for civil engineers. McGraw-Hill, New York*, 1970.

[176] F. J. Dyson and M. L. Mehta, "Statistical theory of the energy levels of complex systems. iv," *Journal of Mathematical Physics*, vol. 4, no. 5, pp. 701–712, 1963.

[177] D. M. Jaffee and T. Russell, "Catastrophe insurance, capital markets, and uninsurable risks," *Journal of Risk and Insurance*, pp. 205–230, 1997.

[178] W. Yao, J. Guo, X. Chen, and M. van Tooren, "Utilizing uncertainty multidisciplinary design optimization for conceptual design of space systems," in *Proc. of the 8th Conference on Systems Engineering Research, Hoboken, NJ, USA*, 2010.

[179] S. Ferson, C. A. Joslyn, J. C. Helton, W. L. Oberkampf, and K. Sentz, "Summary from the epistemic uncertainty workshop: Consensus amid diversity," *Reliability Engineering & System Safety*, vol. 85, no. 1, pp. 355–369, 2004.

[180] J. C. Helton and F. J. Davis, "Latin hypercube sampling and the propagation of uncertainty in analyses of complex systems," *Reliability Engineering & System Safety*, vol. 81, no. 1, pp. 23–69, 2003.

[181] S. Mahadevan and R. Rebba, "Inclusion of model errors in reliability-based optimization," *Journal of Mechanical Design*, vol. 128, no. 4, pp. 936–944, 2006.

[182] B. R. Baliga and I. Y. Lokhmanets, "Generalized richardson extrapolation procedures for estimating grid-independent numerical solutions," *International Journal of Numerical Methods for Heat & Fluid Flow*, vol. 26, no. 3/4, pp. 1121–1144, 2016.

[183] G de Vahl Davis, "Natural convection of air in a square cavity: A bench mark numerical solution," *International Journal for numerical methods in fluids*, vol. 3, no. 3, pp. 249–264, 1983.

[184] R. S. Parrish, "Generating random deviates from multivariate pearson distributions," *Computational Statistics & Data Analysis*, vol. 9, no. 3, pp. 283–295, 1990.

[185] M. S. Taylor and J. R. Thompson, "A data based algorithm for the generation of random vectors," *Computational Statistics & Data Analysis*, vol. 4, no. 2, pp. 93–101, 1986.

[186] A. I. Fleishman, "A method for simulating non-normal distributions," *Psychometrika*, vol. 43, no. 4, pp. 521–532, 1978.

[187] C. D. Vale and V. A. Maurelli, "Simulating multivariate nonnormal distributions," *Psychometrika*, vol. 48, no. 3, pp. 465–471, 1983.

[188] M. C. Cario and B. L. Nelson, "Modeling and generating random vectors with arbitrary marginal distributions and correlation matrix," Citeseer, Tech. Rep., 1997.

[189] S. Ghosh and S. G. Henderson, "Behavior of the norta method for correlated random vector generation as the dimension increases," *ACM Transactions on Modeling and Computer Simulation (TOMACS)*, vol. 13, no. 3, pp. 276–294, 2003.

[190] S. T. Li and J. L. Hammond, "Generation of pseudorandom numbers with specified univariate distributions and correlation coefficients," *IEEE Transactions on Systems, Man, and Cybernetics*, no. 5, pp. 557–561, 1975.

[191] R. L. Iman and W.-J. Conover, "A distribution-free approach to inducing rank correlation among input variables," *Communications in Statistics-Simulation and Computation*, vol. 11, no. 3, pp. 311–334, 1982.

[192] R. T. Clemen and T. Reilly, "Correlations and copulas for decision and risk analysis," *Management Science*, vol. 45, no. 2, pp. 208–224, 1999.

[193] P. M. Lurie and M. S. Goldberg, "An approximate method for sampling correlated random variables from partially-specified distributions," *Management science*, vol. 44, no. 2, pp. 203–218, 1998.

[194] R. R. Hill and C. H. Reilly, "The effects of coefficient correlation structure in two-dimensional knapsack problems on solution procedure performance," *Management Science*, vol. 46, no. 2, pp. 302–317, 2000.

[195] D. C. Charmpis and P. L. Panteli, "A heuristic approach for the generation of multivariate random samples with specified marginal distributions and correlation matrix," *Computational statistics*, vol. 19, no. 2, p. 283, 2004.

[196] M. Moinester and R. Gottfried, "Sample size estimation for correlations with pre-specified confidence interval," *The Quantitative Methods for Psychology*, vol. 10, no. 2, pp. 124–130, 2014.

[197] M Sklar, "Fonctions de repartition an dimensions et leurs marges," *Publ. inst. statist. univ. Paris*, vol. 8, pp. 229–231, 1959.

[198] R. B. Nelsen, "Introduction," in *An Introduction to Copulas*, Springer, 1999, pp. 1–4.

[199] Y. Noh, K. Choi, and L. Du, "Reliability-based design optimization of problems with correlated input variables using a gaussian copula," *Structural and multidisciplinary optimization*, vol. 38, no. 1, pp. 1–16, 2009.

[200] T. A. Zaidi, "A methodology for probabilistic aircraft technology assessment and selection under uncertainty," PhD thesis, Georgia Institute of Technology, 2016.

[201] (), NASA Common Research Model. https://commonresearchmodel.larc.nasa.gov/. 2019.02.22.

[202] G. Schwarz *et al.*, "Estimating the dimension of a model," *The annals of statistics*, vol. 6, no. 2, pp. 461–464, 1978.

[203] S. Kullback and R. A. Leibler, "On information and sufficiency," *The annals of mathematical statistics*, vol. 22, no. 1, pp. 79–86, 1951.

[204] F. J. Fabozzi, S. M. Focardi, S. T. Rachev, and B. G. Arshanapalli, *The basics of financial econometrics: Tools, concepts, and asset management applications*. John Wiley & Sons, 2014.

[205] G. E. Box, "Science and statistics," *Journal of the American Statistical Association*, vol. 71, no. 356, pp. 791–799, 1976.

[206] T. W. Anderson, D. A. Darling, *et al.*, "Asymptotic theory of certain" goodness of fit" criteria based on stochastic processes," *The annals of mathematical statistics*, vol. 23, no. 2, pp. 193–212, 1952.

[207] L. Devroye, "Nonuniform random variate generation," *Handbooks in operations research and management science*, vol. 13, pp. 83–121, 2006.

[208] S. Demarta and A. J. McNeil, "The t copula and related copulas," *International statistical review*, vol. 73, no. 1, pp. 111–129, 2005.

[209] V. Pareto, *Cours d'économie politique*. Librairie Droz, 1964, vol. 1.

[210] B. C. Airplanes and W. Seattle, *777-200/300 airplane characteristics for airport planning, d6-58329 ed*, 2011.

VITA

John Mark Mines was born in Dallas, Texas in 1991. He first attended Southwestern University to play Men's Soccer before transferring to Virginia Polytechnic Institute and State University to pursue engineering. After graduating summa cum laude with a Bachelor's degree in Engineering Science and Mechanics in May 2014, he joined the Aerospace Systems Design Laboratory at the Georgia Institute of Technology in August.

While at Georgia Tech he completed a Master's of Science in Aerospace Engineering in 2015 and a Master's of Business Administration in 2017. He was the project manager of a missile design team that won first prize for the 2014-15 graduate competition. He was also a leadership coach in Tech's LEAD program, which allowed him to teach an introductory leadership course to incoming university freshmen, conduct interviews for coaches, and coach undergraduate "coachees" and graduate coaches, from 2017-2019.

He has accepted a position at Johns Hopkins University Applied Physics Laboratory in Laurel, Maryland. He will be working with an optimization group within the Air and Missile Defense Sector.